# Operational Robustness of Drinking Water Treatment Plants with Respect to Turbidity Representing Normal, Severe and Unprecedented Weather Events

by

Noshin Nawar Reza

A thesis

presented to the University of Waterloo

in fulfillment of the

thesis requirement for the degree of

Master of Applied Science

in

Civil Engineering (Water)

Waterloo, Ontario, Canada, 2022

## Author's Declaration

I hereby declare that I am the sole author of this thesis. This is a true copy of the thesis, including any required final revisions, as accepted by my examiners.

I understand that my thesis may be made electronically available to the public.

# Abstract

Drinking water treatment plants (DWTPs) are required to supply safe drinking water continuously to the consumers to protect public health and sanitation. The adverse effects of climate change can influence raw water quality, which is likely to worsen in the future as predicted by numerous climate models. The intensity, frequency and duration of precipitation events have been observed to be changed throughout the world as a consequence of natural and anthropogenic climate change. Severe and untimely precipitation events have the potential to deteriorate the water quality in surface water bodies directly and have been associated with water-borne diseases. Many DWTPs in Canada use surface water as their raw water source. Heavy precipitation events can lead to a significant increase in suspended and dissolved particles in surface water bodies by fluvial erosion and transportation of particles, which can result in raw water with elevated turbidity at the intake. Most of the DWTPs are designed based on historical data including past weather events. However, with the rapid change in precipitation patterns leading to very high turbidity levels in raw water more frequently, it can be quite challenging for the DWTPs to maintain regulated water quality during these heavy storm events.

To control such turbidity spikes in raw water, a DWTP should be robust. Robustness of DWTPs is defined as the ability to provide excellent performance under normal conditions and deviate minimally during periods of upsets and challenges, maintaining a set finished water quality. The robustness of the affected treatment steps needs to be quantified to evaluate the robustness of the DWTPs under normal and historical weather scenarios and be improved for future weather scenarios that may occur due to climate change. A robustness framework was applied to two full-scale DWTPs (Plant A and Plant B) from Southern Ontario to assess their robustness with respect to turbidity for three raw water scenarios: (a) baseline turbidity representing normal weather, (b) elevated turbidity representing historical precipitation events, and (c) extremely high turbidity representing future precipitation events that is beyond general experience. For evaluating scenarios (a) and (b), on-line turbidity data for the calendar years 2019 and 2020 were provided by the two plants which have different raw water sources and treatment methods. To quantify the robustness of the affected treatment steps for turbidity removal, the turbidity robustness index (TRI) was used. A lower value of TRI is desired as it implies that the treatment step was robust for the given period. Using the TRI method has the advantage to quantify the robustness of treatment units with one index and one classification system irrespective of the different geographic locations, raw water sources, treatment techniques, and intensity and duration of

precipitation events experienced in the two DWTPs. The weekly TRIs were calculated for each unit of the selected treatment steps during normal weather conditions using the on-line data. A method was developed to distinguish the elevated turbidity events representing heavy precipitation from background turbidity data and the TRIs corresponding to these periods were separated. However, no correlation was observed between higher TRIs and weather events characterized by elevated raw water turbidity, which is an indication of robustness with respect to raw water turbidity. The overall robustness of the two plants was assessed during the study period. Plant A was found to be more robust than Plant B in general. The higher TRIs observed in both plants can be a good tool to evaluate their operational regime retroactively and improve the robustness of the treatment steps.

To assess scenario (c), the full-scale coagulation and sand ballasted clarification (SBC) process of Plant A was simulated using modified bench-scale jar tests where spiked water samples with very high turbidity were assessed in addition to controls at normal turbidity. A factorial design experiment was conducted to determine the significant factors for turbidity removal and optimize the process. The outcome of these experiments suggested that the polymer dosage used in the plant is optimum for extremely high turbidities, but the coagulant and microsand dosages can be increased for better removal. The outcome of the bench-scale simulation can aid in potential pilot- or full-scale studies.

This study focuses on elevated raw water turbidity caused by heavy precipitation events. It is recommended to explore the effects of other climatic events on various raw water quality parameters to evaluate and improve the robustness of DWTPs.

# Acknowledgements

First, I would like to express my gratitude to my supervisors, Dr. Peter M. Huck and Dr. Sigrid Peldszus for their invaluable advice, continuous support and motivation throughout this research. I am grateful for your immense knowledge, insightful feedback, great effort and time that you put into this work. I am thankful to be a part of such an interesting project.

I would like to thank Kirti S. Nemani for her helpful guidance and treasured support in shaping the project. Special thanks to Kimia Aghasadeghi, Katarzyna Maria Jaszczyszyn, Sina Golchi and Mahmoud Badawy in the NSERC Chair in Water Treatment for their constructive suggestions and willingness to help whenever needed. Thanks to Mark Sobon and Mark Merlau for their technical support in the lab, to Steven Ngo for his assistance with zeta potential and TOC/DOC measurements and to Lorena Baku for her assistance with numerous administrative tasks. I would like to extend my sincere thanks to all the members of the NSERC Chair in Water Treatment and my friends and colleagues at the University of Waterloo, whose dedication and pursuit of excellence inspire me every day.

This research was conducted in partnership with Plant A and Plant B. I am deeply grateful to the staff of Plant A and B for their guidance and support at every stage of the project by providing plant data and resources, sharing their insight into plant operations and answering my many questions. Thanks to the staff of Plant A for arranging a field trip to the plant, taking the time to explain every single detail of the plant operations, and collecting and shipping the raw water samples and chemicals, without which this research would not be possible.

I would like to extend my thanks to the readers of this thesis, Dr. William A. Anderson and Dr. Stan Potapenko.

Finally, I would like to thank my parents and my sister for their unconditional love and encouragement. Thanks to my friends whose love and support have brightened this journey thousands of miles away from home.

This project is funded by the Natural Sciences and Engineering Research Council of Canada (NSERC) in the form of an Industrial Research Chair in Water Treatment at the University of Waterloo. The current Chair partners are listed at https://uwaterloo.ca/nserc-chair-water-treatment/partners .

# Table of Contents

# List of Figures

# List of Tables

# List of Abbreviations

ANOVA: analysis of variance

AOGCM: atmosphere-ocean general circulation model

BOD: biological oxygen demand

C: carbon

CART: classification and regression tree

CFS: coagulation-flocculation-sedimentation

CI: confidence interval

DBP: disinfection by-product

DOC: dissolved organic carbon

DOM: dissolved organic matter

DWTP: drinking water treatment plants

FTU: formazin turbidity unit

GAC: granular activated carbon

GHS: greenhouse gas

GI: gastrointestinal

HAA: haloacetic acids

HRT: hydraulic retention time

IPCC: Intergovernmental Panel on Climate Change

MDWL: municipal drinking water license

ML/D: million liters per day

NOM: natural organic matter

NPP: normal probability plot

NTU: nephelometric turbidity unit

PACl: polyaluminum chloride

PF: performance function

POC: particulate organic carbon

QMRA: quantitative microbial risk assessment

RPM: revolutions per minute

SBC: sand ballasted clarification

SDS: simulated distribution system

SOP: standard operating procedure

SRES: special report of emissions scenarios

SS: suspended solids

SUVA: specific ultra-violet absorbance

TCU: True color unit

TMH: trihalomethanes

TOC: total organic carbon

TRI: turbidity robustness index

USA: United States of America

UV: ultra-violet

WTP: water treatment plant

# Disclaimer

In several instances in this study, commercial products and/or trade names were mentioned. The use of commercial names does not constitute endorsement or recommendation of these products and/or instruments by the author.

# Chapter 1: Introduction

## 1.1 Problem Statement

Drinking water treatment plants (DWTPs) are required to supply safe drinking water at all times (Hartshorn et al., 2015; Huck & Coffey, 2004; Li & Huck, 2008; Upton et al., 2017; Zhang et al., 2012). Many DWTPs in Canada use surface water (e.g., lakes, rivers, streams) as their raw water source. Due to the rapid changes in climate in the past decades, the duration, intensity, frequency, and timing of extreme hydrological events such as heavy precipitation have changed (Delpla et al., 2009; Füssel, 2009; Kim et al., 2017; Min et al., 2011; Semenza & Menne, 2009; Staben et al., 2015). The water quality in surface water bodies tends to show immediate changes to extreme weather conditions (Staben et al., 2015). Moreover, the overall increase in global temperature results in early snow-melting (Bates et al., 2008). Snow melting and spring storms often occur at the same time and provide the greatest negative impact on surface water quality (Pešić et al., 2020). Intense precipitation leads to increased turbidity levels in surface water (Atherholt et al., 1998; Bates et al., 2008; Crittenden et al., 2012; Khan et al., 2015; Lawler et al., 2006). Elevated raw water turbidity caused by extreme rainfall has been associated with several water-borne diseases and gastrointestinal (GI) hospitalizations (Curriero et al., 2001; De Roos et al., 2017; Delpla et al., 2009; Tinker et al., 2010). Various climate projection models predict that the intensity of precipitation is likely to increase in most areas in the world, while the mean precipitation would decrease (Bates et al., 2008). Consequently, more frequent heavy precipitation will take place in the future resulting in raw water quality parameter changes beyond the general experience, and newer and more difficult challenges for the DWTPs. Most water treatment utilities are designed based on historical data. When raw water with unusually high turbidity that is beyond the design capacity is recorded at the intake, DWTPs may fail to cope with the situation and consequently shut down the plant. Following the plant shutdown, if the finished water reservoir capacity is crossed and the DWTPs cannot meet the demand, it leads to extensive economic loss and social impacts (Qiu et al., 2019; Staben et al., 2015).

Climate change may not be preventable, but necessary measures have to be taken to maintain a set finished drinking water quality during extreme events. A DWTP must be robust in order to ensure the unchanged and desired performance despite the variations in raw water quality following an extreme weather event. Robustness is defined as the competence of a system to perform excellently under normal conditions, deviate minimally during periods of challenges, and continue to provide the desired

service (Huck & Coffey, 2002). Quantification of robustness is important to ensure and improve the robustness of a DWTP. Several researchers have evaluated the robustness of filtration units as well as clarification processes based on turbidity (García-Ávila et al., 2021; Hartshorn et al., 2015; Huck & Coffey, 2004; Li & Huck, 2008; Zoric et al., 2020). However, there has been limited focus on the robustness of the other treatment steps and the overall robustness of full-scale plants. There has been only one study that focused on an integrated framework for performance assessment (Zhang et al., 2012). Furthermore, all these studies emphasize historical data for the water quality parameters investigated, which is likely to be invalid very soon considering the current impacts of climate change on raw water quality.

## 1.2 Research Objectives and Scope

The primary objective of this research is to apply the robustness framework developed by Nemani (2021a) to two DWTPs with respect to turbidity to evaluate the robustness of the affected treatment steps and provide guidance towards testing and implementing short-term operational responses to mitigate the complications caused by a water quality event. This study mainly focuses on the impact on treatment steps of elevated raw water turbidity caused by heavy precipitation.

The main objectives of this research are:

1. To apply the robustness framework with respect to turbidity to two drinking water treatment plants with different raw water sources and treatment trains.
2. To simulate the current and projected effects of extreme precipitation on raw water turbidity at bench-scale to provide guidance for optimizing the current treatment process accordingly.

The sub-objectives relating to the first main objective are:

- Develop a method for separating the turbidity events from background turbidity for Plant A and Plant B.
- Evaluate the robustness of the identified critical treatment steps of Plant A and Plant B using the Turbidity Robustness Index (TRI) during normal and historical high turbidity events.
- Integrate the robustness of different treatment steps and assess the overall robustness of Plant A and Plant B.

The sub-objectives relating to the second main objective are:

- Perform bench-scale simulations of the coagulation and sand ballasted clarification (SBC) process, commercially known as the ACTIFLO® process in Plant A using raw water samples collected during normal weather and historical extreme weather.
- Perform bench-scale simulations of the ACTIFLO® process in Plant A using spiked water samples that reflect the effects of future extreme weather on source water turbidity.
- Provide guidance for optimizing the ACTIFLO® process in Plant A by using a factorial design experiment on spiked water samples that simulates the effects of future extreme weather on source water turbidity.

## 1.3 Structure of the Thesis

The thesis contains six chapters. Table 1.1 summarizes the key points provided in each chapter.

Table 1.1: Thesis structure

| Chapters | Content |
|---|---|
| Chapter 1: Introduction | • Provides problem statement, research objectives and scope, and thesis structure. |
| Chapter 2: Literature review | • Literature review to provide an overview of climate change effects on raw water quality and public health, the concept of robustness in DWTPs, the robustness framework, and methods developed to evaluate robustness.<br>• Identifies research gaps. |
| Chapter 3: Evaluation of robustness in Plant A | • Describes the method developed to separate turbidity events from background turbidity. |

| | |
|---|---|
| | • Evaluates the robustness of Plant A for normal and historical high turbidity events by analyzing data provided by the utility. |
| Chapter 4: Evaluation of robustness in Plant B | • Describes the method developed to separate turbidity events from background turbidity.<br>• Evaluates the robustness of Plant B for normal and historical high turbidity events by analyzing data provided by the utility. |
| Chapter 5: Bench-scale simulation of the ACTIFLO® process in Plant A | • Discusses the results of bench-scale simulations of the ACTIFLO® process during normal weather and historical weather events characterized by turbidity.<br>• Discusses the results of bench-scale simulations to optimize the ACTIFLO® process for future unprecedented extreme weather events. |
| Chapter 6: Comparisons, conclusions and recommendations | • Assesses the applicability of the robustness framework to Plants A and B.<br>• Compares the results of Plants A and B obtained from Chapters 3 and 4.<br>• Summarizes key findings of the research based on the results of Chapters 3, 4, and 5.<br>• Offers recommendations for future research. |

# Chapter 2: Literature Review

## 2.1 Introduction

Safe drinking water is one of the most important factors for protecting public health and sanitation. Rapid and unpredictable changes in weather patterns have an adverse effect on raw water sources and water quality parameters, thus potentially making the water treatment utilities vulnerable. The presence of robustness in the design and operation of DWTPs can substantially overcome the challenges brought by the imminent threat of climate change on water quality and aid in continuing to provide high-quality drinking water in any situation. This chapter discusses the current and projected impact of climate change on raw water quality as well as a robustness framework and its applicability to DWTPs to assess and improve the robustness of the said treatment plants.

## 2.2 Climate Change and Drinking Water Supply

Extreme weather events caused by climate change include cyclones, hurricanes, typhoons, floods, droughts, wildfires, heat waves, cold waves and many more. These events are driven by several factors caused by both natural (e.g., geographic location, topography, air temperature, wind speed, cloud cover, solar radiation, etc.) and anthropogenic (e.g., air, soil and water pollution, greenhouse gas emission, radioactive contamination, etc.) sources (Helmuth, 2002). This section focuses on heavy and/or unusual precipitation due to climate change as extreme weather events and its impact on raw water quality.

### 2.2.1 Observed Effects of Climate Change of Drinking Water Supply

Surface water resources (e.g., lakes, reservoirs, rivers, and streams) provide drinking water to approximately 70% of the population of the United States of America (USA) (Levine et al., 2016). It is certain that the surface water bodies respond directly to the fluctuating weather conditions (Staben et al., 2015). Climate change influences the intensity, frequency, and duration of extreme hydrological events such as excessive precipitation, floods, and droughts (Delpla et al., 2009; Füssel, 2009; Kim et al., 2017; Min et al., 2011; Semenza & Menne, 2009; Staben et al., 2015). Precipitation and air temperature are dependent on each other since precipitation is mainly driven by the generation and transport of water vapor among other factors. 1ºC change in temperature can lead to a 7% increase in

water vapor generation (Alduchov & Eskridge, 1996). Extreme precipitation is controlled by water vapor, which is increasing due to global warming caused by escalated amounts of greenhouse gases (GHGs) in the atmosphere caused by human activities. Well-mixed GHGs are considered as the main drivers of tropospheric warming since 1979. The global surface temperature increased from 0.95 to 1.20ºC from 1900 to 2020, with a larger increase over land (1.59ºC) than over the oceans (0.88ºC). From trend analysis of observational data, it is reported that the frequency and intensity of heavy precipitation events have increased since the 1950s due to human-induced climate change (IPCC, 2021). Several studies have reported a statistically significant increase in the frequency of heavy precipitation across Europe and North America in certain areas, while the total amount of precipitation has decreased (Bates et al., 2008; Groisman et al., 2005). From historical data, it is evident that the increase in severe storm events since 1970 is extensively greater than the projections by the simulated models for that period. The increasing proportion of heavy rainfall to total rainfall was observed over most of the land areas over the late 20th century (Bates et al., 2008).

### 2.2.2 Projected Effects of Climate Change on Drinking Water Supply

Multi-model climate projections reveal that the intensity of precipitation will increase in most regions in the world, particularly in mid- and high-latitude areas where the mean precipitation will also increase. Figure 2.1 shows the annual mean changes in precipitation (%) from fifteen atmosphere-ocean general circulation models (AOGCMs) for the Special Report of Emissions Scenarios (SRES) for the period of 2080-2099 relative to 1980-1999. Increases in precipitation in Canada are projected to be in the range of +20% for the annual mean and +30% for winter (IPCC, 2007).

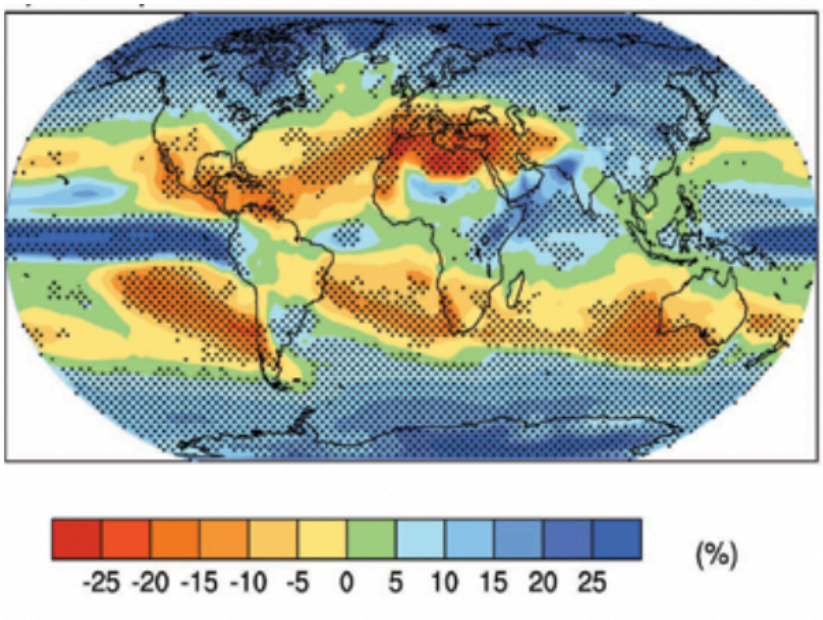


Figure 2.1: Mean changes in precipitation (Bates et al., 2008)

From the year 1936 to 2000, in Western USA, England and Canada, peak streamflow has been observed 1-2 weeks earlier due to early warming-driven snowmelt. Higher temperatures during late winter and changes in the timing and amount of precipitation will be very likely to lead to earlier melting and significant reductions in the snowpack in the western mountains in North America by the middle of the 21st century. In projections for mountain snowmelt-dominated watersheds, it is observed that advances in snowmelt runoff led to increasing winter and early spring flows and decreasing summer flows (Bates et al., 2008). Snow melting combined with storm rainfall has the greatest negative effect on water quality (Pešić et al., 2020).

An increase in temperature up to 2°C is predicted by 2070 in European lakes depending on lake characteristics and season (Singh et al., 2014). Deep lakes are most sensitive to global warming because of their greater heat storage capacity (George et al., 2007).

### 2.2.3 Impacts of Extreme Weather on Water Quality Parameters

Increased intensity of precipitation exacerbates various forms of water pollution including sediments, nutrients, organic matter, pathogens, pesticides, salts, and toxic chemicals (Bates et al., 2008; Curriero et al., 2001; Hurst et al., 2004). Intense rainstorm events lead to an increase in suspended solids (SS), resulting in elevated turbidity levels in freshwater (Atherholt et al., 1998; Bates et al., 2008; Crittenden, 2012; Khan et al., 2015; Lawler et al., 2006) due to fluvial erosion of soil (Bates et al., 2008; Khan et al., 2015). Climate and seasonality are the primary drivers to predict the relationship between precipitation and turbidity. Spatial features including land cover, discharge area, elevation, type of soil and impervious surfaces influence turbidity dynamics in watersheds by affecting sediment source, transport, and delivery (Chen & Chang, 2019). Furthermore, heavy precipitation also raises natural organic matter (NOM) concentration in surface water bodies (Gregory, 1994; Jung et al., 2014; Sharp et al., 2006). Dissolved organic carbon (DOC) concentration can rapidly increase 4-5 times during precipitation or snowmelt events flushing terrestrial NOM into water bodies (Saraceno et al., 2009). The changes in turbidity can directly affect the change in organic matter quantity in water (Hartshorn et al., 2015; Naceradska et al., 2017; Pešić et al., 2020). Besides, NOM levels are observed to remain elevated after turbidity and flow have returned to baseline conditions (Gregory, 1994; Ruecker et al., 2017; Tseng et al., 2000). Delpla et al., (2009) summarize the impact of climate change on surface water quality in Figure 2.2, considering the effects (droughts and floods) of the two main factors (temperature and rainfall). These impacts depend on natural or man-built environments, and the consequences can be different according to the type and characteristics of the water bodies. For streams and rivers, the main water quality parameters affected are organic matter and nutrients, whereas pathogens and cyanobacteria or cyanotoxins are more related to lakes. Micropollutants (inorganic or organic) are also frequently affected in both rivers and lakes.

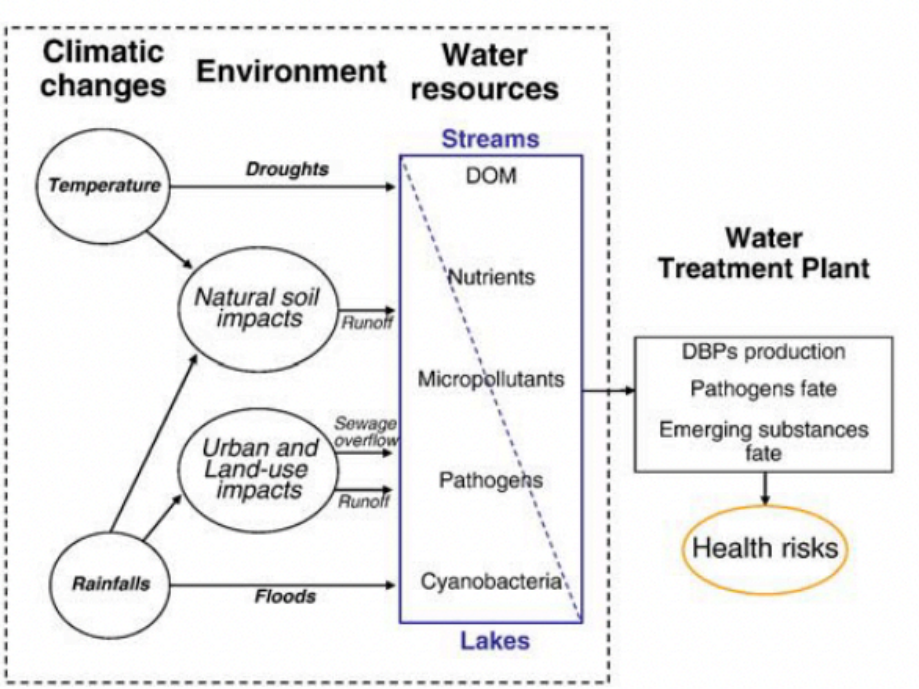


*DOM: dissolved organic matter, DBP: disinfection by-product

Figure 2.2: Impacts of climate change on water resources and drinking water quality (Delpla et al., 2009)

NOM is defined as a complex matrix of organic chemicals present in all water bodies, originating from natural sources such as biological activity, secretions from metabolic activities, and excretions from fish or other aquatic organisms (Crittenden et al., 2012; Health Canada, 2019). As carbon is the key constituent of NOM, particulate organic carbon (POC), total organic carbon (TOC), dissolved organic carbon (DOC) as well as ultra-violet (UV) absorbance are considered as indicators of organic matter in water (Health Canada, 2019). NOM is the major precursor to form disinfection by-products (DBPs) during chlorination (Crittenden et al., 2012; Marhaba & Van, 2000; Sharp et al., 2006). Chlorine for disinfection reacts with organic substances to form DBPs, some of which are highly toxic and carcinogenic compounds such as trihalomethanes (THM) and haloacetic acids (HAA) (Richardson, 2002; Selvam et al., 2018). A simulated distribution system (SDS) test conducted in Quebec, Canada reported that after rainfall events, the concentration of THMs and HAAs were doubled in water samples at the distribution system within 20 hours of contact period due to a considerable rise in the organic

carbon reactivity of filtered water and linked the increases to a rise in non-brominated DBPs (Delpla & Rodriguez, 2016).

High turbidity from an extreme rainfall event can overwhelm a water treatment infrastructure and deteriorate treatment performance (Atherton et al., 1995; Delpla et al., 2009; Fox & Lytle, 1996; Hurst et al., 2004). The Bearspaw water treatment plant (WTP) in Calgary, Alberta, experienced 3750 nephelometric turbidity unit (NTU) of turbidity following an extreme rainfall event in 2013, and Red Deer WTP in Alberta faced around 3000 NTU of turbidity spike due to flooding in 2005 (Yarahmadi, 2019). A study reports that, in 2001, the turbidity in the Tame River in England increased substantially by an order of magnitude to >300-500 formazin turbidity unit (FTU) followed by spring storm events (Lawler et al., 2006). Turbidity peaks ranging from 53-1021 NTU have been observed after rainfall events (>10 mm) in a watershed in Fiji in 2009 and 2010 (Ram & Terry, 2016). The water utility serving New York City, USA has recognized heavy precipitation events as one of its major climate change related concerns. Intense precipitation events have the ability to elevate turbidity levels in some of the main reservoirs of the city up to 100 times the legal limit for source quality at the intake of the utilities, which can result in additional treatment and monitoring costs (IPCC, 2007). In 2011, a DWTP in Alabama, USA, using the Tennessee River as the raw water source, experienced a surge of finished water turbidity of 15 NTU after a severe winter storm, whereas the standard was 0.3 NTU. As a result, the DWTP was forced to shut down for 3 days, alarming the residents and resulting in huge economic loss. The coagulation-flocculation process was affected by the type and concentration of SS, DOM and temperature (Qiu et al., 2019). The treatment process failed to meet the standard due to the storm event, indicating that the system lacked robustness. In 2015, as an aftermath of a hurricane in South Carolina, USA, more than 500 mm of rainfall had taken place in 5 days, which is 5 times more rain than the average precipitation of the entire month, which led to a turbidity spike in water bodies up to 56 NTU during the first few days of flooding, whereas the baseline turbidity was lower than 10 NTU. Moreover, up to 66% of the total annual DOC export occurred during the 5-day long event and the elevated DOC levels in water bodies were observed for 8 weeks (Ruecker et al., 2017). Therefore, controlling the effluent water quality should be the first priority in extreme weather conditions (Qiu et al., 2019). Most water treatment facilities are designed based on historical meteorological data that includes past records of storms and heavy precipitation events. However, DWTPs are now encountering more frequent and intense extreme weather conditions that were not experienced in the past. The affected DWTPs are not

often prepared to take proper and immediate response actions to mitigate the impacts (Qiu et al., 2019; Staben et al., 2015).

### 2.2.4 Impacts of Extreme Weather on Public Health

Water-borne diseases are likely to be increased with frequent heavy rainfall as more pathogens can be transported by higher runoff following a severe rainfall event (Delpla et al., 2009). Half of the waterborne disease outbreaks in the USA during the last half-century were observed to be preceded by rainfall events above the 90th percentile of the monthly accumulated rainfall (Curriero et al., 2001). It is reported that in Alberta, Canada, the ambient temperature, which somewhat controls precipitation events, is strongly, but non-linearly associated with the occurrence of enteric pathogens in water (Bates et al., 2008). Rainfall events above the 93rd percentile of the 5-day average accumulated rainfall resulted in 2.3 times increased risk of an outbreak (Thomas et al., 2006). Elevated raw water turbidity resulting from extreme precipitation has been found to be associated with GI illness (Tinker et al., 2010). Increase in NOM may also enhance bacterial regrowth in water distribution networks (Abokifa et al., 2016). A study in New Jersey, USA, reports to find a positive association between GI hospitalizations and rainfall that impacts drinking water sources in warm seasons (Gleason & Fagliano, 2017). Communities served by public water system are at high risk for GI illness when extreme precipitation damages water treatment infrastructures, subsequently compromising the finished water quality (Exum et al., 2018). Drinking water turbidity has been discovered to be positively associated with acute GI illnesses (De Roos et al., 2017). Moreover, an increase in adenovirus and rotavirus concentrations in raw water by approximately 0.5-log was reported in a study in two full-scale DWTPs in Quebec, Canada, during two snowmelt and rainfall episodes (Sylvestre et al., 2021). A study in Pennsylvania, USA, reported that an increase in finished water turbidity of 0.04 NTU (in compliance with federal standards) correlated to a 9% and 31% increase in hospital admissions for elderly and pediatric patients (Schwartz et al., 1997; Schwartz et al., 2000). It should be noted that turbidity does not provide an indication of water safety from pathogens, but it is useful as an indicator for further investigation (Health Canada, 2012).

## 2.3 Robustness in Drinking Water Treatment

The concept of robustness has been explored in many fields from evolutionary biology to computer operating systems. It is the competence of a system to heal, self-repair, self-regulate, self-assemble, and/or self-replicate and maintain the desired characteristics despite fluctuations in the behavior of its components or the surrounding environment (Li, 2004). Robustness is defined as the ability of a system to provide excellent performance under normal conditions and deviate minimally during periods of upsets or challenges (Huck & Coffey, 2002). A DWTP is considered robust if its performance is insensitive to the variation of source water quality and changing operational conditions, thus continuing to achieve the desired drinking water quality (Zhang et al., 2012). DWTPs are expected to provide safe drinking water to their customers at all times (Hartshorn et al., 2015; Huck & Coffey, 2004; Li & Huck, 2008; Upton et al., 2017; Zhang et al., 2012). To fulfill this goal, several drinking water quality parameters that have a direct or indirect link to public health, are regulated by the federal or provincial government. Five elements were identified to provide safe drinking water under the appropriate regulatory framework (Huck et al., 2001a):

1. Start with the best possible source.
2. Design and operate appropriate treatment.
3. Provide secure distribution.
4. Conduct appropriate monitoring.
5. Respond appropriately to any adverse monitoring results.

The concept of robustness typically emphasizes treatment and monitoring, since in most cases it is almost impossible to change the raw water source (Huck & Coffey, 2004). The concept of robustness is shown graphically in Figure 2.3 in terms of filter performance with varying influent water quality or coagulant dose. When a system is robust, the output of the system does not have a wide variation with changing operating conditions. Although the peak performance of an optimal system is greater than that of a robust system, a robust system may be preferred considering the greater range of operating conditions (Huck et al., 2001b).

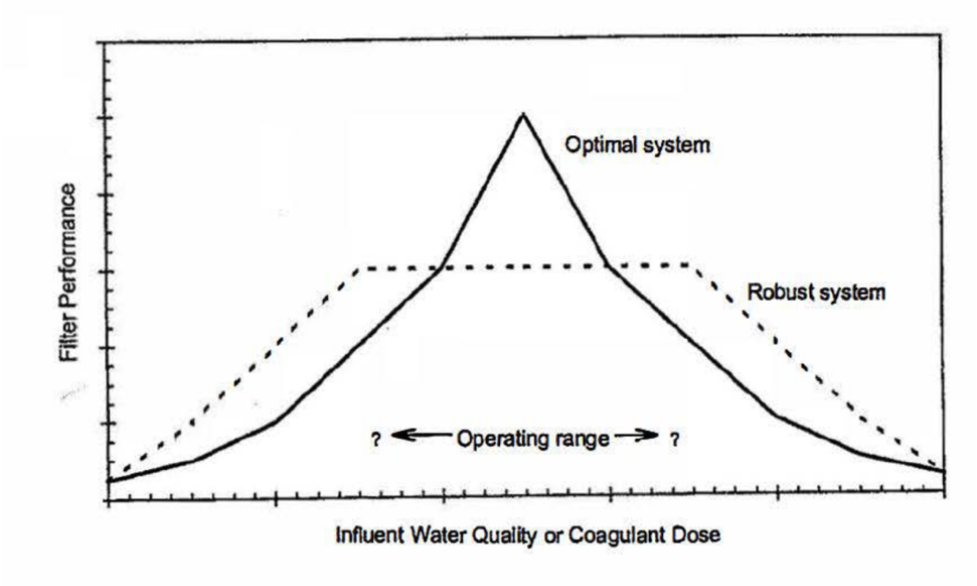


Figure 2.3: Representation of a hypothetical filtration robustness concept (Huck et al., 2001b)

The concept of robustness is closely related to resilience. Resilience of a system is defined as the duration of an unsatisfactory condition following a failure event until the original performance is recovered (Hashimoto et al., 1982). The resilience of a DWTP is a measure of how quickly the system recovers from an upset. It is case-specific and depends on the location, size, availability of trained technicians and the number of operators (Zhang et al., 2012). In Figure 2.4, Levine et al. (2016) show the capacity reserve of DWTPs as a function of recovery time for different types of climate-related disruptions. This concept can be useful to distinguish between robustness and resilience (Nemani, 2021a). Capacity reserve is defined as the difference between design capacity and minimum treatment capacity to maintain the water quality and quantity requirements. After a climate event, in Scenario I, it can be observed that there is a lapse in the capacity to provide safe drinking water. In Scenario II, the capacity fails to provide the desired service for a while before recovering. Scenarios III and IV reflect a breaking point for the system due to insufficient capacity to implement appropriate operational changes or upgrades (Levine et al., 2016). A robust system can be explained with Scenario I as the system recovered quickly from a climate event and met the desired service criteria for the entire duration of the event.

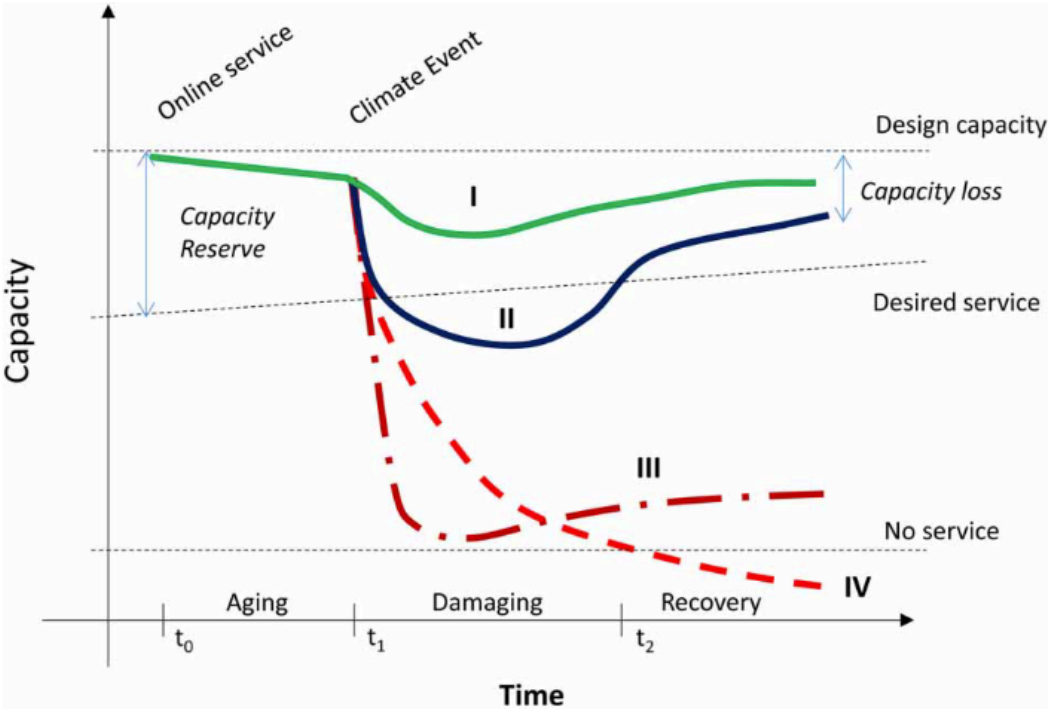


Figure 2.4: Robustness and resilience in the context of DWTPs (Levine et al., 2016)

The importance of robustness in DWTPs can be comprehended from the microbial contamination incident in Walkerton, Canada, in the year 2000, causing GI symptoms in 1300 individuals and 7 deaths (Huck et al., 2001a). Upon investigation and assessment, Huck and Coffey (2004) concluded that the Walkerton water system could not be considered robust, and hence the system was unable to prevent this tragic incident.

## 2.4 Robustness Framework for Drinking Water Treatment Plants

A DWTP should be robust in order to supply drinking water with set finished water quality parameters. As mentioned before, most DWTPs are designed based on historical data including past weather events (Qiu et al., 2019; Staben et al., 2015). With the growing effects of climate change on raw water quality, it is essential for DWTPs to be robust. However, there are numerous variables involved in the process of water treatment, and the variation of raw water quality and performance of one treatment step can

affect the performance of the following steps, which makes evaluation and assessment of the overall performance of DWTPs a very complex problem (Oliveira et al., 2014).

Zakarian et al. (2007) discussed the necessity for a systematic, well-defined methodology to design robust systems, and developed a methodology combining three major techniques: system modeling, integration analysis and quality engineering techniques. The overall methodology is illustrated in Figure 2.5.

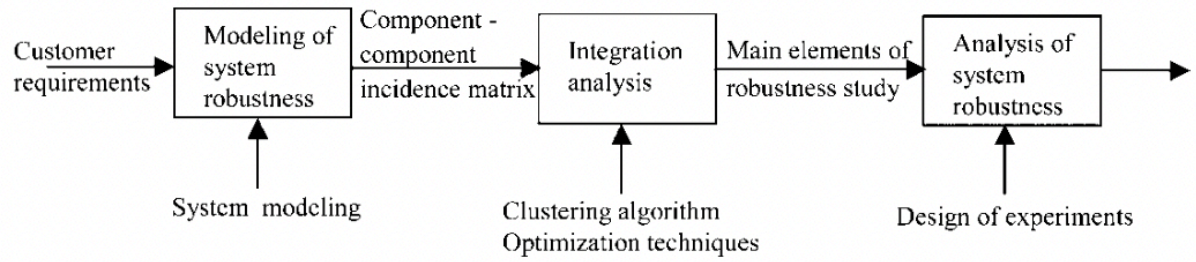


Figure 2.5: Robust system design methodology (Zakarian et al., 2007)

In this study, system robustness was achieved by specifying subsystem configurations within the overall system to minimize subsystem-to-subsystem interactions and overall system sensitivity to noise factors. Although this approach was developed for mechanical and electrical systems, the principle can be applied to the concept of robustness in DWTPs by identifying the treatment steps affected by raw water quality changes, evaluating the robustness of the identified steps, assessing the overall robustness of the utilities, and exploring operational changes to mitigate the impacts by design of experiments.

Nemani (2021a) proposed a robustness framework for DWTPs to evaluate, synthesize and improve the robustness of DWTPs. This framework can be modified to any utility and raw water quality parameters and can facilitate the development of improved standard operating procedures (SOPs) according to the author. Figure 2.6 shows the main steps of the framework.

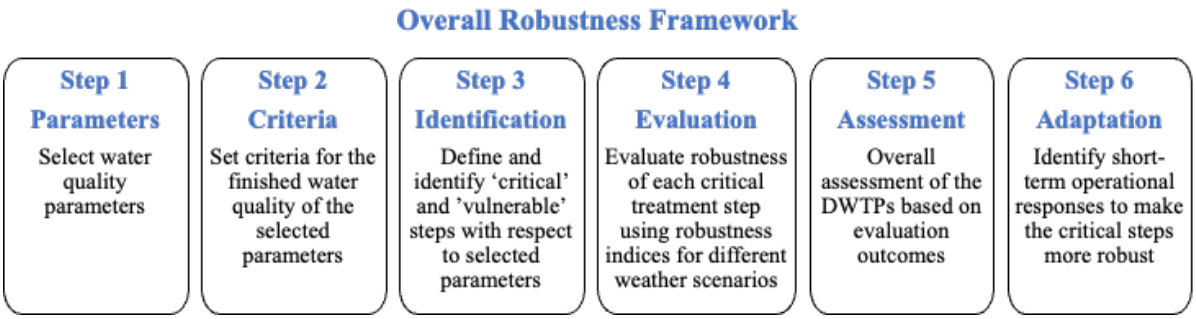


Figure 2.6: Overall robustness framework (adapted from Nemani, 2021a)

The aspects of each step and their applicability in this study are discussed in the sub-sections 2.4.1 to 2.4.6.

### 2.4.1 Step 1: Parameters

Several raw water quality parameters are affected by increasing heavy precipitation caused by climate change. The robustness framework can be applied for different parameters and the robustness of the plant can be assessed in terms of the selected parameter(s). Huck and Coffey (2004) listed turbidity, NOM, pH, temperature, microorganism concentrations (e.g., *Giardia* and *Cryptosporidium*), susceptibility to organic and inorganic contamination as key raw water quality parameters regarding robustness. These parameters are likely to change during precipitation events and have a direct or indirect association with public health as discussed in sub-section 2.2.4. The degree of robustness is a function of both average raw water quality, and the extent and rapidity of variation in raw water quality parameters (Huck & Coffey, 2004). Several studies have reported elevated turbidity and natural organic matter (in terms of TOC, DOC and specific ultraviolet absorbance, SUVA) in raw water sources following an extreme precipitation event (Hurst et al., 2019; Lawler et al., 2006; Qiu et al., 2019; Ruecker et al., 2017). As discussed before, turbidity can be associated with the presence of organic matter (Delpla et al., 2009; Delpla et al., 2015; Pešić et al., 2020) and microorganisms like *Cryptosporidium* (Atherholt et al., 1998; Emelko & Brown, 2002). Turbidity is the most widely used parameter for monitoring plant performance because turbidity measurements are simple, rapid, economical and can be measured continuously (Gregory, 1994; Health Canada, 2012; Huck et al., 2001b; Upton et al., 2017). It is considered as an important water quality variable because of its relation

to biological oxygen demand (BOD) impact, sediment-associated contaminant transport, and suspended sediment effects of organisms and habitats (Lawler et al., 2006). Increase in turbidity in finished drinking water can be associated with GI illness (De Roos et al., 2017; Gleason & Fagliano, 2017; Tinker et al., 2010) and can be a good indicator of pathogens that may need further investigation. Because of its connection to public health, turbidity is a regulated parameter. Moreover, turbidity measurements are useful for comparing different water sources or treatment facilities and are used for process control and regulatory compliance (Crittenden et al., 2012). Considering all these facts, turbidity is selected as the water quality parameter to assess the robustness of the DWTPs in this study.

#### 2.4.1.1 Turbidity

Turbidity is defined as an expression of the optical property that causes light to be scattered and absorbed rather than transmitted with no change in direction or flux level through the sample (Standard Methods, 2005). Turbidity in water is caused by the presence of suspended particles that reduce the clarity of the water. The size of particles in water can vary from 0.001µm to 100µm. Particles that are larger than 1µm, are considered as suspended. Regulations concerning particle measurements are generally based on turbidity measurements (Crittenden et al., 2012), although turbidity is not a direct measure of suspended particles. It is a general measure based on the light scattering and absorbing capacity of suspended particles. Turbidity is expressed in nephelometric turbidity units (NTU) and measured with a device called turbidimeter.

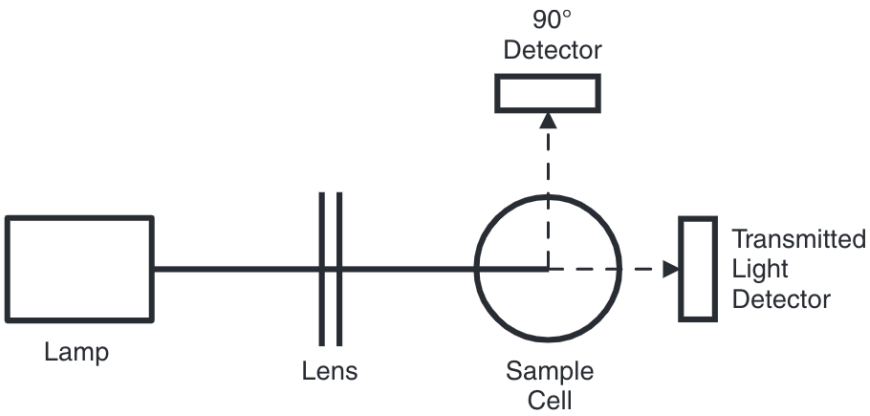


Figure 2.7: General turbidimeter optical system (Hach, 2013)

The principle of measuring turbidity is that when a beam of light passes through the water, the particles, if present, can cause the light to be scattered or absorbed. Figure 2.7 shows a general turbidimeter optical system. The instrument generally includes a lamp, lenses, aperture to focus the light, a 90-degree detector to monitor scattered light and optionally, a forward-scatter light detector, a transmitted-light detector and a back-scatter light detector. The optional detectors may be added to minimize the impact of color, stray light and lamp and optical variabilities (Hach, 2013).

Although particle interference with light depends on the shape, size, number, composition, color, refractive index, etc., it has been generalized that the intensity of light scattering increases with increasing turbidity (Health Canada, 2012).

There can be various sources of suspended particles in water, which are listed in Table 2.1.

Table 2.1: Source of suspended particulates in water (Crittenden et al., 2012)

| **Source** | **Particulate constituents** |
|---|---|
| Contact of water with minerals, rocks, and soil (e.g., weathering) | Clay, silt, sand, and other inorganic soils |
| Decomposition of organic matter in the environment | Cell fragments |
| Living organisms | Algae, diatoms, minute animals, fish |
| Municipal, industrial, and agricultural sources and other human activity | Clay, silt, grit and other inorganic solids, organic compounds, oil, corrosion products |

Turbidity is commonly stable over time and ranges from about 1.0 to 20 NTU in lakes and reservoirs, excluding storm events. Turbidity in rivers is more variable due to storm events, runoff and changes in flow rate in the river and can range from under 10 to over 4000 NTU. Turbidity can change by several hundred NTU in a matter of hours in streams and rivers (Crittenden et al., 2012).

The nature of turbidity has different effects on raw water quality and treatment techniques. Table 2.2 summarizes some of the water quality and treatment implications for different types of turbidity.

Table 2.2: Implication for water quality and treatment based on turbidity type (Health Canada, 2012)

| Type of turbidity | Water quality implications | Treatment implications |
|---|---|---|
| Inorganic particles (clay, silt, mineral fragments, natural precipitants, e.g., calcium carbonate, manganese dioxide, iron oxide) | - Raise/lower pH and alkalinity<br>- Source of micronutrients<br>- Affect zeta potential<br>- Source of metals and metal oxides<br>- Cloudy or turbid appearance<br>- Affect taste | - Major influence on coagulation, flocculation, and sedimentation design<br>- Harbor or protect microorganisms<br>- May require chemical adjustments<br>- Can precipitate in the distribution system |
| Natural organic matter (decomposed plant and animal debris) | - Source of energy and nutrients for microorganisms<br>- Cause color | - Increased disinfectant demand<br>- Harbour/protect microorganisms<br>- Potential to form DBPs |
| Organic macromolecules | - Impart taste and odor<br>- Possess ion exchange and complexing properties, association with toxic elements and micropollutants<br>- Affect pH and zeta potential | - Potential to form DBPs<br>- Major influence on coagulation, flocculation, and sedimentation design<br>- Reduce filter runs<br>- Can precipitate in the distribution system |
| Microorganisms (algae, cyanobacteria, zooplankton, bacteria, protozoa) | - Impart taste and odor<br>- Potential source of toxins (e.g., microcystin-LR)<br>- Can cause microbiologically influenced corrosion in system | - Plug filters<br>- Increased disinfectant demand<br>- Need multiple barriers to ensure effective microbial inactivation<br>- Biological growth (biofilm) |

| | | |
|---|---|---|
| | - Stain fixtures<br>- Aesthetic problems: sloughing of growths (tanks, filters, reservoirs, distribution system | - Shielding from disinfection |

### 2.4.2 Step 2: Criteria

The criteria of the selected water quality parameter can be set based on the regulatory limit and/or plant-specific goals. The main purpose of setting a criterion is to have a treatment goal for the selected parameter (Nemani, 2021a).

Turbidity is a regulated parameter. Health Canada (2012) has listed specific guidelines for filtered water turbidity, which are summarized in Table 2.3. The Ontario regulations are based on these guidelines.

Table 2.3: Regulatory limits of turbidity for different filtration techniques (Health Canada, 2012)

| Filtration type | Regulatory limit |
|---|---|
| Conventional and direct filtration | Turbidity level should be always less than or equal to 0.3 NTU for 95% of the measurements per cycle per month, with a target turbidity less than 0.1 NTU. Turbidity can never exceed 1.0 NTU. |
| Slow sand and diatomaceous earth filtration | Turbidity level should be always less than or equal to 1.0 NTU for 95% of the measurements per cycle per month. Turbidity can never exceed 3.0 NTU. |
| Membrane filtration (Reverse osmosis, Nanofiltration, Ultrafiltration, Microfiltration) | Turbidity level should be always less than or equal to 0.1 NTU for 99% of the measurements per cycle per month, with a target turbidity less than 0.1 NTU. Turbidity value greater than 0.1 NTU for more than 15 minutes should be investigated immediately. |

The regulatory limit for turbidity is set for filtered water. However, DWTPs have pre-treatment before filtration and may have set turbidity goals for these treatment steps so that the filters are not overwhelmed. Some DWTPs may have stricter goals for filtered water to ensure desired finished water quality while maintaining the regulatory limits.

Health Canada (2019) set some suggested targets to provide guidance for other quality parameters related to NOM that are not regulated, but are important because of their association with DBP formation, which are listed in Table 2.4.

Table 2.4: Suggested treated water quality targets regarding NOM (Health Canada, 2019)

| | **Suggested limits** | |
|---|---|---|
| **Parameter** | **Source with higher specific DBP yield or system with extensive distribution system** | **Source with lower specific DBP yield** |
| Color | 5 - 10 TCU | < 15 TCU |
| $UV_{254}$ | 0.02 - 0.04 $cm^{-1}$ | 0.02 - 0.07 $cm^{-1}$ |
| UV transmittance | 90-95% | 85-95% |
| DOC (for DBP control) | < 2 mg/L C | < 4 mg/L C |
| DOC (for biological stability) | < 1.8 mg/L C | < 1.8 mg/L C |

TCU: true color unit, C: carbon

### 2.4.3 Step 3: Identification

There are many treatment steps in a DWTP with different goals to control one or more water quality parameters. This step is required to identify the treatment steps that are 'critical' and 'vulnerable' with respect to the removal of the selected water quality parameter, which is selected to be turbidity in this study. Nemani (2021a) defines 'critical' steps as the water treatment steps that are important for the

physical, chemical or biological removal of the selected parameter whereas the 'vulnerable' steps are defined as the treatment steps that are impacted by the increase or change in the nature of the selected parameter. The critical treatment steps with respect to turbidity need to be identified since the evaluation of robustness of a given plant is dependent on the performance of these treatment steps. The identified critical and vulnerable treatment steps with respect to turbidity by Nemani (2021a) are listed in Table 2.5.

Table 2.5: Identification of critical and vulnerable steps for turbidity (adapted from Nemani, 2021a)

| Process | Criticality | Vulnerability |
|---|---|---|
| Intake | Varies[1] | Yes |
| Coagulation | Yes | Yes |
| Flocculation | Yes | Yes |
| Sedimentation | Yes | Yes |
| Dissolved air floatation | Yes | Yes |
| Filtration | Yes | Yes |
| Adsorption | No | Varies[2] |
| Ozonation | No | Yes |
| Disinfection | No | Yes |
| Distribution system | No | Yes |

1. Depends on the design of the intake system, which may include raw water storage
2. Depends on the type and point of usage

### 2.4.4 Step 4: Evaluation

The overall system robustness can be achieved with various means. However, due to numerous water quality parameters and the related variables in the water treatment systems, the process of evaluating and improving robustness can be quite challenging. Quantification of robustness benefits its improvement in a rational way (Huck & Coffey, 2004). The robustness of the identified steps with respect to turbidity can be evaluated for three scenarios characterized by raw water turbidity:

a. Normal turbidity,

b. Historical high turbidity events,

c. Unusually high turbidity that is beyond general experience but may occur in the future due to climate change.

Scenarios (a) and (b) can be evaluated using on-line turbidity data from the plant. Scenario (c) can be assessed with bench-scale simulations.

To evaluate scenarios (a) and (b), a tool is required that can quantify the robustness of the identified treatment steps. The concept of a robustness index has been used by several researchers with this aim.

The first filtration robustness index was developed by Coffey et al. (1998) considering the index as a function of ripening, turbidity, water production and breakthrough. The index was expressed by the following equation:

$$Robustness\ Index\ = \frac{T_{goal}}{T_{ave}} \times \frac{R_{goal}}{R_{max}} \times \frac{LOR_{max}}{LOR_{goal}} \qquad (2.1)$$

where,

$T_{goal}$ = average turbidity goal (NTU),
$T_{ave}$ = average turbidity (NTU),
$R_{goal}$ = maximum ripening turbidity goal (NTU),
$R_{max}$ = maximum ripening turbidity (NTU),
$LOR_{goal}$ = length of run goal ([time]),
$LOR_{max}$ = length of run ([time]).

Equation (2.1) includes various aspects of filter performance. This index aimed to evaluate filter robustness. With the aim to evaluate robustness in terms of turbidity, this index was improved by interpreting data from pilot- and full-scale filtration systems. Huck et al. (2001b) focused on *Cryptosporidium* removal by granular media filtration and examined various conditions (ripening and breakthrough periods, suboptimal coagulation, sudden increase in flow, sudden change in influent water quality) where filtration was not optimal. To develop a filtration robustness index with respect to particle removal, the following robustness index was introduced by Huck et al. (2001b), and Huck and Coffey (2002):

$$TRI_{90} = \frac{1}{2}\left[\frac{T_{90}}{T_{50}} + \frac{T_{50}}{T_{goal}}\right] \quad (2.2)$$

$$TRI_{95} = \frac{1}{2}\left[\frac{T_{95}}{T_{50}} + \frac{T_{50}}{T_{goal}}\right] \quad (2.3)$$

$$TRI_{99} = \frac{1}{2}\left[\frac{T_{99}}{T_{50}} + \frac{T_{50}}{T_{goal}}\right] \quad (2.4)$$

where,

$TRI_{90}$, $TRI_{95}$, $TRI_{99}$ = turbidity robustness index (TRI) using the 90th, 95th and 99th percentile turbidity (dimensionless),

$T_{50}$, $T_{90}$, $T_{95}$, $T_{99}$ = 50th, 90th, 95th and 99th percentile turbidity (NTU),

$T_{goal}$ = filter turbidity goal (NTU).

The turbidity goal can be utility- or plant-specific. The first term in Equations (2.2) to (2.4) represents the uniformity of performance over a specific duration (e.g., a single filter run or a period of 24 hours). The second term represents how well the filter is performing. A lower value of the robustness index indicates that the filter effluent water is meeting the goal with relatively low variation for the specific duration. In contrast, a higher TRI indicates that either the treatment has failed to meet the goal value, or the performance variability is high for the specific duration of time. The lowest possible value of TRI is 0.5 when the second term is tending toward zero since the median value is much lower than the goal. Furthermore, the TRI value is dependent on the goal value, and it can be comprehended from the equations that the TRI value would increase with a stricter goal.

Huck et al. (2001b) reported that the $TRI_{90}$ and $TRI_{95}$ were more suitable to compare major differences in filter performance whereas the $TRI_{99}$ got heavily influenced by noise in the turbidity data. However, equal weighting of the two terms in Equations (2.2) to (2.4) cannot reflect some specific operational conditions of the system and this was stated as one of the major limitations of this index.

To overcome this limitation, Li and Huck (2008) developed a modified robustness index using unequal weighting with weighting factors that can be adjusted accordingly:

$$TRI_{90D} = \left[A_1 \frac{T_{90}}{T_{50}} + A_2 \frac{T_{50}}{T_{goal}}\right] \times 100 \qquad (2.5)$$

where,

$TRI_{90D}$ = turbidity robustness index (TRI) using the 90th percentile turbidity (dimensionless),

$T_{50}$, $T_{90}$ = 50th and 90th percentile turbidity (NTU),

$T_{goal}$ = filter turbidity goal (NTU),

$A_1$, $A_2$ = weighting factors (dimensionless).

If the weighting factor $A_1$ is set to be higher than $A_2$, it indicates that the index emphasizes the variation in performance, whereas when $A_2$ is higher than $A_1$, it means that the index is focusing on the average performance. The sum of $A_1$ and $A_2$ is equal to 1.

The TRI was multiplied by 100 for convenience. Based on the examination of data, it was observed that the preliminary indication of robustness for a given run can be determined by the upper half of the cumulative turbidity distribution curve (i.e., by the turbidity values above the 50th percentile). Since it is good to have five or more points to determine the trend of a line, Li (2004) chose the $\frac{T_{50}}{T_{goal}}$, $\frac{T_{60}}{T_{goal}}$, $\frac{T_{70}}{T_{goal}}$, $\frac{T_{80}}{T_{goal}}$ and $\frac{T_{90}}{T_{goal}}$ values (where $T_{50}$, $T_{60}$, $T_{70}$, $T_{80}$, $T_{90}$ = 50th, 60th, 70th, 80th and 90th percentile turbidity, NTU) as the points to determine the water quality changes for a given filter run. For each cycle, a quantity $W$ was calculated with Equation (2.6).

$$W = \left(\frac{T_{50}}{T_{goal}} + \frac{T_{60}}{T_{goal}} + \frac{T_{70}}{T_{goal}} + \frac{T_{80}}{T_{goal}} + \frac{T_{90}}{T_{goal}}\right) \times 10 \qquad (2.6)$$

Since the sum was not a large number, it was multiplied by a value of 10 to amplify the value of $W$. A critical value $N$ is used to provide an initial determination of the robustness of a specific filter run. The value of $N$ was set to be 50 because a value of 50 would be obtained if the 50th and 90th percentile turbidity values remain at the goal value of filtration. The procedure of selecting different weighing factors by comparing $W$ and $N$ is summarized in Table 2.6.

Table 2.6: Decision process for selecting difference weighting factors (Li & Huck, 2008)

| Systems | Comparison with W and N | If | Then |
|---|---|---|---|
| Robust | $W \leq N$ | $\frac{T_{90}}{T_{50}} \leq \frac{T_{50}}{T_{goal}}$ | $A_1 > A_2$ |
| | | $\frac{T_{90}}{T_{50}} > \frac{T_{50}}{T_{goal}}$ | $A_1 < A_2$ |
| Less robust | $W > N$ | $\frac{T_{90}}{T_{50}} \leq \frac{T_{50}}{T_{goal}}$ | $A_1 < A_2$ |
| | | $\frac{T_{90}}{T_{50}} > \frac{T_{50}}{T_{goal}}$ | $A_1 > A_2$ |

Li (2004) used different ratios (0.6/0.4, 0.75/0.25, 0.8/0.2, 0.9/0.1) for selecting the high and low values of the weighting factors ($A_1$ and $A_2$) and concluded that the ratio of 0.9/0.1 has more impact in determining TRI of a filtration unit for a specific filter run. However, it was recommended in the study to find a more reasonable ratio based on the statistical analysis with a large amount of data from different systems. In the present study, due to the selected timeframe to evaluate the robustness of the identified steps and the large volume of data sets, the 90th percentile turbidity may be influenced by the noise in the data set. To resolve this issue, the ratio 0.6/0.4 was selected for the weighting factors $A_1$ and $A_2$, which puts a greater emphasis on the 2nd term ($T_{50}/T_{goal}$) of Equation (2.5), if the system is initially identified as robust or vice versa according to Table 2.6.

Li (2004) proposed a classification system based on the values of TRI, which is described in Table 2.7. The TRI classes imply how the treatment step was performing during the filter run or selected timeframe based on the variation of $T_{50}$ and $T_{90}$ with respect to $T_{goal}$. This classification system was originally developed for filter runs by analyzing the on-line filter effluent turbidity data for one of the full-scale DWTPs investigated.

Table 2.7: Classification of system operation quality with TRI (adapted from Li, 2004)

| Class | TRI range | Implication | Mathematical significance |
|---|---|---|---|
| Very stable | < 60 | The system produces high quality water for the entire run. | (1) $T_{50}$, $T_{90} \cong$ 50% of $T_{goal}$, or<br>(2) $T_{50} << T_{goal}$ and $T_{90} >$ 50% of $T_{goal}$. |
| Stable | 60 - 100 | The system produces high quality water for the entire run. | (1) $T_{50}$, $T_{90}$ = 60-75% of $T_{goal}$, or<br>(2) $T_{50}$ = 60-75% of $T_{goal}$ and $T_{90} \cong T_{goal}$. |
| Slightly disturbed | 100 - 130 | The system produces high quality water for most of the run. | (1) $T_{50}$, $T_{90} \cong T_{goal}$, or<br>(2) $T_{50} < T_{goal}$ and $T_{90}$ => 30% over $T_{goal}$. |
| Moderately disturbed | 130 - 160 | The system produces water that is not high quality for a short duration during the run. | (1) $T_{50}$, $T_{90}$ => 30-50% over $T_{goal}$, or<br>(2) $T_{50}$ => 20% over $T_{goal}$ and $T_{90}$ => 60-80% over $T_{goal}$. |
| Upset | 160 - 200 | The system produces water that is not high quality for most of the run. | (1) $T_{50}$, $T_{90}$ => 50-80% over $T_{goal}$. |
| Severely upset | > 200 | The system does produce high quality water at no time during the run. | (1) $T_{50}$, $T_{90}$ => 100% over $T_{goal}$. |

Although the TRI was first developed for filters, in several studies, the TRI method was used to evaluate the robustness of the other treatment steps for a given period. Hurst et al. (2004) used Equation (2.3) to evaluate the robustness of the coagulation and clarification process of a DWTP in England for different raw water conditions during certain rainstorm events and concluded that the TRI was an excellent method for analyzing and compacting large volumes of data.

Harshton et al. (2015) commented that the selecting process of the ratio of $A_1$ and $A_2$ was somewhat arbitrary and the non-constant variability of data, which may appear due to extreme weather events resulting in elevated turbidity levels and higher variability, was not considered. An adapted version of the robustness index replacing the weighting factors $A_1$ and $A_2$ by a concept of *G%*, which is the percentage of time when the turbidity was below $T_{goal}$. They developed Equation (2.7) to evaluate filter robustness.

$$TRI_{90J} = \left[\left(1 - \frac{G\%}{100}\right) \times \frac{T_{90}}{T_{50}} + \frac{T_{50}}{T_{goal}} \times \frac{G\%}{100}\right] \qquad (2.7)$$

According to this method, more emphasis is put on the second term of Equation (2.7), when the effluent turbidity is lower than the goal most of the time during a given run. If the effluent turbidity is always lower than the goal, the weighting factor for the first term of Equation (2.7) would be zero, and the TRI calculated with this equation would not consider the variability in performance. Thus, this approach does not focus on variability in performance when the filters seem to be working well, which can be an important aspect to calculate TRI even though the effluent turbidity is lower than the goal turbidity.

Upton et al. (2017) discussed the effect of skewness and kurtosis of the data set in calculating TRI and indicated that the 95th percentile turbidity does not distinguish between the different turbidity risks, which can be interpreted by considering the skewness and kurtosis. The operational causes of elevated filtrate turbidity were framed as a machine learning classification problem and the Classification and Regression Tree (CART) algorithm was applied to model the conditions associated with poor filtration performance. Although the CART algorithm is a good diagnostic tool to describe these conditions, it lacks the simplicity to be applied at a full-scale DWTP on a regular basis. Moreover, this algorithm was developed for rapid gravity filtration, and its applicability to different filtration techniques and/or treatment steps has not been explored yet.

Zhang et al. (2012) introduced a framework to assess the performance of traditional DWTPs by integrating the concept of reliability, robustness, and Quantitative Microbial Risk Assessment (QMRA) for three treatment steps, unit 1: coagulation-flocculation-sedimentation (CFS), unit 2: filtration and unit 3: disinfection, and used TRI (Equation 2.3) to develop performance functions (PFs) for individual CFS and filtration units as well as the combined units. The framework is illustrated in Figure 2.8.

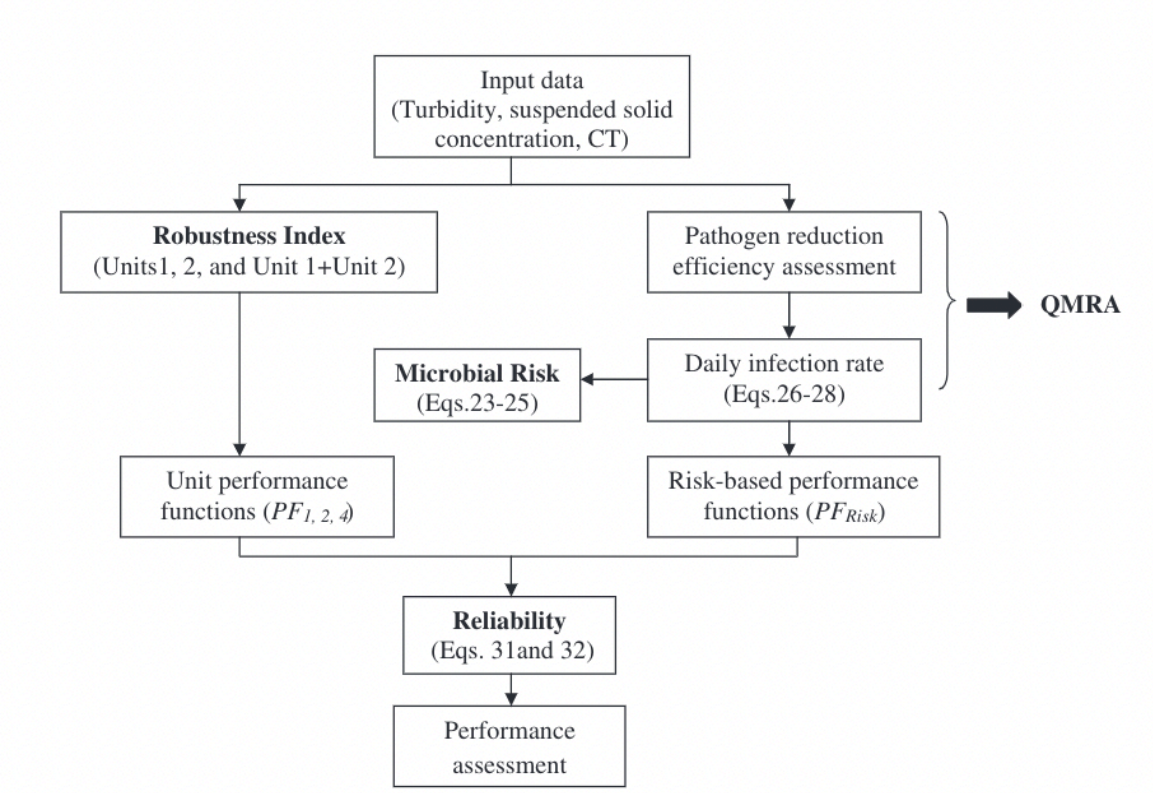


Figure 2.8: Application of reliability, risk and QMRA in DWTP performance assessment (Zhang et al., 2012)

This framework incorporates different aspects of performance assessment. However, it includes more than one water quality parameter, which makes the framework somewhat complex to apply to a full-scale DWTP.

There have been only two studies (Harshton et al., 2015; Upton et al., 2017) that compared the original TRI concept with other methods for evaluating robustness to date, so it is difficult to assess which one is more accurate than the other. However, considering the simplicity and availability of on-line turbidity data, the TRI concept developed by Li and Huck (2008) is proven to be a useful tool to evaluate the robustness of individual treatment steps (García-Ávila et al., 2021; Hurst et. al., 2004; Zhang et al., 2012; Zoric et al., 2020). This method allows evaluation of TRIs of each critical treatment step throughout the plant. These TRIs can be folded into an overall robustness assessment, which can be useful to evaluate the performance of the overall DWTP under normal weather and weather events

caused by the rising impacts of climate change. Therefore, in this study, the robustness index developed by Li and Huck (2008) for evaluating filter performance for a given filter run has been modified for different critical treatment steps based on Table 2.6.

### 2.4.5 Step 5: Assessment

The various evaluation methods of the robustness index determine the robustness of a specific treatment step for a given duration. However, to comprehend the complete impact of the selected raw water quality parameter changes due to climate change, the overall robustness of the plant should be assessed. This step aims to integrate the results from Step 4: Evaluation and determine the overall robustness of a plant. As discussed in sub-section 2.4.4, there have been several studies to evaluate the robustness of individual treatment steps, but none of them attempted to assess the overall robustness of DWTPs. For evaluating robustness with respect to turbidity, the TRIs would indicate the robustness of each critical treatment step for a given duration. Nemani (2021b) has assigned a robustness category number to the classifications of the system operations based on TRI which is listed in Table 2.8.

Table 2.8: Legend of robustness category based on TRIs (Nemani, 2021b)

| **Robustness category number** | **Class** | **TRI range** |
|---|---|---|
| 1 | Very stable | < 60 |
| 2 | Stable | 60 - 100 |
| 3 | Slightly disturbed | 100 - 130 |
| 4 | Moderately disturbed | 130 - 160 |
| 5 | Upset | 160 - 200 |
| 6 | Severely upset | > 200 |

Table 2.9: Demonstration of determining overall system robustness (Nemani, 2021b)

| **Type of data** | **TRI and TRI categories** | | | | | | **Overall robustness category** | **Overall system robustness** |
|---|---|---|---|---|---|---|---|---|
| | **Intake, $T_{goal}$ = 25 NTU** | **Robustness category** | **CFS, $T_{goal}$ = 2.0 NTU** | **Robustness category** | **Filtration, $T_{goal}$ = 2.0 NTU** | **Robustness category** | | |
| Historical data (2019-2020) from a DWTP in southern Ontario | 21 | 1 | 60 | 2 | 45 | 1 | 1 | Very stable |
| | 28 | 1 | 82 | 2 | 46 | 1 | 1 | Very stable |
| | 81 | 1 | 67 | 2 | 47 | 1 | 2 | Stable |
| | 39 | 1 | 84 | 4 | 47 | 1 | 2 | Stable |
| Hypothetical scenarios | 50 | 1 | 250 | 6 | 70 | 2 | 3 | Slightly disturbed |
| | 25 | 1 | 200 | 6 | 180 | 5 | 4 | Moderately disturbed |
| | 250 | 6 | 180 | 5 | 300 | 6 | 6 | Severely upset |

To evaluate the overall TRI of a DWTP, the following approach was proposed. The TRIs calculated for each critical treatment step would be assigned to a robustness category number according to Table 2.8. The average robustness category number would be calculated and rounded to the nearest integer, which would be considered as the overall robustness category. The class corresponding to the overall robustness category number would be determined from Table 2.8, and this class would indicate the overall robustness class of the plant for the given duration.

Nemani (2021b) demonstrated the first iteration of the procedure in Table 2.9 with historical data and hypothetical scenarios by taking the arithmetic average of the robustness categories of each critical step to calculate the overall robustness category.

However, each treatment process may have different levels of significance to remove turbidity. Taking the arithmetic average to calculate the overall robustness category would not consider the fact that one treatment may be more significant than the other in terms of removing turbidity. To resolve this issue, unequal weighting factors can be assigned to the treatment steps according to their level of significance with respect to turbidity removal, and the overall robustness of the plant can be assessed in a more logical way.

### 2.4.6 Step 6: Adaptation

Based on the outcome of Step 4: Evaluation and Step 5: Assessment, if any of the identified treatment steps are found to be less robust with respect to the selected water quality parameter, short-term operational responses will be explored to make the specific treatment step more robust, thus improving the overall robustness of the system. This can include adjusting the dosage of coagulants and other chemicals, changing coagulation type, addition of coagulant aid, pH adjustments, mixing speed and duration and surface loading rate for the CFS process, and hydraulic rate, filter run time and backwash duration for the filtration process (Nemani, 2021a).

In this study, a bench-scale test has been conducted to assess the performance of a critical treatment step with respect to turbidity removal of a DWTP in Southern Ontario for current and predicted future weather scenarios by simulating raw water quality that may occur due to the adverse effect of heavy

precipitation. Spiked raw water samples were prepared in the lab and modified jar test was conducted to simulate the ACTIFLO® process in Plant A. A factorial design experiment was performed to optimize the ACTIFLO® parameters for raw water with extremely high turbidity. The detailed analysis can be found in Chapter 5.

## 2.5 Identification of Research Needs

Since most of the DWTPs are designed based on historical data including past heavy precipitation events, the system is likely to encounter unforeseeable challenges and may even fail under more extreme adverse weather events caused by unusual, untimely, and more frequent and heavy precipitation that changes raw water quality parameters in ways that were never experienced in the past. Therefore, there is an urgent need to comprehend the associated cause and effects and develop knowledge and tools that can diagnose the consequences of these events on treatment beforehand and direct to proper measures to improve the robustness of the plants so that they can withstand these events. When the raw water quality worsens beyond the design capacity, most of the DWTPs tend to shut down during storm events and rely on their reservoirs until the event is passed. This may result in huge economic and social impact on the served population, if the reservoir capacity is crossed. Considering the rapid change in precipitation nature, intensity and frequency, long-term changes like implementation of newer designs and treatment techniques to the pre-existing DWTPs cannot exhibit immediate outcomes. However, if the pre-existing operations within the DWTPs can be modified accordingly, it would ensure that the system is robust against extreme weather events in the near future as well as save the capital cost. The outcome of the short-term operational changes may aid to plan and implement long-term measures later. Therefore, a robustness framework is imperative for water treatment systems to evaluate and assess the robustness of different treatment steps as well as the overall system so that the limitations and complications can be pinned down, and short-term operational changes can be attempted and implemented to prepare the system for more adverse weather effects in the future. Turbidity is an important parameter in water treatment since it has proven to be very responsive to changes in weather by numerous studies. Filter effluent turbidity is a regulated parameter. In addition, due to its ability to indicate changes in other water quality parameters and microbiological quality of water, link to public health, simplicity in measurement and availability of continuous on-line data at several points of the treatment process, evaluation of robustness of different treatment processes

with respect to turbidity can lead to a better understanding of the robustness of DWTPs and assist to develop dynamic approaches to improve their robustness. While there have been several studies that focused on assessing the robustness of treatment steps in terms of turbidity, a complete framework is required to work as a proactive assessment tool in order to guide and prepare DWTPs for the upcoming challenges of climate change impacts on source water.

# Chapter 3: Evaluation of Robustness of Plant A

## 3.1 Introduction

Plant A is a DWTP located in southern Ontario. The Grand River is the only source of raw water in this plant. The Grand River watershed is the largest watershed in Southern Ontario, encompassing almost 7,000 $km^2$ in consultation with the provinces and territories of area. About 80% of the watershed is used for agriculture. Around 500,000 people live in the five municipalities around the watershed (Loomer & Cooke, 2011). Discharge from urban runoff, agricultural lands, and wastewater treatment plants into the Grand River and tributaries make the Grand River a moderately to heavily impacted surface water body (Hamouda et al., 2016). The particles discharged upstream of Plant A are transported to the intake during heavy precipitation, significantly increasing the turbidity in the raw water. According to the plant operators, the plant is experiencing more frequent and severe unseasonal precipitation events in recent years, which may pose a challenge to maintain regulated water quality parameters including turbidity, which is the selected water quality parameter in this study. Health Canada (2012) has recommended regulatory guidelines for turbidity for different filtration techniques (listed in Chapter 2: Table 2.3) and DWTPs have different turbidity goals for the other treatment steps. A robust DWTP performs consistently regardless of the variations in the raw water quality (Zhang et al., 2012). This chapter mainly focuses on two steps of the robustness framework (Chapter 2: Figure 2.6), Step 4: Evaluation which is to evaluate the robustness of the critical treatment steps of the plant that can be affected by elevated raw water turbidity, and Step 5: Assessment which is to assess the overall robustness of the plant with respect to turbidity removal for calendar years 2019 and 2020.

## 3.2 Materials and Methods

### 3.2.1 Plant Description

Plant A has the capacity to treat 150 million liters of water per day (ML/D). The raw water from the Grand River is not directly pumped from the river, it enters the plant through a canal. Low lift pumps are used to pump the water from the canal to the plant (Staff of Plant A, December 2020).

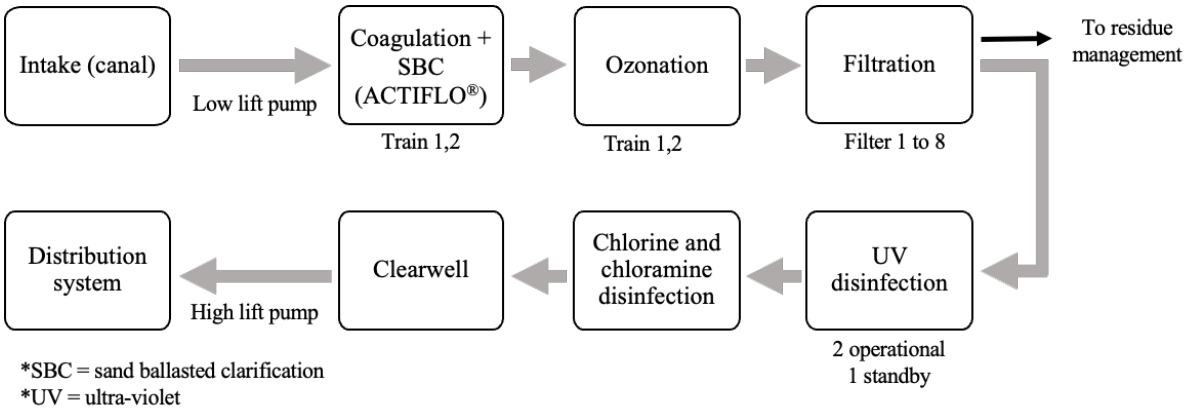


Figure 3.1: Plant A process flow diagram (figure depicts one treatment train and one filter basin)

Figure 3.1 shows the treatment process flow of Plant A. The water pumped by the low lift pumps is divided into two parallel treatment trains and moves on to the next treatment step, which is coagulation with polyaluminum chloride (PACl), followed by SBC. In Plant A, the ACTIFLO® process is used, which is one of the commercially available technologies for SBC. ACTIFLO®, developed by Veolia Water Technologies, is a compact system in which microsand (pure silica) and polymer (anionic) is used to increase the weight of flocs resulting in faster floc settling than in the conventional CFS method (Desjardins et al., 2002; Plum et al., 1998).

Each ACTIFLO® unit consists of an injection tank with a hydrocyclone rapid mixer, a coagulation tank, a maturation tank, and a sedimentation tank. The SBC effluent water from each train moves to the ozone contact chamber for that train.

After ozonation, the water moves to the filters through one pipe, mixing the effluent water from the two trains of SBC. There are eight deep bed bio-filters, each containing 1.6 m of anthracite over 0.4 m of sand. Biological filtration is employed in this plant with the dual objectives of particle and organics removal.

Filtration is followed by UV disinfection, and chlorine and chloramine disinfection. The water is then moved to the underground treated water reservoir, which has a capacity of 18 million liters. With high lift pumps, the finished water is finally moved to the distribution system (Staff of Plant A, December 2020).

### 3.2.2 Available Data

The plant framework (discussed in Chapter 2: section 2.4), developed by Nemani (2021a) was applied to Plant A. The timeframe of the study was selected to be two calendar years, 2019 and 2020. The selected water quality parameter in this study is turbidity. According to Step 3: Identification of the framework (discussed in Chapter 2: sub-section 2.4.3), the critical treatment steps that are affected by turbidity are, coagulation and SBC, i.e., the ACTIFLO® process, and filtration. On-line turbidity and flow data for the years 2019 and 2020 were requested from the plant as well as the dimensions for all the tanks and basins. Table 3.1 provides an overview of the available data.

Table 3.1: On-line monitoring data obtained from Plant A

| Location | Frequency | Frequency |
|---|---|---|
| Raw water turbidity | December 2018 to December 2020 | Every 5-minutes |
| ACTIFLO® effluent turbidity | January 2019 to December 2020 | Every 5-minutes |
| Filter effluent turbidity | January 2019 to December 2020 | Every 1-minute |
| Raw water flow rate | January 2019 to December 2020 | Every 5-minutes |
| Pre-treatment train 1 and 2 flow rate | January 2019 to December 2020 | Every 5-minutes |
| Filtration units (1 to 8) flow rate | January 2019 to December 2020 | Every 1-minute |

### 3.2.3 Identification of Invalid Data

Before analyzing the data, it is important to remove the data points that do not represent the actual condition of the plant. According to the plant operators, these data can result from instrumental error or recordings during maintenance and repair activities, and/or plant shutdowns. The methods developed to identify and remove the invalid data points from the data sets after consulting with the plant operators are discussed in sub-sections 3.2.3.1 to 3.2.3.3.

### 3.2.3.1 Raw water turbidity data

The raw water turbidity data of the year 2019 were plotted in a time series in Figure 3.2. In this figure, some data points were observed to be very high compared to the adjacent data points. There can be two reasons behind this:

1. The turbidity of the raw water rose drastically for 5-10 minutes and then returned to the previous lower level.
2. The on-line turbidimeter recorded a wrong value due to instrumental error or maintenance work during the time of recording.

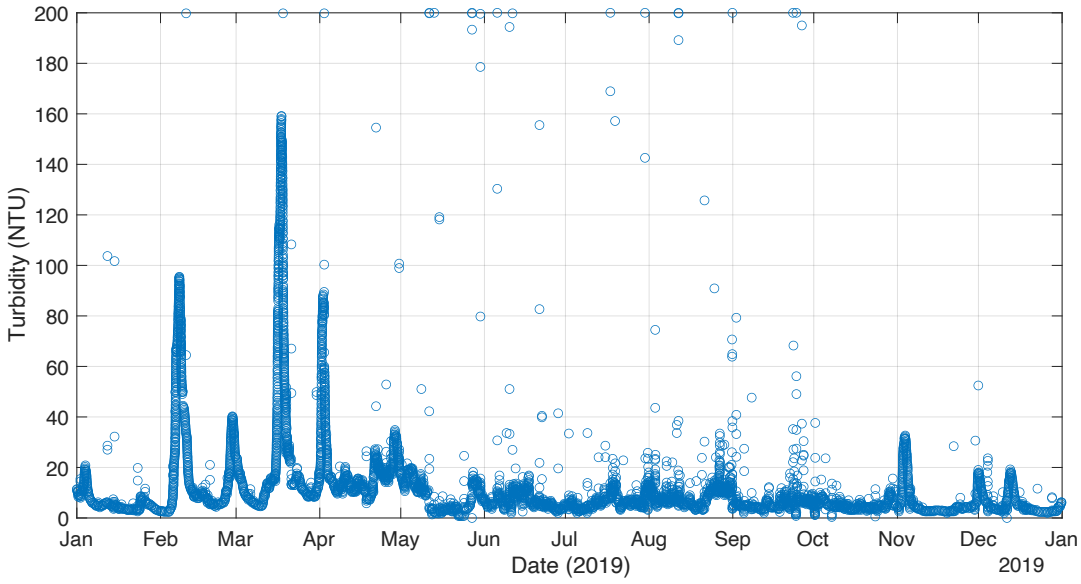


Figure 3.2: Time series of raw water turbidity data (2019)

In the case of the second reason, the data points must be removed before analysis because they do not represent the actual turbidity of the raw water. However, it is not acceptable to remove data that represent actual turbidity peaks in the raw water, which are very important in this study. Therefore, a method was developed that can identify and remove the invalid data points without removing actual turbidity peaks in the raw water.

This method takes the median turbidity for an hour, so it assumes that turbidity peaks lasting less than an hour are not considered as weather events. First, the median of the turbidity values before and 30 minutes (total 1 hour) after "suspected" (suspected to be invalid) data will be calculated. If that "suspected" data is *x%* above the calculated median, that data will be considered invalid. In short, invalid data = x% above the hourly median.

The value of *x* was varied from 50 to 200, to determine which value of *x* removes the obvious (from visual observation) invalid data without removing significant turbidity peaks that represent actual weather events in the Grand River. Finally, the optimum value of *x* was selected to be 100 as higher values of *x* cannot remove all the obvious invalid data points, whereas lower values of *x* remove turbidity peaks that are clearly caused by weather events. Therefore, the final method to identify invalid data points from raw water turbidity data is, invalid data = 100% above the hourly median. The time series of raw water turbidity data with varying values of *x* can be found in Appendix A (Figure A.1).

To illustrate the method, two example raw water turbidity data sets from 2019 are shown in Table 3.2. The data suspected to be invalid are indicated with asterisk (*).

Table 3.2: Demonstrations of the method to identify invalid data points

| **Example Data Set - 1** | | **Example Data Set - 2** | |
|---|---|---|---|
| **Date and Time** | **Turbidity (NTU)** | **Date and Time** | **Turbidity (NTU)** |
| 2019-05-13 8:45 | 3.40 | 2019-03-17 19:10 | 158 |
| 2019-05-13 8:50 | 3.40 | 2019-03-17 19:15 | 157 |
| 2019-05-13 8:55 | 3.47 | 2019-03-17 19:20 | 159 |
| 2019-05-13 9:00 | 5.41 | 2019-03-17 19:25 | 159 |
| 2019-05-13 9:05 | 5.41 | 2019-03-17 19:30 | 159 |
| 2019-05-13 9:10 | 5.41 | 2019-03-17 19:35 | 159 |
| 2019-05-13 9:15 | 200* | 2019-03-17 19:40 | 160* |
| 2019-05-13 9:20 | 2.44 | 2019-03-17 19:45 | 158 |

| | | | |
|---|---|---|---|
| 2019-05-13 9:25 | 2.42 | 2019-03-17 19:50 | 158 |
| 2019-05-13 9:30 | 2.40 | 2019-03-17 19:55 | 158 |
| 2019-05-13 9:35 | 2.40 | 2019-03-17 20:00 | 158 |
| 2019-05-13 9:40 | 2.40 | 2019-03-17 20:05 | 158 |
| 2019-05-13 9:45 | 2.40 | 2019-03-17 20:10 | 159 |
| **Median turbidity (NTU)** | 3.40 | **Median turbidity (NTU)** | 158 |
| **100% above the median** | 6.80 < 200 | **100% above the median** | 316 > 160 |
| **Remarks** | Invalid data point | **Remarks** | Valid data point |

Due to the size of the data set, it is very difficult to manually search data that are suspected to be invalid. Hence, two MATLAB functions (Appendix D: Code D.1 and D.2) were developed and applied to every data point for the raw water turbidity data sets for 2019 and 2020, and the invalid data points were removed prior to analysis.

The time series of the raw water turbidity data after removing the invalid data points for the year 2019 is shown in Figure 3.3. 189 out of 105109 (0.18%) data were removed as invalid data. The same method is applied to the raw water turbidity data for the year 2020 and 89 out of 105397 (0.08%) data were removed. The time series of the raw water turbidity data after removing the invalid data points for the year 2020 is shown in Figure 3.4.

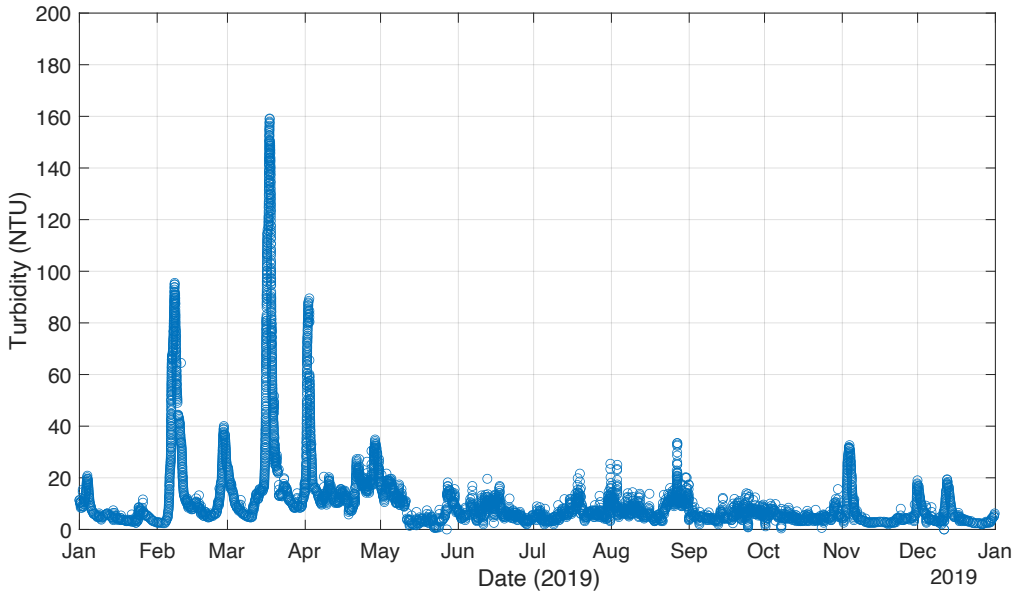


Figure 3.3: Time series of raw water turbidity data (2019) with invalid data points removed

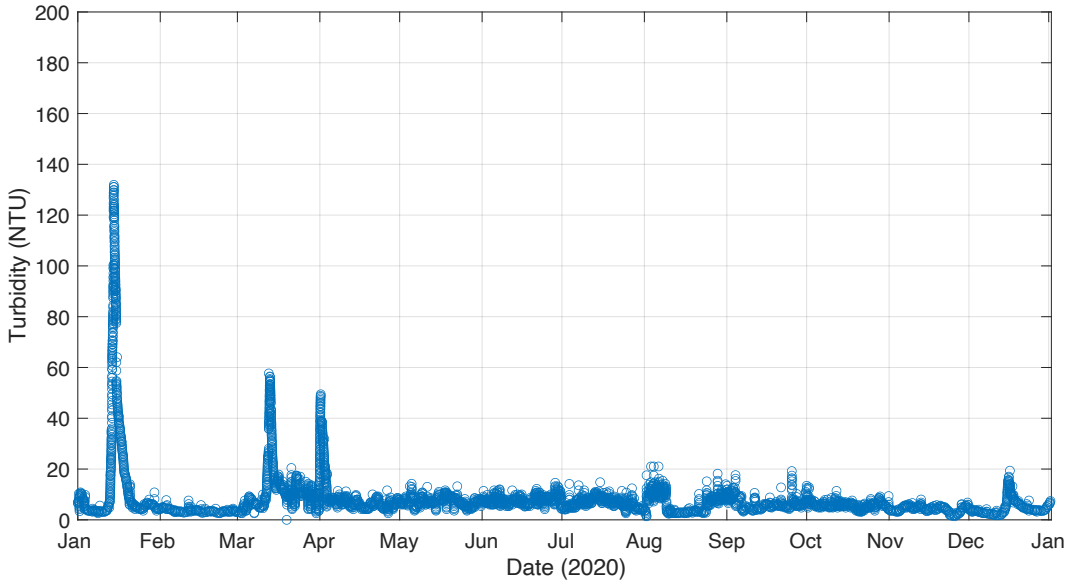


Figure 3.4: Time series of raw water turbidity data (2020) with invalid data points removed

#### 3.2.3.2 ACTIFLO® Effluent Turbidity Data

The flow rates of train 1 and train 2 determine the validity of the ACTIFLO® effluent turbidity data. If the flow rate is zero, it implies that there was no water going into the plant for coagulation and SBC, which may occur due to plant shutdowns for various reasons. The minimum flow rate required for the ACTIFLO® process is 35 ML/D in Plant A (Staff of Plant A, April 2021), so if the flow rate is less than 35 ML/D, it indicates that the plant and/or the ACTIFLO® units are being shut down or started up from a shutdown. Hence, turbidity values recorded in the online turbidimeter during these periods do not represent the actual condition and can be removed as invalid data points. A MATLAB function (Appendix D: Code D.3) was used to identify and remove the data points corresponding to flow rates less than 35 ML/D from the ACTIFLO® effluent turbidity data sets. Overall, 7.36% of the data were removed.

#### 3.2.3.3 Filter Effluent Turbidity Data

Similar to the previous sub-section, the flow rates of each filter determine the validity of the filter effluent turbidity data. If the flow rate is zero, it implies that there was no water going into the filter which may occur due to filter backwash, maintenance work, and/or plant shutdowns for various reasons. As mentioned before, Plant A has 8 filters and usually 6 of them run simultaneously, keeping 2 filters on stand-by. After backwash, for the first 35 minutes of a filter run, the effluent water goes to waste (Staff of Plant A, April 2021), also called the filter-to-waste period. The turbidity values recorded in the on-line turbidimeter during the filter-to-waste periods were removed as invalid data. Therefore, the turbidity data corresponding to filter flow rates equal to zero and the first 35 minutes of a filter run were identified and removed for every filter using a MATLAB function (Appendix D: Code D.4). Overall, 30.4% of the data were removed.

### 3.2.4 Data Analysis Approach

The plant framework developed by Nemani (2021a) was applied in this study. The fourth step "evaluation" in the plant framework (discussed in Chapter 2: sub-section 2.4.4) focused on quantifying the concept of robustness for treatment steps that are affected by changes in raw water quality parameters, which in this study is elevated turbidity caused by heavy and unusual precipitation events.

Thus, it is necessary to distinguish between the raw water turbidity levels during normal weather and weather events that can cause a significant increase in turbidity at the intake. The raw water turbidity data was used to establish two weather scenarios:

1. Normal weather
2. Weather events, characterized by elevated turbidity in the raw water.

The TRI concept developed by Li and Huck (2008) was used to evaluate the turbidity of the coagulation and SBC process, i.e., the ACTIFLO® process and the filtration process for the above-mentioned weather scenarios. Li and Huck (2008) used the length of a filter run as the duration of each TRI calculation. For evaluating the robustness of the ACTIFLO® process, the duration of each TRI calculation was selected to be a week since most of the extreme weather events vary from 4 days to 2 weeks. The TRIs were calculated using Equations 2.5 and 2.6, and Table 2.6. Changing the duration from the duration of one filter run to one week incorporates a much larger volume of data which is why the 90th percentile turbidity ($T_{90}$) is heavily influenced by the noise in the data set. To neutralize this issue, the high and low values of the weighting factors $A_1$ and $A_2$ were selected to be 0.6 and 0.4 instead of 0.9 and 0.1 to shift more weight to the average performance of the treatment units. The timeframe for TRI calculation was selected to be one week for the filters as well so that the TRIs of different treatment steps are comparable with one another, and later can be used to evaluate the overall robustness of the plant. The overall robustness of the plant with respect to turbidity was assessed by a method developed by Nemani (2021b) as discussed in Chapter 2: sub-section 2.4.5.

The flow rate data were used to determine the hydraulic retention times of the treatment units. Hydraulic retention time (HRT) of water treatment units is defined as the ratio between the unit volume and flow rate that represents the average residence time of water within the unit (Crittenden et al., 2012). The calculation of HRTs for different treatment units is important for the analysis. If the ACTIFLO® effluent turbidity data of a given treatment unit were compared with the raw water data for the same timeframe, the comparison would not be accurate as it would take some time for the raw water to flow from the intake and pass the whole ACTIFLO® process. The HRTs of different tanks within the treatment processes were calculated using the median flow rates to offset the data points so that the comparison between raw water turbidity data, and ACTIFLO® unit and filter effluent turbidity data are more logical. The HRTs of the treatments units in Plant A using the median flow rates are shown in Table 3.3.

Table 3.3: HRTs of different treatment units in Plant A

| Unit | | Hydraulic Retention Time (HRT) |
|---|---|---|
| ACTIFLO® unit (trains 1 and 2) | Injection tank | 5m 24s |
| | Coagulation tank | 5m 14s |
| | Maturation tank | 16m 30s |
| | Sedimentation tank | 26m 54s |
| | Total | 54m |
| Ozonation unit (trains 1 and 2) | | 1h 28m |
| Filtration unit (Filters 1 to 8) | | 1h 43m |

## 3.3 Results and Discussion

### 3.3.1 Identification of Normal Turbidity and Turbidity Events

As discussed in sub-section 3.2.4, to evaluate the robustness of the critical treatment steps, it is important to separate the calculated TRIs based on weather to determine whether the treatment steps are affected by weather events or not, which is the main indication of robustness for the factor being addressed in this research. From the time series of the raw water turbidity (Figures 3.3 and 3.4), some turbidity peaks can be observed that indicate precipitation-related weather events in the area. However, there should be a specific criterion to select these peaks and establish them as turbidity events, which refers to precipitation-related weather events characterized by raw water turbidity. Two methods were developed to identify and separate the normal turbidity and turbidity events. The development process and applicability of these two methods are discussed in sub-sections 3.3.1.1 and 3.3.1.2.

#### 3.3.1.1 Method 1: Yearly Median Raw Water Turbidity

The yearly median of the raw water turbidity data was calculated. If the turbidity values are *y%* over the yearly median, they are considered as turbidity events. Therefore, turbidity event = y% above the yearly median, for at least one hour.

According to this method, the elevated turbidity levels have to continue for at least an hour to be considered as a weather event. Turbidity peaks lasting less than an hour are considered as invalid data in this study and removed prior to the analysis as has been discussed in sub-section 3.2.3.1.

The yearly median turbidity of the year 2019 was 5.81 NTU. The value of *y* was ranged from 25 to 100, and the method was applied to the raw water turbidity data of 2019, which is shown in Figure 3.5.

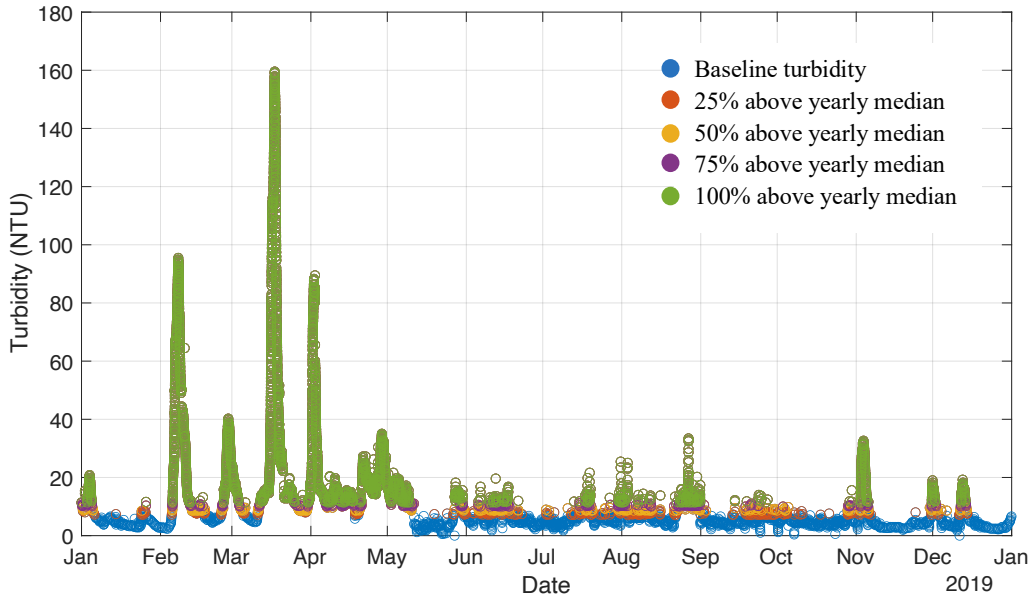


Figure 3.5: Time series of raw water data (2019) with turbidity peak events using yearly median raw water turbidity (5.81 NTU)

To check the applicability of the method, three weather events were selected based on their durations.

**1. Short duration turbidity event**

The short duration turbidity event occurred in mid-December 2019, which may have caused by heavy precipitation. The details of this event are described in Table 3.4 and shown in Figure 3.6. For the value of *y* ranging from 25% to 100%, the duration of this event varied by 1 day 4 hours, and the median turbidities varied by 2 NTU. Therefore, if the value of *y* is decreased, more data before and after the turbidity peak is considered as a turbidity event as shown in Figure 3.6. However, one particular value of *y* cannot be selected with certainty after scrutinizing this short duration turbidity event only.

Table 3.4: Short duration turbidity event in mid-December 2019

| **Percentage (%) above the yearly median (5.81 NTU)** | **Trigger turbidity of the events (NTU)** | **Event start date and time** | **Event end date and time** | **Event Duration** | **Median turbidity of the event (NTU)** | **Maximum turbidity of the event (NTU)** |
|---|---|---|---|---|---|---|
| 25% | 7.26 | 12/11/2019 17:10 | 12/14/2019 15:55 | 2d 22h 45m | 13.0 | 19.4 |
| 50% | 8.72 | 12/11/2019 21:15 | 12/14/2019 9:20 | 2d 12h 5m | 14.0 | 19.4 |
| 75% | 10.1 | 12/12/2019 1:20 | 12/14/2019 3:45 | 2d 2h 25m | 14.6 | 19.4 |
| 100% | 11.6 | 12/12/2019 3:55 | 12/13/2019 22:05 | 1d 18h 10m | 15.2 | 19.4 |

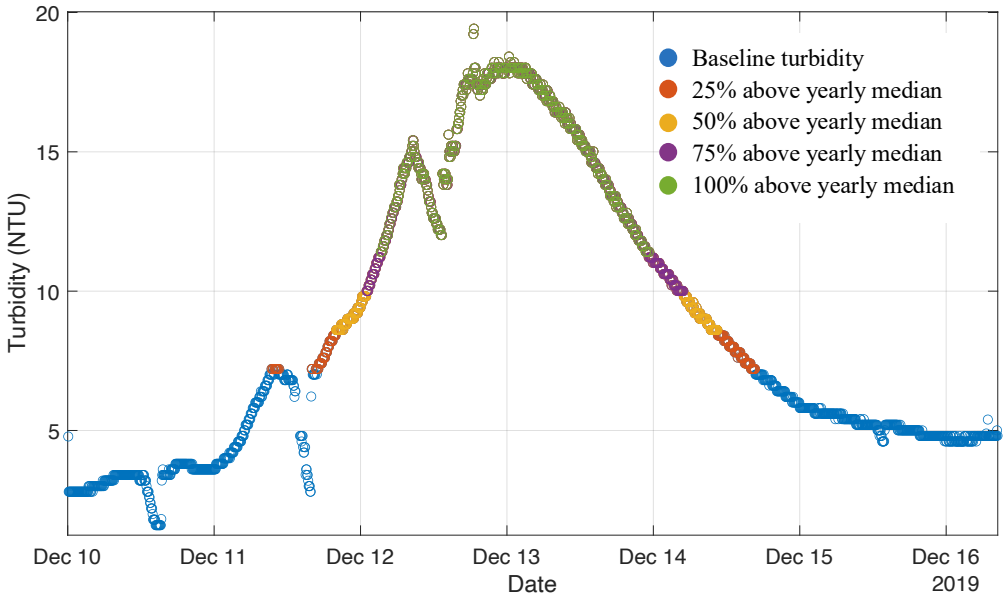


Figure 3.6: Time series of raw water turbidity during turbidity event (mid-December 2019) using yearly median raw water turbidity (5.81 NTU)

**2. Medium duration turbidity event**

The medium duration turbidity event occurred in February 2019, which may have been caused by unseasonal heavy precipitation resulting in snow-melting and runoff in the Grand River. The details of this event are described in Table 3.5 and shown in Figure 3.7. For the value of *y* ranging from 25% to 100%, the duration of this event varied by more than 6 days, and the median turbidities varied by 30.4 NTU. For the higher values (75-100%) of *y*, it is evident in Figure 3.7 that some elevated turbidity values are being cut off from the turbidity event, which may be critical to the analysis. As listed in Table 3.5, the median turbidity of the event was 26.8 NTU for y = 50%, which increased to 36.2 NTU for y = 75%. This substantial change in median turbidity values was not observed in the short duration turbidity event. Therefore, it is obvious that the higher values (75-100%) of *y* do not consider some elevated turbidity values as turbidity events.

Table 3.5: Medium duration turbidity event in February 2019

| Percentage (%) above the yearly median (5.81 NTU) | Trigger turbidity of the events (NTU) | Event start date and time | Event end date and time | Event Duration | Median turbidity of the event (NTU) | Maximum turbidity of the event (NTU) |
|---|---|---|---|---|---|---|
| 25% | 7.26 | 2/5/2019 12:05 | 2/18/2019 7:35 | 12d 19h 30m | 11.8 | 95.6 |
| 50% | 8.72 | 2/5/2019 14:20 | 2/14/2019 15:45 | 9d 1h 25m | 26.8 | 95.6 |
| 75% | 10.1 | 2/5/2019 15:50 | 2/13/2019 3:00 | 7d 11h 10m | 36.2 | 95.6 |
| 100% | 11.6 | 2/5/2019 17:10 | 2/12/2019 4:45 | 6d 11h 35m | 42.2 | 95.6 |

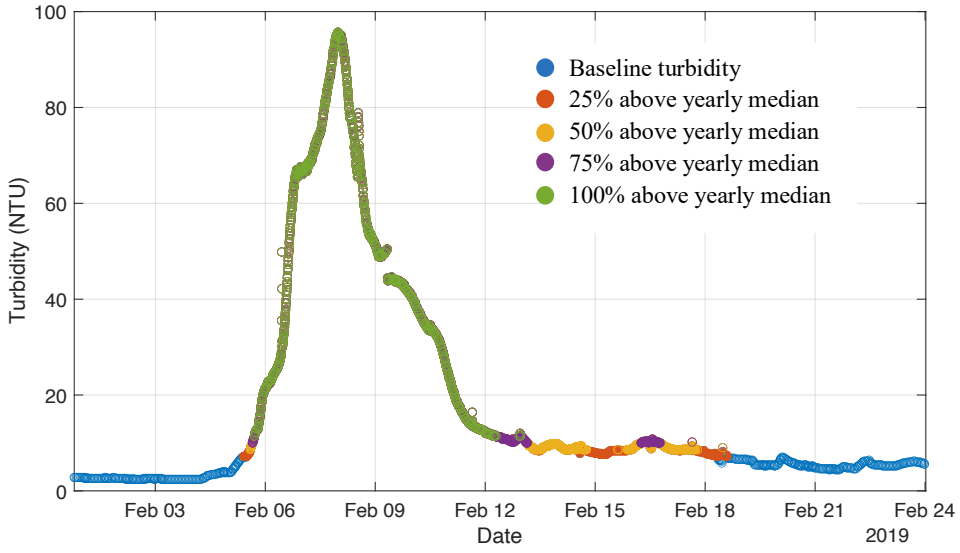


Figure 3.7: Time series of raw water turbidity during turbidity event (February 2019) using yearly median raw water turbidity (5.81 NTU)

### 3. Long duration turbidity event

The long event occurred from mid-March to the first week of May 2019, mostly caused by spring run-off and heavy precipitation. The details of this event are described in Table 3.6 and shown in Figure 3.8. For the value of *y* ranging from 25% to 100%, the duration of this event varied by almost 6 days, and the median turbidities varied by 2 NTU. Thus, the variation in median turbidity of the event is similar to the short event, but drawing a conclusion regarding the selection of an appropriate value of *y* became even more complicated.

Table 3.6: Long duration turbidity event in March-April-May 2019

| **Percentage (%) above the yearly median (5.81 NTU)** | **Trigger turbidity of the events (NTU)** | **Event start date and time** | **Event end date and time** | **Event Duration** | **Median turbidity of the event (NTU)** | **Maximum turbidity of the event (NTU)** |
|---|---|---|---|---|---|---|
| 25% | 7.26 | 3/11/2019 2:45 | 5/11/2019 13:05 | 61d 10h 20m | 14.6 | 159.6 |
| 50% | 8.72 | 3/11/2019 17:00 | 5/11/2019 13:05 | 60d 20h 5m | 15.0 | 159.6 |
| 75% | 10.1 | 3/11/2019 19:50 | 5/11/2019 13:05 | 60d 17h 15m | 15.2 | 159.6 |
| 100% | 11.6 | 3/12/2019 5:05 | 5/6/2019 22:45 | 55d 17h 40m | 16.6 | 159.6 |

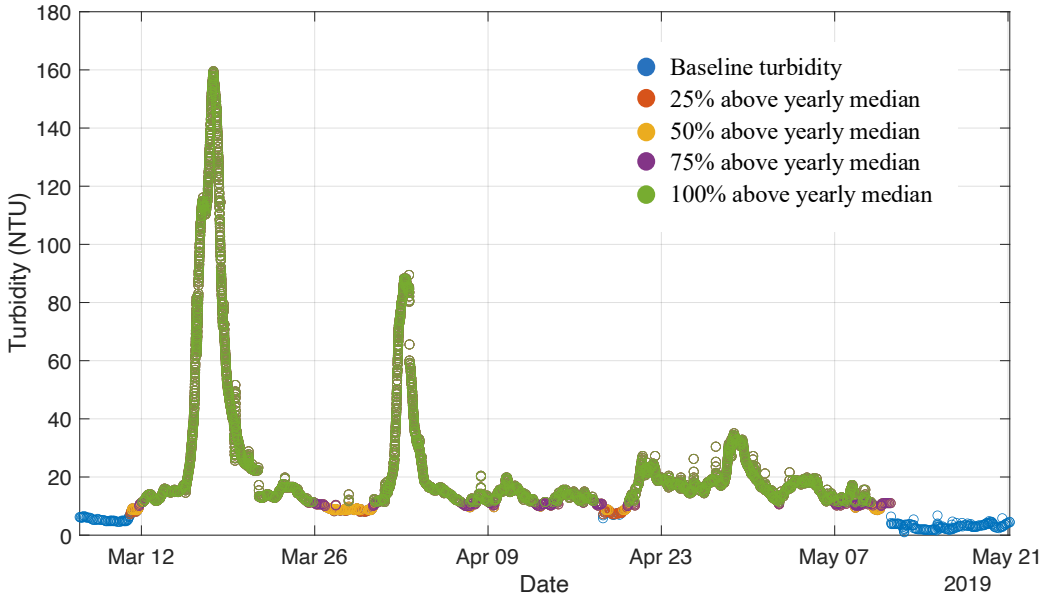


Figure 3.8: Time series of raw water turbidity during turbidity event (March-April-May 2019) using yearly median raw water turbidity (5.81 NTU)

The limitation of using the yearly median to find weather events is evident in the case of this event. From Figure 3.8, it can be observed that there are multiple peaks, unlike Figures 3.6 and 3.7. Although there have been several weather events from March to May 2019, this method considers them as one big event. The baseline turbidity during these months was higher because of snow-melting and spring runoff, but since this method considered the yearly median, it failed to separate multiple events during this period. Therefore, the yearly median turbidity cannot be used to select weather events characterized by turbidity, and another method was developed which aims to overcome the limitations of this method.

#### 3.3.1.2 Method 2: Seasonal Median Raw Water Turbidity

The year is separated into 4 seasons (winter, spring, summer, and fall) and the median turbidity of each season is calculated, which are shown in Table 3.7.

Table 3.7: Yearly and seasonal raw water median turbidities of 2019

| Season | Winter | Spring | Summer | Fall | Yearly |
|---|---|---|---|---|---|
| **Duration** | Dec 2018 - Feb 2019 | Mar 2019 - May 2019 | Jun 2019 - Aug 2019 | Sep 2019 - Nov 2019 | Jan 2019 - Dec 2019 |
| **Median turbidity (NTU)** | 5.21 | 12.2 | 6.00 | 4.40 | 5.81 |

The differences between the respective seasonal and the yearly median turbidities for winter, summer, and fall varied from -0.6 to +1.4 NTU, but in spring it varied by +6.4 NTU, indicating the baseline turbidity was higher in spring than in other seasons, and the weather events cannot be separated using the yearly median turbidity.

Therefore, the revised method is: if the turbidity values are *y%* above the seasonal median, they will be considered as weather event turbidity. In short, turbidity event = y% above the seasonal median, for at least one hour.

This method was applied to the raw water turbidity data for spring 2019. Figure 3.9 shows that using the seasonal median turbidity distinguishes among multiple weather events successfully.

Using the seasonal median turbidity instead of the yearly median turbidity should not have any significant difference in the other seasons since the seasonal median turbidities are close to the yearly median turbidity. The time series plots of raw water turbidity for the other seasons are in Appendix A (Figure A.2).

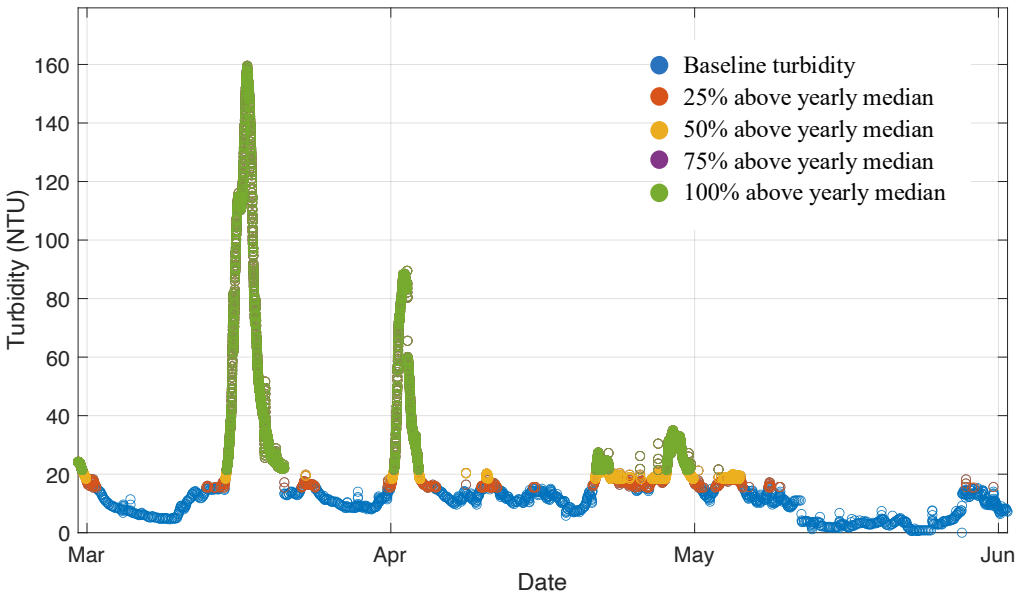


Figure 3.9: Time series of raw water turbidity of spring 2019 using seasonal median raw water turbidity (12.2 NTU)

As observed in Figures 3.6 to 3.9 (and Figure A.2 in Appendix A), the higher values (75-100%) of *y* eliminate turbidity data that clearly indicates the start and end of an event whereas a low value (25%) of *y* takes some of the baseline turbidity values as weather events. Therefore, the optimum value of *y* is selected to be 50% to identify weather events from raw water turbidity data, and the final method is: turbidity event = 50% above the seasonal median turbidity, for at least one hour. Two MATLAB functions (Appendix D: Code D.5 and D.6) were used to apply this method to the raw water data points and identify the weather events characterized by the raw water turbidity. Figures 3.10 and 3.11 show the time series of raw water turbidity of the year 2019 and 2020 respectively indicating normal turbidity levels and turbidity events characterized by raw water turbidity.

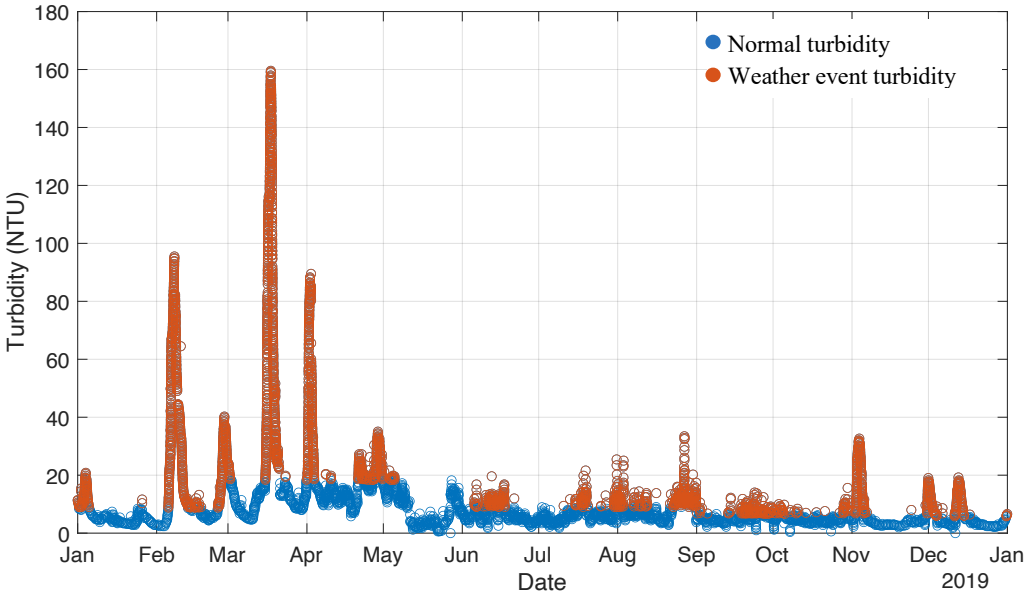


Figure 3.10: Time series of raw water turbidity (2019) showing normal turbidity and turbidity events

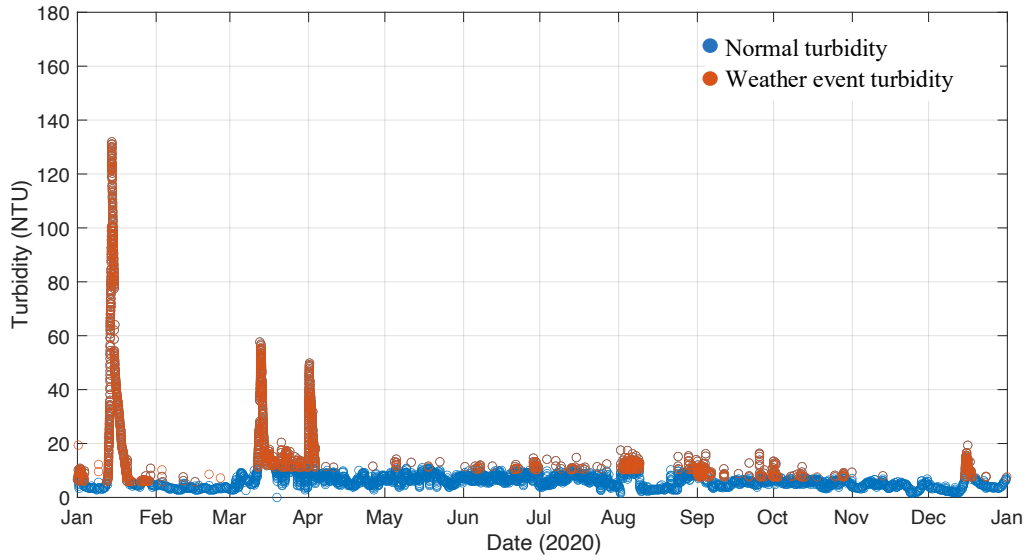


Figure 3.11: Time series of raw water turbidity (2020) showing normal turbidity and turbidity events

### 3.3.2 Robustness of the ACTIFLO® Units

According to Step 4: Evaluation of the plant framework, the TRIs were calculated for the ACTIFLO® units with Equation 2.5. To calculate the TRIs for every week of the year 2019 and 2020, a goal turbidity is required as stated in Step 2: Criteria of the plant framework. There is no regulatory limit set for coagulation and SBC effluent water since it is not the final treatment step to remove turbidity. DWTPs generally have a goal turbidity for conventional CFS or SBC effluent water so that elevated effluent turbidity cannot overwhelm the filters and/or fail to produce filtered water maintaining the regulatory limit (listed in Chapter 2: Table 2.3). In Plant A, the goal turbidity (Tgoal) of the ACTIFLO® effluent water is 1.0 NTU (Staff of Plant A, April 2021). A stricter goal (Tgoal = 0.5 NTU) was selected during the initial analysis to observe the effects of different turbidity goals in calculating TRIs. In Figure 3.12, the TRIs of the train 1 ACTIFLO® unit for the year 2019 are calculated for two TRI goals, 0.5 NTU shown by the blue bars and 1.0 NTU shown by the orange bars. The lower the turbidity goal, the stricter the criterion, which should lead to higher TRI values. All the TRIs with Tgoal = 0.5 NTU are higher than those with Tgoal = 1.0 NTU as expected. The classes of the TRIs are discussed later in this chapter.

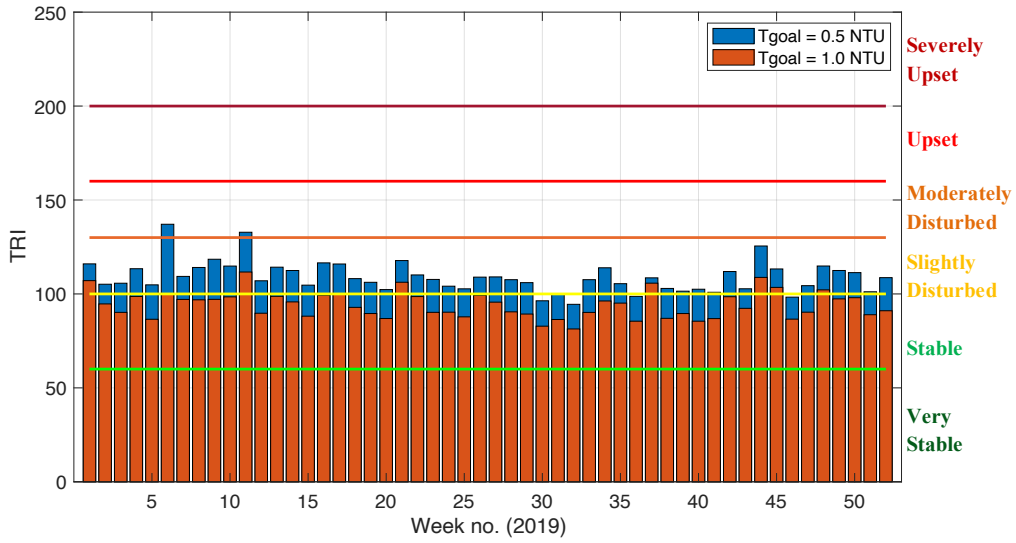


Figure 3.12: Weekly TRIs of the train 1 ACTIFLO® unit (2019) with varying Tgoals

According to the plant operators, the goal turbidity of the ACTIFLO® units in Plant A is 1.0 NTU, which is why the goal value of 1.0 NTU was used to calculate the TRIs of the ACTIFLO® units in

further analysis. Figures 3.13 and 3.14 show the weekly TRIs of the train 1 ACTIFLO® unit for the years 2019 and 2020 respectively.

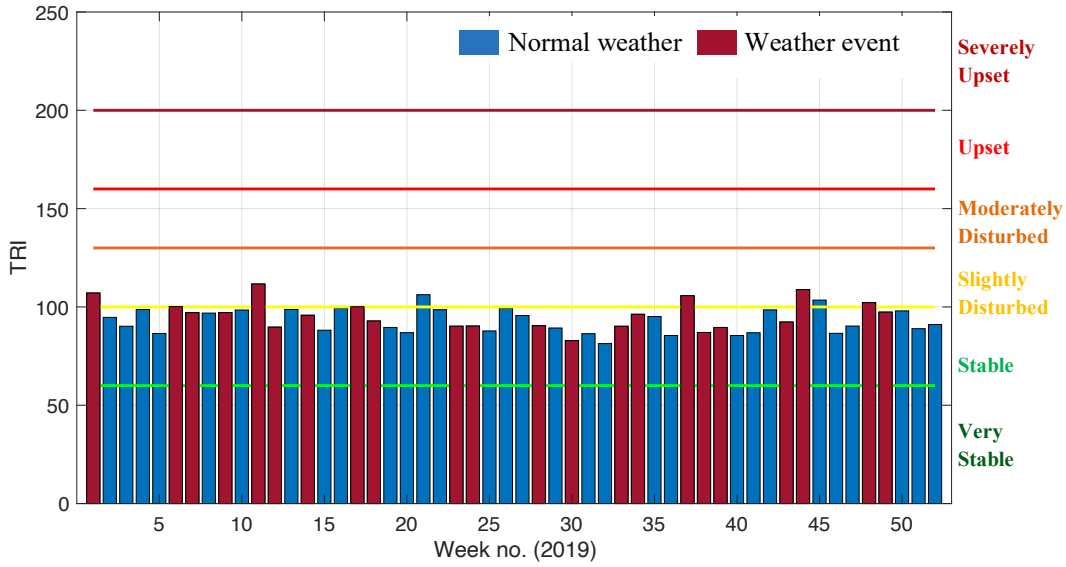


Figure 3.13: Weekly TRIs of the train 1 ACTIFLO® unit (2019) during normal weather and weather events characterized by raw water turbidity (Tgoal = 1.0 NTU)

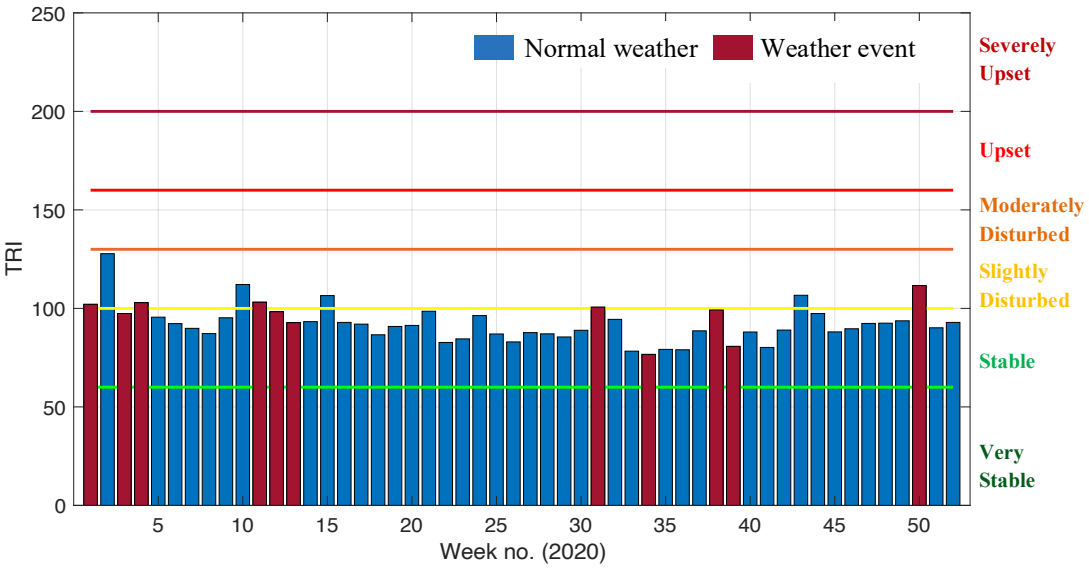


Figure 3.14: Weekly TRIs of the train 1 ACTIFLO® unit (2020) during normal weather and weather events characterized by raw water turbidity (Tgoal = 1.0 NTU)

The blue bars represent the TRIs during normal weather and the red bars represent the TRIs corresponding to the weeks that were affected by weather events, which were identified using the method developed in sub-section 3.3.1.2. Most of the TRIs fall into the "stable" (60-100) class, which indicates that the 50th and the 90th percentile turbidity were below the goal turbidity and the ACTIFLO® units always maintained desired quality (effluent turbidity < 1.0 NTU) for the respective weeks. For 7 weeks in 2019 and 8 weeks in 2020 the TRIs fall into the "slightly disturbed" (100-130) class, which indicate that either both 50th and 90th percentile turbidity was close to the goal turbidity and/or the 90th percentile turbidity was greater than the goal turbidity in some cases and the ACTIFLO® units produced effluent water with desired quality most of the time during the given weeks. This should be noted that the classification system regarding the TRI values was developed based on the turbidity data analysis for filter runs, so the name of the classes may not be as precise in this case as this is an entirely different treatment step with different duration, but the mathematical interpretation of TRI should be valid.

The definition of robustness implies that if the performance of a system is observed to exacerbate during upsets, the system would not be considered robust. However, there is no visible trend in Figures 3.13 and 3.14 that shows that the TRIs are only higher during weather events, which indicates the ACTIFLO® units were robust. Similar results are found for train 2, which is shown in Appendix A (Figure A.3).

Although there is no observed difference between TRIs during normal weather and weather events, to confirm the visual observation from Figures 3.13 and 3.14, in Figure 3.15 the TRIs corresponding to weather events as characterized by raw water turbidity were plotted against the maximum or 'peak' turbidity of the event, which represents the extremity of the event. A similar figure has been plotted for train 2, which can be found in Appendix A (Figure A.4). However, no positive correlation ($R^2 \approx 0$) was observed between the TRIs and peak turbidities of a weather event, implying that weather events did not affect TRIs in 2019 and 2020, confirming that the ACTIFLO® operation of Plant A was robust according to the definitions used in this analysis.

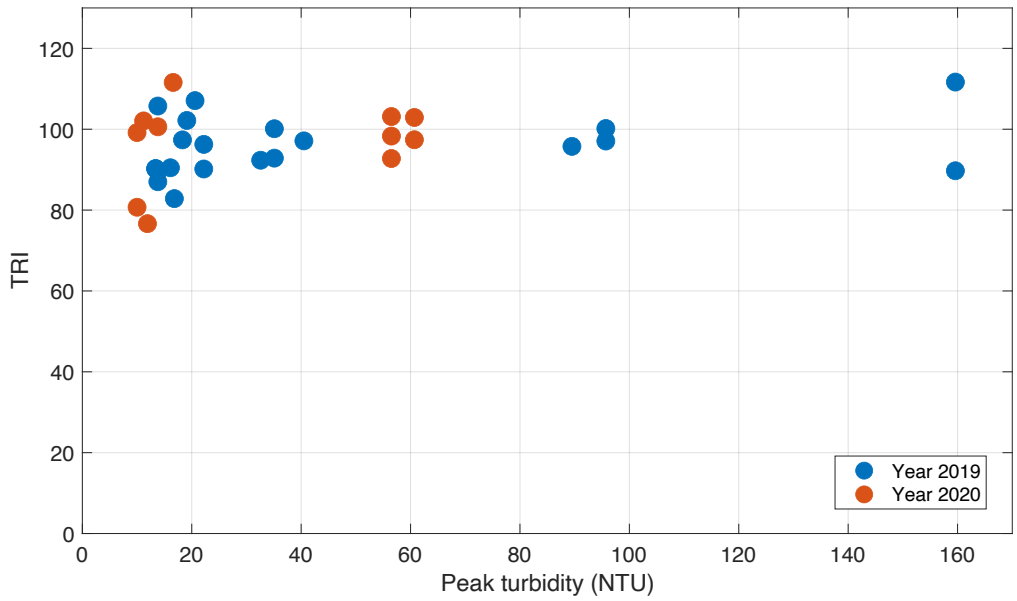


Figure 3.15: Weekly TRIs of the train 1 ACTIFLO® unit in relation to the maximum values of raw water turbidity during weather events

In addition to the TRI plots, in order to visualize the overall performance of the ACTIFLO® units, the weekly average raw water turbidities are plotted against the weekly average train 1 ACTIFLO® effluent turbidity for the years 2019 and 2020 in Figures 3.16 and 3.17 respectively to observe the weekly turbidity removal by the ACTIFLO® units.

In both figures, the weekly average train 1 ACTIFLO® effluent turbidities are below the goal turbidity 1.0 NTU during both normal weather and weather events characterized by turbidity. Train 2 ACTIFLO® unit shows similar results, which can be found in Appendix A (Figure A.5). After ozonation, the effluent water from both trains is mixed and flows through a common pipe, before it enters the filter gallery. Overall, the two ACTIFLO® units successfully removed 82.0% to 98.7% on average (Table A.1 in Appendix A) per week of raw water turbidity throughout the years 2019 and 2020.

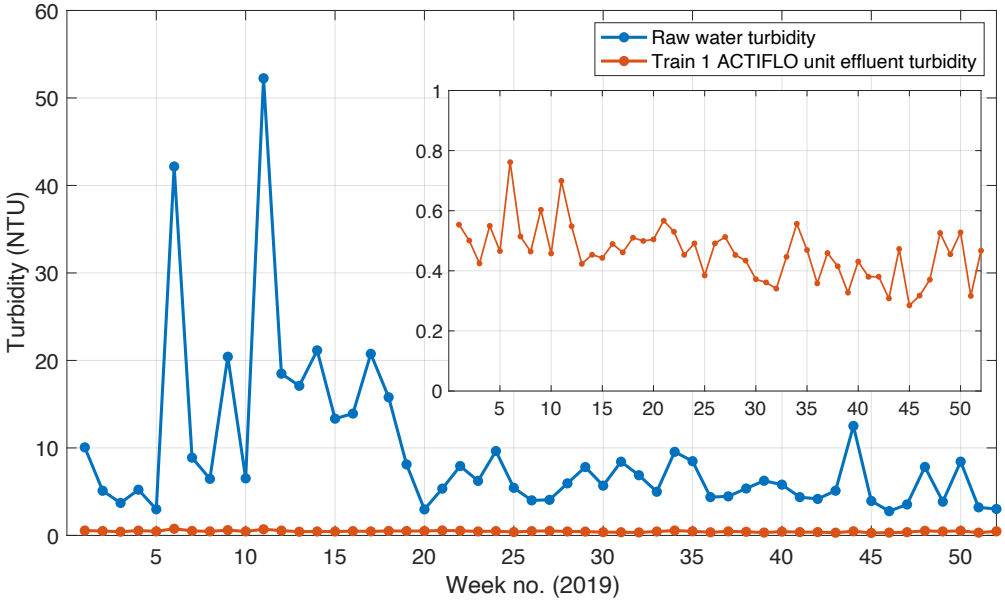


Figure 3.16: Weekly average raw water and train 1 ACTIFLO® influent and effluent turbidity (2019)

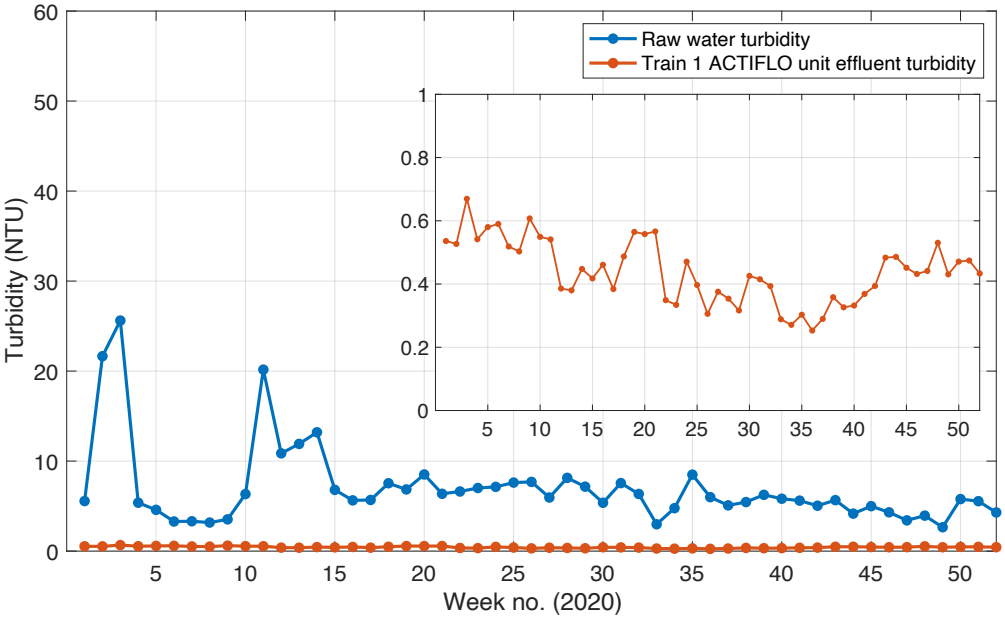


Figure 3.17: Weekly average raw water and train 1 ACTIFLO® influent and effluent turbidity (2020)

### 3.3.3 Robustness of the Filtration Units

In Plant A, filtration is the last step to remove particles, i.e., turbidity. In 2019 and 2020, the ACTIFLO® units of Plant A removed about 92% of the raw water turbidity on average, and the filters removed the rest, maintaining finished water turbidity within the regulatory limits. To evaluate the robustness of the filtration units with TRI, a goal turbidity is required as specified by Step 2: Criteria (Chapter 2: sub-section 2.4.2) in the plant framework. Plant A follows the regulatory limit set by the Government of Ontario based on Health Canada (2012), which states that the effluent turbidity of every filter must be less than or equal to 0.3 NTU for at least 95% of the measurement per cycle per month, with a target of less than 0.1 NTU, and the turbidity can never exceed 1.0 NTU. Plant A strictly maintains the effluent turbidity of each filter below 0.1 NTU. If the effluent turbidity exceeds 0.2 NTU, the water is directed to waste and if it increases over 0.3 NTU, the filter will automatically shutdown (Staff of Plant A, December 2020). Considering these facts, the goal turbidity of the filter is selected to be 0.1 NTU. Since there are 8 filters in Plant A, only the data analysis result of 2 representative filters (Filter 2 from the north side and Filter 7 from the south side of the plant) is discussed in this chapter. The results of the other filters can be found in Appendix A (Figures A.6 and A.7).

Figures 3.18 and 3.19 show the weekly TRIs of Filter 2 for the years 2019 and 2020 respectively. The blue bars represent the TRIs during normal weather and the red bars represent the TRIs corresponding to the weeks that were affected by weather events characterized by raw water turbidity. Most of the TRIs fall into the “stable” (60-100) class and for 4 weeks in 2019 and 4 weeks in 2020 the TRIs fall into the “slightly disturbed” (100-130) class. The TRI falls into “moderately disturbed” (130-160) class during one week in 2020.

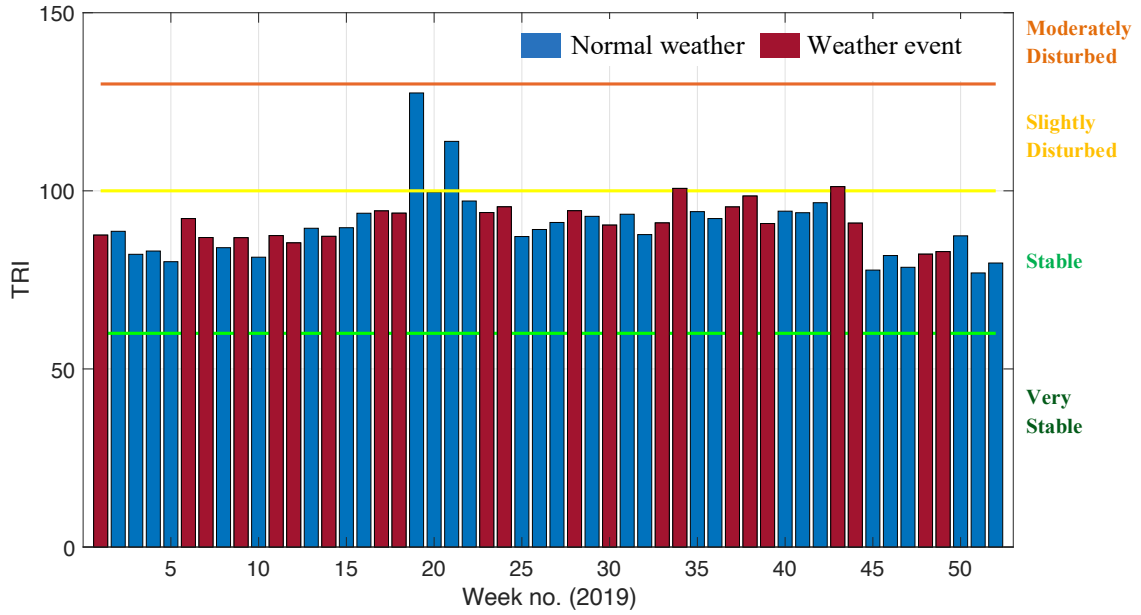


Figure 3.18: Weekly TRIs of Filter 2 (2019) during normal weather and weather events characterized by raw water turbidity (Tgoal = 0.1 NTU)

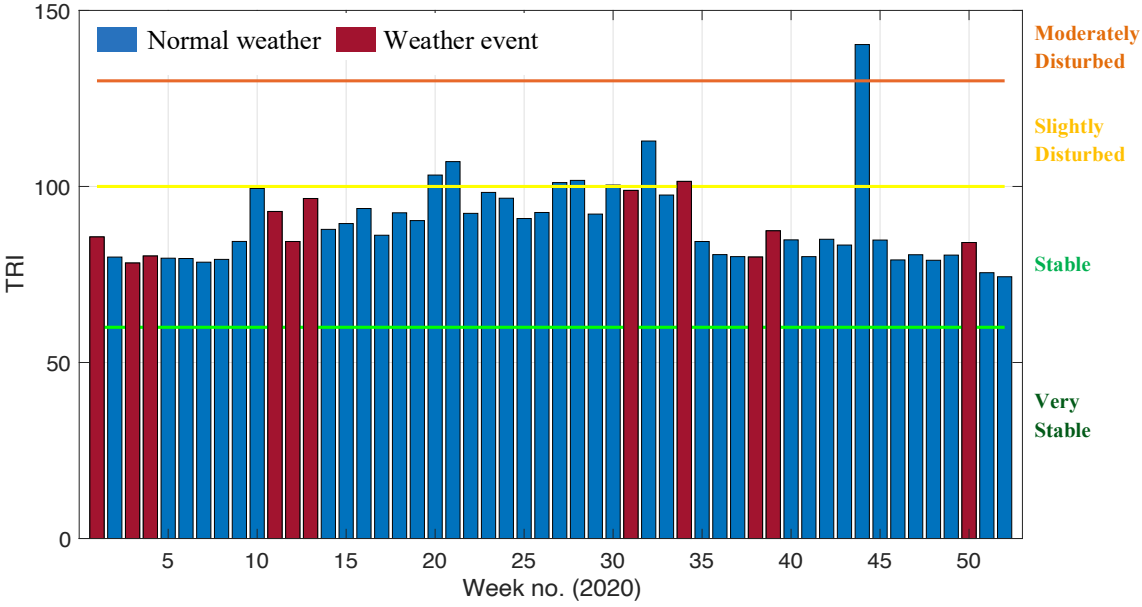


Figure 3.19: Weekly TRIs of Filter 2 (2020) during normal weather and weather events characterized by raw water turbidity (Tgoal = 0.1 NTU)

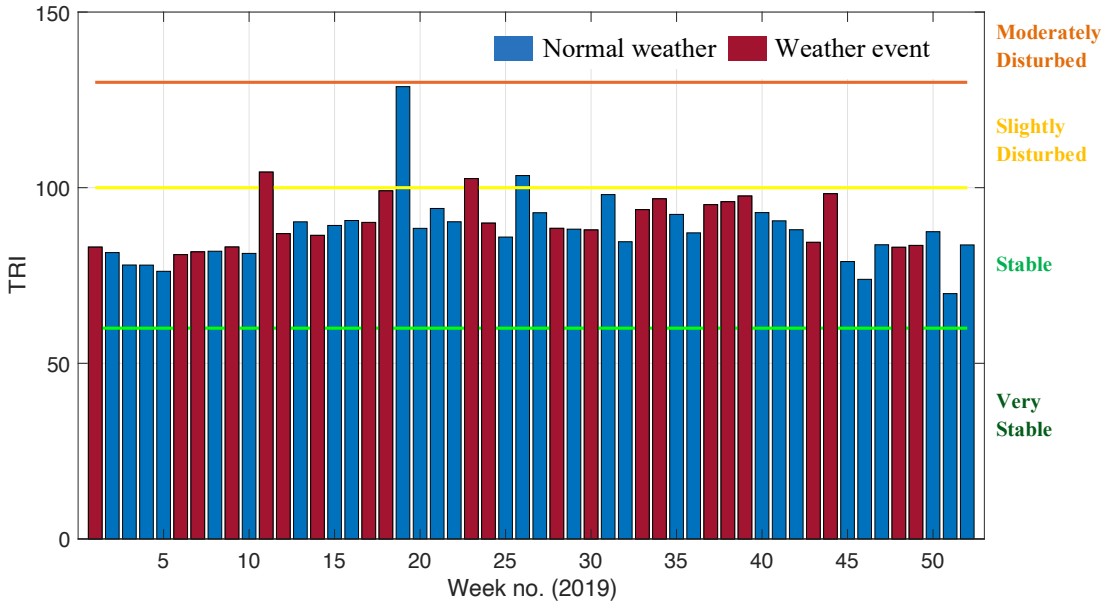


Figure 3.20: Weekly TRIs of Filter 7 (2019) during normal weather and weather events characterized by raw water turbidity (Tgoal = 0.1 NTU)

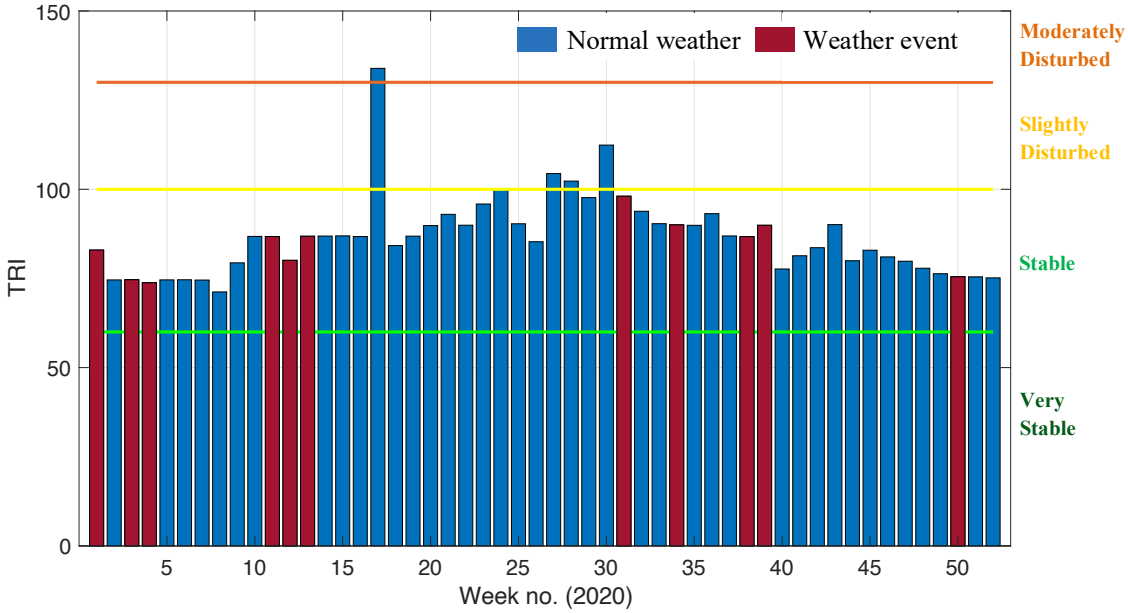


Figure 3.21: Weekly TRIs of Filter 7 (2020) during normal weather and weather events characterized by raw water turbidity (Tgoal = 0.1 NTU)

Similarly, Figures 3.20 and 3.21 show the weekly TRIs of Filter 7 for the years 2019 and 2020 respectively. The blue bars represent the TRIs during normal weather and the red bars represent the TRIs corresponding to the weeks that were affected by weather events characterized by raw water turbidity. Most of the TRIs fall into the "stable" (60-100) class, for 4 weeks in 2019 and 2 weeks in 2020 the TRIs fall into "slightly disturbed" (100-130) class, and for 1 week of 2020 the TRI falls into the "moderately disturbed" (130-160) class.

The "stable" TRIs indicate that the 50th and the 90th percentile turbidities were below the goal turbidity and the filters always maintained desired quality (effluent turbidity < 0.1 NTU) for the respective weeks. The "slightly disturbed" TRIs indicate that either both the 50th and 90th percentile turbidities were close to the goal turbidity and/or the 90th percentile turbidity was greater than the goal turbidity in some cases and the filters produced effluent water with desired quality most of the time during the given weeks. The "moderately disturbed" TRIs indicate that both the 50th and 90th percentile turbidity were greater than the goal turbidity and the filters did not generate effluent water with desired quality for a short duration during the given weeks. From Figures 3.18 to 3.21 and A.6 and A.7, it is observed that there are some TRIs that fall into the "moderately disturbed" class but there was no weather event taking place during those weeks. Although the "moderately disturbed" TRIs imply that the performance of the filters was not satisfactory during a short period of time in the given weeks, they do not always correspond to the weather events characterized by raw water turbidity, indicating that the reason behind this undesirable performance is not weather-related. It should be noted that the classification system based on the TRI values (Li & Huck 2008) was developed based on the turbidity data analysis for individual filter runs. Therefore, the name of the classes may not be as accurate in this case as the duration that was considered to calculate TRIs is much larger than a filter run, but the mathematical interpretation of TRI should be valid. Moreover, these TRIs were calculated considering Tgoal = 0.1 NTU, which is one-third of the regulatory limit (0.3 NTU) making this analysis a bit strict, which can act as a safety factor in the future if any operational changes are needed to be made.

Similar to the ACTIFLO® unit TRIs, there is no visible trend in Figures 3.18 to 3.21 that shows that the TRIs are only higher during weather events, which indicates that Filters 2 and 7 were robust. Similar results were found for the other filters, which are shown in Appendix A (Figures A.6 and A.7).

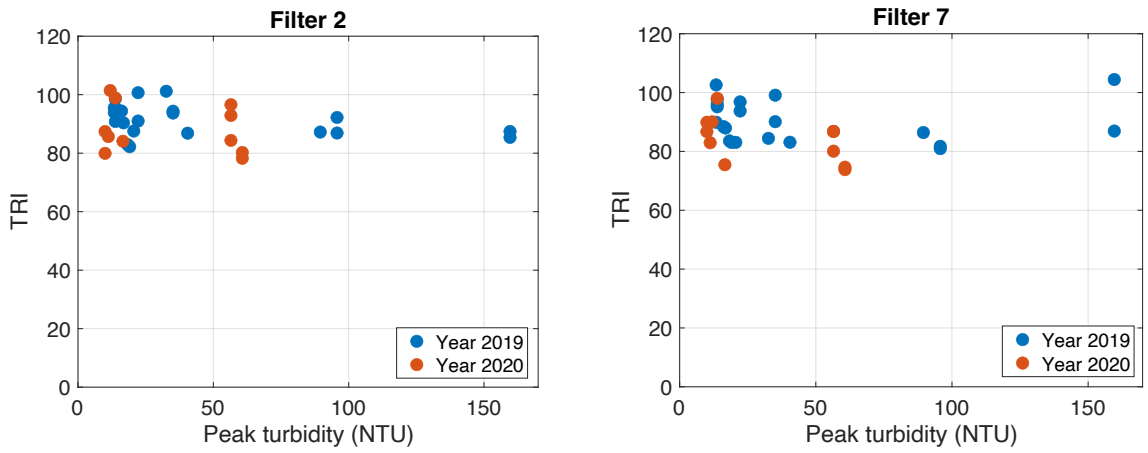


(a) (b)

Figure 3.22: Weekly TRIs of (a) Filter 2 and (b) Filter 7 in relation to the maximum values of raw water turbidities during weather events

Although there is no observed difference between TRIs during normal weather and weather events, to confirm the visual observation from Figures 3.18 to 3.21, in Figure 3.22 the TRIs corresponding to weather events as characterized by raw water turbidity were plotted against the maximum or 'peak' turbidity of the event. However, no positive correlation ($R^2 \approx 0$) has been observed between the TRIs and peak turbidities of a weather event, implying that weather events did not affect TRIs in 2019 and 2020. This confirms that Filters 2 and 7 of Plant A were robust with respect to higher raw water turbidity. Similar results were found for the other filters, which are shown in Appendix A (Figure A.8), which verifies that the overall filtration system of Plant A was robust in 2019 and 2020 according to the definitions used in this analysis.

In addition to the TRI plots, in order to visualize the overall performance of the filters, the weekly average filter influent turbidities are plotted against the weekly average Filter 2 and Filter 7 effluent turbidity for the years 2019 and 2020 in Figures 3.23 and 3.24 respectively, to observe the weekly turbidity removal by these two filters.

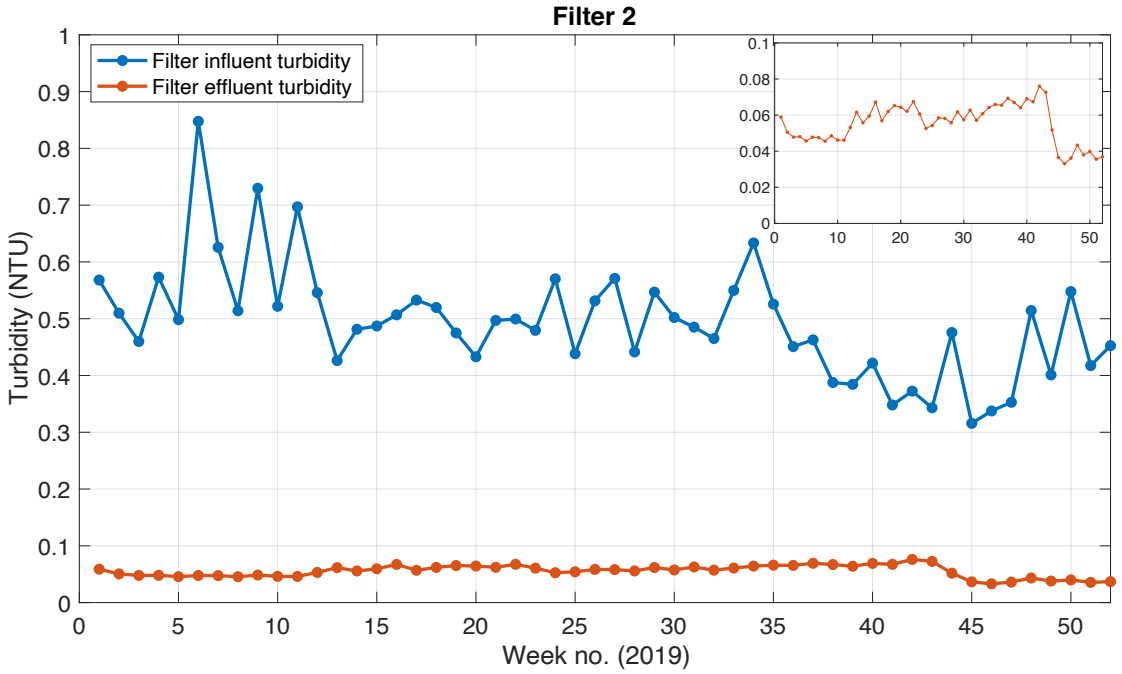


(a)

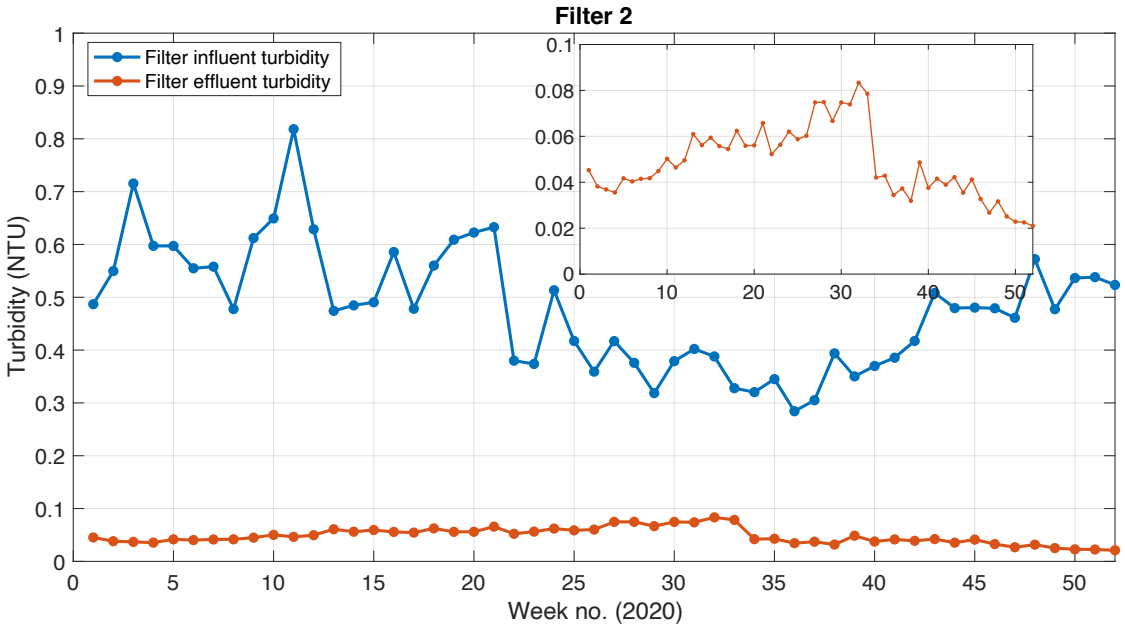


(b)

Figure 3.23: Weekly average filter influent and effluent turbidity of Filter 2 in (a) 2019 and (b) 2020

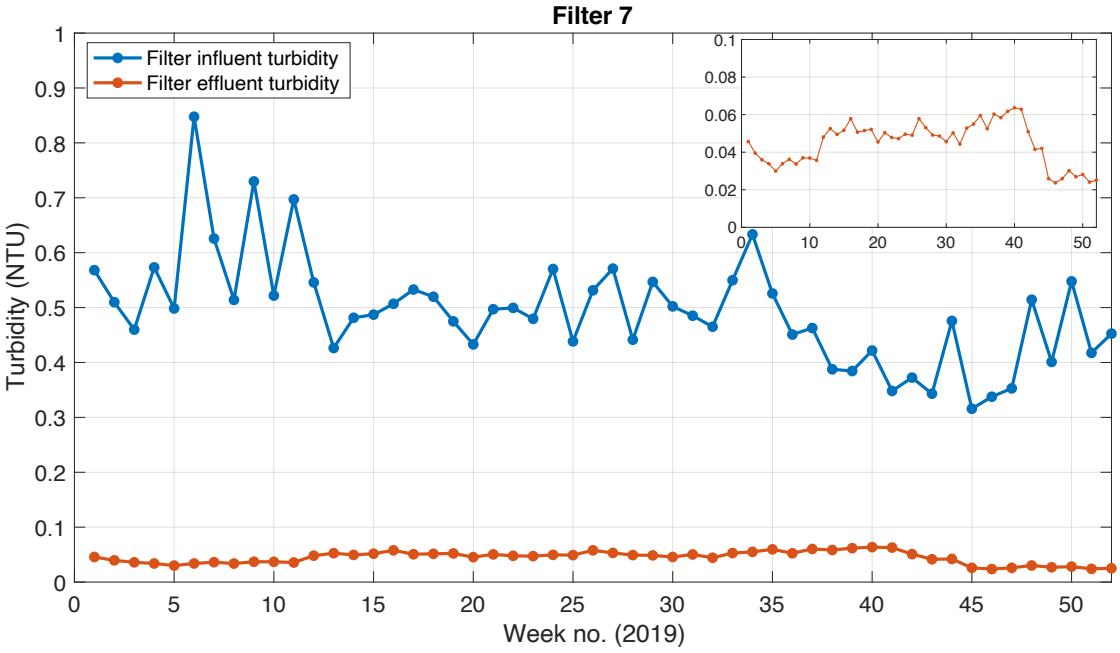


(a)

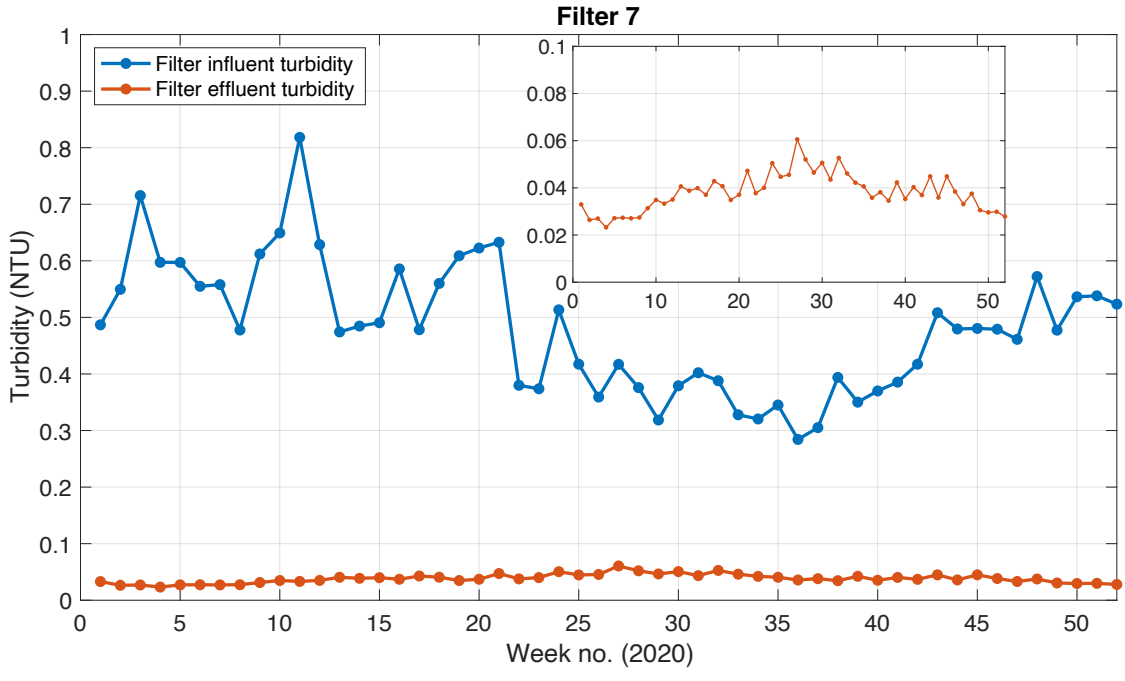


(b)

Figure 3.24: Weekly average filter influent and effluent turbidity of Filter 7 in (a) 2019 and (b) 2020

Figures 3.23 and 3.24 show that all the Filter 2 and Filter 7 effluent turbidities are below the goal turbidity 0.1 NTU during normal weather and weather events. The effluent water from all the filters is mixed and the water moves to the UV disinfection units. Overall, the process culminating in the eight filters successfully removes 98.1% to 99.9% (Table A.1 in Appendix A) of raw water turbidity per week on average throughout the years 2019 and 2020, maintaining the effluent turbidity below 0.1 NTU, which is well below the regulatory limit (0.3 NTU).

### 3.3.4 Overall Robustness of Plant A

Since in Plant A the two critical treatments steps for turbidity are the ACTIFLO® process and filtration, the overall robustness of the plant is dependent on the robustness of these two steps. As the two treatment trains are parallel and identical, the average TRI of the train 1 and 2 ACTIFLO® units represents the total TRI of the ACTIFLO® process. Again, since all the filters are operated randomly throughout the year, the average TRI of the eight filters represents the total TRI of the filtration step (Staff of Plant A, April 2021). To calculate the overall TRI of the plant, the overall robustness category (Chapter 2: Table 2.8) developed by Nemani (2021b) was used. According to the first iteration of this method, the overall robustness category is the average of the TRIs of all the critical treatment steps in the plant. However, one step can be more significant than the other in terms of removing turbidity. Thus, the overall robustness of Plant A can be assessed considering the following scenarios:

1. Equal weighting of the ACTIFLO® and filtration process assuming both processes are equally important.
2. Unequal weighting:
    i. The ACTIFLO® process is more significant as it removed around 92% of the raw water turbidity on average per week in 2019 and 2020 and aims to provide filter influent water with turbidity less than or equal to 1.0 NTU.
    ii. The filtration process is more significant as it is the final step to remove turbidity.

The overall robustness category and the overall robustness class evaluated by equal weighting of the two processes for the year 2019 is demonstrated in Table 3.8.

Table 3.8: Overall robustness of Plant A by weeks in 2019 using equal weighting

| Week no. | 2019 | | | | | |
|---|---|---|---|---|---|---|
| | ACTIFLO® Units | | Filters | | Plant | |
| | TRI | Category | TRI | Category | Overall Robustness Category | Overall System Robustness |
| 1 | 110 | 3 | 86 | 2 | 3 | slightly disturbed |
| 2 | 97 | 2 | 86 | 2 | 2 | stable |
| 3 | 91 | 2 | 80 | 2 | 2 | stable |
| 4 | 99 | 2 | 81 | 2 | 2 | stable |
| 5 | 89 | 2 | 78 | 2 | 2 | stable |
| 6 | 104 | 3 | 91 | 2 | 3 | slightly disturbed |
| 7 | 99 | 2 | 87 | 2 | 2 | stable |
| 8 | 101 | 3 | 82 | 2 | 3 | slightly disturbed |
| 9 | 104 | 3 | 86 | 2 | 3 | slightly disturbed |
| 10 | 102 | 3 | 80 | 2 | 3 | slightly disturbed |
| 11 | 106 | 3 | 91 | 2 | 3 | slightly disturbed |
| 12 | 93 | 2 | 88 | 2 | 2 | stable |
| 13 | 97 | 2 | 94 | 2 | 2 | stable |
| 14 | 105 | 3 | 88 | 2 | 2 | stable |
| 15 | 95 | 2 | 90 | 2 | 2 | stable |
| 16 | 104 | 3 | 90 | 2 | 3 | slightly disturbed |
| 17 | 101 | 3 | 95 | 2 | 3 | slightly disturbed |
| 18 | 95 | 2 | 103 | 3 | 3 | slightly disturbed |
| 19 | 91 | 2 | 108 | 3 | 3 | slightly disturbed |
| 20 | 92 | 2 | 92 | 2 | 2 | stable |
| 21 | 116 | 3 | 99 | 2 | 3 | slightly disturbed |
| 22 | 108 | 3 | 93 | 2 | 3 | slightly disturbed |
| 23 | 97 | 2 | 95 | 2 | 2 | stable |
| 24 | 95 | 2 | 92 | 2 | 2 | stable |
| 25 | 91 | 2 | 91 | 2 | 2 | stable |

| | | | | | | |
|---|---|---|---|---|---|---|
| 26 | 102 | 3 | 96 | 2 | 3 | slightly disturbed |
| 27 | 98 | 2 | 94 | 2 | 2 | stable |
| 28 | 96 | 2 | 94 | 2 | 2 | stable |
| 29 | 95 | 2 | 94 | 2 | 2 | stable |
| 30 | 92 | 2 | 93 | 2 | 2 | stable |
| 31 | 96 | 2 | 97 | 2 | 2 | stable |
| 32 | 89 | 2 | 88 | 2 | 2 | stable |
| 33 | 95 | 2 | 94 | 2 | 2 | stable |
| 34 | 98 | 2 | 101 | 3 | 3 | slightly disturbed |
| 35 | 96 | 2 | 96 | 2 | 2 | stable |
| 36 | 92 | 2 | 91 | 2 | 2 | stable |
| 37 | 111 | 3 | 96 | 2 | 3 | slightly disturbed |
| 38 | 89 | 2 | 99 | 2 | 2 | stable |
| 39 | 88 | 2 | 91 | 2 | 2 | stable |
| 40 | 87 | 2 | 94 | 2 | 2 | stable |
| 41 | 84 | 2 | 92 | 2 | 2 | stable |
| 42 | 92 | 2 | 94 | 2 | 2 | stable |
| 43 | 89 | 2 | 98 | 2 | 2 | stable |
| 44 | 101 | 3 | 99 | 2 | 3 | slightly disturbed |
| 45 | 94 | 2 | 80 | 2 | 2 | stable |
| 46 | 83 | 2 | 78 | 2 | 2 | stable |
| 47 | 91 | 2 | 80 | 2 | 2 | stable |
| 48 | 104 | 3 | 85 | 2 | 3 | slightly disturbed |
| 49 | 95 | 2 | 81 | 2 | 2 | stable |
| 50 | 106 | 3 | 91 | 2 | 3 | slightly disturbed |
| 51 | 90 | 2 | 78 | 2 | 2 | stable |
| 52 | 91 | 2 | 81 | 2 | 2 | stable |

For the unequal weighting scenarios, the ratio between weighting factors was selected to be 0.6/0.4. The overall robustness category and the overall robustness class evaluated by higher weighting of the

ACTIFLO® process and higher weighting of the filtration process for the year 2019 are demonstrated in Table 3.9 and 3.10 respectively.

Table 3.9: Overall robustness of Plant A by weeks in 2019 by unequal weighting (considering the ACTIFLO® process is more significant)

| Week no. | 2019 | | | | | |
|---|---|---|---|---|---|---|
| | ACTIFLO® Units | | Filters | | Plant | |
| | TRI | Category | TRI | Category | Overall Robustness Category | Overall System Robustness |
| 1 | 110 | 3 | 86 | 2 | 3 | slightly disturbed |
| 2 | 97 | 2 | 86 | 2 | 2 | stable |
| 3 | 91 | 2 | 80 | 2 | 2 | stable |
| 4 | 99 | 2 | 81 | 2 | 2 | stable |
| 5 | 89 | 2 | 78 | 2 | 2 | stable |
| 6 | 104 | 3 | 91 | 2 | 3 | slightly disturbed |
| 7 | 99 | 2 | 87 | 2 | 2 | stable |
| 8 | 101 | 3 | 82 | 2 | 3 | slightly disturbed |
| 9 | 104 | 3 | 86 | 2 | 3 | slightly disturbed |
| 10 | 102 | 3 | 80 | 2 | 3 | slightly disturbed |
| 11 | 106 | 3 | 91 | 2 | 3 | slightly disturbed |
| 12 | 93 | 2 | 88 | 2 | 2 | stable |
| 13 | 97 | 2 | 94 | 2 | 2 | stable |
| 14 | 105 | 3 | 88 | 2 | 3 | slightly disturbed |
| 15 | 95 | 2 | 90 | 2 | 2 | stable |
| 16 | 104 | 3 | 90 | 2 | 3 | slightly disturbed |
| 17 | 101 | 3 | 95 | 2 | 3 | slightly disturbed |
| 18 | 95 | 2 | 103 | 3 | 2 | stable |
| 19 | 91 | 2 | 108 | 3 | 2 | stable |

| | | | | | | |
|---|---|---|---|---|---|---|
| 20 | 92 | 2 | 92 | 2 | 2 | stable |
| 21 | 116 | 3 | 99 | 2 | 3 | slightly disturbed |
| 22 | 108 | 3 | 93 | 2 | 3 | slightly disturbed |
| 23 | 97 | 2 | 95 | 2 | 2 | stable |
| 24 | 95 | 2 | 92 | 2 | 2 | stable |
| 25 | 91 | 2 | 91 | 2 | 2 | stable |
| 26 | 102 | 3 | 96 | 2 | 3 | slightly disturbed |
| 27 | 98 | 2 | 94 | 2 | 2 | stable |
| 28 | 96 | 2 | 94 | 2 | 2 | stable |
| 29 | 95 | 2 | 94 | 2 | 2 | stable |
| 30 | 92 | 2 | 93 | 2 | 2 | stable |
| 31 | 96 | 2 | 97 | 2 | 2 | stable |
| 32 | 89 | 2 | 88 | 2 | 2 | stable |
| 33 | 95 | 2 | 94 | 2 | 2 | stable |
| 34 | 98 | 2 | 101 | 3 | 2 | stable |
| 35 | 96 | 2 | 96 | 2 | 2 | stable |
| 36 | 92 | 2 | 91 | 2 | 2 | stable |
| 37 | 111 | 3 | 96 | 2 | 3 | slightly disturbed |
| 38 | 89 | 2 | 99 | 2 | 2 | stable |
| 39 | 88 | 2 | 91 | 2 | 2 | stable |
| 40 | 87 | 2 | 94 | 2 | 2 | stable |
| 41 | 84 | 2 | 92 | 2 | 2 | stable |
| 42 | 92 | 2 | 94 | 2 | 2 | stable |
| 43 | 89 | 2 | 98 | 2 | 2 | stable |
| 44 | 101 | 3 | 99 | 2 | 3 | slightly disturbed |
| 45 | 94 | 2 | 80 | 2 | 2 | stable |
| 46 | 83 | 2 | 78 | 2 | 2 | stable |
| 47 | 91 | 2 | 80 | 2 | 2 | stable |
| 48 | 104 | 3 | 85 | 2 | 3 | slightly disturbed |
| 49 | 95 | 2 | 81 | 2 | 2 | stable |

| | | | | | | |
|---|---|---|---|---|---|---|
| 50 | 106 | 3 | 91 | 2 | 3 | slightly disturbed |
| 51 | 90 | 2 | 78 | 2 | 2 | stable |
| 52 | 91 | 2 | 81 | 2 | 2 | stable |

Table 3.10: Overall robustness of Plant A by weeks in 2019 by unequal weighting (considering the filtration process is more significant)

| **Week no.** | **2019** | | | | | |
|---|---|---|---|---|---|---|
| | **ACTIFLO® Units** | | **Filters** | | **Plant** | |
| | **TRI** | **Category** | **TRI** | **Category** | **Overall Robustness Category** | **Overall System Robustness** |
| 1 | 110 | 3 | 86 | 2 | 2 | stable |
| 2 | 97 | 2 | 86 | 2 | 2 | stable |
| 3 | 91 | 2 | 80 | 2 | 2 | stable |
| 4 | 99 | 2 | 81 | 2 | 2 | stable |
| 5 | 89 | 2 | 78 | 2 | 2 | stable |
| 6 | 104 | 3 | 91 | 2 | 2 | stable |
| 7 | 99 | 2 | 87 | 2 | 2 | stable |
| 8 | 101 | 3 | 82 | 2 | 2 | stable |
| 9 | 104 | 3 | 86 | 2 | 2 | stable |
| 10 | 102 | 3 | 80 | 2 | 2 | stable |
| 11 | 106 | 3 | 91 | 2 | 2 | stable |
| 12 | 93 | 2 | 88 | 2 | 2 | stable |
| 13 | 97 | 2 | 94 | 2 | 2 | stable |
| 14 | 105 | 3 | 88 | 2 | 2 | stable |
| 15 | 95 | 2 | 90 | 2 | 2 | stable |
| 16 | 104 | 3 | 90 | 2 | 2 | stable |
| 17 | 101 | 3 | 95 | 2 | 2 | stable |

| | | | | | | |
|---|---|---|---|---|---|---|
| 18 | 95 | 2 | 103 | 3 | 3 | slightly disturbed |
| 19 | 91 | 2 | 108 | 3 | 3 | slightly disturbed |
| 20 | 92 | 2 | 92 | 2 | 2 | stable |
| 21 | 116 | 3 | 99 | 2 | 2 | stable |
| 22 | 108 | 3 | 93 | 2 | 2 | stable |
| 23 | 97 | 2 | 95 | 2 | 2 | stable |
| 24 | 95 | 2 | 92 | 2 | 2 | stable |
| 25 | 91 | 2 | 91 | 2 | 2 | stable |
| 26 | 102 | 3 | 96 | 2 | 2 | stable |
| 27 | 98 | 2 | 94 | 2 | 2 | stable |
| 28 | 96 | 2 | 94 | 2 | 2 | stable |
| 29 | 95 | 2 | 94 | 2 | 2 | stable |
| 30 | 92 | 2 | 93 | 2 | 2 | stable |
| 31 | 96 | 2 | 97 | 2 | 2 | stable |
| 32 | 89 | 2 | 88 | 2 | 2 | stable |
| 33 | 95 | 2 | 94 | 2 | 2 | stable |
| 34 | 98 | 2 | 101 | 3 | 3 | slightly disturbed |
| 35 | 96 | 2 | 96 | 2 | 2 | stable |
| 36 | 92 | 2 | 91 | 2 | 2 | stable |
| 37 | 111 | 3 | 96 | 2 | 2 | stable |
| 38 | 89 | 2 | 99 | 2 | 2 | stable |
| 39 | 88 | 2 | 91 | 2 | 2 | stable |
| 40 | 87 | 2 | 94 | 2 | 2 | stable |
| 41 | 84 | 2 | 92 | 2 | 2 | stable |
| 42 | 92 | 2 | 94 | 2 | 2 | stable |
| 43 | 89 | 2 | 98 | 2 | 2 | stable |
| 44 | 101 | 3 | 99 | 2 | 2 | stable |
| 45 | 94 | 2 | 80 | 2 | 2 | stable |
| 46 | 83 | 2 | 78 | 2 | 2 | stable |
| 47 | 91 | 2 | 80 | 2 | 2 | stable |

| | | | | | | |
|---|---|---|---|---|---|---|
| 48 | 104 | 3 | 85 | 2 | 2 | stable |
| 49 | 95 | 2 | 81 | 2 | 2 | stable |
| 50 | 106 | 3 | 91 | 2 | 2 | stable |
| 51 | 90 | 2 | 78 | 2 | 2 | stable |
| 52 | 91 | 2 | 81 | 2 | 2 | stable |

Similar tables for the year 2020 can be found in Appendix A (Tables A.2 to A.4).

To visualize the overall robustness of the plant in 2019 and 2020 with different weighting scenarios, a histogram is plotted in Figure 3.23, which summarizes the findings in Tables 3.8 to 3.10, and A.2 to A.4.

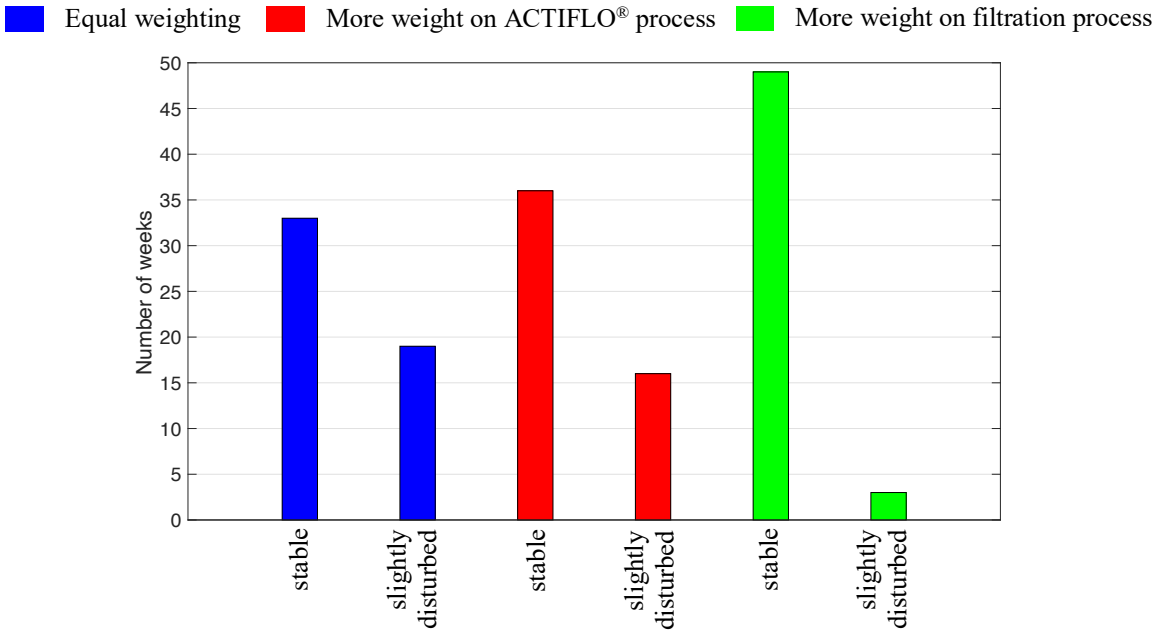

(a)

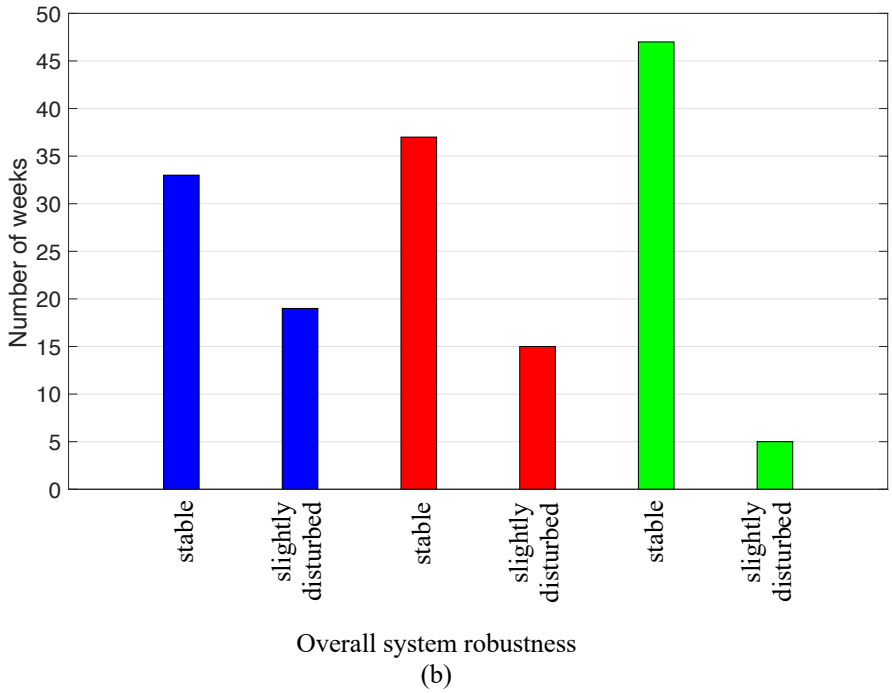


Figure 3.25: Overall robustness category of Plant A in (a) 2019 and (b) 2020 with equal and unequal weightings

It should be noted that the "slightly disturbed" class implies that the system performed excellently during most of the period, and no overall system robustness was found to be greater than 3, which refers to the "slightly disturbed" class (Chapter 2: Table 2.8).

From Figure 3.25, it is clear that changing the weighting of the treatment processes has an effect on the overall robustness category. With equal weighting of the two processes, larger number of "slightly disturbed" TRIs are observed, but its applicability is not ideal. If the robustness category of one process is equal to 3, and the other is 2, the arithmetic average is 2.5, which becomes 3 with upper rounding corresponding to the "slightly disturbed" class. Thus, using the same weighting may not be logical since different processes have different purposes.

Putting more weight to the ACTIFLO® process, it is found that the system was "slightly disturbed" for 31 weeks out of 104 weeks in 2019 and 2020. 15 weeks (48.4%) of those weeks were affected by weather events characterized by higher raw water turbidity. In contrast, when more weighting was put

to the filtration process, for 8 weeks in two years, the overall system was in the "slightly disturbed" class, among which 2 weeks (25%) were affected by weather events according to the method described in sub-section 3.3.1.2. Therefore, it can be said that the ACTIFLO® process is more sensitive to elevated turbidity in raw water, which is expected because it is the first process to encounter the turbidity rise in raw water. These results also indicate that the system was "slightly disturbed" in some weeks when the turbidity was considered normal, and there may be operational factors behind this. Therefore, the overall robustness of the plant did not depend on raw water turbidity events.

## 3.4 Conclusion

Due to the geographic location and raw water source of Plant A, it is very vulnerable to elevated turbidity in the raw water caused by weather events. Nevertheless, the TRIs of the ACTIFLO® and filtration process, which are the critical treatment steps in terms of turbidity removal, suggest that the treatment steps are meeting the goal turbidity of each step. No positive correlation is found between weather events characterized by elevated turbidity and the TRIs of these treatment steps. Finally, the overall plant robustness indicates that Plant A has successfully delivered treated water with desired quality in terms of turbidity in the years 2019 and 2020.

# Chapter 4: Evaluation of Robustness of Plant B

## 4.1 Introduction

Plant B is a DWTP located in southern Ontario, using Lake Ontario as the source. As of 2021, the plant supplies drinking water to a large municipal residential system serving a population of 536,917 (Ontario Regulation, 2021). Since the plant draws water from Lake Ontario and the opening of the intake pipe is at a substantial distance from the shore, the raw water is less likely to be affected by municipal and agricultural runoff like rivers and creeks. During heavy precipitation events, the plant experiences elevated turbidity in the raw water, which is mostly caused by the wind direction (easterly wind) transporting particles from resuspended sediments and run-off towards intake pipes. The plant used to face 2-3 heavy precipitation events per year, but the number has increased to 4-5 in recent years (Staff of Plant B, July 2021). With the rise of climate change, more frequent and severe unseasonal precipitation events may occur in the near future. This may pose a challenge to maintain regulated water quality parameters including turbidity, which is the selected water quality parameter in this study. Health Canada (2012) has suggested regulatory limits for turbidity for different filtration techniques (listed in Table 2.3). This chapter aims to apply two steps of the robustness framework (shown in Figure 2.6) to Plant B, Step 4: Evaluation, which is to evaluate the robustness of the critical treatment steps of the plant that can be affected by elevated raw water turbidity, and Step 5: Assessment, which is to assess the overall robustness of the plant with respect to turbidity removal for calendar years 2019 and 2020.

## 4.2 Materials and Methods

### 4.2.1 Plant Description

Plant B is a conventional treatment plant. The monthly drinking water production of Plant B ranged from 186 to 235 ML/D in the year 2021, while the Municipal Drinking Water License (MDWL) daily rated capacity was 926 ML/D. It has three raw water intake pipes with 1.22 m, 1.52 m, and 2.44 m diameters, which can draw raw water from Lake Ontario at distances of 640 m, 915 m, and 945 m from the shore. Two intake pipes (1.52 m and 2.44 m diameters) are currently in use (Ontario Regulation, 2021; Staff of Plant B, January 2022).

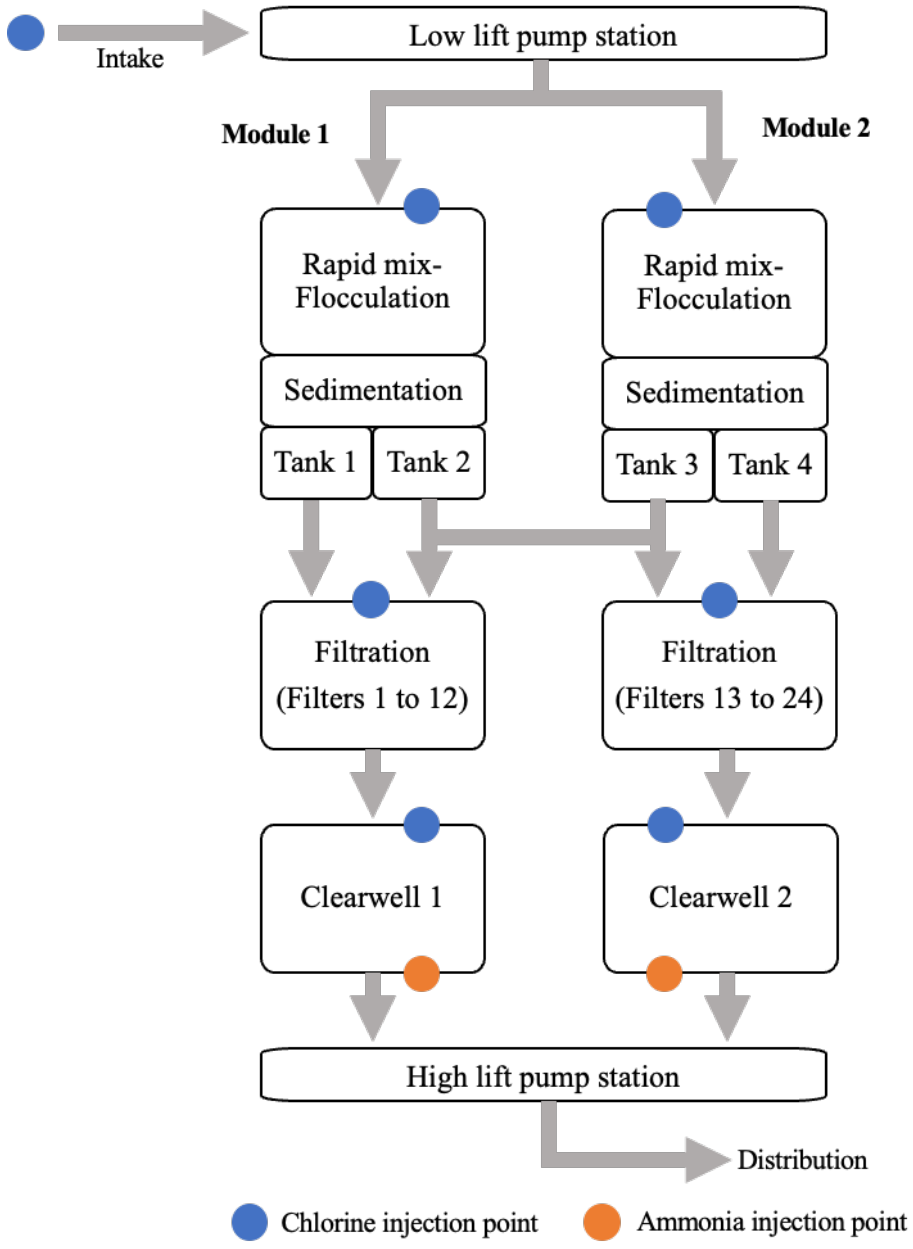


Figure 4.1: Plant B process flow diagram

Figure 4.1 shows the treatment process flow of Plant B. The water is pumped by the low lift pump from the intake pipes. There are 3 traveling screens at the low lift pumping station to screen the water before pumping the water into the treatment plant (Ontario Regulation, 2021).

The intake water is split into two parallel treatment trains (modules 1 and 2). The facility employs year-round pre-chlorination at the intake, followed by coagulation (rapid mix), flocculation, and sedimentation as pre-treatment. PACl is injected as a coagulant. Additional chlorine is also added to ensure disinfection. Five PACl pumps draw from two PACl tanks to pump PACl to four rapid mix tanks. The suspended solids in the water collide with one another due to the action of the mixers the coagulant assists in their clumping together. The flocs are carried along with the outflow from the rapid mix tanks into the flocculation tanks and then the sedimentation tanks, where the flocs settle to the bottom of the tanks. The effluent water moves to the filters (Eramosa Engg. Inc. et al., 2015; Singh, 2018).

There are 24 dual media filters containing sand (depth: 150-230 mm) and granular activated carbon (GAC) (depth: 740 mm). As shown in Figure 4.1, sedimentation tank 1 can only feed Filters 1 to 12, and tank 4 can only feed Filters 13 to 24. Tanks 2 and 3 can feed all the filters if the interconnecting valve is open. If the interconnecting valve is closed, tanks 1 and 2 can only feed Filters 1 to 12, and tanks 3 and 4 can only feed Filters 3 and 4, separating the treatment process into two independent trains (Staff of Plant B, January 2022). A chlorine residual is present through filtration, where the GAC adsorbs any remaining chlorine (Singh, 2018).

After filtration, the effluent water from Filters 1 to 12 moves to clearwell 1, and the effluent water from Filters 13 to 24 moves to clearwell 2. Chlorine is added again in the clearwells. Ammonia is added before the treated water enters the distribution system to convert chlorine into mono-chloramine to help maintain stable chloramine residuals (Ontario Regulation, 2021; Singh, 2018).

Using the high lift pumps, the finished water is finally moved to the distribution system (Ontario Regulation, 2021).

### 4.2.2 Available Data

The plant framework (discussed in Chapter 2: section 2.4), developed by Nemani (2021a) was applied to Plant B. The timeframe of the study was selected to be two calendar years, 2019 and 2020, the same

as Plant A. The selected water quality parameter in this study is turbidity. According to Step 3: Identification of the framework (discussed in Chapter 2: sub-section 2.4.3), the critical treatment steps that are affected by turbidity are, CFS and filtration. On-line turbidity and flow data from January 2019 to December 2020 were requested from the plant as well as the dimensions for all the tanks and basins. Table 4.1 provides an overview of the available data.

Table 4.1: On-line monitoring data obtained from Plant B

| Location | Frequency |
|---|---|
| Raw water turbidity | Every 5-minutes |
| CFS (modules 1 and 2) effluent turbidity | Every 5-minutes |
| Filter (1 to 24) effluent turbidity | Every 1-minute |
| Pre-treatment (modules 1 and 2) flow rate | Every 5-minutes |
| Filtration units (1 to 24) flow rate | Every 1-minute |
| PACl flow rate (lines 1 to 4) | Every 1-minute |

### 4.2.3 Identification of Invalid Data

Similar to Plant A, the data points that do not represent the actual condition of Plant B were removed before analysis. According to the plant operators, these data can result from instrument errors or recordings during maintenance and repair activities, and/or plant shutdowns. The same methods that were developed to identify and remove the invalid data points from the data set for Plant A were applied to Plant B, and modified where required after consulting with the plant operators. The methods were modified to identify the invalid data points from the CFS and filter effluent turbidity data.

#### 4.2.3.1 Raw Water Turbidity Data

The raw water turbidity data of the year 2019 were plotted in a time series in Figure 4.2. Similar to Plant A (shown in Figure 3.2), in this figure, some data points were observed to be very high compared to the adjacent data points.

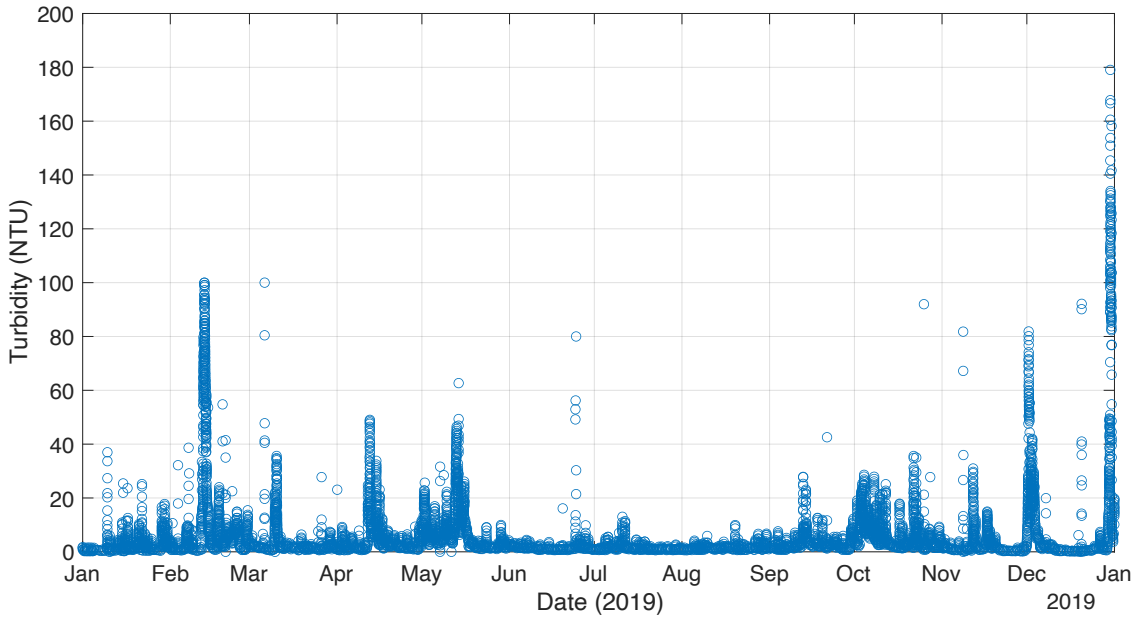


Figure 4.2: Time series of raw water turbidity data (2019)

From Chapter 3: sub-section 3.2.3.1, the final method to identify invalid data points from raw water turbidity data is as follows: invalid data = 100% above the hourly median. This is the same method that was developed for Plant A. MATLAB functions (Appendix D: Code D.1 and D.2) were used to remove the invalid data points prior to analysis.

The time series of the raw water turbidity data after removing the invalid data points for the year 2019 is shown in Figure 4.3. 161 out of 105108 (0.15%) data points were removed as invalid data. The same method is applied to the raw water turbidity data for the year 2020, which is shown in Figure 4.4. 232 out of 105396 (0.22%) data points were removed as invalid data.

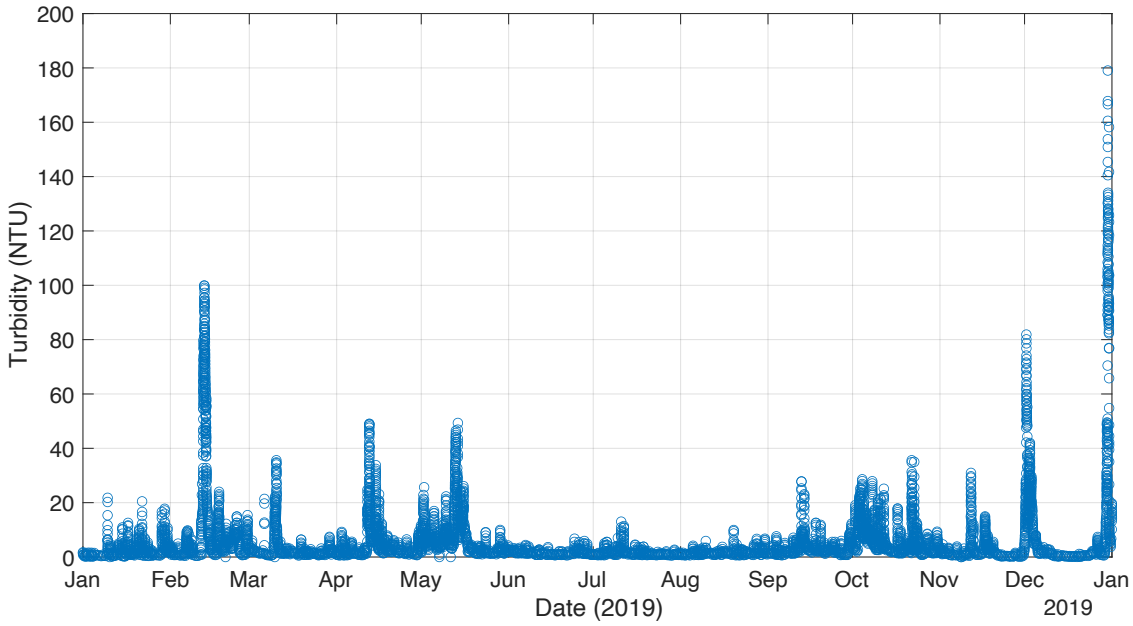


Figure 4.3: Time series of raw water turbidity data (2019) with invalid data points removed

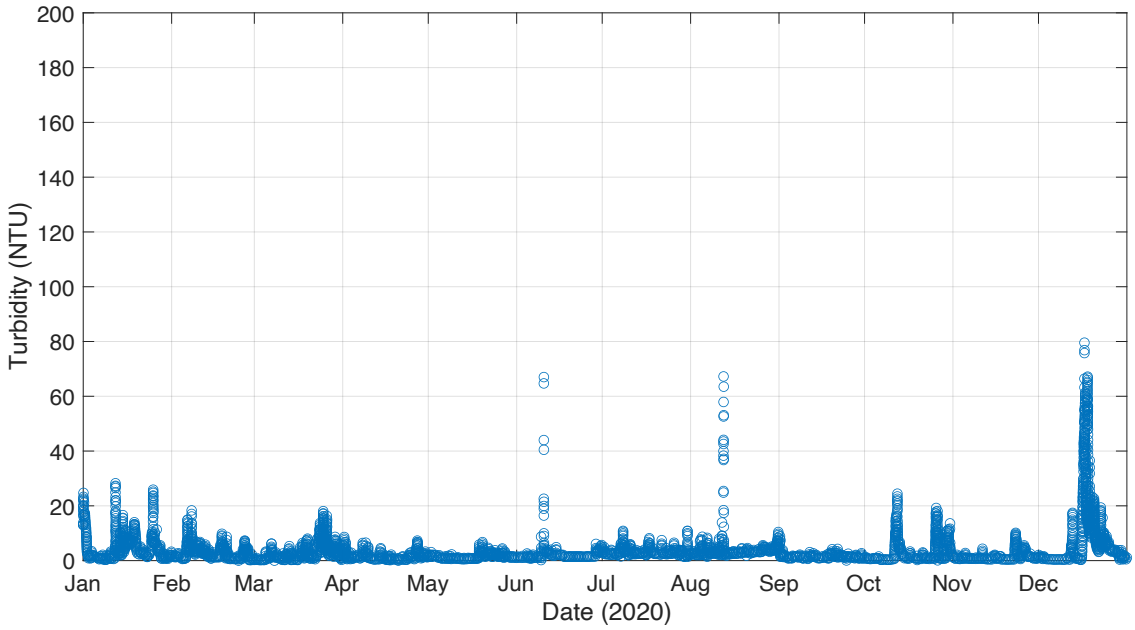


Figure 4.4: Time series of raw water turbidity data (2020) with invalid data points removed

#### 4.2.3.2 CFS Effluent Turbidity Data

The validity of the CFS effluent turbidity data can be determined by analyzing the following data:

1. Pre-treatment water flow rates to the rapid mix tanks.
2. PACl flow rates to the rapid mix tanks.

If the pre-treatment water flow rate is zero, it implies that there was no water going into the coagulation tanks, which may occur due to plant/module shutdowns for various reasons. If the flow rate is below 5 ML/D, no coagulant is added to the coagulation tanks (Eramosa Engg. Inc. et al., 2015; Staff of Plant B, July 2021). Thus, if the pre-treatment water flow rate is less than 5 ML/D, it indicates that the plant and/or the CFS units are being shut down or started up from a shutdown.

In addition to the pre-treatment water flow rates, the PACl flow rate also determines the validity of the CFS effluent turbidity data. Figure 4.5 shows the time series of PACl flow data of each line for the year 2019. A similar figure for the year 2020 can be found in Appendix B (Figure B.1). From Figures 4.5 and B.1, it is observed that one or more PACl lines were shut down during the study period as the flow continued to be zero.

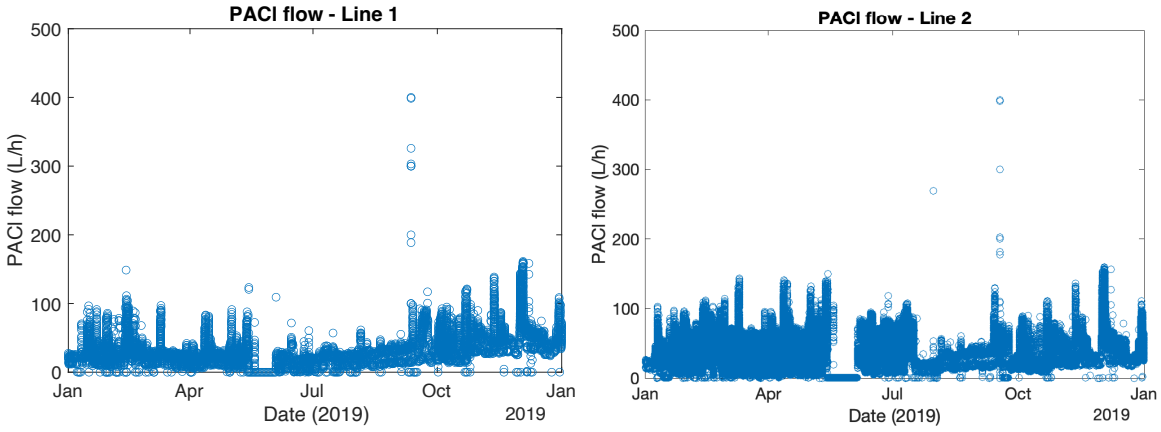


(a) (b)

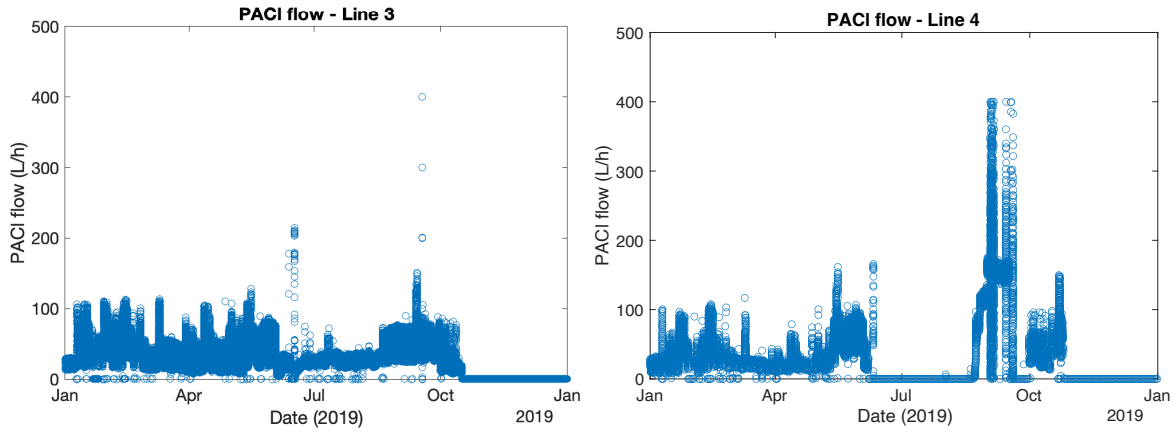


(c) (d)

Figure 4.5: Timeseries of PACl flow (L/h) (a) line 1, (b) line 2, (c) line 3 and (d) line 4 for the year 2019

Lines 1 and 2 feed the module 1 CFS unit and lines 3 and 4 feed the module 2 CFS unit. If the total PACl flow of lines 1 and 2 is equal to zero, it implies that no coagulation was taking place during those periods in module 1. The total flow of lines 3 and 4 has similar implications. From Figures 4.5 and B.1, Table 4.2 was generated indicting the shutdown periods of the PACl lines and corresponding modules.

Table 4.2: PACl line and module shutdown periods based on PACl flow data

| **Line/Module** | **Shutdown periods** |
|---|---|
| PACl line 1 | 13 May 2019 to 3 June 2019, 19 February 2020 to 4 June 2020, 19 August 2020 to 12 November 2020. |
| PACl line 2 | 13 May 2019 to 5 June 2019, 19 February 2020 to 8 June 2020. |
| CFS module 1 | 13 May 2019 to 3 June 2019, 19 February 2020 to 4 June 2020. |
| PACl line 3 | 16 October 2019 to 16 February 2020, 13 November 2020 to 20 November 2020. |
| PACl line 4 | 7 June 2019 to 22 August 2019, 19 September 2019 to 30 September 2019, 25 October 2019 to 18 February 2020, 12 June 2020 to 16 June 2020. |
| CFS module 2 | 25 October 2019 to 16 February 2020. |

Hence, turbidity values recorded in the online turbidimeter during these periods do not represent the actual condition and can be removed as invalid data points. A MATLAB function (Appendix D: Code D.8) was used to identify and remove the data points corresponding to raw water flow rates less than 5 ML/D and PACl flow rates in both lines for the corresponding module equal to zero from the CFS effluent turbidity data sets. Overall, 21.3% of the data were removed.

#### 4.2.3.3 Filter Effluent Turbidity Data

Similar to the previous sub-section, the flow rates of each filter determine the validity of the filter effluent turbidity data. If the flow rate is zero, it implies that there was no water going into the filter which may occur due to filter backwash, maintenance work, and plant shutdowns for various reasons. As mentioned before, Plant B has 24 filters and usually, 12 to 18 of them run simultaneously while the others are kept on stand-by (Staff of Plant B, July 2021). After backwash when putting filters to service again, filters are operated at 5 ML/D flow rate for around 20 minutes and the effluent turbidity is checked (Staff of Plant B, January 2022). If the effluent turbidity is under the regulatory limit (0.3 NTU), the filters are ramped up to a higher flow rate (15 to 22 ML/D) (Staff of Plant B, July 2021). In the study period, no effluent turbidity data in the first 20 minutes of a filter run was found to be greater than 0.3 NTU. Therefore, the turbidity data corresponding to filter flow rates equal to zero were identified and removed for every filter using a MATLAB function (Appendix D: Code D.9).

As discussed in sub-section 4.2.1, due to the interconnecting valve it cannot be said that Filters 1 to 12 were not operated when the CFS unit of module 1 was shut down, and Filters 13 to 24 were not operated when the CFS unit of module 2 was shut down, because tanks 2 and 3 can feed all the filters if the interconnecting valve is open. The opening and closing log of all the valves connecting the sedimentation tanks and the filters during the study period was provided by the utility, which was used to determine when the filters were not operating, and the corresponding filter effluent turbidity data were removed. Overall, 45.7% data were removed.

### 4.2.4 Data Analysis Approach

The plant framework developed by Nemani (2021a) was applied in this study. Step 4: Evaluation in the plant framework (discussed in Chapter 2: sub-section 2.4.4) focused on quantifying the robustness of

the treatment steps that are affected by changes in the selected raw water quality parameter(s), which is elevated turbidity caused by heavy and unusual precipitation events in this study. Thus, it is necessary to distinguish between the raw water turbidity levels during normal weather and weather events that can cause a significant increase in turbidity at the intake. The same two scenarios as Plant A were established for Plant B using raw water turbidity data, which are:

1. Normal weather characterized by baseline raw water turbidity.
2. Weather events, characterized by elevated turbidity in the raw water.

The same methods discussed in Chapter 3: sub-section 3.2.4 were used to evaluate the TRIs of the CFS units and the filters. The HRTs of different tanks within the CFS processes were calculated using the median flow rates, and then used to offset the turbidity data points so that the comparisons between raw water turbidity data, and CFS unit and filter effluent turbidity data are more logical. The HRTs of the treatments units in Plant B using the median flow rates are shown in Table 4.3.

Table 4.3: HRTs of different treatment units in Plant B

| **Unit** | | | **Hydraulic Retention Time (HRT)** |
|---|---|---|---|
| CFS unit | Module 1 | Coagulation tank | 3m 20s |
| | | Flocculation tank | 1h 59m |
| | | Sedimentation tank | 5h 19m |
| | | Total | 7h 22m |
| | Module 2 | Coagulation tank | 3m 23s |
| | | Flocculation tank | 2h 1m |
| | | Sedimentation tank | 5h 24m |
| | | Total | 7h 29m |

## 4.3 Results and Discussion

### 4.3.1 Identification of Normal Turbidity and Turbidity Events

As discussed in Chapter 3: sub-section 3.2.4, to evaluate the robustness of the critical treatment steps, it is important to separate the calculated TRIs based on weather to determine whether the treatment steps are affected by weather events or not. From the time series of the raw water turbidity (Figures 4.3 and 4.4), some turbidity peaks can be observed that indicate precipitation-related weather events in the area. For Plant A, two methods were developed using yearly (Chapter 3: sub-section 3.3.1.1) and seasonal (Chapter 3: sub-section 3.3.1.2) median raw water turbidity. The latter was selected because the difference between yearly and seasonal median turbidities in Plant A was too high for the spring season, and so the method using the yearly median turbidity could not distinguish between separate weather events. However, in Plant B the difference between the yearly and seasonal median raw water turbidity is not that high. Table 4.4 shows the yearly and seasonal median raw water turbidity of Plant B for the years 2019 and 2020.

Table 4.4: Yearly and seasonal raw water median turbidities of 2019 and 2020

| **Season** | **Winter** | **Spring** | **Summer** | **Fall** | **Yearly** |
|---|---|---|---|---|---|
| **Duration** | Jan 2019 - Feb 2019 | Mar 2019 - May 2019 | Jun 2019 - Aug 2019 | Sep 2019 - Nov 2019 | Jan 2019 - Dec 2019 |
| **Median turbidity (NTU)** | 0.99 | 1.87 | 1.14 | 1.94 | 1.39 |
| **Duration** | Dec 2019 - Feb 2020 | Mar 2020 - May 2020 | Jun 2020 - Aug 2020 | Sep 2020 - Nov 2020 | Jan 2020 - Dec 2020 |
| **Median turbidity (NTU)** | 1.48 | 1.08 | 2.40 | 1.01 | 1.45 |

The differences between the respective seasonal and the yearly median turbidities varied from -0.40 to +0.55 NTU in 2019 and -0.44 to +0.95 NTU in 2020, which is substantially lower compared to Plant A. The revised method developed for Plant A (turbidity event = y% above the seasonal median, for at least one hour) was applied to the raw water turbidity data of Plant B varying the value of y from 25% to 100%, which is shown in Figure 4.6.

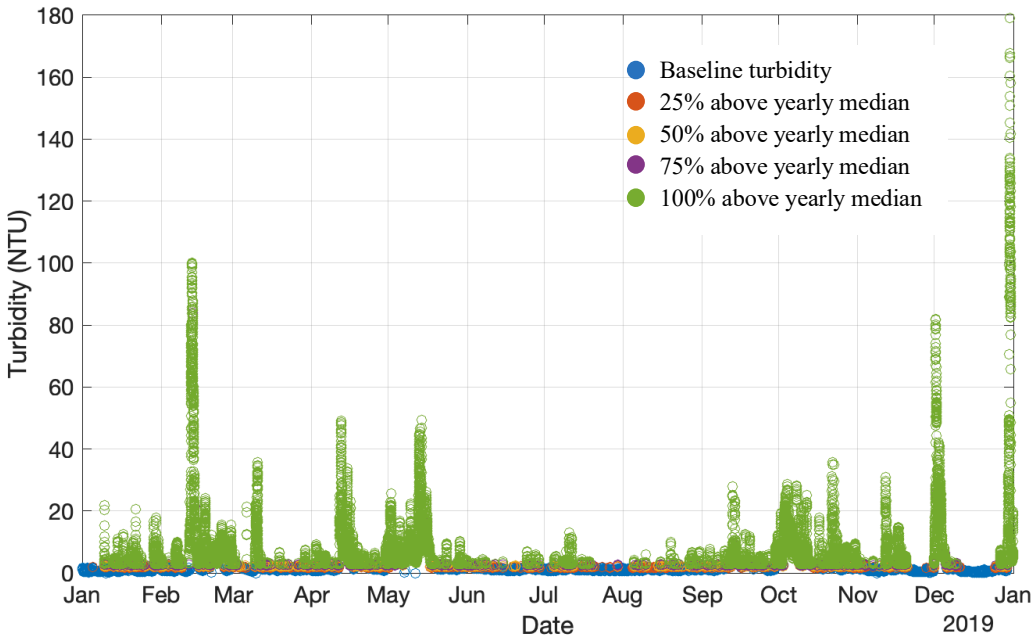


Figure 4.6: Time series of raw water data (2019) with turbidity peak events using corresponding seasonal median raw water turbidity

In Figure 4.6, it is very difficult to visualize the data points that are not green, which represents the turbidity data that are 100% above the seasonal median raw water turbidity. Since the seasonal median turbidities are very low compared to the peak turbidities, this method is considering almost all the raw water turbidity data points as weather events, which is not possible. Therefore, the method developed for Plant A cannot be applied to Plant B.

According to the plant operators, if the raw water turbidity is lower than 10 NTU, it is considered normal (Staff of Plant B, July 2021). To make this analysis a bit stricter, the following method was used to identify normal weather and weather events: turbidity event = 100% above the seasonal median + 5

NTU, for at least one hour. The value “5 NTU” was selected so that the baseline turbidity values that represent normal weather cannot exceed 10 NTU. For instance, in the case of the season summer 2020, the median turbidity is 2.40 NTU, which is the highest median raw water turbidity in the study period. According to this method, if the raw water turbidity in summer 2020 is below 9.80 NTU, it represents normal weather characterized by raw water turbidity.

Figures 4.7 and 4.8 show the time series of raw water turbidity of the year 2019 and 2020 respectively, indicating normal turbidity levels and turbidity events characterized by raw water turbidity using this method.

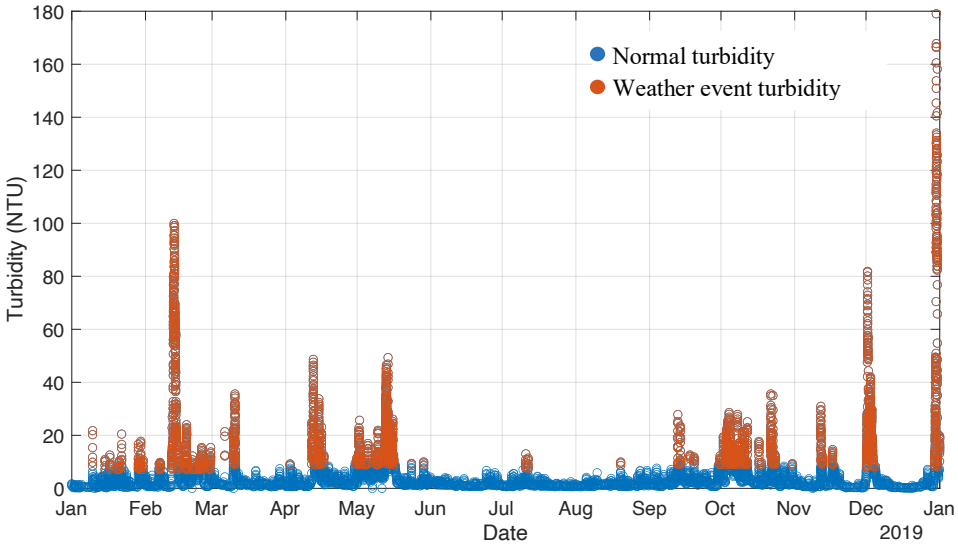


Figure 4.7: Time series of raw water turbidity (2019) showing normal turbidity and turbidity events

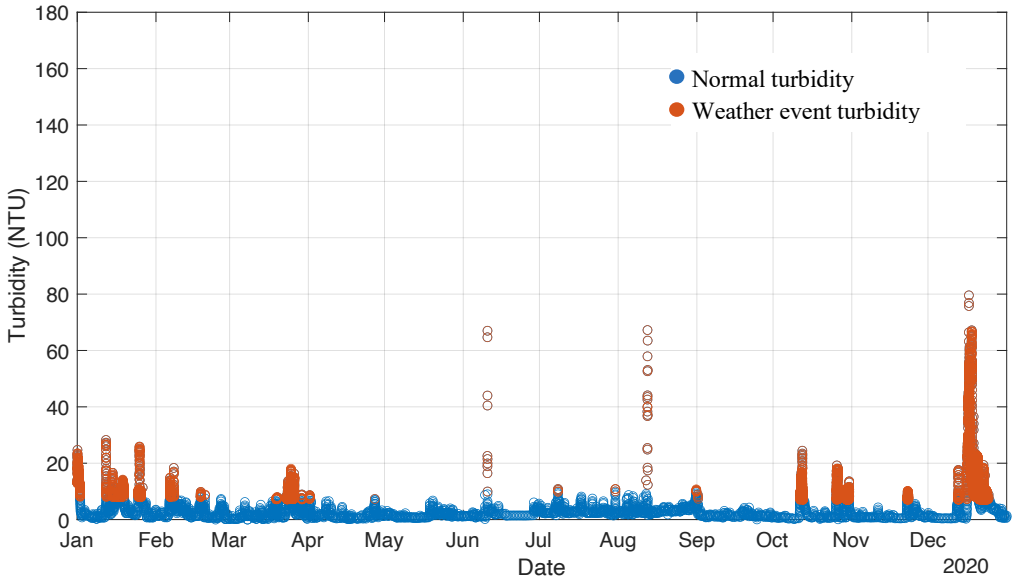


Figure 4.8: Time series of raw water turbidity (2020) showing normal turbidity and turbidity events

### 4.3.2 Robustness of the CFS Units

According to the fourth step "evaluation" of the plant framework, the TRIs were calculated for the CFS units with Equation 2.5. To calculate the TRIs for every week of the year 2019 and 2020, a goal turbidity is required as stated in Step 2: Criteria of the plant framework. There is no regulatory limit set for CFS effluent water, since it is not the final treatment step to remove turbidity. DWTPs generally have a goal turbidity for conventional CFS effluent water so that elevated effluent turbidity cannot overwhelm the filters and/or fail to produce filtered water maintaining the regulatory limit (listed in Table 2.3). In Plant B, the goal turbidity (Tgoal) of the CFS effluent water is 1.0 NTU. A stricter goal (Tgoal = 0.5 NTU) was selected during the initial analysis to observe the effects of different turbidity goals in calculating TRIs. In Figure 4.9, the TRIs of the module 1 CFS unit for the year 2019 are calculated for two TRI goals, 0.5 NTU shown by the blue bars, and 1.0 NTU shown by the orange bars. The lower the turbidity goal, the stricter the criterion, which should lead to higher TRI values. All the TRIs with Tgoal = 0.5 NTU are higher than those with Tgoal = 1.0 NTU as expected. The classes of the TRIs are discussed later in this section.

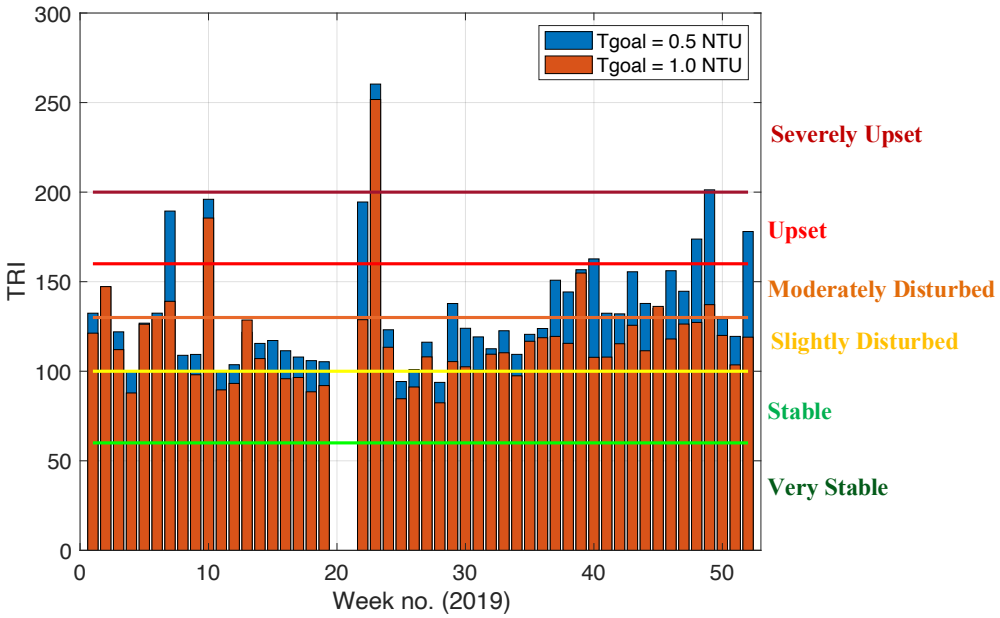


Figure 4.9: Weekly TRIs of the module 1 CFS unit (2019) with varying Tgoals

According to the plant operators, the goal turbidity of the CFS units in Plant B is 1.0 NTU, so the goal value of 1.0 NTU was used to calculate the TRIs of the CFS units in further analysis. Figures 4.10 and 4.11 show the weekly TRIs of modules 1 and 2 CFS units respectively for the years 2019 and 2020.

The blue bars represent the TRIs during normal weather and the red bars represent the TRIs corresponding to the weeks that were affected by weather events, which were identified using the method developed in sub-section 4.3.1. The empty spaces in the figure represent unit shutdown during the corresponding weeks due to maintenance or repair work.

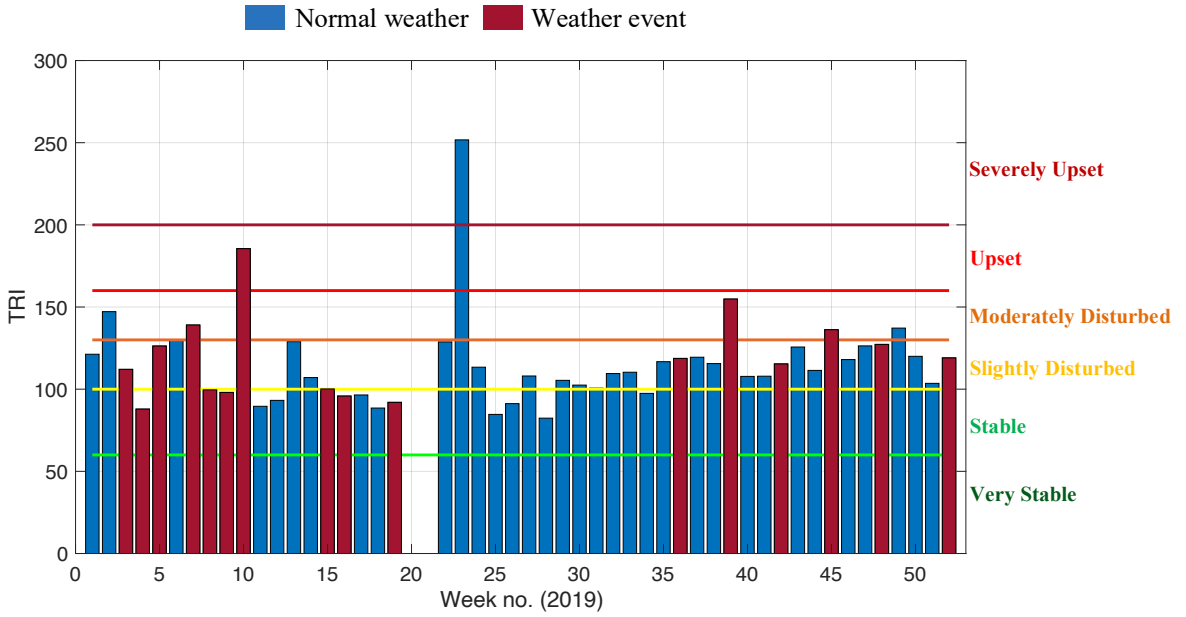


(a)

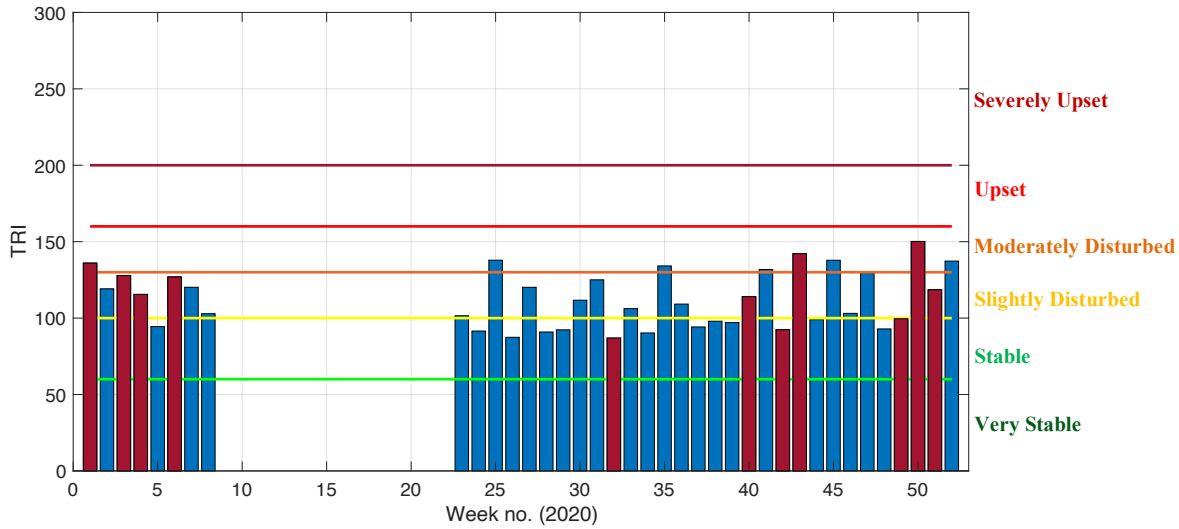


(b)

Figure 4.10: Weekly TRIs during normal weather and weather events characterized by raw water turbidity of module 1 CFS unit in (a) 2019 and (b) 2020 (Tgoal = 1.0 NTU)

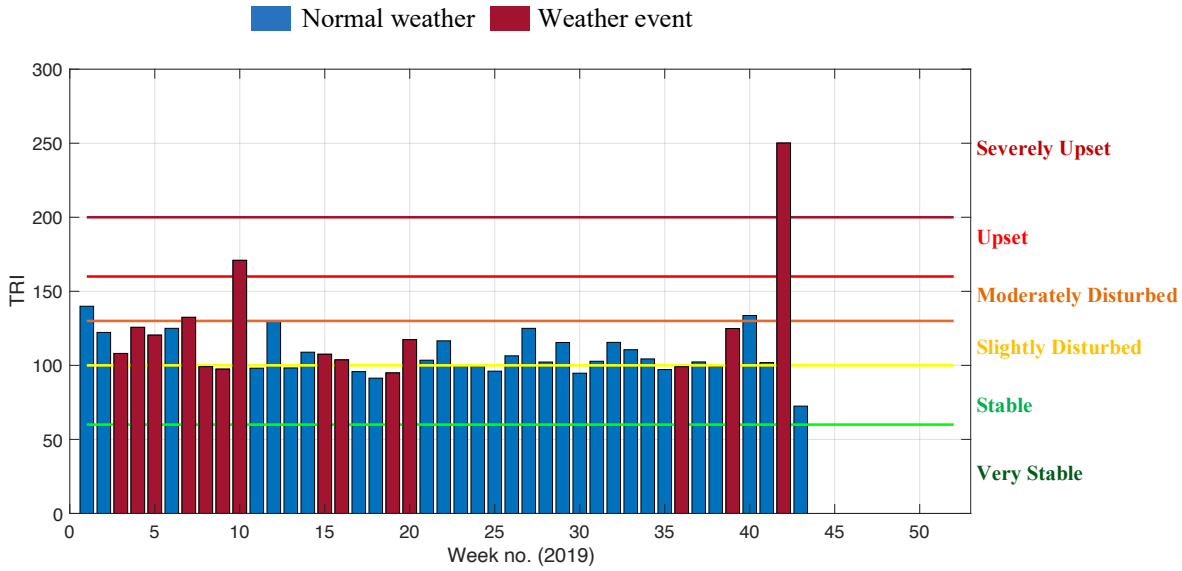


(a)

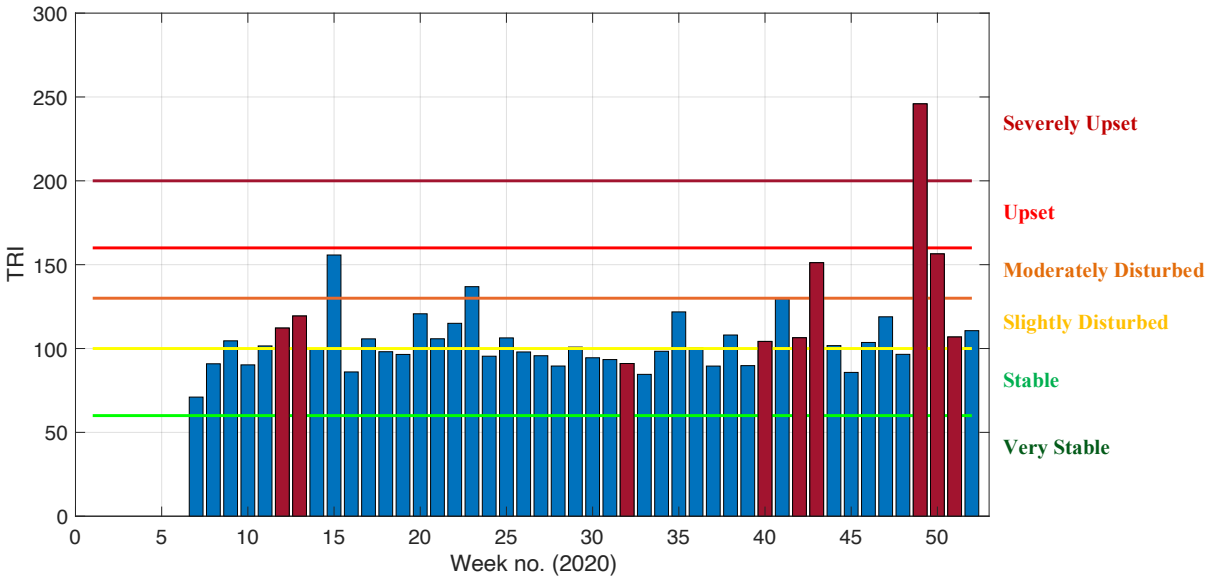


(b)

Figure 4.11: Weekly TRIs during normal weather and weather events characterized by raw water turbidity of module 2 CFS unit in (a) 2019 and (b) 2020 (Tgoal = 1.0 NTU)

For 27 weeks in the study period (104 weeks), TRIs fall into the “stable” (60-100) class, which indicates that the 50th and the 90th percentile turbidity were below the goal turbidity and the CFS unit always maintained the desired quality (effluent turbidity < 1.0 NTU) for the respective weeks.

For 46 weeks in the study period, the TRIs fall into the “slightly disturbed” (100-130) class, which indicates that either both 50th and 90th percentile turbidity was close to the goal turbidity and/or the 90th percentile turbidity was greater than the goal turbidity in some cases. The CFS unit produced effluent water with the desired quality most of the time during the given weeks.

For 13 weeks in the study period, the TRIs fall into the “moderately disturbed” (130-160) class, which indicates that both 50th and 90th percentile turbidity was higher than the goal turbidity. The CFS unit could not produce effluent water with the desired quality for a short duration (around 30% of the week) during the given weeks.

For one week in the study period, the TRI falls into the “upset” (160-200) class, and for one week the TRI falls into the “severely upset” (>200) category, which indicate that both 50th and 90th percentile turbidity was almost two times higher than the goal turbidity. The CFS unit could not produce effluent water with the desired quality.

It should be noted that the classification system regarding the TRI values was developed based on the turbidity data analysis for filter runs, so the name of the classes may not be as precise in this case as this is an entirely different treatment step with different duration, but the mathematical interpretation of the TRI should be valid.

The definition of robustness implies that if the performance of a system is observed to exacerbate during upsets, the system would not be considered robust. In Figures 4.10 and 4.11, it is observed that the TRIs corresponding to weather events (red bars) are mostly (75 out of 80) greater than 130, which indicates that the performance of the CFS units may not be robust, according to the definition used in this analysis.

The high TRI values during normal weather (blue bars) were investigated and it was found that the influent turbidity was very low. It is reasonable to infer that there were not enough particles in the water to react with the coagulant, which resulted in a higher CFS effluent water turbidity.

To investigate the effect of the extremity of weather events on TRI, Figure 4.12 was generated. In this figure, the TRIs corresponding to weather events as characterized by raw water turbidity were plotted

against the maximum or 'peak' turbidity of the event, which represents the extremity of the event. However, no positive correlation ($R^2 \approx 0$) was observed between the TRIs and peak turbidities of a weather event, implying that the peak turbidity of the weather events did not affect TRIs in 2019 and 2020.

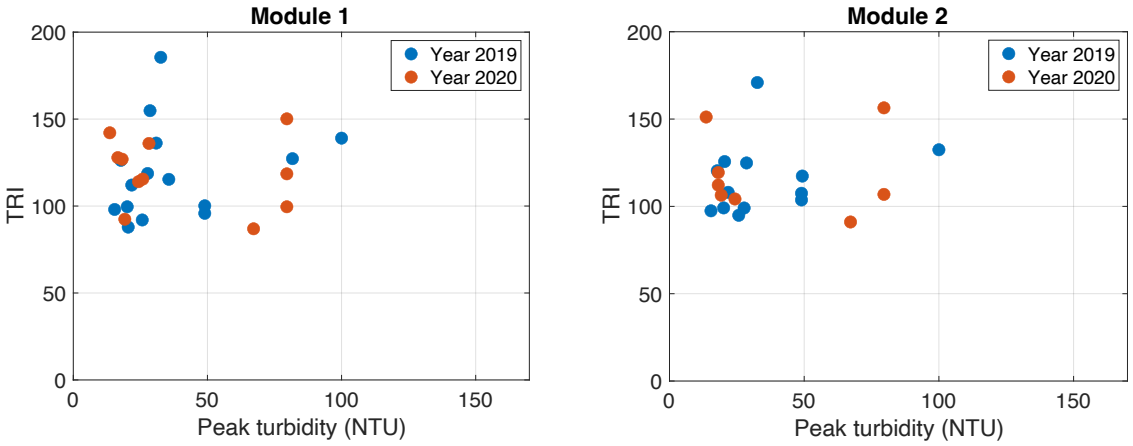


(a) (b)

Figure 4.12: Weekly TRIs of the (a) module 1 and (b) module 2 CFS unit in relation to the maximum values of raw water turbidity during weather events

In addition to the TRI plots, in order to visualize the overall performance of the CFS units, the weekly average raw water turbidities are plotted against the weekly average module 1 and module 2 CFS effluent turbidity for the years 2019 and 2020 in Figures 4.13 and 4.14 respectively to observe the weekly turbidity removal by the CFS units.

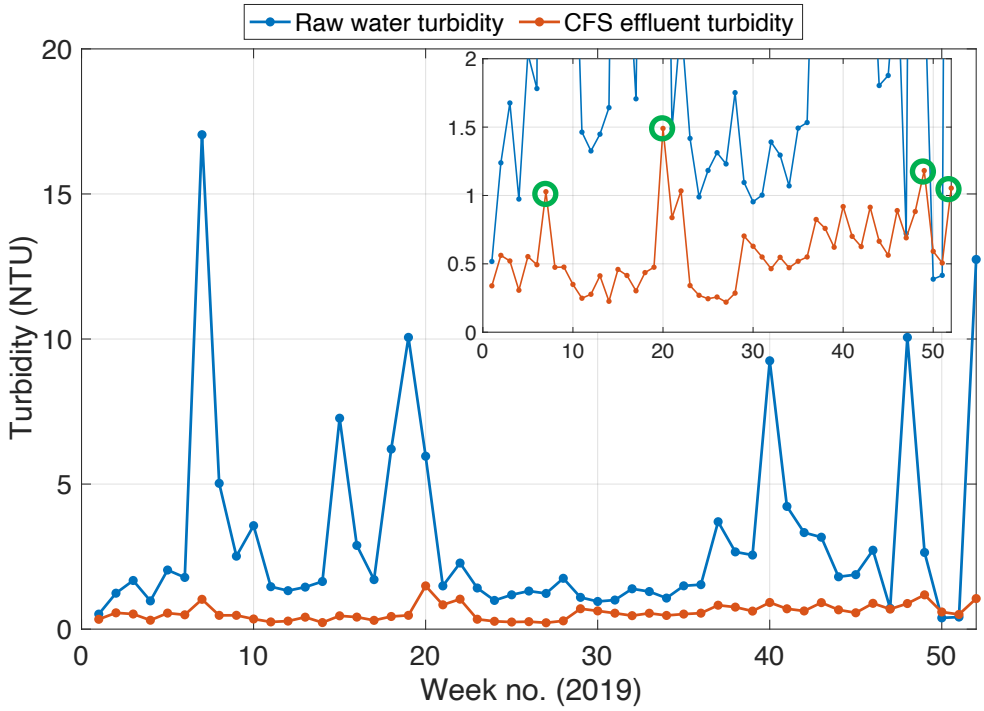


(a)

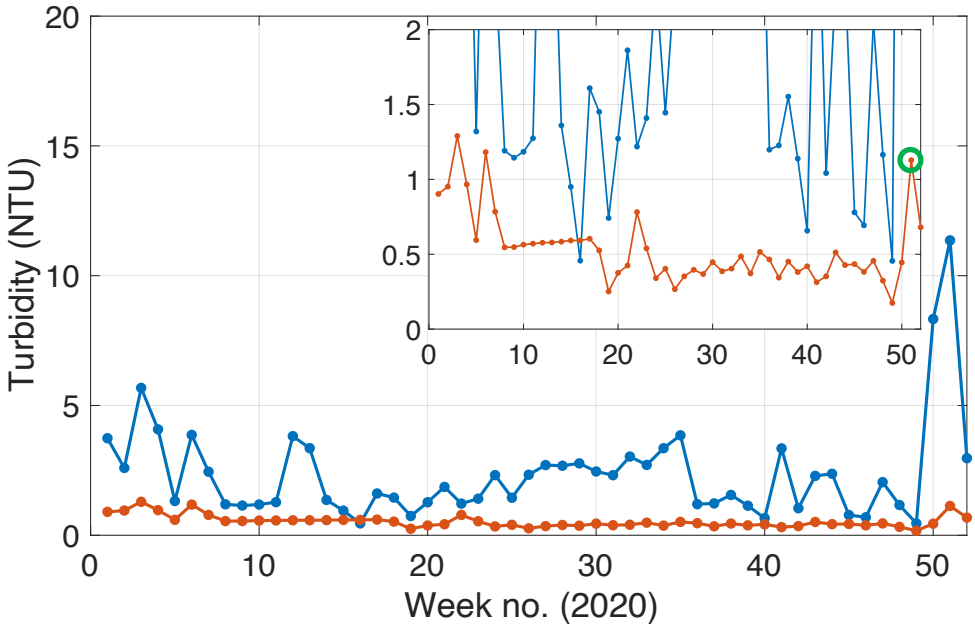


(b)

Figure 4.13: Weekly average raw water and module 1 CFS influent and effluent turbidity in (a) 2019 and (b) 2020

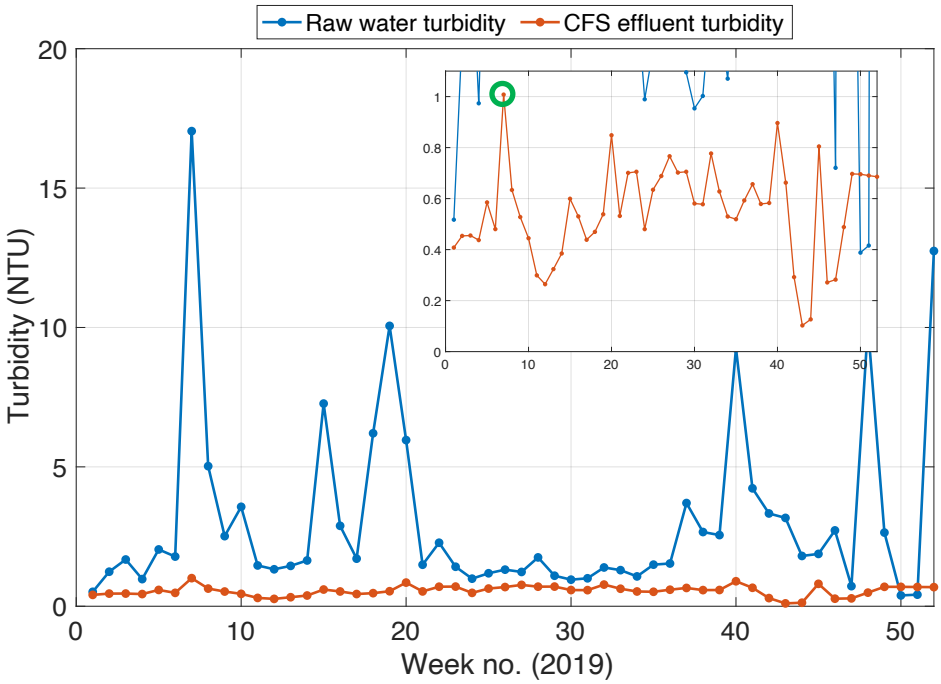


(a)

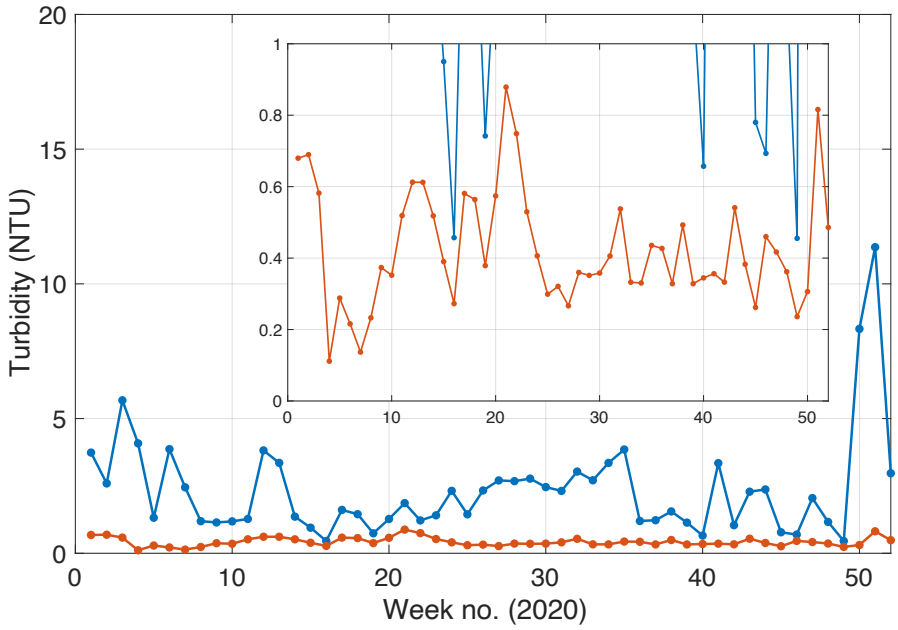


(b)

Figure 4.14: Weekly average raw water and module 2 CFS influent and effluent turbidity in (a) 2019 and (b) 2020

In both figures, it is observed the weekly average module 1 and 2 CFS effluent turbidities are above the goal turbidity (1.0 NTU) during some weather events characterized by turbidity (indicated with green circles in the figures), which explains the high TRIs during these events. For the TRIs in the "upset" and "severely upset" class, the weekly average CFS effluent turbidities were lower than the goal turbidity. However, the 90th percentile turbidity was significantly higher than the goal turbidity, which resulted in these "upset" and "severely upset" TRIs. In module 1, for 2 weeks in 2019 and 1 week in 2020 and in module 2 for 2 weeks in 2019, the weekly average CFS effluent turbidity is found to be higher than the weekly average raw water turbidity. In these cases, the raw water turbidity was very low, which may have impacted the coagulation mechanism.

### 4.3.3 Robustness of Filtration Units

In Plant B, filtration is the last step to remove particles, i.e., turbidity. To evaluate the robustness of the filtration units with TRI, a goal turbidity is required as specified by the second step "criteria" (Chapter 2: sub-section 2.4.2) in the plant framework. Plant B follows the regulatory limit set by the Government of Ontario based on Health Canada (2012), which states that the effluent turbidity of every filter must be less than or equal to 0.3 NTU for at least 95% of the measurement per cycle per month, with a target of less than 0.1 NTU, and the turbidity can never exceed 1.0 NTU (listed in Chapter 2: Table 2.3). Since there are 24 filters in Plant B, only the data analysis result of two representative filters (Filter 2 from module 1 and Filter 18 from module 2) is discussed in this chapter. Filter 2 represents the average performance of all the filters in Plant B. Filter 18 shows some of the highest TRIs observed in this analysis, so it was chosen to discuss the worst-case scenario. The TRIs of the other filters are shown in Appendix B (Figures B.2 to B.8).

Initially, the TRIs were calculated using two goals, 0.3 NTU and 0.1 NTU to observe the effect of goal turbidity values in TRI calculation. Figure 4.15 shows the TRIs of Filter 2 for the year 2019 for the two goals, 0.3 NTU shown by the orange bars and 0.1 NTU shown by the blue bars. All the TRIs with Tgoal = 0.3 NTU are lower than those with Tgoal = 0.1 NTU as expected. The class of the TRIs is discussed later in this chapter.

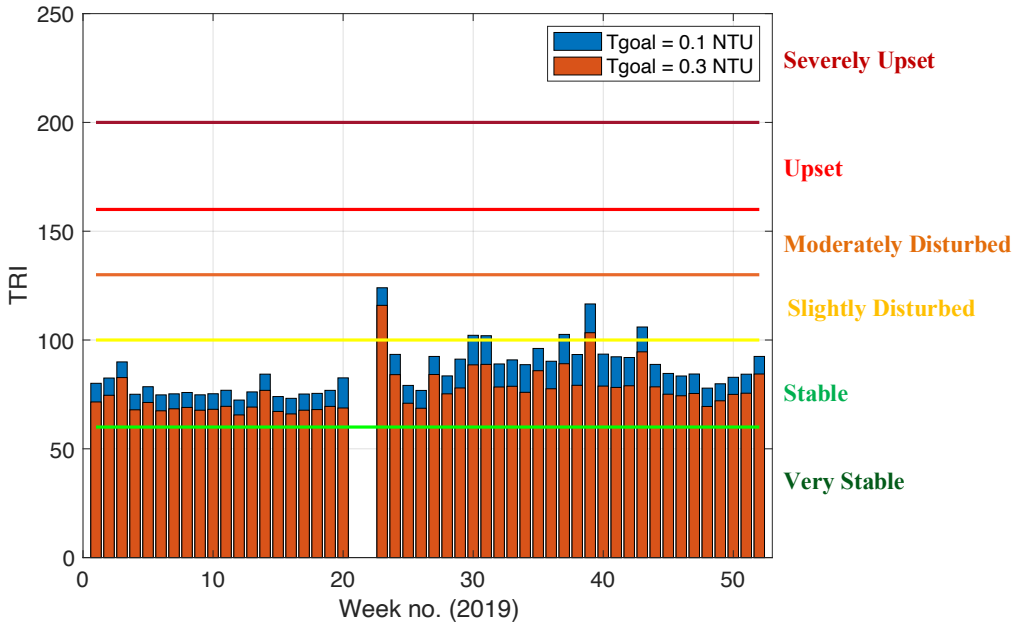


Figure 4.15: Weekly TRIs of Filter 2 (2019) with varying Tgoals

According to the plant operators, Plant B aims to maintain the filter effluent turbidity below 0.1 NTU, so the goal turbidity was used as 0.1 NTU for all the filters in further analysis.

Figures 4.16 and 4.17 show the weekly TRIs of Filter 2 and Filter 18 respectively for the years 2019 and 2020. The blue bars represent the TRIs during normal weather and the red bars represent the TRIs corresponding to the weeks that were affected by weather events characterized by raw water turbidity. The empty spaces in the figure represent filter shutdown during the corresponding weeks due to maintenance or repair work.

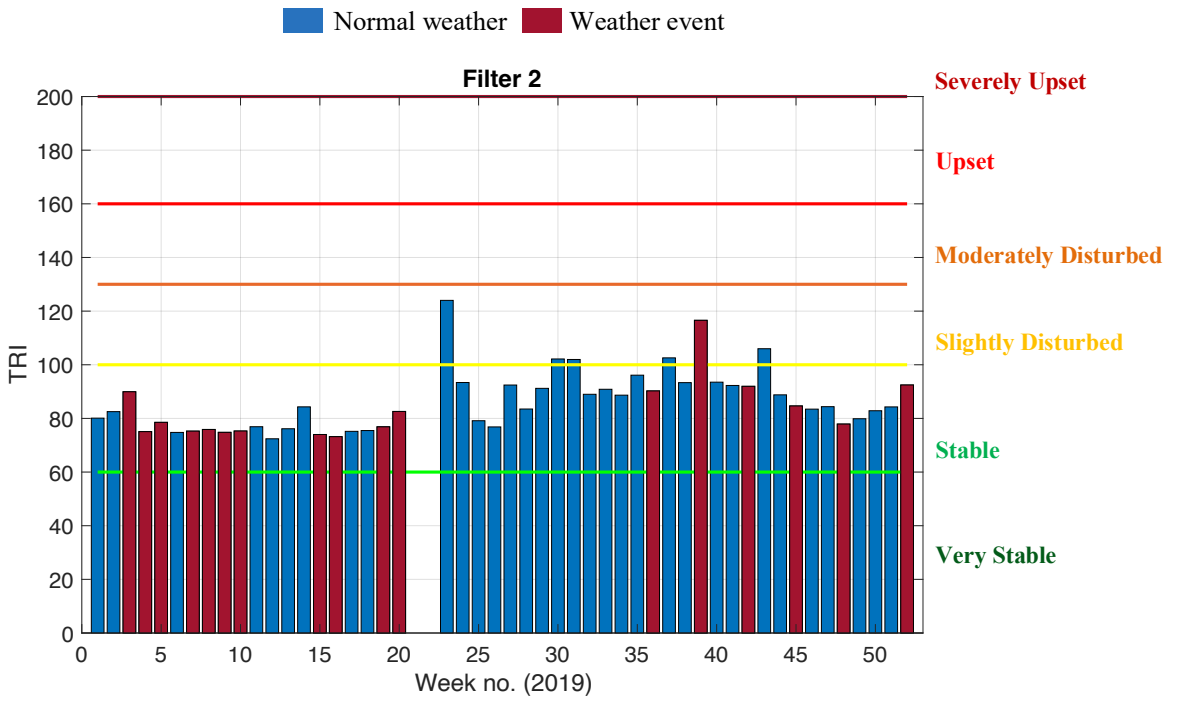


(a)

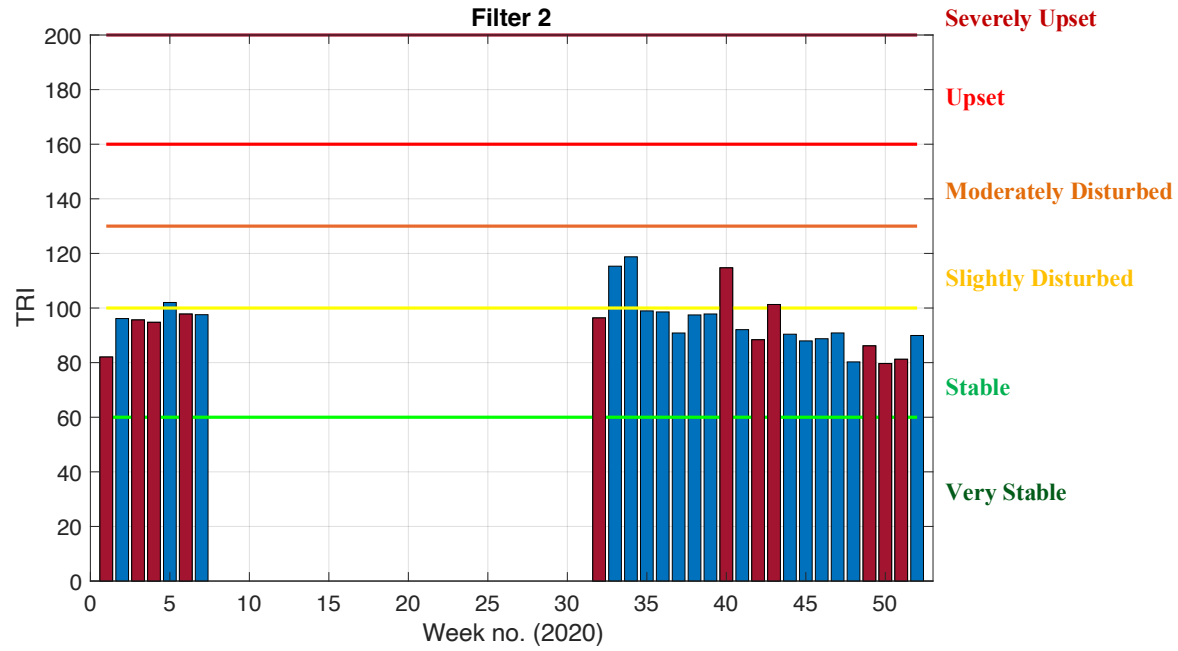


(b)

Figure 4.16: Weekly TRIs of Filter 2 in (a) 2019 and (b) 2020 during normal weather and weather events characterized by raw water turbidity (Tgoal = 0.1 NTU)

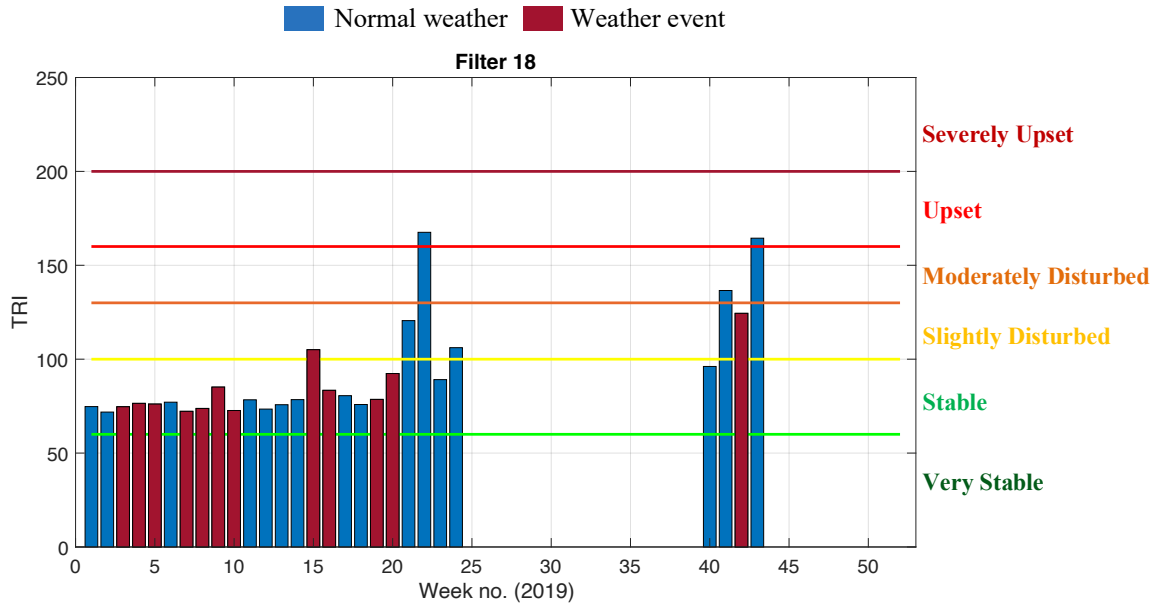


(a)

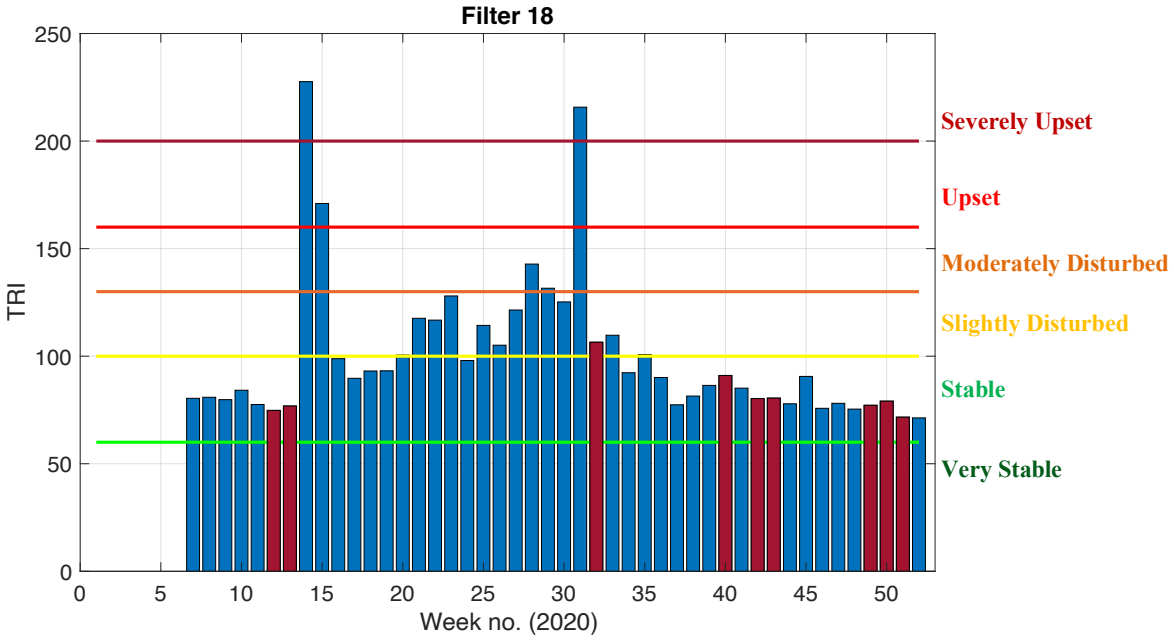


(b)

Figure 4.17: Weekly TRIs of Filter 18 in (a) 2019 and (b) 2020 during normal weather and weather events characterized by raw water turbidity (Tgoal = 0.1 NTU)

For both Filters 2 and 18, most of the TRIs fall into the "stable" (60-100) class, which indicates that the 50th and the 90th percentile turbidity were below the goal turbidity, and the filters always maintained the desired quality (effluent turbidity < 0.1 NTU) for the respective weeks.

For Filter 2, the TRIs fall into the "slightly disturbed" (100-130) class for 11 weeks during the study period (104 weeks). For Filter 18, the TRIs fall into the "slightly disturbed" (100-130) class for 15 weeks during the study period. These TRIs indicate that either both 50th and 90th percentile turbidity was close to the goal turbidity and/or the 90th percentile turbidity was greater than the goal turbidity in some cases and the filters produced effluent water with desired quality most of the time during the given weeks. For Filter 2, none of the TRIs are observed beyond this class.

The TRI falls into the "moderately disturbed" (130-160) class for 3 weeks for Filter 18. The "moderately disturbed" TRIs indicate that both the 50th and 90th percentile turbidity were greater than the goal turbidity and the filters did not generate effluent water with desired quality for a short duration (almost 30% of the time) during the given weeks.

For Filter 18, the TRIs fall into the "upset" (160-200) class for 3 weeks and into the "severely upset" (>200) category for 2 weeks during the study period, which indicates that both 50th and 90th percentile turbidity was almost two times higher than the goal turbidity and the filter could not produce effluent water with desired quality.

The weekly TRI plots for the other filters can be found in Appendix B (Figures B.2 to B.8), which show similar results. In most filters, the TRIs are in the "stable" and "slightly disturbed" class like Filter 2, which implies that the filters were successful to keep the effluent turbidity at 0.1 NTU. However, for some filters like Filter 18, some high TRIs (>130) were observed. For these TRIs, although the filter effluent turbidity met the regulatory limit, which is 0.3 NTU for 95% of the measurements per cycle per month, the effluent turbidity exceeded the target turbidity, which is 0.1 NTU. This implies that the filters met the regulatory limits set by the Government of Ontario, but could not meet the target set by Health Canada (2012) during the weeks corresponding to the high TRIs. Thus, the analysis of the filter effluent turbidity data using TRI can be a useful tool for utilities to investigate their operational details during those weeks and take appropriate measures to improve the performance of the filters.

Filter 7 was shut down for decades and put in service at the end of 2020, which is why no on-line turbidity data was available to calculate TRI except for the last two weeks of 2020 (Staff of Plant B, July 2021).

From Figures 4.16 and 4.17, and B.2 to B.8, some high TRI values are observed but there was no weather event taking place during those weeks. Although these high TRIs imply that the performance of the filters was not satisfactory during some periods in the given weeks, they do not always correspond to the weather events characterized by raw water turbidity, indicating that the reason behind this undesirable performance is not weather-related. It should be noted that the classification system for the TRI values was developed based on the turbidity data analysis for individual filter runs. Therefore, the names of the classes may not be as accurate in this case as the duration that was considered to calculate TRIs is much larger than a filter run, but the mathematical interpretation of TRI should be valid.

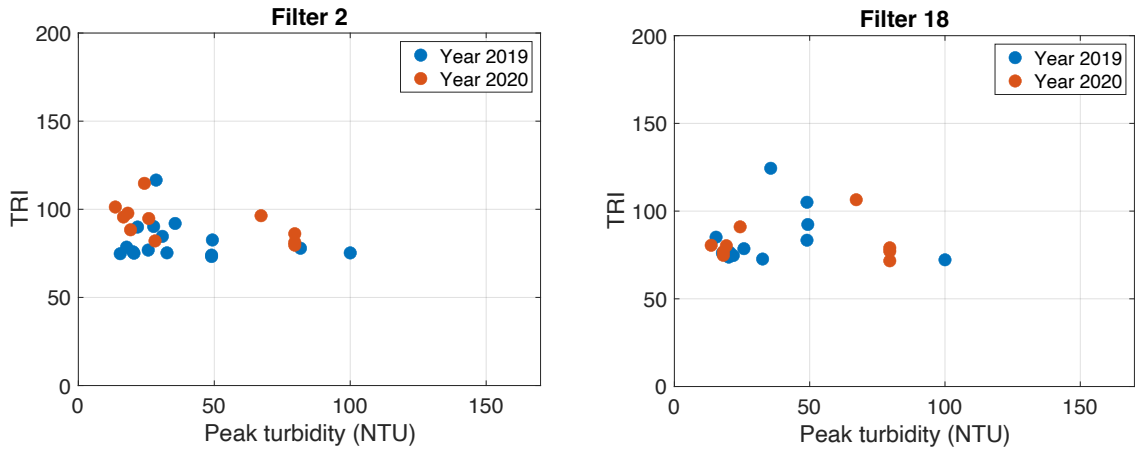


(a) (b)

Figure 4.18: Weekly TRIs of (a) Filter 2 and (b) Filter 18 in relation to the maximum values of raw water turbidities during weather events

Although there is no observed difference between TRIs during normal weather and weather events, to confirm the visual observation from Figures 4.16 and 4.17, in Figure 4.18 the TRIs corresponding to turbidity events were plotted against the maximum or 'peak' turbidity of the event. However, no positive correlation ($R^2 \approx 0$) has been observed between the TRIs and peak turbidities of a weather event, implying that weather events did not affect TRIs in 2019 and 2020, confirming that Filters 2 and 18 of Plant B were robust with respect to higher raw water turbidity. Similar results were found for the other filters, which are shown in Appendix B (Figures B.9 to B.12).

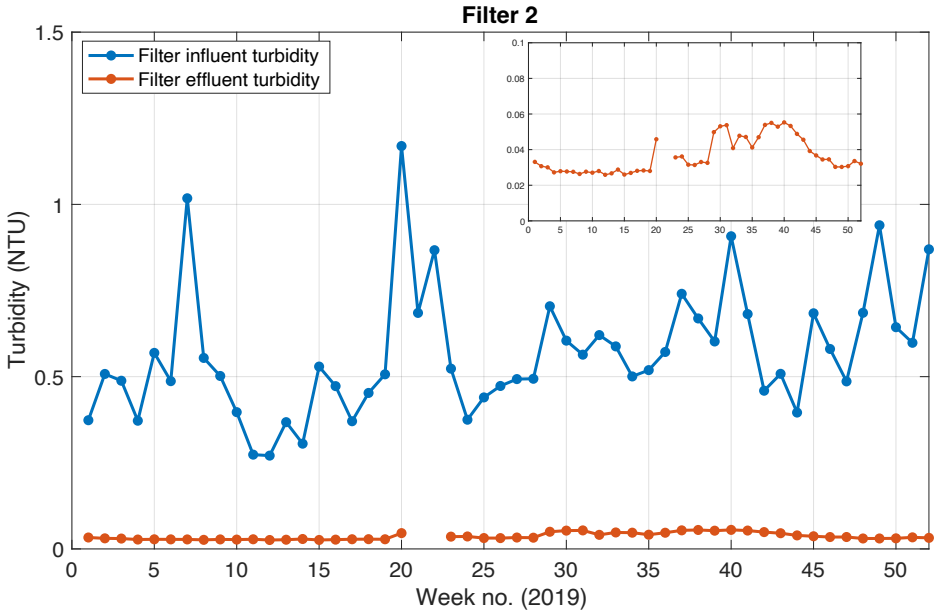


(a)

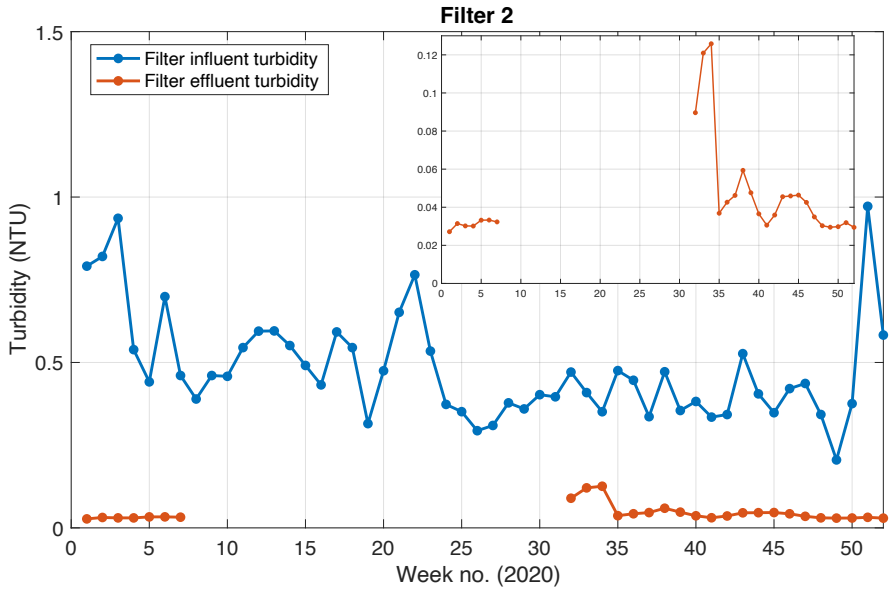


(b)

Figure 4.19: Weekly average filter influent and effluent turbidity of Filter 2 in (a) 2019 and (b) 2020

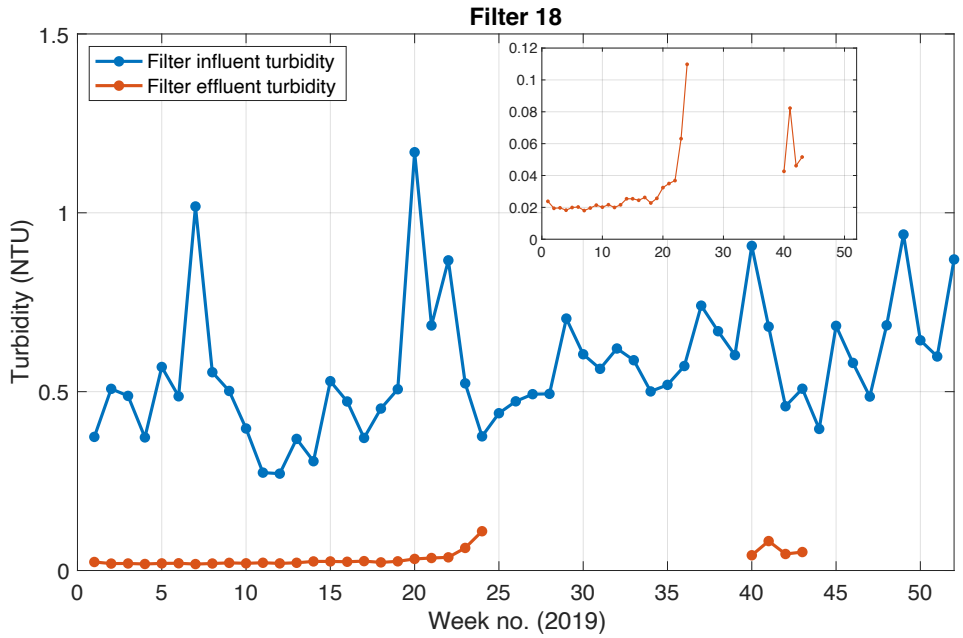


(a)

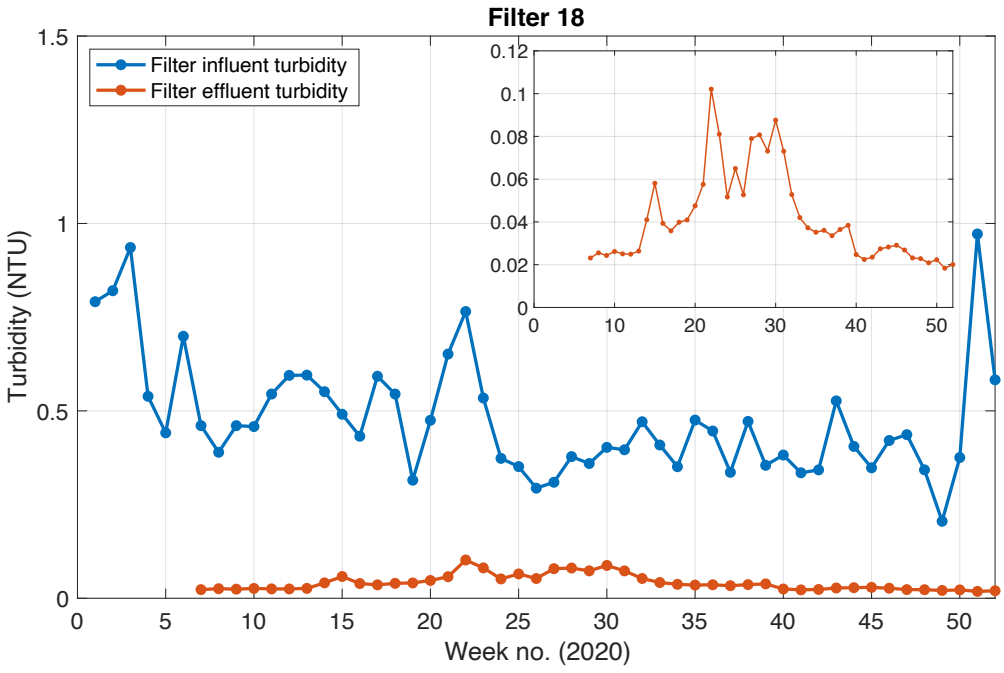


(b)

Figure 4.20: Weekly average filter influent and effluent turbidity of Filter 18 in (a) 2019 and (b) 2020

In addition to the TRI plots, in order to visualize the overall performance of the filters, the weekly average filter influent turbidities are plotted against the weekly average Filter 2 and Filter 18 effluent turbidity for the years 2019 and 2020 in Figures 4.19 and 4.20 to observe the weekly turbidity removal by these two filters. These figures show that almost all the weekly average Filter 2 and Filter 18 effluent turbidities are below the goal turbidity of 0.1 NTU. For 2 weeks in Filter 2 and 2 weeks in Filter 18, the weekly average turbidities are found a bit higher than 0.1 NTU, but well below the regulatory limit (0.3 NTU). The effluent water from Filters 1 to 12 moves to clearwell 1 and the effluent water from Filters 13 to 24 moves to clearwell 2. After disinfection, the water from clearwells 1 and 2 enters the distribution system with the high lift pump. Overall, 76.8% to 99.9% (Table B.1 in Appendix B) of raw water turbidity is removed after filtration per week on average throughout the years 2019 and 2020, maintaining the effluent turbidity below the regulatory limit.

### 4.3.4 Overall Robustness of Plant B

Since the two critical treatments steps for turbidity are the CFS process and filtration, the overall robustness of the plant is dependent on the robustness of these two steps. As the treatment trains are parallel and identical, the average TRI of the modules 1 and 2 CFS units represents the total TRI of the CFS process. Again, since all the filters are operated randomly throughout the years, the average TRI of the 24 filters represents the total TRI of the filtration step. To calculate the overall TRI of the plant, the overall robustness category (Chapter 2: Table 2.8) developed by Nemani (2021b) was used. The overall robustness of Plant B can be assessed considering the following scenarios:

1. Equal weighting of the CFS and filtration process assuming both processes are equally important.
2. Unequal weighting:
    i. The CFS process is more significant.
    ii. The filtration process is more significant as it is the final step to remove turbidity.

The overall robustness category and the overall robustness class evaluated by equal weighting of the two processes for the year 2019 are demonstrated in Table 4.5.

Table 4.5: Overall robustness of Plant B by week in 2019 using equal weighting

| Week no. | 2019 | | | | | |
|---|---|---|---|---|---|---|
| | CFS Units | | Filters | | Plant | |
| | TRI | Category | TRI | Category | Overall Robustness Category | Overall System Robustness |
| 1 | 131 | 4 | 75 | 2 | 3 | slightly disturbed |
| 2 | 135 | 4 | 83 | 2 | 3 | slightly disturbed |
| 3 | 110 | 3 | 83 | 2 | 3 | slightly disturbed |
| 4 | 107 | 3 | 77 | 2 | 3 | slightly disturbed |
| 5 | 123 | 3 | 87 | 2 | 3 | slightly disturbed |
| 6 | 127 | 3 | 85 | 2 | 3 | slightly disturbed |
| 7 | 136 | 2 | 81 | 2 | 2 | stable |
| 8 | 99 | 2 | 76 | 2 | 2 | stable |
| 9 | 98 | 2 | 79 | 2 | 2 | stable |
| 10 | 178 | 5 | 80 | 2 | 4 | moderately disturbed |
| 11 | 94 | 2 | 77 | 2 | 2 | stable |
| 12 | 112 | 3 | 75 | 2 | 3 | slightly disturbed |
| 13 | 113 | 3 | 79 | 2 | 3 | slightly disturbed |
| 14 | 108 | 3 | 84 | 2 | 3 | slightly disturbed |
| 15 | 104 | 3 | 81 | 2 | 3 | slightly disturbed |
| 16 | 100 | 3 | 80 | 2 | 3 | slightly disturbed |
| 17 | 96 | 2 | 81 | 2 | 2 | stable |
| 18 | 90 | 2 | 81 | 2 | 2 | stable |
| 19 | 93 | 2 | 81 | 2 | 2 | stable |
| 20 | 117 | 3 | 98 | 2 | 3 | slightly disturbed |
| 21 | 103 | 3 | 128 | 3 | 3 | slightly disturbed |
| 22 | 123 | 3 | 125 | 3 | 3 | slightly disturbed |

| | | | | | | |
|---|---|---|---|---|---|---|
| 23 | 176 | 5 | 105 | 3 | 4 | moderately disturbed |
| 24 | 107 | 3 | 94 | 2 | 3 | slightly disturbed |
| 25 | 90 | 2 | 93 | 2 | 2 | stable |
| 26 | 99 | 2 | 97 | 2 | 2 | stable |
| 27 | 117 | 3 | 103 | 3 | 3 | slightly disturbed |
| 28 | 92 | 2 | 95 | 2 | 2 | stable |
| 29 | 110 | 3 | 92 | 2 | 3 | slightly disturbed |
| 30 | 99 | 2 | 94 | 2 | 2 | stable |
| 31 | 102 | 3 | 109 | 3 | 3 | slightly disturbed |
| 32 | 113 | 3 | 99 | 2 | 3 | slightly disturbed |
| 33 | 110 | 3 | 98 | 2 | 3 | slightly disturbed |
| 34 | 101 | 3 | 92 | 2 | 3 | slightly disturbed |
| 35 | 107 | 3 | 93 | 2 | 3 | slightly disturbed |
| 36 | 109 | 3 | 94 | 2 | 3 | slightly disturbed |
| 37 | 111 | 3 | 97 | 2 | 3 | slightly disturbed |
| 38 | 107 | 3 | 98 | 2 | 3 | slightly disturbed |
| 39 | 140 | 4 | 112 | 3 | 4 | moderately disturbed |
| 40 | 121 | 3 | 92 | 2 | 3 | slightly disturbed |
| 41 | 105 | 3 | 91 | 2 | 3 | slightly disturbed |
| 42 | 183 | 5 | 89 | 2 | 4 | moderately disturbed |
| 43 | 99 | 2 | 96 | 2 | 2 | stable |
| 44 | 111 | 3 | 85 | 2 | 3 | slightly disturbed |
| 45 | 136 | 4 | 84 | 2 | 3 | slightly disturbed |
| 46 | 118 | 3 | 89 | 2 | 3 | slightly disturbed |
| 47 | 126 | 3 | 85 | 2 | 3 | slightly disturbed |
| 48 | 127 | 3 | 87 | 2 | 3 | slightly disturbed |
| 49 | 137 | 4 | 92 | 2 | 3 | slightly disturbed |
| 50 | 120 | 3 | 90 | 2 | 3 | slightly disturbed |

| | | | | | | |
|---|---|---|---|---|---|---|
| 51 | 104 | 3 | 91 | 2 | 3 | slightly disturbed |
| 52 | 119 | 3 | 95 | 2 | 3 | slightly disturbed |

For the unequal weighting scenarios, the ratio between weighting factors was selected to be 0.6/0.4, the same as Plant A. The overall robustness category and the overall robustness class evaluated by a higher weighting of the CFS and filtration process for the year 2019 are demonstrated in Table 4.6 and Table 4.7 respectively.

Table 4.6: Overall robustness of Plant B by weeks in 2019 using unequal weighting (considering the CFS process is more significant)

| **Week no.** | **2019** | | | | | |
|---|---|---|---|---|---|---|
| | **CFS Units** | | **Filters** | | **Plant** | |
| | **TRI** | **Category** | **TRI** | **Category** | **Overall Robustness Category** | **Overall System Robustness** |
| 1 | 131 | 4 | 75 | 2 | 3 | slightly disturbed |
| 2 | 135 | 4 | 83 | 2 | 3 | slightly disturbed |
| 3 | 110 | 3 | 83 | 2 | 3 | slightly disturbed |
| 4 | 107 | 3 | 77 | 2 | 3 | slightly disturbed |
| 5 | 123 | 3 | 87 | 2 | 3 | slightly disturbed |
| 6 | 127 | 3 | 85 | 2 | 3 | slightly disturbed |
| 7 | 136 | 2 | 81 | 2 | 2 | stable |
| 8 | 99 | 2 | 76 | 2 | 2 | stable |
| 9 | 98 | 2 | 79 | 2 | 2 | stable |
| 10 | 178 | 5 | 80 | 2 | 4 | moderately disturbed |
| 11 | 94 | 2 | 77 | 2 | 2 | stable |
| 12 | 112 | 3 | 75 | 2 | 3 | slightly disturbed |
| 13 | 113 | 3 | 79 | 2 | 3 | slightly disturbed |

| | | | | | | |
|---|---|---|---|---|---|---|
| 14 | 108 | 3 | 84 | 2 | 3 | slightly disturbed |
| 15 | 104 | 3 | 81 | 2 | 3 | slightly disturbed |
| 16 | 100 | 3 | 80 | 2 | 3 | slightly disturbed |
| 17 | 96 | 2 | 81 | 2 | 2 | stable |
| 18 | 90 | 2 | 81 | 2 | 2 | stable |
| 19 | 93 | 2 | 81 | 2 | 2 | stable |
| 20 | 117 | 3 | 98 | 2 | 3 | slightly disturbed |
| 21 | 103 | 3 | 128 | 3 | 3 | slightly disturbed |
| 22 | 123 | 3 | 125 | 3 | 3 | slightly disturbed |
| 23 | 176 | 5 | 105 | 3 | 4 | moderately disturbed |
| 24 | 107 | 3 | 94 | 2 | 3 | slightly disturbed |
| 25 | 90 | 2 | 93 | 2 | 2 | stable |
| 26 | 99 | 2 | 97 | 2 | 2 | stable |
| 27 | 117 | 3 | 103 | 3 | 3 | slightly disturbed |
| 28 | 92 | 2 | 95 | 2 | 2 | stable |
| 29 | 110 | 3 | 92 | 2 | 3 | slightly disturbed |
| 30 | 99 | 2 | 94 | 2 | 2 | stable |
| 31 | 102 | 3 | 109 | 3 | 3 | slightly disturbed |
| 32 | 113 | 3 | 99 | 2 | 3 | slightly disturbed |
| 33 | 110 | 3 | 98 | 2 | 3 | slightly disturbed |
| 34 | 101 | 3 | 92 | 2 | 3 | slightly disturbed |
| 35 | 107 | 3 | 93 | 2 | 3 | slightly disturbed |
| 36 | 109 | 3 | 94 | 2 | 3 | slightly disturbed |
| 37 | 111 | 3 | 97 | 2 | 3 | slightly disturbed |
| 38 | 107 | 3 | 98 | 2 | 3 | slightly disturbed |
| 39 | 140 | 4 | 112 | 3 | 4 | moderately disturbed |
| 40 | 121 | 3 | 92 | 2 | 3 | slightly disturbed |
| 41 | 105 | 3 | 91 | 2 | 3 | slightly disturbed |

| | | | | | | |
|---|---|---|---|---|---|---|
| 42 | 183 | 5 | 89 | 2 | 4 | slightly disturbed |
| 43 | 99 | 2 | 96 | 2 | 2 | stable |
| 44 | 111 | 3 | 85 | 2 | 3 | slightly disturbed |
| 45 | 136 | 4 | 84 | 2 | 3 | slightly disturbed |
| 46 | 118 | 3 | 89 | 2 | 3 | slightly disturbed |
| 47 | 126 | 3 | 85 | 2 | 3 | slightly disturbed |
| 48 | 127 | 3 | 87 | 2 | 3 | slightly disturbed |
| 49 | 137 | 4 | 92 | 2 | 3 | slightly disturbed |
| 50 | 120 | 3 | 90 | 2 | 3 | slightly disturbed |
| 51 | 104 | 3 | 91 | 2 | 3 | slightly disturbed |
| 52 | 119 | 3 | 95 | 2 | 3 | slightly disturbed |

Table 4.7: Overall robustness of Plant B by weeks in 2019 using unequal weighting (considering the filtration process is more significant)

| **Week no.** | **2019** | | | | | |
|---|---|---|---|---|---|---|
| | **CFS Units** | | **Filters** | | **Plant** | |
| | **TRI** | **Category** | **TRI** | **Category** | **Overall Robustness Category** | **Overall System Robustness** |
| 1 | 131 | 4 | 75 | 2 | 3 | slightly disturbed |
| 2 | 135 | 4 | 83 | 2 | 3 | slightly disturbed |
| 3 | 110 | 3 | 83 | 2 | 2 | stable |
| 4 | 107 | 3 | 77 | 2 | 2 | stable |
| 5 | 123 | 3 | 87 | 2 | 2 | stable |
| 6 | 127 | 3 | 85 | 2 | 2 | stable |
| 7 | 136 | 2 | 81 | 2 | 2 | stable |
| 8 | 99 | 2 | 76 | 2 | 2 | stable |

| | | | | | | |
|---|---|---|---|---|---|---|
| 9 | 98 | 2 | 79 | 2 | 2 | stable |
| 10 | 178 | 5 | 80 | 2 | 3 | slightly disturbed |
| 11 | 94 | 2 | 77 | 2 | 2 | stable |
| 12 | 112 | 3 | 75 | 2 | 2 | stable |
| 13 | 113 | 3 | 79 | 2 | 2 | stable |
| 14 | 108 | 3 | 84 | 2 | 2 | stable |
| 15 | 104 | 3 | 81 | 2 | 2 | stable |
| 16 | 100 | 3 | 80 | 2 | 2 | stable |
| 17 | 96 | 2 | 81 | 2 | 2 | stable |
| 18 | 90 | 2 | 81 | 2 | 2 | stable |
| 19 | 93 | 2 | 81 | 2 | 2 | stable |
| 20 | 117 | 3 | 98 | 2 | 2 | stable |
| 21 | 103 | 3 | 128 | 3 | 3 | slightly disturbed |
| 22 | 123 | 3 | 125 | 3 | 3 | slightly disturbed |
| 23 | 176 | 5 | 105 | 3 | 4 | moderately disturbed |
| 24 | 107 | 3 | 94 | 2 | 2 | stable |
| 25 | 90 | 2 | 93 | 2 | 2 | stable |
| 26 | 99 | 2 | 97 | 2 | 2 | stable |
| 27 | 117 | 3 | 103 | 3 | 3 | slightly disturbed |
| 28 | 92 | 2 | 95 | 2 | 2 | stable |
| 29 | 110 | 3 | 92 | 2 | 2 | stable |
| 30 | 99 | 2 | 94 | 2 | 2 | stable |
| 31 | 102 | 3 | 109 | 3 | 3 | slightly disturbed |
| 32 | 113 | 3 | 99 | 2 | 2 | stable |
| 33 | 110 | 3 | 98 | 2 | 2 | stable |
| 34 | 101 | 3 | 92 | 2 | 2 | stable |
| 35 | 107 | 3 | 93 | 2 | 2 | stable |
| 36 | 109 | 3 | 94 | 2 | 2 | stable |

| | | | | | | |
|---|---|---|---|---|---|---|
| 37 | 111 | 3 | 97 | 2 | 2 | stable |
| 38 | 107 | 3 | 98 | 2 | 2 | stable |
| 39 | 140 | 4 | 112 | 3 | 3 | slightly disturbed |
| 40 | 121 | 3 | 92 | 2 | 2 | stable |
| 41 | 105 | 3 | 91 | 2 | 2 | stable |
| 42 | 183 | 5 | 89 | 2 | 3 | slightly disturbed |
| 43 | 99 | 2 | 96 | 2 | 2 | stable |
| 44 | 111 | 3 | 85 | 2 | 2 | stable |
| 45 | 136 | 4 | 84 | 2 | 3 | slightly disturbed |
| 46 | 118 | 3 | 89 | 2 | 2 | stable |
| 47 | 126 | 3 | 85 | 2 | 2 | stable |
| 48 | 127 | 3 | 87 | 2 | 2 | stable |
| 49 | 137 | 4 | 92 | 2 | 3 | slightly disturbed |
| 50 | 120 | 3 | 90 | 2 | 2 | stable |
| 51 | 104 | 3 | 91 | 2 | 2 | stable |
| 52 | 119 | 3 | 95 | 2 | 2 | stable |

Similar tables for the year 2020 can be found in Appendix B (Tables B.2 to B.4).

To visualize the overall robustness of the plant in 2019 and 2020 with different weighting scenarios, a histogram is plotted in Figure 4.21, which summarizes the finding in Tables 4.5 to 4.7, and B.2 to B.4.

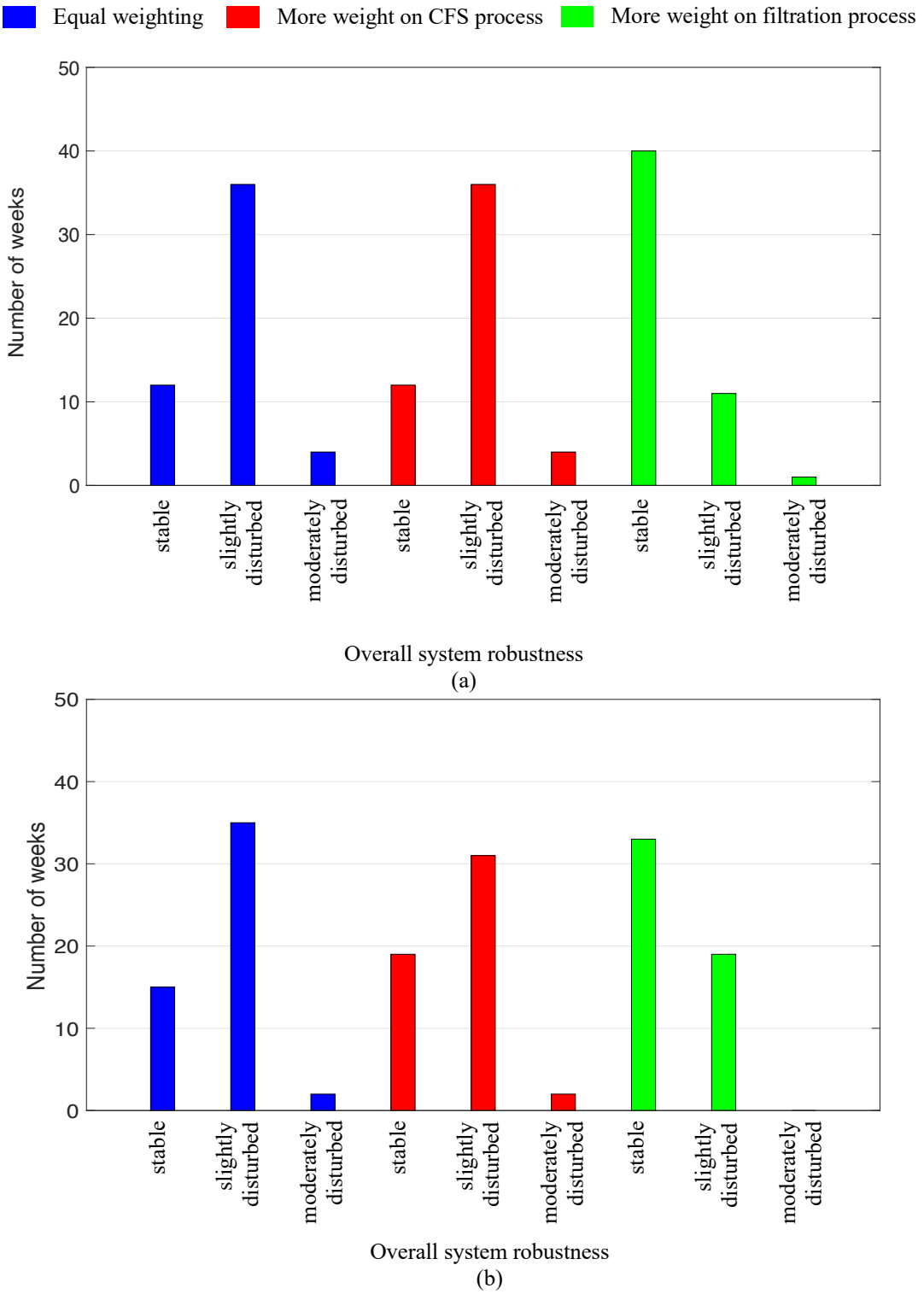


Figure 4.21: Overall robustness category of Plant B in (a) 2019 and (b) 2020 with equal and unequal weighting

From Figure 4.21, it is clear that changing the weighting of the treatment processes has an effect on the overall robustness category. With equal weighting of the two processes and more weighting on the CFS process, larger number of "slightly disturbed" and "moderately disturbed" TRIs are observed. This is caused by the high TRIs of the CFS units in some weeks.

Putting more weight on the filtration process seems more logical as it is the final step to remove turbidity. With unequal weighting (more weight on the filtration process), it is found that the system was "slightly disturbed" for 11 weeks in 2019 and 19 weeks in 2020. The system was in the "moderately disturbed" class for only 1 week in 2019. It should be noted that the "slightly disturbed" class implies that the system performed excellently during most of the period, and no overall system robustness, except for week no. 23 in 2019, was found to be greater than 3, which refers to the "slightly disturbed" class (listed in Table 2.8). 12 (39%) of those weeks had weather events characterized by higher raw water turbidity. These results indicate that the system was "slightly disturbed" and "moderately disturbed" in some weeks (61% during the study period) when the turbidity was considered normal, and there may be some operational factors behind this. Therefore, the overall robustness of the plant did not depend on raw water turbidity events.

## 4.4 Conclusion

The raw water turbidity of Plant B is relatively low most of the time, which is expected because the source water of Plant B is one of the Great Lakes. The plant uses the conventional CFS process, which performs adequately most of the time, but the performance was unsatisfactory during some weeks as indicated by the higher (>130) TRIs. The filters are meeting the regulatory limit (0.3 NTU, 95% of the measurements per cycle per month), but the high TRIs imply that the filter effluent turbidity exceeded the target turbidity (0.1 NTU) in some weeks. No positive correlation is found between weather events characterized by elevated turbidity and the TRIs of the filters, indicating that the filters were robust with respect to high raw water turbidity. There can be several operational factors behind the high TRIs of the filters. Hence, the TRI is a useful tool as it helps the utilities to pinpoint the times of less robust operational performance of the filters in the past and re-evaluate their operational process to make the filters more robust. In conclusion, the high TRIs of the CFS units and some filters indicate that the overall treatment process in Plant B may be vulnerable in the future if the occurrence of more severe, unusual and untimely precipitation events increase given the current trend of climate change.

# Chapter 5: Bench-scale Simulation of the ACTIFLO® Process in Plant A

## 5.1 Introduction

The last step of the robustness framework discussed in Chapter 2: sub-section 2.4.6 is Step 6: Adaptation, which is to improve the robustness of the treatment steps by making short-term operational changes. The coagulation and SBC process, commercially named the ACTIFLO® process of Plant A has been identified as a critical treatment step and the robustness of this step has been evaluated in Chapter 3. The ACTIFLO® process has been found to be quite robust in terms of turbidity removal during normal weather and weather events characterized by raw water turbidity. However, it is unknown how the ACTIFLO® units will perform, if the raw water turbidity increases beyond general experience due to an extreme weather event. In this chapter, bench-scale jar tests were performed to simulate the full-scale ACTIFLO® process on water samples with baseline turbidity representing normal weather and with elevated turbidity representing historical weather events. Finally, a factorial design experiment was conducted on water samples representing extremely high turbidity to determine the significant parameters affecting the ACTIFLO® process. The results of this analysis provide information that would be helpful in optimizing the treatment step. It is possible that detailed optimization of the full-scale process could require additional work beyond bench-scale studies.

## 5.2 The ACTIFLO® Process

Most surface water based DWTPs use the conventional CFS process to remove a large portion of particles and sometimes organic matter from raw water (Desjardins et al., 2002). However, some plants including Plant A use ballasted flocculation, followed by ballasted clarification, which is a relatively new technology. This process involves the injection of a ballasting agent during flocculation to increase the size and density of the flocs (Lapointe et al., 2017; Zafisah et al., 2020). Typically, microsand is used as a ballasting agent, and the process is called SBC. Ballasted flocs have greater mass than micro flocs that are produced in the conventional CFS process, which affects the size of the flocs and increases the settling velocity (Desjardins et al., 2002; Dianous & Dernaucourt, 1991; Ghanem et al., 2007; He et al., 2019). Moreover, ballasting agents have low surface charge density compared to colloidal particles in water. Hence, the addition of ballasting agents does not chemically disrupt the interaction

between the coagulant/flocculant and colloidal particles (Young & Edwards, 2003; Zafisah et al., 2020). SBC process offers a more compact process leading to a smaller system footprint, faster start-up, higher settling rate, and treated water with equal or better quality than conventional CFS systems (Desjardins et al., 2002; Lapointe & Barbeau, 2018; Zafisah et al., 2020). The time required for 80% turbidity removal can decrease from 10 minutes to 3 minutes when conventional flocculation is replaced by ballasted flocculation (Dianous & Dernaucourt, 1991).

The capacity of an ACTIFLO® unit can be up to 800,000 $m^3/d$ (Haarbo et al., 1998). The full-scale ACTIFLO® process is shown in Figure 5.1.

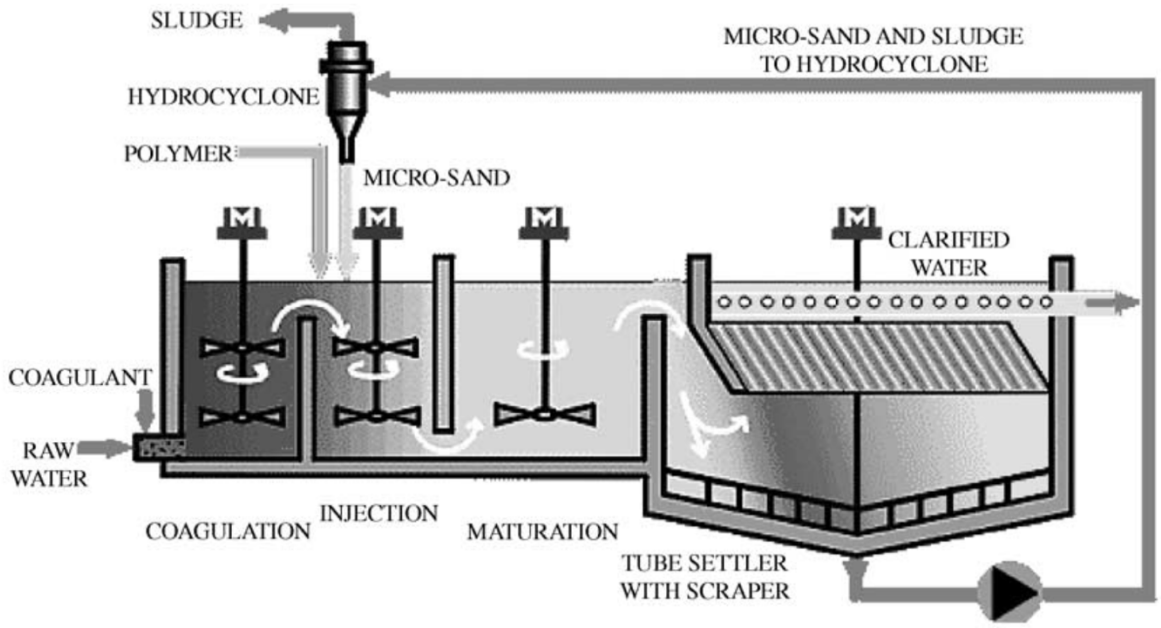


Figure 5.1: Schematic of the ACTIFLO® process (Desjardins et al., 2002)

One ACTIFLO® unit consists of four tanks: coagulation tank, injection tank, maturation tank and sedimentation tank. Coagulant is added to the raw water in the coagulation tank to destabilize the colloids. The coagulated water then enters the injection tank where microsand and polymer are introduced simultaneously to initiate floc formation. The polymer helps the microsand to become attached to the flocs. Both coagulation and injection tanks are equipped with mixers with high mixing

intensity. The flocs grow in the maturation tank at a lower mixing intensity, keeping the ballasted flocs in suspension (Desjardins et al., 2002; Plum et al., 1998). The flocculation mixing gradient, G can be as high as 700/s without floc breakage, but it is typically kept at 60-200/s at full-scale plants, which is adequate and cost-effective (Dianous & Dernaucourt, 1991). The water finally moves to the settling tank. Microsand is incorporated into the flocs through polyelectrolyte bridges, making the flocs heavier, which increases their settling velocity in the lamella separator. The flocs settle very quickly on the large surface developed by the lamellae, where a laminar counterflow settling takes place. The water passes the lamella and leaves the plant over outlet weirs above the lamellas. The settled mixture of sludge and microsand is recirculated and the microsand is separated from the sludge by the hydrocyclone, which is an intense vortex, and then redirected to the injection tank maintaining a typical microsand concentration of 2-4 g/L, ensuring very low sand loss. The on-going loss of is adjusted by feeding microsand as required in the injection tank. The microsand-free sludge is diverted into the sewer or sludge treatment units depending on the applicable regulations. The sludge flow generally makes up 6% of the total water flow treated (Desjardins et al., 2002; Guibelin et al., 1990; Plum et al., 1998). At the designed flow rate, the surface loading rate in a typical ACTIFLO® unit is 40 $m^3/hr/m^2$. This loading rate corresponds to hydraulic contact times of respectively 2, 2, 6 and 3 minutes in the coagulation, injection, maturation and settling tanks at common design conditions (Desjardins et al., 2002).

## 5.3 Materials and Methods

Modified jar tests were performed to simulate the full-scale ACTIFLO® process at bench-scale in the laboratory. Three chemicals (coagulant, polymer and microsand) were obtained from Plant A, which are used in the full-scale ACTIFLO® units in Plant A:

i. **Coagulant:** Polyaluminum chloride (PACl), manufactured by Kemira Chemicals Inc. (product name: Kemira SternPAC) was used as the coagulant. The chemical formula of PACl is $Al_{13}(OH)_{20}(SO_4)_2Cl_{15}$.

ii. **Microsand:** Silica, mainly in the form of quartz was used as the ballasting agent (product name: filter sand and gravel, all grades), manufactured by Anthrafilter Media and Coal Ltd.

iii. **Polymer:** Anionic polymer is used in the plant (product name: FLOPAM™ AN 934 PWG), manufactured by SNF Canada Ltd.

The modified jar tests were performed on two types of water:

i. **Raw water samples:** Raw water samples were collected from the plant intake during normal weather when the turbidity was considered regular, and during a heavy precipitation event when the turbidity increased due to the weather.

ii. **Spiked water samples:** The turbidity of the raw water samples was spiked artificially in the laboratory to achieve historical high turbidity and extremely high turbidity beyond general experience by adding industrial mineral clay (kaolin, manufactured by Sigma-Aldrich) in raw water samples collected from Plant A.

The methods used in the laboratory to perform the bench-scale tests are discussed in subsections 5.3.1 to 5.3.4.

### 5.3.1 Modified Jar Test Procedure

To simulate the ACTIFLO® process at bench scale, a modified jar test procedure was developed by John Meunier Inc. (2005). The simulation method has proven to reproduce results that are very close to full-scale unit results (Desjardins et al., 2002; He et al., 2019; Lapointe et al., 2017; Lapointe & Barbeau, 2018; Murujew et al., 2020; Nam et al., 2013; Zafisah et al., 2020). Figure 5.2 shows the timeline of the jar tests used in the bench-scale simulation. The duration of each process adjusted to reflect the full-scale durations in Plant A.

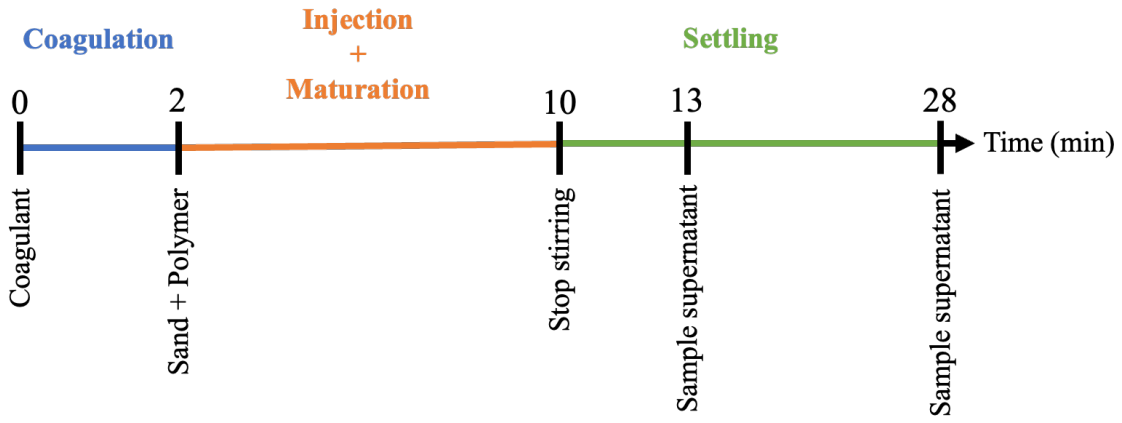


Figure 5.2: Timeline (not to scale) of the ACTIFLO® jar test (adapted from John Meunier Inc., 2005)

A standard jar test apparatus (PB-700™ Jar Tester, Phipps and Bird™, Richmond, Virginia) was used for the experiments. As mentioned previously, the chemicals for the jar tests were collected from the plant. The coagulant (PACl) and the polymer were sent as stock solutions. The microsand was sent in dry form.

One liter of raw water was measured by a graduated cylinder and square beakers were filled with the raw water. The raw water turbidity in each beaker was measured using a turbidimeter (2100Q Portable Turbidimeter, Hach, Canada). For each jar, the apparatus was equipped with a single, flat impeller. The mixing paddles were set between 0.5 and 1.0 cm from the bottom of the beaker to ensure the ballast stays in suspension. The mixing speed was adjusted to 150 revolutions per minute (RPM). After initiating stirring, the appropriate amount of coagulant was added to the jar at time zero. Two minutes after adding coagulant, required amounts of microsand and polymer were added. After the supplementary maturation contact time, the apparatus was turned off to stop stirring and allow the water to settle. The lamellar settling of the full-scale units could not be reproduced in jar tests. Preliminary results from previous studies suggest that 15 seconds was sufficient for settling in the jar test, but it is practical to keep the water for 3 minutes (Desjardins et al., 2002). The clarified water was sampled from 5 to 10 cm below the supernatant surface for two settling times, after 3 minutes and an additional 15 minutes. The sampling after 15 minutes was done to ensure maximum settling. After sampling, the clarified water quality parameters were measured.

The experiments were divided into three phases. The overview of the experimental design is shown in Figure 5.3.

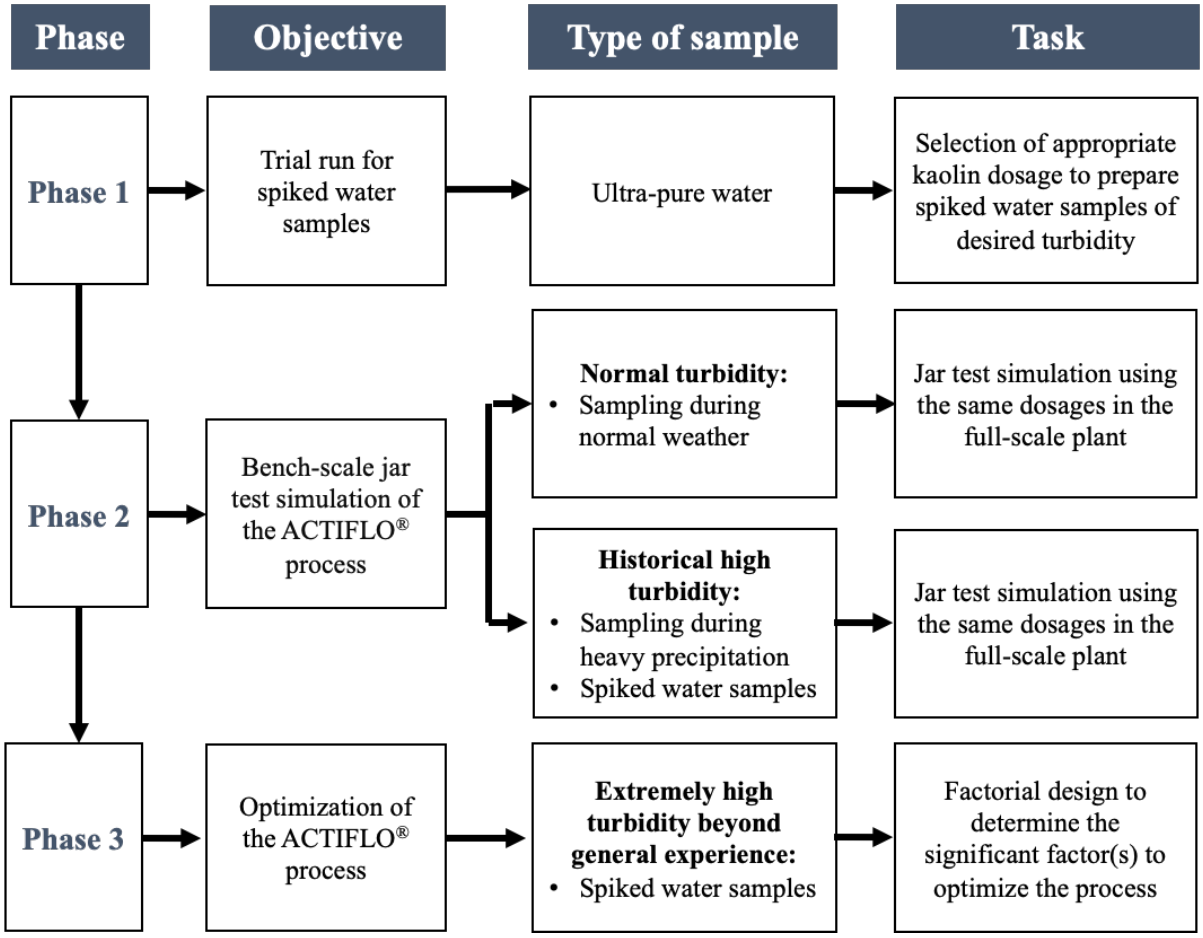


Figure 5.3: Overview of the experiments

### 5.3.2 Sampling

As shown in Figure 5.3, in phase 2, bench-scale tests were performed on water samples collected from the intake of Plant A. Samples were collected in 3-gallons plastic jars. Three batches of raw water samples were collected for this study. The first two batches of samples were collected during normal weather and the last one was collected during a precipitation event, which caused elevated turbidity in the raw water. Table 5.1 lists the relevant data of the day of samplings. The tests were done within 3 days after the samples were collected.

Table 5.1: Data from the full-scale plant on the day of sampling

| Sampling date | Raw water turbidity (NTU) | Coagulant dosage (mg/L) | Microsand dosage (g/L) | Polymer dosage (mg/L) | ACTIFLO® effluent turbidity (NTU) | Percentage of turbidity removal (%) |
|---|---|---|---|---|---|---|
| 10-Sep-21 | 5.12 | 35.0 | 1.6 | 0.17 | 0.22 | 95.8 |
| 14-Oct-21 | 5.08 | 50.0 | 1.0 | 0.13 | 0.34 | 93.4 |
| 14-Dec-21 | 37.4 | 40.0 | 1.9 | 0.22 | 0.70 | 98.1 |

### 5.3.3 Preparation of Spiked Water Samples

Several researchers have used industrial mineral clay, kaolin to prepare water samples with high turbidity in the laboratory (He et al., 2019; Lee et al., 2010; Nam et al., 2013; Okuda et al., 1999; Zafisah et al., 2020). In this study, to prepare spiked water samples with high turbidity for the experiments in phases 2 and 3, kaolin (hydrated aluminum silicate), manufactured by Sigma-Aldrich, was used. Initially, to provide an indication of how much would be required, different amounts of kaolin were added to ultra-pure water, which resulted in synthetic water with very high turbidity, which is shown as phase 1 in Figure 5.3. Figure 5.4 shows the turbidity of water samples after adding varying concentrations of kaolin to ultra-pure water. The limit of the turbidimeter was 999 NTU. The turbidity of ultra-pure water crossed this limit after adding 0.6 g/L of kaolin.

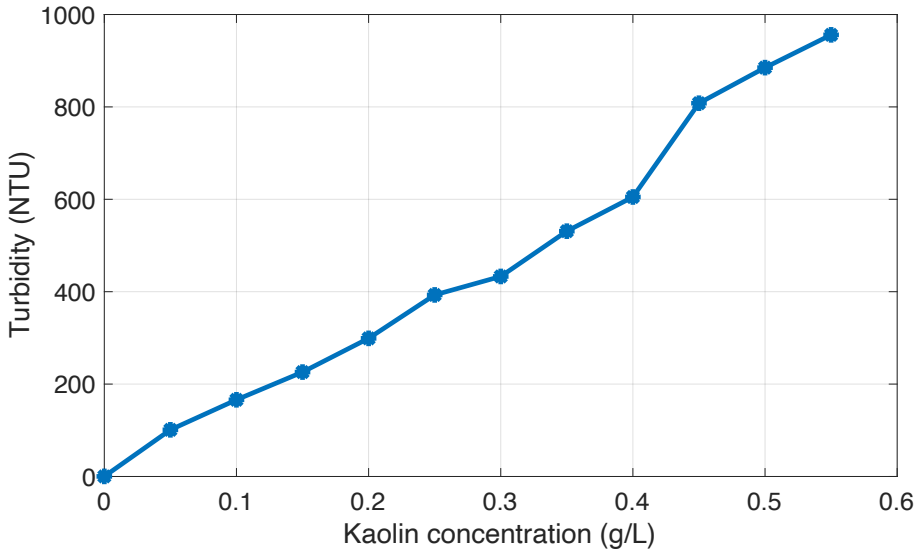


Figure 5.4: Turbidity of ultra-pure water samples with varying concentrations of kaolin

Figure 5.4 was used as a reference to prepare water samples with desired turbidity levels in the later experiments.

### 5.3.4 Raw Water Turbidity Scenarios

For phases 2 and 3 of the experiment shown in Figure 5.3, jar tests were conducted on three raw water turbidity scenarios that may occur due to varying weather at the raw water source. The scenarios and the methodologies used for each scenario are discussed in sub-sections 5.3.4.1 to 5.3.4.3.

#### 5.3.4.1 Regular Turbidity Representing Normal Weather

For the first scenario in phase 2 (shown in Figure 5.3), the ACTIFLO® process in Plant A was simulated at bench-scale on water samples collected from the plant intake when the weather was considered normal, and the raw water turbidity was average or lower than average for the corresponding season. The purpose of these tests is to observe how well the results of bench-scale simulations of the ACTFLO® unit work at regular turbidity conditions compared to the full-scale plant. The coagulant,

microsand and polymer dosage data were collected from the plant during the day of sampling. These dosages were used in the jar tests and the post-jar test water turbidity was compared with the full-scale ACTIFLO® effluent turbidity, which are listed in Table 5.1.

#### 5.3.4.2 Historical High Turbidity Representing Past Weather Events

For the second scenario in phase 2 (shown in Figure 5.3), the ACTIFLO® process was simulated at bench-scale on water samples with elevated turbidity that occurred due to a heavy precipitation event in the past. Plant A does not have any specific regime or SOPs for storm events that increase raw water turbidity. During storm events, the operators in the plant change the dosages based on experience (Staff of Plant A, June 2021). From the raw water turbidity data collected from the plant, some of the elevated turbidity events in 2019 were identified. The events were selected in a way so that all the turbidity events with different intensities during all seasons were covered. The ACTIFLO® operations during those events were simulated at bench-scale. Table 5.2 lists the mean and peak turbidities of the events and the dates when the peak turbidities were observed along with the coagulant, microsand and polymer dosages that were used on those dates.

Table 5.2: Historical turbidity events in Plant A

| **Event no.** | Event 1 | Event 2 | Event 3 | Event 4 | Event 5 |
|---|---|---|---|---|---|
| **Season** | Winter | Spring | Spring | Spring | Fall |
| **Date** | 07-Feb-19 | 17-Mar-19 | 02-Apr-19 | 29-Apr-19 | 04-Nov-19 |
| **Mean (daily) raw water turbidity (NTU)** | 80.0 | 125 | 65.2 | 31.2 | 27.0 |
| **Maximum raw water turbidity (NTU)** | 96.6 | 159 | 88.5 | 34.4 | 32.6 |
| **Coagulant dosage (mg/L)** | 37.7 | 40.0 | 40.0 | 35.0 | 40.0 |

| | | | | | |
|---|---|---|---|---|---|
| **Microsand dosage (g/L)** | 2.3 | 1.1 | 1.1 | 1.3 | 1.6 |
| **Polymer dosage (mg/L)** | 0.28 | 0.27 | 0.22 | 0.13 | 0.22 |
| **ACTIFLO® effluent turbidity (NTU)** | 0.91 | 0.81 | 0.57 | 0.66 | 0.69 |
| **Percentage of turbidity removal (%)** | 98.9 | 99.4 | 99.1 | 97.9 | 97.4 |

Two types of water samples were used for these tests:

i. **Direct sampling:** Water samples were collected during a storm event on 14 December 2021, which caused elevated turbidity in the raw water. The same coagulant, microsand and polymer dosages that were used in the full-scale plant on the day of sampling (shown in Table 5.1) were used in the jar tests.

ii. **Spiked water sample:** Water samples were prepared by adding the appropriate amount of kaolin to the raw water collected from Plant A (batch 2) representing historical high turbidity levels in Table 5.2. Jar tests were performed using the dosages listed in Table 5.2 that were used during these events to observe how well the bench-scale simulation of the ACTFLO® unit using kaolin works at elevated turbidity conditions in the plant. The characteristics of the particles in these water samples would differ from those in the actual raw water samples.

#### 5.3.4.3 Extremely High Turbidity Representing Future Weather Events

In phase 3 (shown in Figure 5.3), the ACTIFLO® process was simulated at bench-scale on water samples with extremely and unusually high turbidity that was not experienced yet in Plant A, but may occur in the future due to extreme weather events caused by climate change. The water samples with very high turbidity (400-500 NTU) were prepared by adding 0.35 g/L of kaolin to the raw water. The characteristics of the particles in these water samples are very likely to differ from those in the actual

raw water samples. Since the dosages of coagulant, microsand and polymer have been found to have the most impact on turbidity removal on jar tests, a factorial design was conducted by using these three dosages as the independent variables to determine the significant parameter(s) and optimize the process. A full factorial design was performed with center point replicates using spiked raw water samples (batch 3) with turbidity ranging from 400 to 500 NTU, which was not observed in the raw water of Plant A in the years 2019 and 2020 as shown in Figures 3.3 and 3.4. The dependent variable or the yield in the factorial experiment was the percentage of turbidity removed after 15 minutes of settling. For the factorial design, the low values of the independent variables were selected as the highest dosages used in the plant from past data, and the high values were selected by doubling these low values. The middle values were calculated from the high and low values. In these experiments, coded values of the independent variables were used as it has been found beneficial to identify the relative impact of the parameters by comparing the factor coefficients (Ezemagu et al., 2021). The high and low coded and uncoded values of the independent variables are related by the following equation:

$$Coded\ value = \frac{Uncoded\ value - Mean}{\frac{Range}{2}} \qquad (5.1)$$

Table 5.3 lists the coded and uncoded values of the independent variables for the experiments in the jar tests representing the high, low and middle levels.

Table 5.3: Coded and uncoded values of factors

| Independent variables | Symbols | Coded value | Uncoded value |
|---|---|---|---|
| Coagulant dosage | C | +1 | 100 mg/L |
| | | 0 | 75 mg/L |
| | | -1 | 50 mg/L |
| Microsand dosage | M | +1 | 8.0 g/L |
| | | 0 | 6.0 g/L |
| | | -1 | 4.0 g/L |

| | | | |
|---|---|---|---|
| Polymer dosage | P | +1 | 0.56 mg/L |
| | | 0 | 0.42 mg/L |
| | | -1 | 0.28 mg/L |

The coded values +1, 0 and -1 represent the high, middle and low values of the independent variables respectively. Since there are three factors, the factorial design was a $2.2^3$ full factorial design with each run replicated and 3 center point replications, which means 19 experimental runs in total. The order in which each run, statistically known as a treatment, was conducted was randomized to minimize the unpredicted variations in the observed responses caused by uncontrolled irrelevant issues (Ezemagu et al., 2021). Table 5.4 lists the treatments of the experiments.

Table 5.4: Combinations of coded variables for the factorial design

| **Treatments** | **ID** | **Replicates** | **Coagulant dosage (C)** | **Microsand dosage (M)** | **Polymer dosage (P)** |
|---|---|---|---|---|---|
| 1 | (1) | 2 | -1 | -1 | -1 |
| 2 | C | 2 | +1 | -1 | -1 |
| 3 | M | 2 | -1 | +1 | -1 |
| 4 | P | 2 | -1 | -1 | +1 |
| 5 | C*M | 2 | +1 | +1 | -1 |
| 6 | M*P | 2 | -1 | +1 | +1 |
| 7 | P*C | 2 | +1 | -1 | +1 |
| 8 | C*M*P | 2 | +1 | +1 | +1 |
| 9 | center point | 3 | 0 | 0 | 0 |

The design responses obtained from the factorial design experiments were analyzed by fitting the yield to a second-order polynomial model. The relationship between the expected response and the coded independent variables is shown by a second-order polynomial regression equation in Equation 5.2.

$$Y_i = \beta_0 + \beta_C C + \beta_M M + \beta_P P + \beta_{CM} CM + \beta_{MP} MP + \beta_{PC} PC + \beta_{CMP} CMP + e_i , \quad (5.2)$$

where, $\beta_0$ is the intercept, $\beta_C$, $\beta_M$ and $\beta_P$ are the coefficients for linear terms for C, M and P respectively, $\beta_{CM}$, $\beta_{MP}$, $\beta_{PC}$ and $\beta_{CMP}$ are the coefficients for interaction terms for C*M, M*P, P*C and C*M*P respectively. The statistical error ($e_i$) in Equation (5.2) can be estimated using Equation (5.3).

$$e_i = Y_{i\,exp} - Y_{i\,fit} , i = 1\ to\ n \quad (5.3)$$

where, $e_i$ represents the residual, which is the difference between the experimental value of yield ($Y_{iexp}$) and the fitted value ($Y_{i\,fit}$), and $n$ is the total number of experimental runs.

Residual plots were used to check the nature of the residuals in the regression model. The coefficient of determination, $R^2$ and adjusted $R^2$ were calculated. $R^2$ is loosely interpreted as the proportion of the variability in the data explained by the model. $R^2$ can be calculated using Equation (5.4).

$$R^2 = 1 - \frac{RSS}{SST}, \quad (5.4)$$

where RSS is the residual sum of squares and SST is the total sum of squares. The value of $R^2$ ranges from 0 to 1. Larger values are more desirable since it would mean the model is able to explain a higher ratio of the variability. The adjusted $R^2$ is a variation of the ordinary $R^2$ which incorporates the number of factors in the model.

$$R^2_{adj} = 1 - \frac{n-1}{n-p}\frac{RSS}{SST}, \quad (5.5)$$

where, $p$ is the number of factors. The adjusted $R^2$ is a measure of the adequacy of the model. It should be always less than $R^2$ (Montgomery, 2013).

A hypothesis test was done on the coefficients by means of the Student's t-test of the null hypothesis that a coefficient equals zero. The 95% confidence intervals (CIs) of the coefficients were also calculated.

The effects of each factor and their interactions were calculated. The effect for a factor represents the predicted change in the mean response when the factor changes from the low level to the high level. Effects are twice the value of the coded coefficients. The sign of the effect indicates the direction of the

relationship between the term and the response (Montgomery, 2013). The normal probability plot (NPP) of the effects of the factors and interactions was used to determine the significant parameter(s). Marginal means plots were used to comprehend the interaction between the factors.

Analysis of variance (ANOVA) was used as a model-independent approach to find the significant parameter(s). ANOVA states the total variability in the data measured by the total corrected sum of squares and can be partitioned into a sum of squares of the differences between the treatment averages and the grand average plus a sum of squares of the differences of observations within treatments from the treatment average (Montgomery, 2013). The statistical significance of the factors and their interactions were determined using F-value (Fisher's test), and the variation of the calculated F-value (F-probe) with the critical F-value at 95% confidence level by p-value (probability). Hence the significance level, $\alpha$ is equal to 5% and if the p-value for a factor is found to be less than 0.05, the factor would be statistically significant.

## 5.4 Results and Discussion

### 5.4.1 Bench-scale Simulation of the ACTIFLO® Process Water Samples with Regular Turbidity

The jar tests were performed on two batches of water samples collected from the intake of Plant A. The coagulant, polymer and microsand dosages that were used on the day of sampling were used in the jar tests as well. The raw water turbidity in each jar, dosages and the post-jar test turbidities are summarized in Table 5.5.

Table 5.5: Results of bench-scale simulations using raw water samples of batches 1 and 2

| **Batch no.** | Batch 1 (10 Sep. 2021) | | | Batch 2 (14 Oct. 2021) | | |
|---|---|---|---|---|---|---|
| **Sample no.** | 1 | 2 | 3 | 1 | 2 | 3 |
| **Raw water turbidity (NTU)** | 8.23 | 6.71 | 6.66 | 3.75 | 3.63 | 3.66 |
| **Coagulant dosage (mg/L)** | 35.0 | | | 50.0 | | |

| **Microsand dosage (g/L)** | 1.6 | | | 1.0 | | |
|---|---|---|---|---|---|---|
| **Polymer dosage (mg/L)** | 0.17 | | | 0.13 | | |
| **Mean (n=3) post-jar test water turbidity (NTU) (Settling time = 15 min)** | 1.04 | 0.64 | 0.65 | 0.93 | 0.88 | 0.89 |
| **Percentage (%) of turbidity removal** | 87.4 | 90.5 | 90.2 | 75.2 | 75.8 | 75.7 |

The raw water turbidity of batches 1 and 2 were recorded as 5.12 NTU and 5.08 NTU respectively (listed in Table 5.1). However, as shown in Table 5.5, the turbidity varied from 8.23 NTU to 6.66 NTU for batch 1 and 3.63 NTU to 3.75 NTU for batch 2 in the sampling containers. This variation was observed because particle distribution in the raw water is not homogenous. When the raw water was poured into different containers, the unequal distribution of particles caused different turbidity in different sampling containers.

The results of the jar tests for batch 1 and batch 2 water samples were plotted in Figure 5.5. The goal turbidity of the full-scale ACTIFLO® unit in Plant A is 1.0 NTU. For one sample in batch 1, the post-jar test water turbidity is a little higher than the goal. For all the other samples in batches 1 and 2, the post-jar test water turbidity was lower than the goal. The full-scale ACTIFLO® effluent turbidity for batches 1 and 2 were 0.22 NTU and 0.34 NTU respectively. All the jar tests resulted in higher post-jar test turbidity than the full-scale units. Nonetheless, the turbidity was found to be below the goal turbidity after the jar test in almost all cases and the jar tests removed 75.2% to 90.5% of raw water turbidity, which indicates that the bench-scale simulation can fairly reproduce the full-scale unit and can be used as an initial decision-making tool.

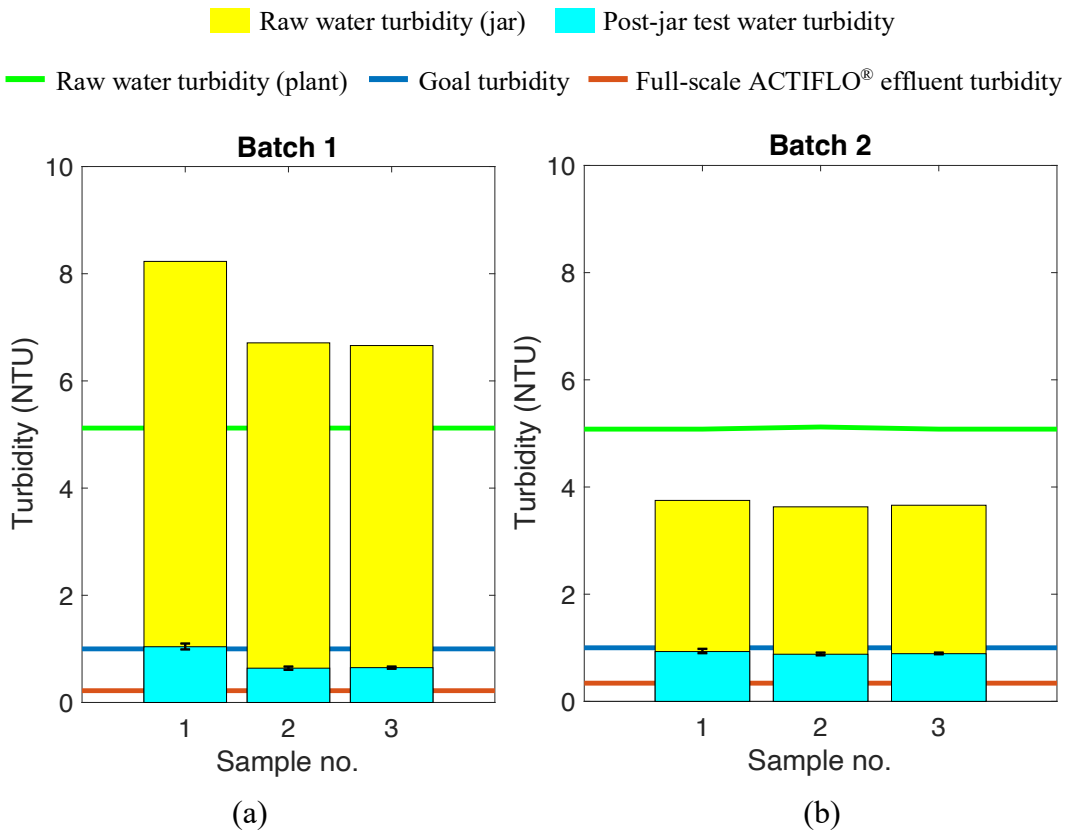


Figure 5.5: Bench-scale jar test results of raw water samples with regular turbidity during normal weather, (a) batch 1 (10 Sep. 2021) and (b) batch 2 (14 Oct. 2021)

### 5.4.2 Bench-scale Simulation of the ACTIFLO® Process Water Samples with Historical High Turbidity

The jar tests were performed on the water samples collected during a heavy precipitation event on 14 December 2021 (batch 3). Although the average raw water turbidity was 37.4 NTU recorded in the plant, the turbidity varied from 25.6 NTU to 63.0 NTU from container to container. This was caused by the non-homogenous distribution of particles in each sampling container. However, the variation in batch 3 was much larger than in batches 1 and 2. Since the raw water turbidity of batch 3 was substantially higher than the previous batches, there were more particles in the raw water, which led to a higher variation of turbidity in the sampling containers. The coagulant, polymer and microsand dosages that were used in the plant on the day of sampling were used in the jar tests as shown in Table

5.1. The raw water turbidity in each jar, dosages and the post-jar test turbidities are summarized in Table 5.6.

Table 5.6: Results of bench-scale simulations using water samples of batch 3

| **Sample no.** | 1 | 2 | 3 | 4 | 5 | 6 |
|---|---|---|---|---|---|---|
| **Raw water turbidity (NTU)** | 25.6 | 29.1 | 31.4 | 61.5 | 62.8 | 63.0 |
| **Coagulant dosage (mg/L)** | 40.0 | | | | | |
| **Microsand dosage (g/L)** | 1.9 | | | | | |
| **Polymer dosage (mg/L)** | 0.22 | | | | | |
| **Mean (n=3) post-jar test water turbidity (NTU) (Settling time = 15 min)** | 3.94 | 5.30 | 6.29 | 11.0 | 16.8 | 14.7 |
| **Percentage (%) of turbidity removal** | 84.6 | 81.8 | 80.0 | 82.1 | 73.2 | 76.7 |

The results for batch 3 water samples are plotted in Figure 5.6. As stated previously, the goal turbidity of the full-scale ACTIFLO® unit in Plant A is 1.0 NTU. For all the samples in batch 3, the post-jar test water turbidity was significantly higher than the goal. The full-scale ACTIFLO® effluent turbidity was 0.70 NTU. All the jar tests resulted in much higher post-jar test turbidity than the full-scale units. As shown in Figure 5.5, the post-jar test turbidity was also higher than the full-scale ACTIFLO® effluent turbidity for batches 1 and 2, but the difference is not as high as batch 3. One reason may be the high raw water turbidity in batch 3. Moreover, the raw water turbidity in batch 3 was significantly higher than that of batches 1 and 2, but there is not much difference in the coagulant, microsand and polymer dosage that were used in the full-scale plant. In fact, the coagulant dosage used for batch 3 was much lower (40 mg/L) than that of batch 2 (50 mg/L), which worked for the full-scale plant, but may have caused the higher post-jar turbidity in batch 3 at bench-scale. Furthermore, the full-scale impeller design, lamella settling and the upflow velocity of the water could not be replicated in jar tests (Desjardins et al., 2002), which is why the post-jar test turbidity varied from the full-scale effluent

turbidity and the variation becomes larger with increasing raw water turbidity. However, the jar tests removed 73.2% to 84.6% of raw water turbidity, indicating that the bench-scale jar tests can be used as an initial tool to optimize the full-scale although the accuracy may be a bit lower.

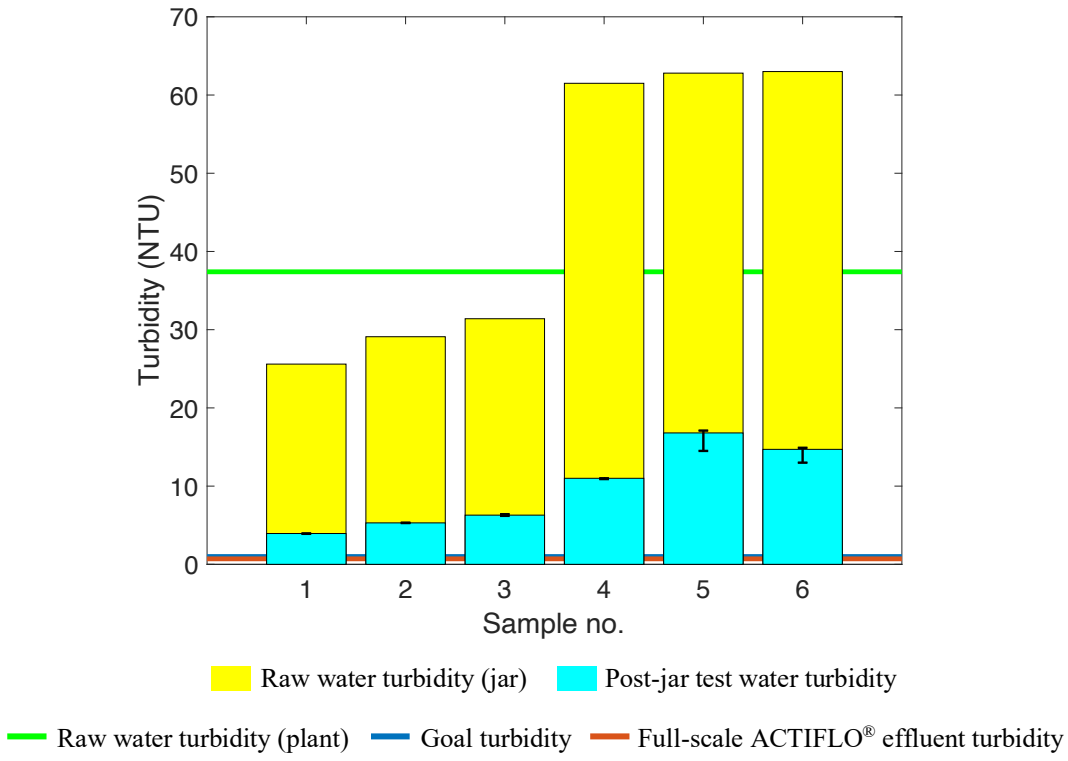


Figure 5.6: Bench-scale jar test results for water samples with high turbidity collected during a heavy precipitation event (14 Dec. 2021)

To recreate the turbidity events listed in Table 5.2, spiked raw water samples were prepared by adding kaolin to the raw water collected from Plant A with the same turbidity as the mean turbidity of the events. However, it is almost impossible to prepare a spiked water sample with an exact turbidity value, so the spiked water turbidity was kept between the daily mean and peak turbidity during the events and the same coagulant, microsand and polymer dosages as in the full-scale plant (listed in Table 5.2) were applied in the jar tests. Table 5.7 shows the results of the jar tests using the spiked water samples representing some historical high turbidity events experienced in Plant A.

Table 5.7: Results of bench-scale simulations for spiked water samples representing historical high turbidity events

| **Event no.** | Event 1 | Event 2 | Event 3 | Event 4 | Event 5 |
|---|---|---|---|---|---|
| **Sample no.** | 1 | 2 | 3 | 4 | 5 |
| **Spiked raw water turbidity (NTU)** | 91.4 | 141 | 70.2 | 33.7 | 27.8 |
| **Coagulant dosage (mg/L)** | 37.7 | 40.0 | 40.0 | 35.0 | 40.0 |
| **Microsand dosage (g/L)** | 2.3 | 1.1 | 1.1 | 1.3 | 1.6 |
| **Polymer dosage (mg/L)** | 0.28 | 0.27 | 0.22 | 0.13 | 0.22 |
| **Mean (n=3) post-jar test water turbidity (NTU) (Settling time = 15 min)** | 19.5 | 21.6 | 17.6 | 6.04 | 8.85 |
| **Percentage (%) of turbidity removal** | 78.7 | 84.8 | 75.0 | 82.1 | 68.1 |

Figure 5.7 illustrates the result of the jar tests simulating the historical turbidity events in Plant A. Applying the same coagulant, microsand and polymer dosages that were used during these events in the full-scale units removed 68.1% to 84.8% turbidity at bench-scale, but all the post-jar test turbidities were significantly higher than both the goal and full-scale ACTIFLO® effluent raw water turbidity. The difference between the post-jar test turbidity and full-scale effluent turbidity is much higher than that of batches 1, 2 and 3. One reason may be that the characteristics of the particles in the spiked water were different from the actual raw water as the raw water was spiked artificially using kaolin. Moreover, the raw water turbidity during the events was significantly higher than that of batches 1, 2 and 3, but the coagulant dosages that were used in the plant during those events, were lower or equal to the coagulant dosages that were used in the plant during normal weather (batch 1 and 2). These coagulant dosages worked in the full-scale plant with similar or increased microsand and polymer dosages (listed in Table 5.2). However, at bench-scale, the post-jar test turbidity varied significantly from the full-scale effluent turbidity, and other limitations (impeller design, absence of lamella settling and upflow velocity of water, etc.) may have played a role. Nonetheless, the percentage of turbidity removal

suggests that the jar tests can remove a considerable amount of the spiked water turbidity, which can be used for further investigation to optimize the full-scale ACTIFLO® process.

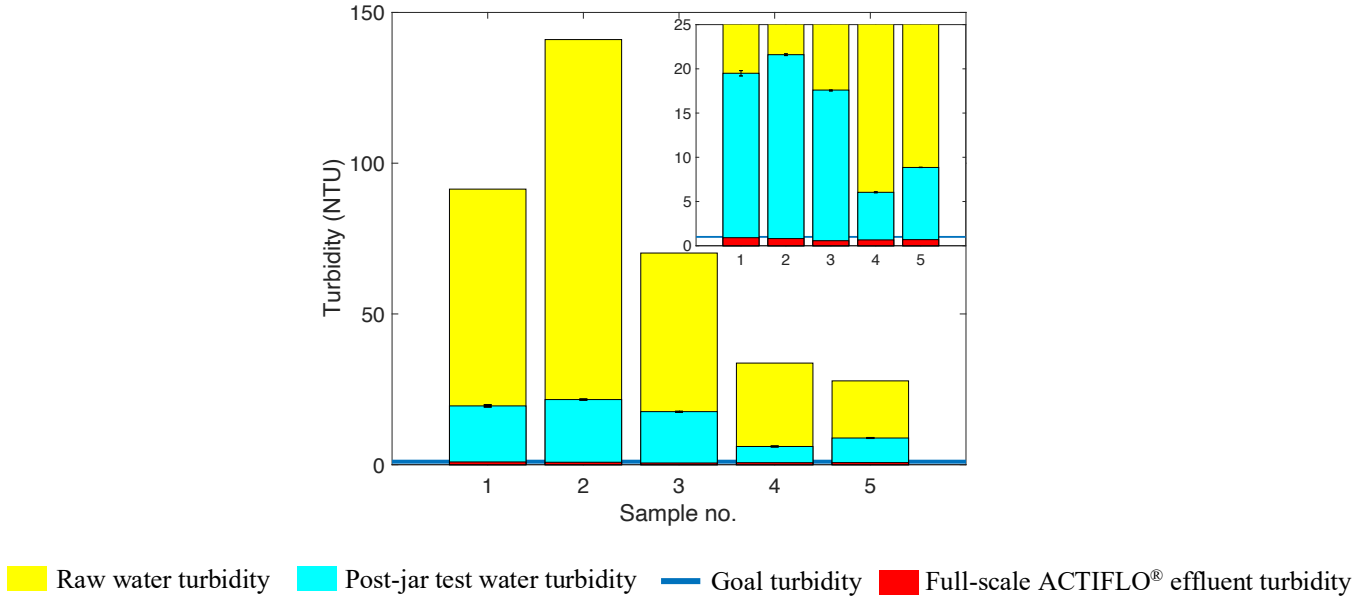


Figure 5.7: Bench-scale simulation results of spiked water samples with historical high turbidity

### 5.4.3 Bench-scale Simulation of the ACTIFLO® Process Water Samples with Extremely High Turbidity

The jar tests were performed on spiked water samples that were prepared in the laboratory by adding kaolin to the raw water collected from Plant A. Table 5.8 lists the results of the factorial design experiments on water samples with extremely high turbidity that may occur in the future due to climate change. The post-jar test turbidity of these tests varied from 11.3 NTU to 193 NTU, which are significantly higher than the goal turbidity, 1.0 NTU. Although the spiked water turbidity for each run was very high, the percentage of turbidity removal for almost all the experimental runs are higher than the jar tests for spiked water samples with historical high turbidity (listed in Table 5.7). The reason behind this higher removal may be the increased coagulant, microsand and polymer dosages since the low values of these dosages in the factorial design were the highest dosages used in the plant in the years 2019 and 2020. The difference between post-jar test turbidities of the duplicate runs is observed to be very close except for run 7. The post-jar test turbidities were substantially higher for this run, and

the difference between the two duplicates was 52 NTU. In run 7, higher dosages of coagulant and polymer were used, but the microsand dosage was low (P*C). The reason behind the low removal in this run may be the lower dosage of microsand compared to the coagulant and polymer dosages, because the flocs in the jars did not have enough ballasting agent to attach and settle. The higher post-jar test turbidity led to more unsettled particles in the jars, which resulted in more variation in turbidity than in any other run.

Table 5.8: Result of the factorial design experiment with coded independent variables

| **Run** | **ID** | **Coagulant dose (a)** | **Microsand dose (b)** | **Polymer dose (c)** | **Spiked water turbidity (NTU)** | **Post-jar test turbidity (NTU)** | **Yield, Y = Percent turbidity removal (%)** |
|---|---|---|---|---|---|---|---|
| 1-1 | (1) | -1 | -1 | -1 | 462 | 28.9 | 93.7 |
| 1-2 | (1) | -1 | -1 | -1 | 441 | 21.1 | 95.2 |
| 2-1 | C | +1 | -1 | -1 | 432 | 23.2 | 94.6 |
| 2-2 | C | +1 | -1 | -1 | 422 | 18.0 | 95.7 |
| 3-1 | M | -1 | +1 | -1 | 443 | 25.6 | 94.2 |
| 3-2 | M | -1 | +1 | -1 | 477 | 25.3 | 94.7 |
| 4-1 | P | -1 | -1 | +1 | 440 | 41.2 | 90.6 |
| 4-2 | P | -1 | -1 | +1 | 469 | 37.1 | 92.1 |
| 5-1 | C*M | +1 | +1 | -1 | 467 | 11.3 | 97.6 |
| 5-2 | C*M | +1 | +1 | -1 | 448 | 14.4 | 96.8 |
| 6-1 | M*P | -1 | +1 | +1 | 436 | 45.4 | 89.6 |
| 6-2 | M*P | -1 | +1 | +1 | 479 | 36.7 | 92.3 |

| | | | | | | | |
|---|---|---|---|---|---|---|---|
| 7-1 | P*C | +1 | -1 | +1 | 443 | 141 | 68.2 |
| 7-2 | P*C | +1 | -1 | +1 | 439 | 193 | 56.0 |
| 8-1 | C*M*P | +1 | +1 | +1 | 462 | 32.1 | 93.1 |
| 8-2 | C*M*P | +1 | +1 | +1 | 452 | 37.9 | 91.6 |
| 9-1 | center point | 0 | 0 | 0 | 426 | 16.6 | 96.1 |
| 9-2 | center point | 0 | 0 | 0 | 422 | 12.3 | 97.1 |
| 9-3 | center point | 0 | 0 | 0 | 468 | 17.4 | 96.3 |

The results of the factorial design experiment were analyzed by a second-order polynomial model. The fitted model is:

$$Y = 90.8 - 3.01C + 3.98M - 5.57P + 4.08CM + 3.48MP - 3.91PC + 3.58CMP + e \qquad (5.6)$$

To find the significant effects or interactions, the t-test was performed and 95% CI of the coefficients were calculated, which are listed in Table 5.9.

Table 5.9: t-test and 95% CI of the regression coefficients

| **Coefficients** | | **t-probe** | **95% CI** |
|---|---|---|---|
| $\beta_0$ (intercept) | 90.8 | 93.6 | [88.7 93.0] |
| $\beta_C$ | -3.06 | -2.89 | [-5.38 -0.73] |
| $\beta_M$ | 3.98 | 3.76 | [1.65 6.30] |
| $\beta_P$ | -5.57 | -5.27 | [-7.89 -3.24] |
| $\beta_{CM}$ | 4.08 | 3.86 | [1.75 6.41] |
| $\beta_{MP}$ | 3.48 | 3.29 | [1.15 5.81] |

| | | | |
|---|---|---|---|
| $\beta_{PC}$ | -3.91 | -3.70 | [-6.24 -1.59] |
| $\beta_{CMP}$ | 3.58 | 3.38 | [1.25 5.90] |

The value of t-critical was found to be 2.20 for $\alpha = 5\%$. All of the absolute values of t-probe were found to be higher than t-critical, which means all the factors and the interactions are significant. The CIs of the coefficients also indicate that the errors associated with the coefficients are not larger than the coefficients, and the CIs do not include zero which represents that the model is a good fit.

To visualize the effects of different factors and their interactions, the effect (percentage of turbidity removal) of each factor and their interactions are plotted in Figure 5.8.

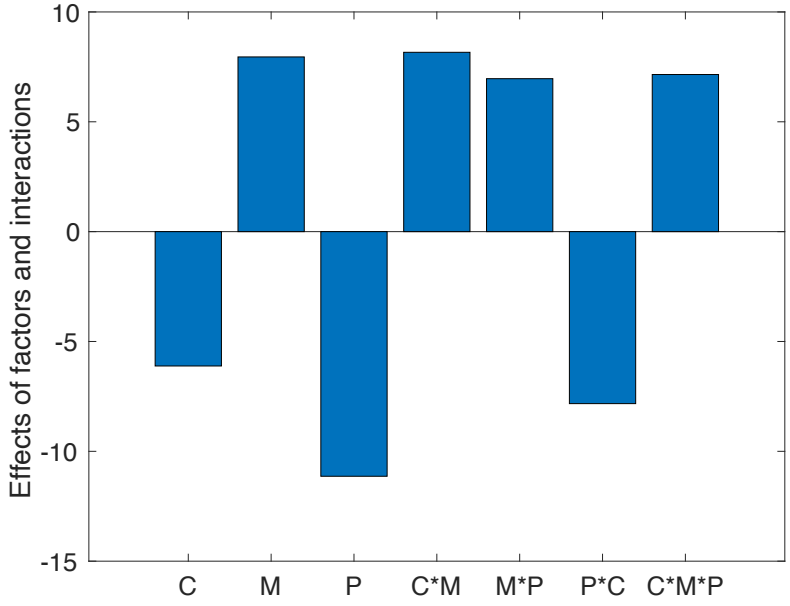


Figure 5.8: Effects of the factors and interactions

Although from the t-test it was found that all the factors and their interactions were significant, from Figure 5.8 it is visible that they have different levels of significance. If the microsand dosage (M), and combination of coagulant and microsand dosage (C*M), microsand and polymer dosage (M*P) and the combinations of the three main factors, coagulant, microsand and polymer dosage (C*M*P) are changed from the low value to high value, it is predicted that the mean percent turbidity removal would

increase. Similarly, if the coagulant dosage (C), polymer dosage (P) and the combination of coagulant and polymer dosage (P*C) are changed from high value to low value, the mean percent turbidity removal would increase.

The marginal means plots are presented in Figure 5.9 to understand the nature of interactions between the main factors. It is visible that all the factors are correlated. The coagulant and microsand dosages (C*M) have the most interaction, followed by microsand and polymer dosages (M*P), and the polymer and coagulant dosages (P*C), which is similar to the findings from the effects of the factors in Figure 5.8.

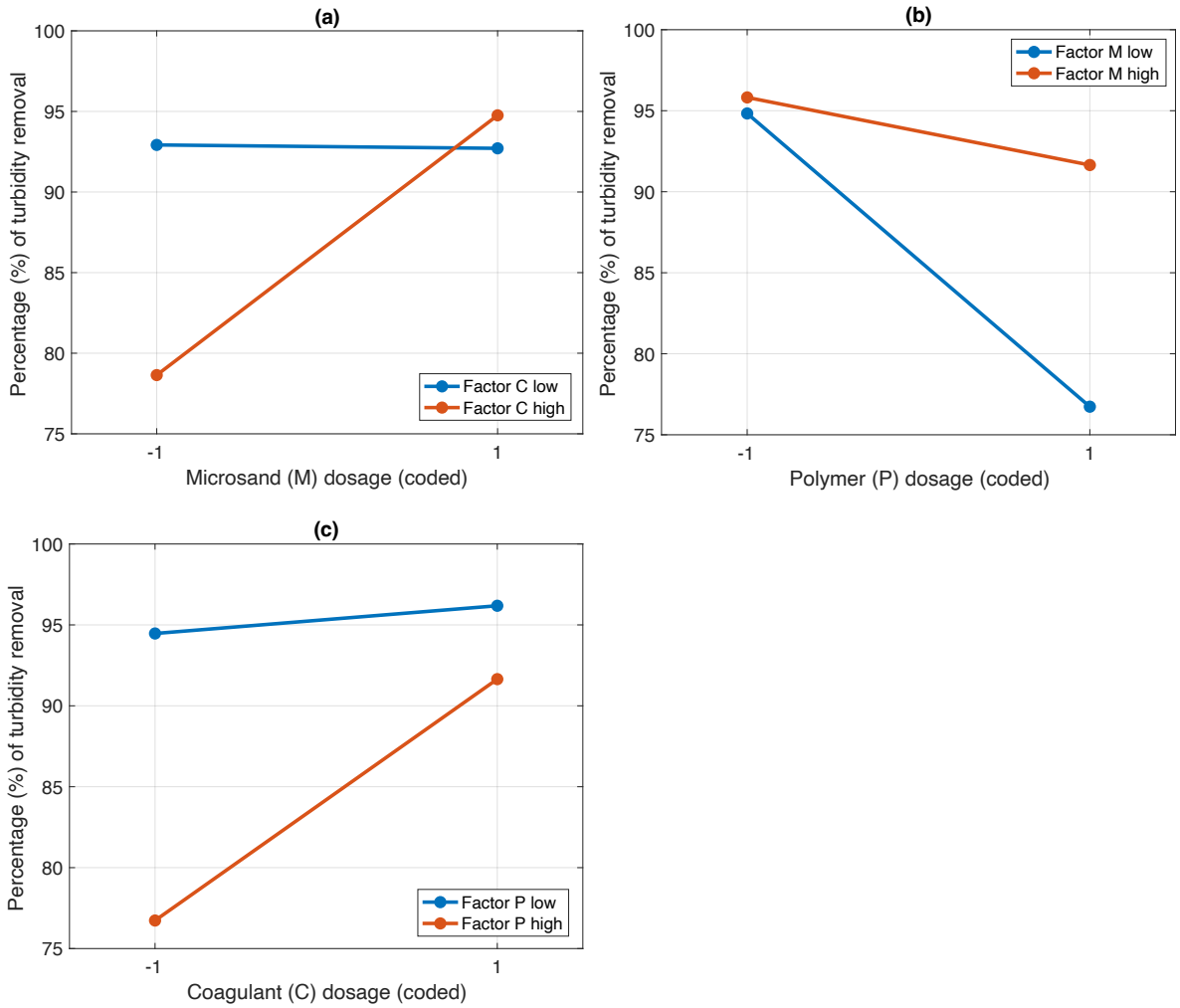


Figure 5.9: Marginal means plot of the interactions between (a) coagulant and microsand dosage (C*M), (b) microsand and polymer dosage (M*P), and (c) polymer and coagulant dosage (P*M)

The NPP of the effects of the main factors and their interactions are shown in Figure 5.10. From this figure, it is visible that the polymer dosage is the most significant effect as it deviates from the normal distribution of the other effects.

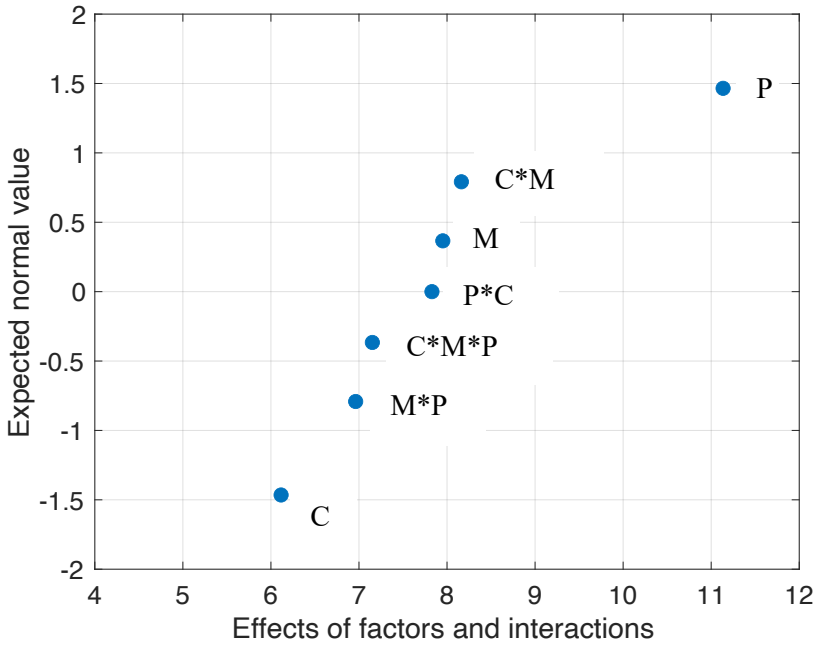


Figure 5.10: Normal distribution of the effects of the main factors and their interactions

The coefficient of determination, $R^2$ of the model is found to be 0.90, which is close to 1.0 indicating that the predicted and experimental responses were close and 90% of the data fit the model and 90% of the variability in the yield is associated to the independent variables. However, the adjusted $R^2$ was found to be 0.85, which indicates that the accuracy of the model may be adequate.

The nature of the residuals can be a good indicator of the model fit. Figure 5.11 shows the residual plots with the independent variables (data shown in Appendix C: Table C.2). The residuals are scattered both above and below the zero line, but all the residuals for the center-points are positive. This indicates that the fit of the model may be adequate since the experimental values of the percentage of turbidity removal for the all center-point runs were higher than the predicted values.

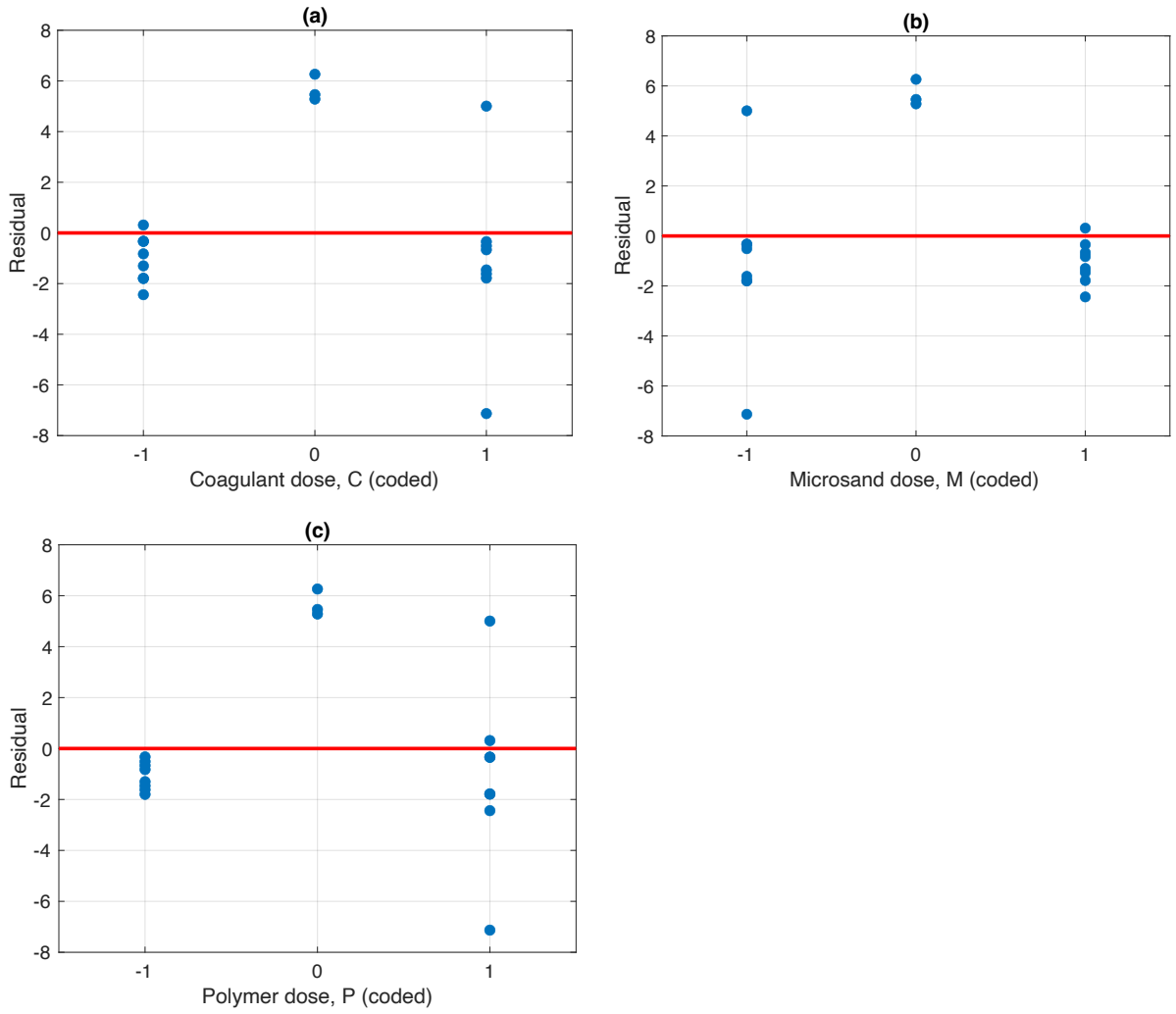


Figure 5.11: Residuals of the model with respect to (a) coagulant dosage (coded), (b) microsand dosage (coded) and (c) polymer dosage (coded)

The ANOVA table shown in Table 5.10 was generated from the experimental data to determine the statistical significance of the factors and their interactions. From Table 5.10, it is observed that the p-value for the microsand dosage (M), polymer dosage (P) and the interaction of coagulant and microsand dosage (C*M) are less than or equal to 0.05, which indicates that these are the significant factors in the factorial design experiments from a model-independent approach.

Table 5.10: ANOVA table for the factors and their interactions

| Source | Sum of squares | Degree of freedom | Mean sum of squares | F-probe | p-value |
|---|---|---|---|---|---|
| C | 126.0 | 1 | 126.0 | 2.87 | 0.118 |
| M | 213.0 | 1 | 213.0 | 4.86 | 0.050* |
| P | 417.7 | 1 | 417.7 | 9.53 | 0.010* |
| C*M | 224.5 | 1 | 224.5 | 5.12 | 0.045* |
| M*P | 163.3 | 1 | 163.3 | 3.72 | 0.080 |
| P*C | 206.4 | 1 | 206.4 | 4.71 | 0.053 |
| C*M*P | 172.3 | 1 | 172.3 | 3.93 | 0.073 |
| Error | 482.2 | 11 | 43.84 | | |
| Total | 2005.4 | 18 | | | |

*significant (<= 0.05)

To summarize the findings from the analysis of the factorial design experiments, it is observed that polymer dosage is the most significant factor and increasing the polymer dosage without increasing the microsand dosage can result in decreased turbidity removal. The excess polymer can trap the coagulated particles in the settled water (Desjardins et al., 2002), which may lead to higher post-jar test turbidity. The role of polymer in the ACTIFO® system is to assist the bridging action between microsand and pre-formed flocs (Desjardins et al., 2002; He et al., 2019; Lapointe et al., 2017; Zafisah et al., 2020). However, if the polymer dosage is high, but the microsand dosage is low, the flocs cannot settle as effectively, leading to higher post-jar test turbidity. The microsand dosage has also been found significant in some analyses and increasing the microsand dosage can lead to higher turbidity removal by adding more ballasting agent for the flocs to attach with. The role of microsand is unquestionable since ballasted flocculation is based on the use of microsand (Desjardins et al., 2002). Coagulant dosage was not found to be significant, but increasing both coagulant and microsand dosage can lead to higher

removal since increased coagulant dosage can destabilize the particles and form flocs in the water and the microsand acts as the ballasting agent for the flocs to settle. Therefore, optimal turbidity removal can be achieved by using low polymer dosage, and high coagulant and microsand dosages. It should be noted that the low values in these experiments are the highest dosages that have been used in the full-scale plant. Hence, the results of this factorial design experiment suggest that the polymer dosage used in the plant is optimum for extremely high turbidities, but the coagulant and microsand dosages can be increased for better removal.

### 5.4.4 Limitations of the bench-scale Simulation

There are some differences observed between the post-jar test turbidity and full-scale ACTIFLO® effluent turbidity in the jar tests that simulate the full-scale procedure at bench-scale with the raw water samples collected from the plant. Although the jar test is essentially a batch reactor simulating a flow-through system, the upflow velocity of water, lamellar settling, exact impeller and basin design of the full-scale units cannot be simulated in jar tests (Desjardins et al., 2002), which may be the reason behind the variations.

In the bench-scale simulations using the spiked water samples representing the historical high turbidity events and unprecedented extremely high turbidity events, it has been observed that higher removal efficiency was achieved when the spiked water turbidity was very high. The percentage of turbidity removal for the jar tests using the raw water samples of batch 3 (shown in Table 5.6) was lower than that for most of the runs of the factorial design experiments (shown in Table 5.8). The spiked water samples were prepared by adding kaolin to the raw water samples of batch 3, so the property of kaolin may have affected the overall nature of turbidity and thus the simulation results. This can be explained by the zeta potential of the raw and spiked water samples, which is summarized in Figure 5.12 (data shown in Appendix C: Table C.1). The green bars correspond to the average zeta potential, for the raw water samples it was -12.3 mV but in the spiked water samples, the average zeta potential was found to be -18.5 mV. The error bars in the figure represent the maximum and minimum zeta potential of the samples. The addition of kaolin increases the turbidity, but it also adds more negatively charged particles to the water. One explanation could be that the particles react more with the positively charged coagulant (ranging from +18.2 to +26.2 mV for the used dosages, data shown in Appendix C: Table C.1), which resulted in higher turbidity removal in the jar tests.

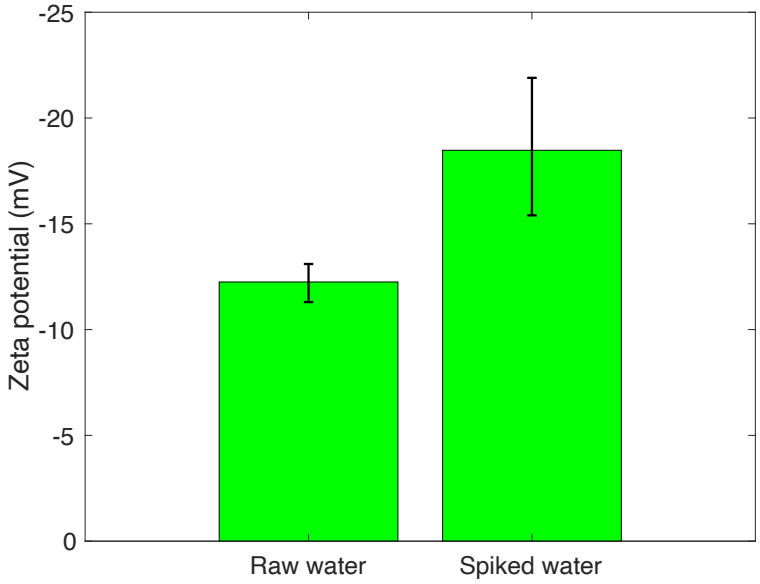


Figure 5.12: Mean zeta potential of different types of water samples (n = 4)

It has been observed during the experiments that the turbidity of spiked water samples tended to decrease if stirring was stopped, whereas the turbidity of raw water samples was almost constant. Kaolin has a higher density than the typical particles in the raw water and settles very quickly. The rate of settling depends on the kaolin concentration. It has been found that for lower concentrations of kaolin (0.025 to 0.050 g/L), the turbidity (27.7 to 70.2 NTU) dropped by 2-5 NTU, and for higher concentrations of kaolin (0.35 to 0.55 g/L), the turbidity (496 to 874 NTU) dropped by 15-20 NTU in a span of 2 minutes. To understand the influence of kaolin in the jar tests, two jar tests were performed on spiked water with 432 and 468 NTU turbidity (same as the factorial design experiments) without adding any chemicals. It was found that only mixing, followed by sedimentation removed 128 and 143 NTU of turbidity respectively. Thus, it is obvious that higher removals were achieved in the experiments using spiked raw water samples which may not be representative of the raw water with elevated turbidity caused by a heavy precipitation event. The particle characteristics in the spiked water samples seem to differ with respect to settleability and zeta potential compared to the actual raw water samples at the intake. Therefore, the bench-scale simulations using spiked water samples can be considered as a primary tool, and the results obtained from these experiments can aid in potential bench-

scale studies using soil sediments collected from the bottom of the intake to prepare spiked water samples to improve the robustness of the ACTIFLO® process.

## 5.5 Conclusion

The bench-scale simulations on raw water samples with regular turbidity representing the normal weather fairly reproduced the operations of the full-scale ACTIFLO® units, keeping the effluent turbidity below the goal turbidity of the full-scale unit. The simulation on the water samples collected during the heavy precipitation events and spiked water samples with historical high turbidity representing the past weather events showed adequate removal although the post-jar test turbidity was significantly higher than the full-scale effluent turbidity, which may have been caused by the limitations of bench-scale (impeller design, lamellar settling, upflow velocity of water, etc.). The results obtained from the factorial design performed on spiked water samples with extremely high turbidity representing future weather events were fitted into a second-order polynomial model, which represented the experimental outputs with moderate accuracy. The significant factors obtained from the analysis of the model suggest that a lower dosage of polymer and higher dosage of microsand with a higher dosage of coagulant can lead to higher turbidity removal. Although the bench-scale tests have some limitations, the implication of these tests can be used in future studies.

# Chapter 6: Comparisons, Conclusions and Recommendations

## 6.1 Comparisons

The robustness framework was applied to two DWTPs with different raw water sources and treatment trains. There can be two aspects of comparison: how the robustness framework was tailored to these plants, and how the results vary for similar treatment steps in the plants.

### 6.1.1 Applicability of the Robustness Framework

**Step 1 – Parameters:** For both plants, the first step of the robustness framework was the same because the selected water quality parameter in this study was turbidity.

**Step 2 – Criteria:** Filter effluent turbidity is a regulated parameter. As both plants are in Ontario, they follow the same provincial regulations regarding drinking water quality. The criteria set by the staff of Plants A and B were at least as stringent as prescribed regulated values. However, as Plant A uses bio-filtration and Plant B uses conventional dual media filtration, the criteria set by the staff of the two plants can be different.

**Step 3 – Identification:** The critical treatment steps were the ACTIFLO® and filtration for Plant A, and conventional CFS and filtration for Plant B. Both ACTIFLO® and conventional CFS processes removed the particles from the raw water before filtration. It should be noted that Plant A has ozonation between the ACTIFLO® units and filtration, however since ozonation is not a particle removal step, it is not considered in the analysis.

**Step 4 – Evaluation:** The robustness of the identified critical steps of both plants was quantified using the same tool, TRI. However, the method to identify turbidity events from background turbidity was different. From the raw water turbidity data, it is visible that the baseline turbidity of Plant A is much higher than Plant B, and Plant A experienced much longer and more frequent elevated turbidity events than Plant B. This is expected because the raw water source of Plant A is a river, so the raw water is more influenced by heavy precipitation events. In contrast, the source water of Plant B is one of the Great Lakes, which is why the baseline raw water turbidity is very low. During heavy precipitation events, the raw water turbidity in Plant B increases, but not as much as in Plant A. Due to these variances, slightly different methods were applied to separate the turbidity events from background

turbidity. Therefore, for this step of the robustness framework, the same tool (TRI) can be applied to quantify robustness, but to compare the robustness based on turbidity events, the method to separate the events needed to be modified based on the raw water source.

**Step 5 – Assessment:** The average robustness class was used in both plants to assess the overall robustness of the plants. However, the importance of different treatment steps for the removal of turbidity can vary from plant to plant. To calculate the overall robustness class, the weights of different steps were varied in each plant to give an identification of their contribution to turbidity removal.

**Step 6 – Adaptation:** This step can be very different from plant to plant and from one treatment step to another. In this study, only the ACTIFLO® process in Plant A was optimized at bench-scale by modified jar tests. To optimize the conventional CFS units at bench-scale, the conventional jar test is the most popular approach. Bench-scale setups can be designed for the filtration step to find short-term operational responses to make the steps more robust. Based on the results of the bench-scale experiments, pilot-scale set-ups can be planned for more detailed analysis.

Therefore, all the steps of the robustness framework were efficiently applied to Plant A and Plant B (except for step 6), which are very different in terms of raw water source and treatment trains. The results obtained from the application of the framework can be a diagnostic tool for the water treatment utilities to improve the robustness of their plants.

### 6.1.2 Comparisons between Plant A and Plant B

The ACTIFLO® process in Plant A and the CFS process in Plant B have the same goal: achieving a turbidity of 1.0 NTU. Almost all the TRIs of the ACTIFLO® units of Plant A fell into the “stable” (60-100) class, only a few fell into the “slightly disturbed” (130-160) class. For the same goal, the TRIs of the CFS units of Plant B were found to be much higher. Most of them fell into the “slightly disturbed” (130-160) class. Some of them fell into the “moderately disturbed” (130-160), “upset” (160-200) and “severely upset” (>200) classes. Some of the very high TRIs observed in the CFS units of Plant B can be explained by the very low raw water turbidity as there were not enough particles to react with the coagulant and achieve good floc formation. However, this was not an issue with the ACTIFLO® units for two reasons: the raw water turbidity in Plant A was never as low as in Plant B, and the particles were attached to the ballasting agent (microsand) by the polymer. For both plants, no noteworthy trend

was found between elevated raw water turbidity and high TRIs. This is encouraging from an operational perspective.

The filter performance of both plants was rather similar. The goal turbidity was 0.1 NTU for each individual filter in both plants. For both plants, most of the TRIs fell into the "stable" (60-100) class, only a few in the "slightly disturbed" (130-160) class, and one or two in the "moderately disturbed" (130-160) class. However, the high TRIs do not always correspond to the weather events characterized by raw water turbidity, indicating that the reason behind this is not weather-related. All the filters in both plants met the regulatory criterion set by the Government of Ontario (effluent turbidity < 0.3 NTU, 95% of the measurements per cycle per month).

The overall robustness of both plants was found to be stable for most weeks during the study period. The higher overall robustness categories could not be related to weather events characterized by raw water turbidity in the plants.

## 6.2 Summary of Conclusions

This study focused on the treatment steps that are more likely to be affected by elevated raw water turbidity due to heavy precipitation events caused by climate change. The following conclusions were made by applying the robustness framework to the two DWTPs:

- Plant A is very susceptible to elevated turbidity in their raw water caused by heavy precipitation events as it uses a river as its source. However, the TRIs of the critical treatment steps with respect to turbidity, which are the ACTIFLO® and filtration process indicate that the treatment steps are successful in maintaining the effluent turbidity under the regulatory limits. The overall plant robustness suggests that Plant A has effectively delivered treated water with desired quality during the study period.
- The raw water turbidity of Plant B was relatively low most of the time during the study period since the source water is one of the Great Lakes. The TRIs of the critical treatment steps with respect to turbidity, which are the CFS and filtration process, indicate that the treatment steps were adequate in maintaining the effluent turbidity under the regulatory limits. Some of the high TRIs of the CFS process and their association with the weather events characterized by elevated turbidity suggest that the CFS process may be vulnerable in the future, if the

occurrence of more severe, unusual, and untimely precipitation events becomes more common given the current trend of climate change.

- In both plants, most of the higher (>130) TRIs were not associated with any weather events characterized by raw water turbidity, which implies that the plants were robust during the study period. Therefore, the reason behind the high TRIs was not weather-related. However, the high TRIs can be a good indicator for the operators to review and assess the performances of the treatment steps in the corresponding weeks and re-evaluate their operational regimes.
- The bench-scale simulations of the ACTIFLO® units reproduced the full-scale performance with adequate accuracy. The factorial design experiment on spiked water samples representing unprecedented turbidity events that may occur in the future due to climate change predicted that, in the ranges tested, the polymer dosage used in the plant at present is optimum, but higher dosage of microsand with a higher dosage of coagulant can lead to higher turbidity removal. The spiked water samples may not be representative of the actual raw water experiencing the same level of turbidity, but these experiments can aid in potential pilot- or full-scale studies to improve the robustness of the ACTIFLO® process for extremely high raw water turbidity.
- All the steps of the robustness framework were successfully applied to the two DWTPs with different raw water and treatment trains. The applicability of the framework implies that the robustness framework can be tailored for any utility and used as a comprehensive tool to assess and improve the robustness of the DWTPs.

## 6.3 Recommendations for Future Studies

Based on the above-mentioned conclusions, the recommendations for future research are summarized below:

- In this study, only the effects of heavy precipitation events on raw water were considered as a consequence of climate change. However, the occurrence of several natural and anthropogenic climate-induced phenomena, such as drought, wildfire, cyclones, glacial melting, etc. throughout the world may have diverse repercussions on drinking water quality. There is an urgent need to evaluate and improve the robustness of the DWTPs that are likely to be affected by these events.

- Other than turbidity, unprecedented, intense and untimely precipitation events caused by climate change affect other raw water quality parameters, such as NOM and characteristics and microbiological quality of water. The robustness framework can be modified for these parameters and applied to the DWTPs to evaluate and improve their robustness.
- The TRI method used to quantify the robustness of the critical treatment steps with respect to turbidity has proven to be an effective tool, but it is only based on the 50th and 90th percentile values in the data set. The potential of new or modified robustness indices can be explored, which is not too complicated to apply to a full-scale DWTP and can incorporate the other statistical parameters of the data set, such as the distribution of the data.
- In this study, the sixth step, adaptation of the robustness framework, was applied to only one critical step (ACTIFLO® process in Plant A) at bench-scale by modified jar tests due to time limitations. There is scope to design experiments to simulate the other critical steps at bench-scale and pilot-scale to find short-term operational responses to improve the robustness of these steps, if the raw water quality deteriorates beyond general experience due to climate change in the future.
- The spiked water samples used in the bench-scale experiments were prepared with kaolin, which may not exemplify the real raw water condition because of the higher specific weight and negative charge of the kaolin particles, as well as the fact that they have not interacted with other components of the water such as NOM. Raw water samples collected from the plants can be spiked using soil sediments collected from the bottom of the intake, and can be an alternate way to carry out the experiments that may be more representative of the particles of the raw water.

# References


Abokifa, A. A., Yang, Y. J., Lo, C. S., & Biswas, P. (2016). Investigating the role of biofilms in trihalomethane formation in water distribution systems with a multicomponent model. *Water research*, *104*, 208–219. https://doi.org/10.1016/j.watres.2016.08.006

Alduchov, O. A., & Eskridge, R. E. (1996). Improved magnus form approximation of saturation vapor pressure. *Journal of Applied Meteorology*, *35*(4), 601-609. https://doi.org/10.1175/1520-0450(1996)035<0601:IMFAOS>2.0.CO;2

Atherholt, T. B., LeChevallier, M. W., Norton, W. D., & Rosen, J. S. (1998). Effect of rainfall on giardia and crypto. *Journal / American Water Works Association, 90*(9), 66-80. doi:10.1002/j.1551-8833.1998.tb08499.x

Atherton, F., Newman, C. P., & Casemore, D. P. (1995). An outbreak of waterborne cryptosporidiosis associated with a public water supply in the UK. *Epidemiology and infection*, *115*(1), 123–131. https://doi.org/10.1017/s0950268800058180

Bates, B.C., Kundzewicz, Z.W., Wu, S., & Palutikof, J.P. (2008). Climate Change and Water: Technical Paper of the Intergovernmental Panel on Climate Change. *IPCC Secretariat*, Geneva.

Chen, J., & Chang, H. (2019). Dynamics of wet-season turbidity in relation to precipitation, discharge, and land cover in three urbanizing watersheds, Oregon. *River Research and Applications*, *35*(7), 892–904. https://doi.org/10.1002/rra.3487

Coffey, B. M., Liang, S., Green, J. F., & Huck, P. M. (1998). Quantifying performance and robustness of filters during non-steady state and perturbed conditions. *Proc. AWWA Water Quality Technology Conference, CD-ROM. Denver, CO: AWWA.*

Crittenden, J., Trussell, R. R., Hand, D. W., Howe, K. J., & Tchobanoglous, G. (2012). MWH's water treatment: principles and design (3rd ed.). *Hoboken, N.J: John Wiley & Sons.*

Curriero, F. C., Patz, J. A., Rose, J. B., & Lele, S. (2001). The association between extreme precipitation and waterborne disease outbreaks in the United States, 1948-1994. *American journal of public health*, *91*(8), 1194–1199. https://doi.org/10.2105/ajph.91.8.1194

De Dianous, F., & Dernaucourt, J. C. (1991). Advantages of weighted flocculation in water treatment. *Water Supply, 9*(3-4 supp), S43-S46.

De Roos, A. J., Gurian, P. L., Robinson, L. F., Rai, A., Zakeri, I., & Kondo, M. C. (2017). Review of epidemiological studies of drinking-water turbidity in relation to acute gastrointestinal illness. *Environmental health perspectives*, *125*(8), 086003. https://doi.org/10.1289/EHP1090

Delpla, I., & Rodriguez, M. J. (2016). Experimental disinfection by-product formation potential following rainfall events. *Water Research*, *104*, 340–348. https://doi.org/10.1016/j.watres.2016.08.031

Delpla, I., Jones, T. G., Monteith, D. T., Hughes, D. D., Baurès, E., Jung, A.-V., Thomas, O., & Freeman, C. (2015). Heavy rainfall impacts on trihalomethane formation in contrasting northwestern european potable waters. *Journal of Environmental Quality*, *44*(4), 1241–1251. https://doi.org/10.2134/jeq2014.10.0442

Delpla, I., Jung, A. v., Baures, E., Clement, M., & Thomas, O. (2009). Impacts of climate change on surface water quality in relation to drinking water production. *Environment International*, *35*(8), 1225–1233. https://doi.org/10.1016/j.envint.2009.07.001

Desjardins, C., Koudjonou, B., & Desjardins, R. (2002). Laboratory study of ballasted flocculation. In *Water Research* (Vol. 36).

Emelko, M.B., & Brown, T. (2003). Granular media provide effective pathogen removal. *Water Serv.*, 106:2:11-13.

Eramosa Engineering Inc., Westin Engineering Inc., XCG Consultants Ltd., & R.E. Poisson Engineering Inc. (2015). Pretreatment (flocculation and coagulation) HWFLS (Woodward WTP): Process control narrative. Version 2.5 (Narrative format: SCADA Standards Version 4.4).

Exum, N. G., Betanzo, E., Schwab, K. J., Chen, T. Y. J., Guikema, S., & Harvey, D. E. (2018). Extreme precipitation, public health emergencies, and safe drinking water in the USA. *Current Environmental Health Reports, 5*(2), 305–315. https://doi.org/10.1007/s40572-018-0200-5

Ezemagu, I. G., Ejimofor, M. I., Menkiti, M. C., & Nwobi-Okoye, C. C. (2021). Modeling and optimization of turbidity removal from produced water using response surface methodology and artificial neural network. *South African Journal of Chemical Engineering*, *35*, 78–88. https://doi.org/10.1016/j.sajce.2020.11.007

Fox, K. R., & Lytle, D. A. (1996). Milwaukee's crypto outbreak: investigation and recommendations. *Journal / American Water Works Association*, *88*(9), 87-94.

Füssel, H. (2009). An updated assessment of the risks from climate change based on research published since the IPCC Fourth Assessment Report. *Climatic change, 97*, 469-482. doi: 10.1007/s10584-009-9648-5

García-Ávila, F., Avilés-Añazco, A., Sánchez-Cordero, E., Valdiviezo-Gonzáles, L., & Ordoñez, M. D. T. (2021). The challenge of improving the efficiency of drinking water treatment systems in rural areas facing changes in the raw water quality. *South African Journal of Chemical Engineering*, *37*, 141–149. https://doi.org/10.1016/j.sajce.2021.05.010

George, G., Hurley, M., & Hewitt, D. (2007). The impact of climate change on the physical characteristics of the larger lakes in the English Lake District. *Freshwater Biology, 52*: 1647-1666. https://doi.org/10.1111/j.1365-2427.2007.01773.x

Ghanem, A. V., Young, J. C., & Edwards, F. G. (2007). Mechanisms of ballasted floc formation. Journal of Environmental Engineering, 133(3), 271-277. doi:10.1061/(ASCE)0733-9372(2007)133:3(271)

Gleason, J. A., & Fagliano, J. A. (2017). Effect of drinking water source on associations between gastrointestinal illness and heavy rainfall in New Jersey. *PloS one*, *12*(3), e0173794. https://doi.org/10.1371/journal.pone.0173794

Gregory, J. (1994). Cryptosporidium in water: treatment and monitoring methods. *Filtration & Separation*, *31*(3), 283-268.

Groisman, P. Y., Knight, R. W., Easterling, D. R., Karl, T. R., Hegerl, G. C., & Razuvaev, V. N. (2005). Trends in intense precipitation in the climate record. *Journal of Climate, 18*(9), 1326–1350. https://doi.org/10.1175/JCLI3339.1

Guibelin, E., Delsalle, F., & Binot, P. (1994). The Actiflo® process: A highly compact and efficient process to prevent water pollution by stormwater flows. *Water Science and Technology, 30*(1), 87-96. doi:10.2166/wst.1994.0009

Haarbo, A., Dahl, C., & Rineau, S. (1998). Successful applications: new applications of the Actiflo process. *Water Quality International,* (NOV./DEC.), 29-30.

Hach. (2013). *Water Analysis Handbook*. Hach Company. Loveland, Colorado. https://www.hach.com/wah

Hartshorn, A. J., Prpich, G., Upton, A., Macadam, J., Jefferson, B., & Jarvis, P. (2015). Assessing filter robustness at drinking water treatment plants. *Water and Environment Journal*, *29*(1), 16–26. https://doi.org/10.1111/wej.12094

Hashimoto, T., Stedinger, J. R., & Loucks, D. P. (1982). Reliability, resiliency, and vulnerability criteria for water resource system performance evaluation, *Water Resources Research, 18*(1), 14– 20. doi:10.1029/WR018i001p00014.

He, W., Xie, Z., Lu, W., Huang, M., & Ma, J. (2019). Comparative analysis on floc growth behaviors during ballasted flocculation by using aluminum sulphate (AS) and polyaluminum chloride (PACl) as coagulants. *Separation and Purification Technology,* 213, 176–185. https://doi.org/10.1016/j.seppur.2018.12.043

Health Canada (2012). Guidelines for Canadian Drinking Water Quality: Guideline Technical Document - Turbidity. https://www.canada.ca/en/health-canada/services/publications/healthy-living/guidelines-canadian-drinking-water-quality-turbidity.html

Health Canada (2019). Guidance on Natural Organic Matter in Drinking Water. https://www.canada.ca/en/health-canada/programs/consultation-organic-matter-drinking-water/document.html

Helmuth, B. (2002). How do we Measure the Environment? Linking Intertidal Thermal Physiology and Ecology Through Biophysics. *Integrative and Comparative Biology, 42*(4), 837-845, https://doi.org/10.1093/icb/42.4.837

Huck, P. M., & Coffey, B. M. (2002). Robust drinking water treatment for microbial pathogens—Implications for Cryptosporidium removal. *Proc. 10th International Gothenburg Symposium, Gothenburg, Sweden.*

Huck, P. M., & Coffey, B. M. (2004). The importance of robustness in drinking-water systems. *Journal of Toxicology and Environmental Health -Part A, 67*(20–22), 1581–1590. https://doi.org/10.1080/15287390490491891

Huck, P. M., Payment, P., Hrudey, S. E., & Anderson, W. B. (2001a). A severe waterborne disease outbreak in Walkerton, Ontario: issues relating to treatment and distribution. *AWWA Water Quality Technology Conference (WQTC)*, Nashville, TN, USA, CD-ROM, Paper M8-2.

Huck, P. M., Emelko, M. B., Coffey, B. M., Maurizio, D. D., & O'Melia, C. R. (2001b). Filter operation effects on pathogen passage. *American Water Works Association Research Foundation,* Denver, CO, USA.

Hurst, A. M., Edwards, M. J., Chipps, M., Jefferson, B., & Parsons, S. A. (2004). The impact of rainstorm events on coagulation and clarifier performance in potable water treatment. *Science of the Total Environment*, *321*(1–3), 219–230. https://doi.org/10.1016/j.scitotenv.2003.08.016

IPCC (2007). Climate Change 2007: Impacts, Adaptation and Vulnerability. *Contribution of Working Group II to the Fourth Assessment Report of the Intergovernmental Panel on Climate Change*, M.L. Parry, O.F. Canziani, J.P. Palutikof, P.J. van der Linden and C.E.Hanson, Eds., Cambridge University Press, Cambridge, UK, 976pp.

IPCC (2021). Summary for Policymakers. In: *Climate Change 2021: The Physical Science Basis. Contribution of Working Group I to the Sixth Assessment Report of the Intergovernmental Panel on Climate Change* [Masson-Delmotte, V., P. Zhai, A. Pirani, S. L. Connors, C. Péan, S. Berger, N. Caud, Y. Chen, L. Goldfarb, M. I. Gomis, M. Huang, K. Leitzell, E. Lonnoy, J.B.R. Matthews, T. K. Maycock, T. Waterfield, O. Yelekçi, R. Yu and B. Zhou (eds.)]. Cambridge University Press.

John Meunier Inc. (2005). ACTIFLO® process simulation: laboratory jar tests procedure. Québec, Canada.

Jung, B. J., Lee, J. K., Kim, H., & Park, J. H. (2014). Export, biodegradation, and disinfection byproduct formation of dissolved and particulate organic carbon in a forested headwater stream during extreme rainfall events. *Biogeosciences*, *11*(21), 6119–6129. https://doi.org/10.5194/bg-11-6119-2014

Khan, S. J., Deere, D., Leusch, F. D. L., Humpage, A., Jenkins, M., & Cunliffe, D. (2015). Extreme weather events: should drinking water quality management systems adapt to changing risk profiles? *Water Research, 85*, 124–136. https://doi.org/10.1016/j.watres.2015.08.018

Kim, D., Jacome, G., Lee, S. C., Moya, W., Nam, K. J., & Yoo, C. (2017). Vulnerability assessment index at process-level for the identification of adaptive strategies in wastewater treatment plants under climate change. *Korean Journal of Chemical Engineering, 34*(12), 3054–3066. https://doi.org/10.1007/s11814-017-0218-7

Lapointe, M., & Barbeau, B. (2018). Selection of media for the design of ballasted flocculation processes. Water Research, 147, 25–32. https://doi.org/10.1016/j.watres.2018.09.041

Lapointe, M., Brosseau, C., Comeau, Y., & Barbeau, B. (2017). Characterization of ballasted flocs in water treatment using microscopy. *Water research*, *90*, 119–127. https://doi.org/10.1016/j.watres.2015.12.018

Lawler, D. M., Petts, G. E., Foster, I. D. L., & Harper, S. (2006). Turbidity dynamics during spring storm events in an urban headwater river system: The Upper Tame, West Midlands, UK. *Science of the Total Environment*, *360*(1–3), 109–126. https://doi.org/10.1016/j.scitotenv.2005.08.032

LeChevallier, M. W., Evans, T. M., & Seidler, R. J. (1981). Effect of turbidity on chlorination efficiency and bacterial persistence in drinking water. *Applied and environmental microbiology*, *42*(1), 159–167. https://doi.org/10.1128/aem.42.1.159-167.1981

Lee, K. E., Teng, T. T., Morad, N., Poh, B. T., & Hong, Y. F. (2010). Flocculation of kaolin in water using novel calcium chloride-polyacrylamide (CaCl2-PAM) hybrid polymer. *Separation and Purification Technology, 75(3),* 346–351. https://doi.org/10.1016/j.seppur.2010.09.003

Levine, A. D., Yang, Y. J., & Goodrich, J. A. (2016). Enhancing climate adaptation capacity for drinking water treatment facilities. *Journal of Water and Climate Change, 7*(3), 485–497. https://doi.org/10.2166/wcc.2016.011

Li, T. (2004). Quantifying robustness of water treatment systems. M.A.Sc. thesis, University of Waterloo, Waterloo, Ontario.

Li, T., & Huck, P. M. (2008). Improving the evaluation of filtration robustness. *Journal of Environmental Engineering and Science, 7*(1), 29–37. https://doi.org/10.1139/S07-032

Marhaba, T. F., & Van, D. (2000). The variation of mass and disinfection by-product formation potential of dissolved organic matter fractions along a conventional surface water treatment plant. *Journal of hazardous materials*, *74*(3), 133–147. https://doi.org/10.1016/s0304-3894(99)00190-9

McCoy, W.F., & Olson, B.H. (1986). Relationship among turbidity, particle counts and bacteriological quality within water distribution lines. *Water Research, 20*, 1023-1029.

Min, S.K., Zhang, X., Zwiers, F., & Hegrel, G.C. (2011). Human contribution to more-intense precipitation extremes. *Nature 470*, 378–381. https://doi.org/10.1038/nature09763

Montgomery, D. C. (2013). Design and analysis of experiments. *John Wiley & Sons, Inc.*

Murujew, O., Geoffroy, J., Fournie, E., Socionovo Gioacchini, E., Wilson, A., Vale, P., Jefferson, B., & Pidou, M. (2020). The impact of polymer selection and dose on the incorporation of ballasting agents onto wastewater aggregates. *Water Research*, *170*. https://doi.org/10.1016/j.watres.2019.115346

Naceradska, J., Pivokonsky, M., Pivokonska, L., Baresova, M., Henderson, R. K., Zamyadi, A., & Janda, V. (2017). The impact of pre-oxidation with potassium permanganate on cyanobacterial organic matter removal by coagulation. *Water research*, *114*, 42–49. https://doi.org/10.1016/j.watres.2017.02.029

Nam, S. W., Jo, B. Il, Kim, M. K., Kim, W. K., & Zoh, K. D. (2013). Streaming current titration for coagulation of high turbidity water. *Colloids and Surfaces A: Physicochemical and Engineering Aspects, 419*, 133–139. https://doi.org/10.1016/j.colsurfa.2012.11.051

Nemani, K.S. (2021a). Evaluation and improvement of robustness in drinking water treatment systems to manage turbidity and TOC related water quality upsets during extreme weather. Ph.D. thesis proposal, University of Waterloo, Waterloo, Ontario.

Nemani, K.S. (2021b). Robustness in drinking water treatment systems to manage turbidity- and TOC-related water quality upsets during extreme weather. NSERC chair partner information day, University of Waterloo, Waterloo, Ontario.

Okuda, T., Baes, A. U., Nishijima, W., & Okada, M. (1999). Improvement of extraction method of coagulation active components from Moringa oleifera seed. *Water Research, 33(15)*, 3373–3378. https://doi.org/10.1016/S0043-1354(99)00046-9

Oliveira, M. D., Melo, L. D. V., Queiroga, L. L., Oliveira, S. M. A. C., & Libanio, M. (2014). Applying reliability analysis to evaluate water treatment plants. *Water Science and Technology: Water Supply*, *14*(4), 634–642. https://doi.org/10.2166/ws.2014.019

Ontario regulation (2021). Drinking water systems annual water quality and summary report, Appendix A, Section 11 & Schedule 22. https://www.hamilton.ca/sites/default/files/media/browser/2020-02-27/drinking-water-report-2021.pdf

Pešić, M., Milić, S., Nujkić, M., & Marić, M. (2020). The impact of climatic parameters on the turbidity and natural organic matter content in drinking water in the City of Bor (Eastern Serbia). *Environmental Earth Sciences, 79*(11). https://doi.org/10.1007/s12665-020-09016-0

Plum, V., Dahl, C. P., Bentsen, L., Petersen, C. R., Napstjert, L., & Thomsen, N. B. (1998). The Actiflo method. *Water Science and Technology, 37*(1), 269-275. doi:10.

Qiu, F., Lv, H., Zhao, X., & Zhao, D. (2019). Impact of an extreme winter storm event on the coagulation/flocculation processes in a prototype surface water treatment plant: causes and mitigating measures. *International Journal of Environmental Research and Public Health, 16*(15). https://doi.org/10.3390/ijerph16152808

Ram, A. R., & Terry, J. P. (2016). Stream turbidity responses to storm events in a pristine rainforest watershed on the Coral Coast of southern Fiji. *International Journal of Sediment Research*, *31*(4), 279–290. https://doi.org/10.1016/j.ijsrc.2016.07.002

Richardson, S. D. (2002). The role of GC-MS and LC-MS in the discovery of drinking water disinfection by-products. *Journal of environmental monitoring: JEM*, *4*(1), 1–9. https://doi.org/10.1039/b105578j

Ruecker, A., Uzun, H., Karanfil, T., Tsui, M. T. K., & Chow, A. T. (2017). Disinfection byproduct precursor dynamics and water treatability during an extreme flooding event in a coastal blackwater river in southeastern United States. *Chemosphere*, *188*, 90–98. https://doi.org/10.1016/j.chemosphere.2017.08.122

Saraceno, J. F., Pellerin, B. A., Downing, B. D., Boss, E., Bachand, P. A. M., & Bergamaschi, B. A. (2009). High-frequency in situ optical measurements during a storm event: Assessing relationships between dissolved organic matter, sediment concentrations, and hydrologic processes. *Journal of Geophysical Research: Biogeosciences, 114*(4), 1–11. https://doi.org/10.1029/2009JG000989

Schwartz, J., Levin, R., & Goldstein, R. (2000). Drinking water turbidity and gastrointestinal illness in the elderly of Philadelphia. *Journal of epidemiology and community health*, *54*(1), 45–51. https://doi.org/10.1136/jech.54.1.45

Schwartz, J., Levin, R., & Hodge, K. (1997). Drinking water turbidity and pediatric hospital use for gastrointestinal illness in Philadelphia. *Epidemiology (Cambridge, Mass.)*, *8*(6), 615–620. https://doi.org/10.1097/00001648-199710000-00001

Selvam, R., Muniraj, S., Duraisamy, T., & Muthunarayanan, V. (2018). Identification of disinfection by-products (DBPs) halo phenols in drinking water. *Applied Water Science*, *8*(5), 1-8.

Semenza, J. C., & Menne, B. (2009). Climate change and infectious diseases in Europe. *The Lancet Infectious Diseases 9*(6), 365–375.

Sharp, E. L., Parsons, S. A., & Jefferson, B. (2006). Seasonal variations in natural organic matter and its impact on coagulation in water treatment. *The Science of the total environment*, *363*(1-3), 183–194. https://doi.org/10.1016/j.scitotenv.2005.05.032

Singh, S. (2018). Evaluating expected microcystin removal at three Ontario drinking water treatment plants. M.A.Sc. thesis, University of Waterloo, Waterloo, Ontario.

Singh, V.P., Mishra, A.K., Chowdhary, H., & Khedun, C.P. (2014). Climate Change and Its Impact on Water Resources. In: *Wang, L., Yang, C. (eds) Modern Water Resources Engineering. Handbook of Environmental Engineering, vol 15. Humana Press, Totowa, NJ.* https://doi.org/10.1007/978-1-62703-595-8_11

Staben, N., Nahrstedt, A., & Merkel, W. (2015). Securing safe drinking water supply under climate change conditions. *Water Science and Technology: Water Supply, 15*(6), 1334–1342. https://doi.org/10.2166/ws.2015.099

Staff of Plant A, (April 2021). Personal communication (Meeting minutes from 6 April 2021).

Staff of Plant A, (December 2020). Personal communication (Plant visit on 11 December 2020).

Staff of Plant A, (June 2021). Personal communication (Meeting minutes from 24 June 2021).

Staff of Plant B, (January 2022). Personal communication (Meeting minutes from 20 January 2022).

Staff of Plant B, (July 2021). Personal communication (Meeting minutes from 14 July 2022).

Standard Methods (2005). Standard Methods for the Examination of Water and Wastewater, 21st ed. *American Public Health Association (APHA), American Water Works Association (AWWA), and Water Environment Federation (WEF)*, Washington, DC.

Sylvestre, É., Prévost, M., Burnet, J. B., Pang, X., Qiu, Y., Smeets, P., Medema, G., Hachad, M., & Dorner, S. (2021). Demonstrating the reduction of enteric viruses by drinking water treatment during snowmelt episodes in urban areas. *Water Research*, *11*. https://doi.org/10.1016/j.wroa.2021.100091

Thomas, K. M., Charron, D. F., Waltner-Toews, D., Schuster, C., Maarouf, A. R., & Holt, J. D. (2006). A role of high impact weather events in waterborne disease outbreaks in Canada, 1975 - 2001. *International journal of environmental health research*, *16*(3), 167–180. https://doi.org/10.1080/09603120600641326

Tinker, S. C., Moe, C. L., Klein, M., Flanders, W. D., Uber, J., Amirtharajah, A., Singer, P., & Tolbert, P. E. (2010). Drinking water turbidity and emergency department visits for gastrointestinal illness in Atlanta, 1993-2004. *Journal of exposure science & environmental epidemiology*, *20*(1), 19–28. https://doi.org/10.1038/jes.2008.68

Tseng, T., Segal, B.D., & Edwards, M. (2000). Increasing alkalinity to reduce turbidity. *Journal / American Water Works Association, 92*: 44-54. https://doi.org/10.1002/j.1551-8833.2000.tb08958.x

Upton, A., Jefferson, B., Moore, G., & Jarvis, P. (2017). Rapid gravity filtration operational performance assessment and diagnosis for preventative maintenance from on-line data. *Chemical Engineering Journal*, *313*, 250–260. https://doi.org/10.1016/j.cej.2016.12.047

Yarahmadi, H. (2019). Ultimate performance, continuous development. *Ontario Pipeline*. Vol 15, No. 3, Fall 2019.

Young, J. C., & Edwards, F. G. (2003). Factors affecting ballasted flocculation reactions. *Water Environment Research, 75*(3), 263-272. doi:10.2175/106143003X141051

Zafisah, N. S., Ang, W. L., Mohammad, A. W., Hilal, N., & Johnson, D. J. (2020). Interaction between ballasting agent and flocs in ballasted flocculation for the removal of suspended solids in water. *Journal of Water Process Engineering,* 33. https://doi.org/10.1016/j.jwpe.2019.101028

Zakarian, A., Knight, J. W., & Baghdasaryan, L. (2007). Modelling and analysis of system robustness. *Journal of Engineering Design*, *18*(3), 243–263. https://doi.org/10.1080/09544820600804939

Zhang, K., Achari, G., Sadiq, R., Langford, C. H., & Dore, M. H. I. (2012). An integrated performance assessment framework for water treatment plants. *Water Research*, *46*(6), 1673–1683. https://doi.org/10.1016/j.watres.2011.12.006

Zoric, S., Becelic-Tomin, M., & Dalmacija, B. (2020). Robustness analysis of technological units for drinking water clarification: Normal and emergency operating conditions. *Hemijska Industrija*, *74*(2), 91–102. https://doi.org/10.2298/HEMIND190909009Z

# Appendices

## Appendix A: Supplementary Information of Plant A

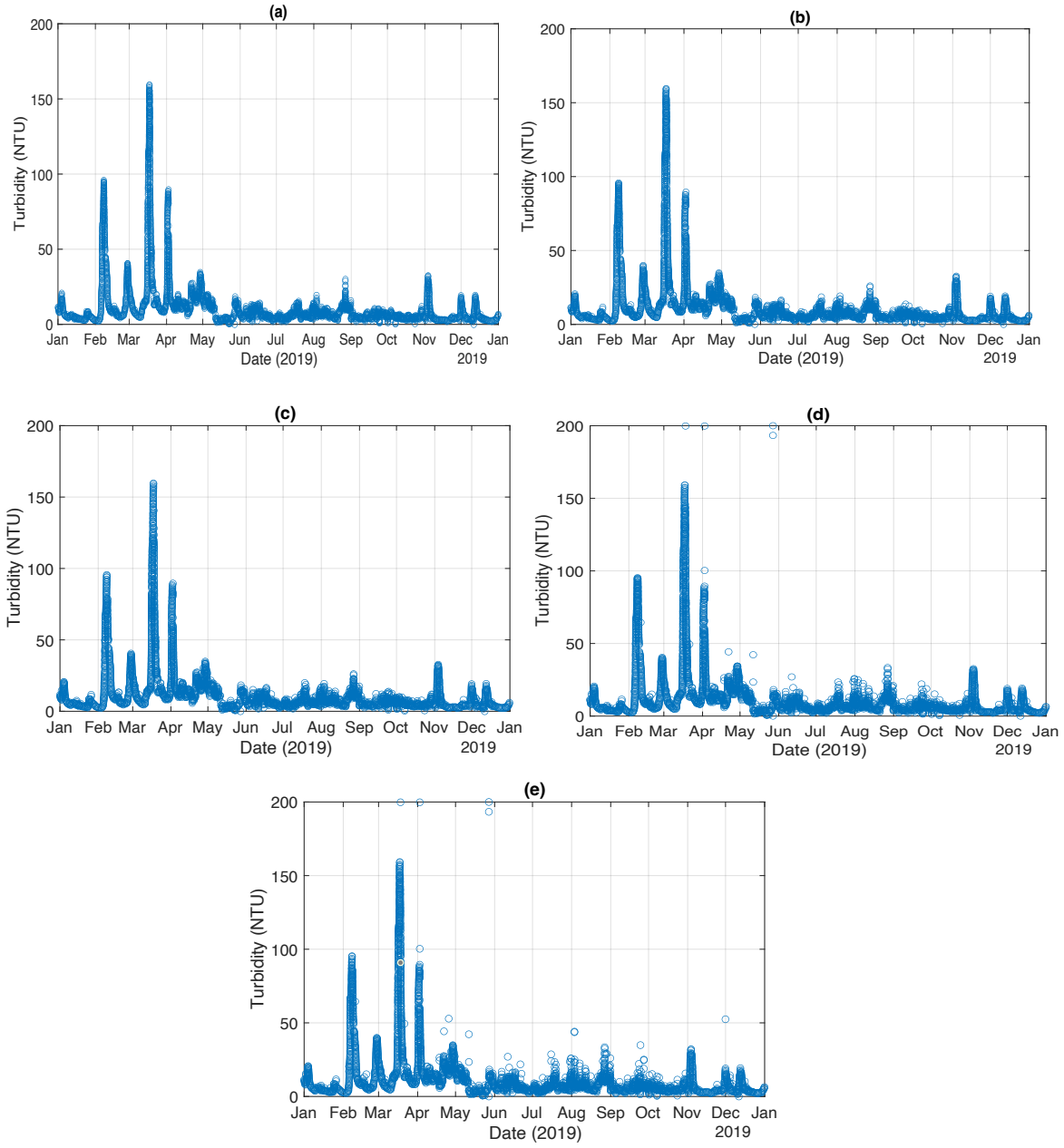


Figure A.1: Time series of raw water turbidity data (2019) with invalid data points removed varying values of x, (a) x = 25%, (b) x = 50%, (c) x = 75%, (d) x = 150%, (e) x = 200% (invalid data = x% above the hourly median)

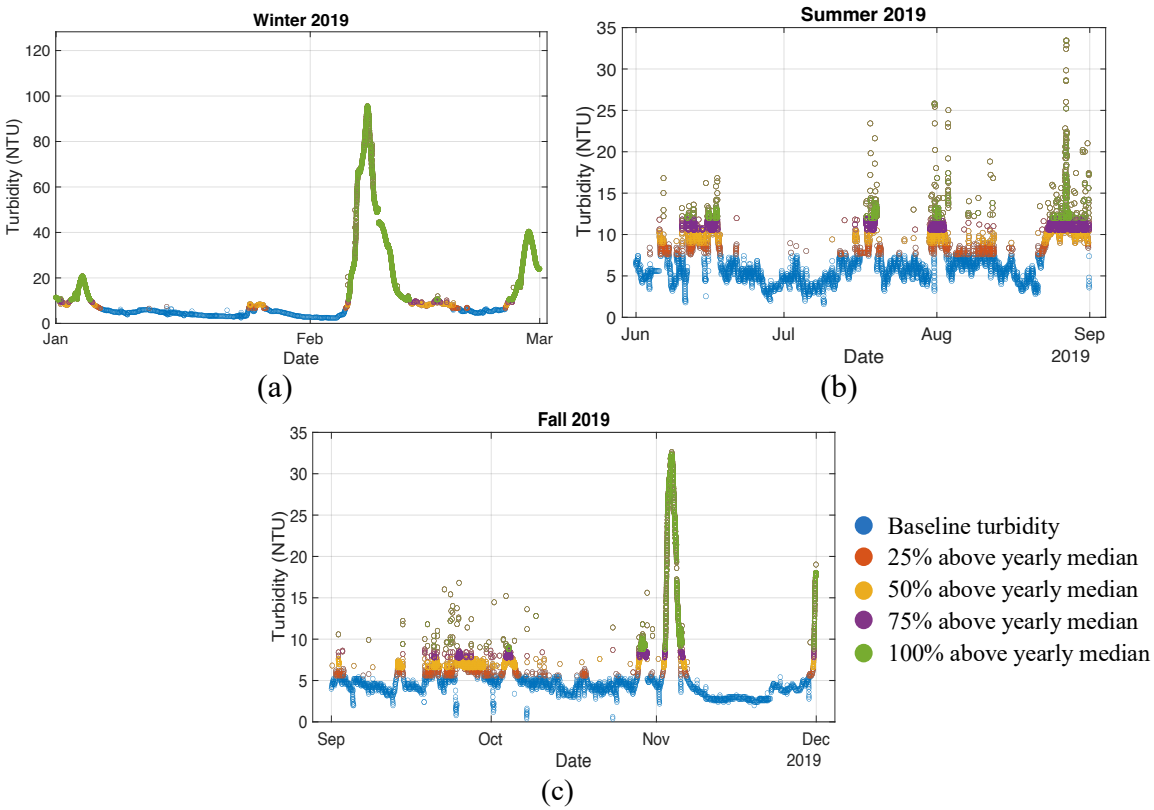


Figure A.2: Time series of raw water turbidity showing normal and weather events characterized by turbidity using seasonal median turbidity for (a) winter 2019, (b) summer 2019 and (c) fall 2019

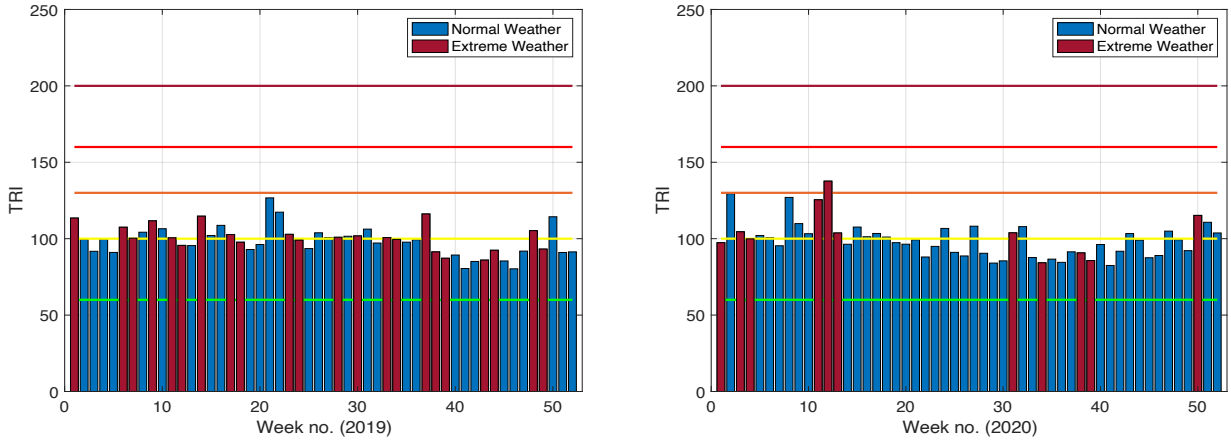


Figure A.3: Weekly TRIs of the train 2 ACTIFLO® unit during normal and weather events characterized by raw water turbidity (Tgoal = 1.0 NTU)

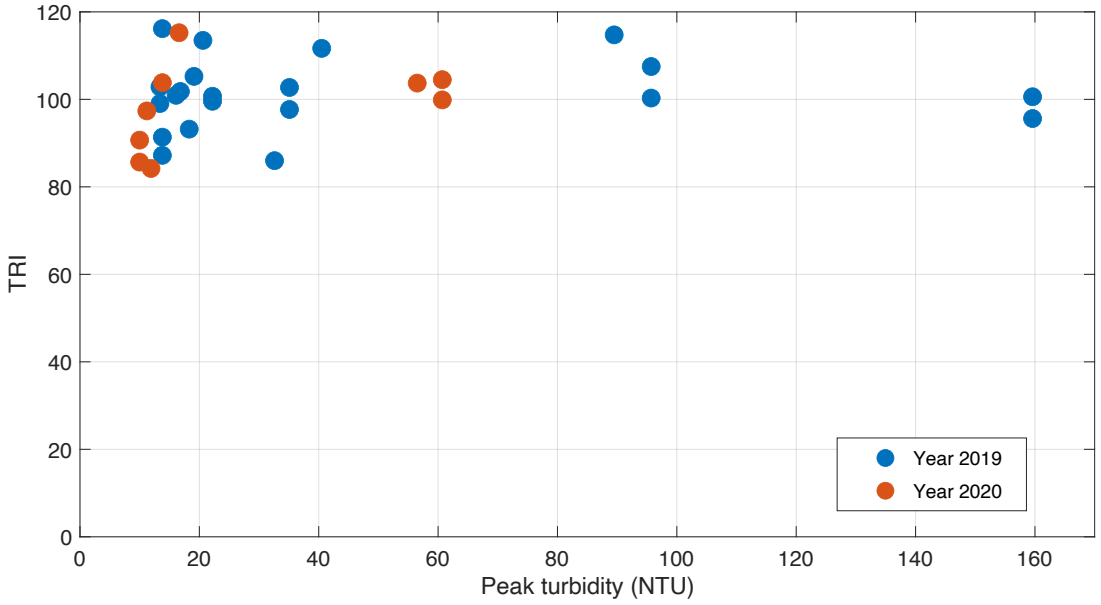


Figure A.4: Weekly TRIs of the train 2 ACTIFLO® unit in relation to the maximum values of raw water turbidities during weather events

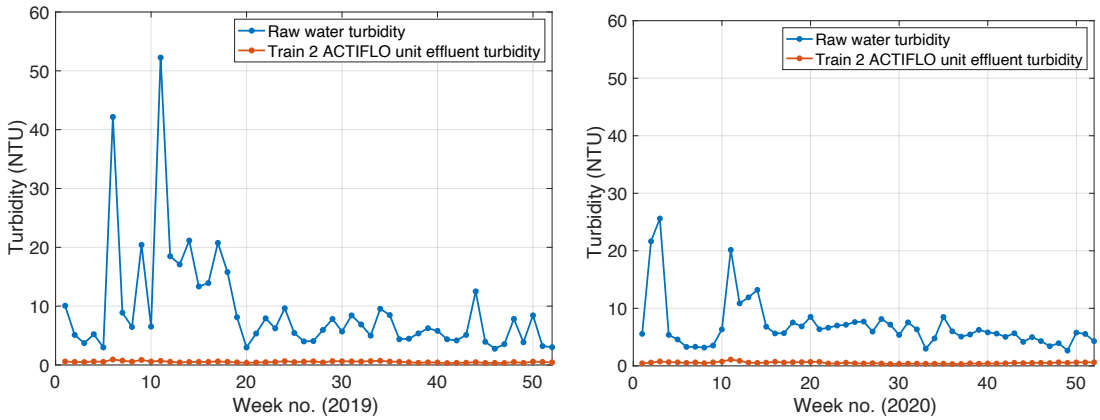


Figure A.5: Weekly average raw water and train 2 ACTIFLO® influent and effluent turbidity for 2019 and 2020

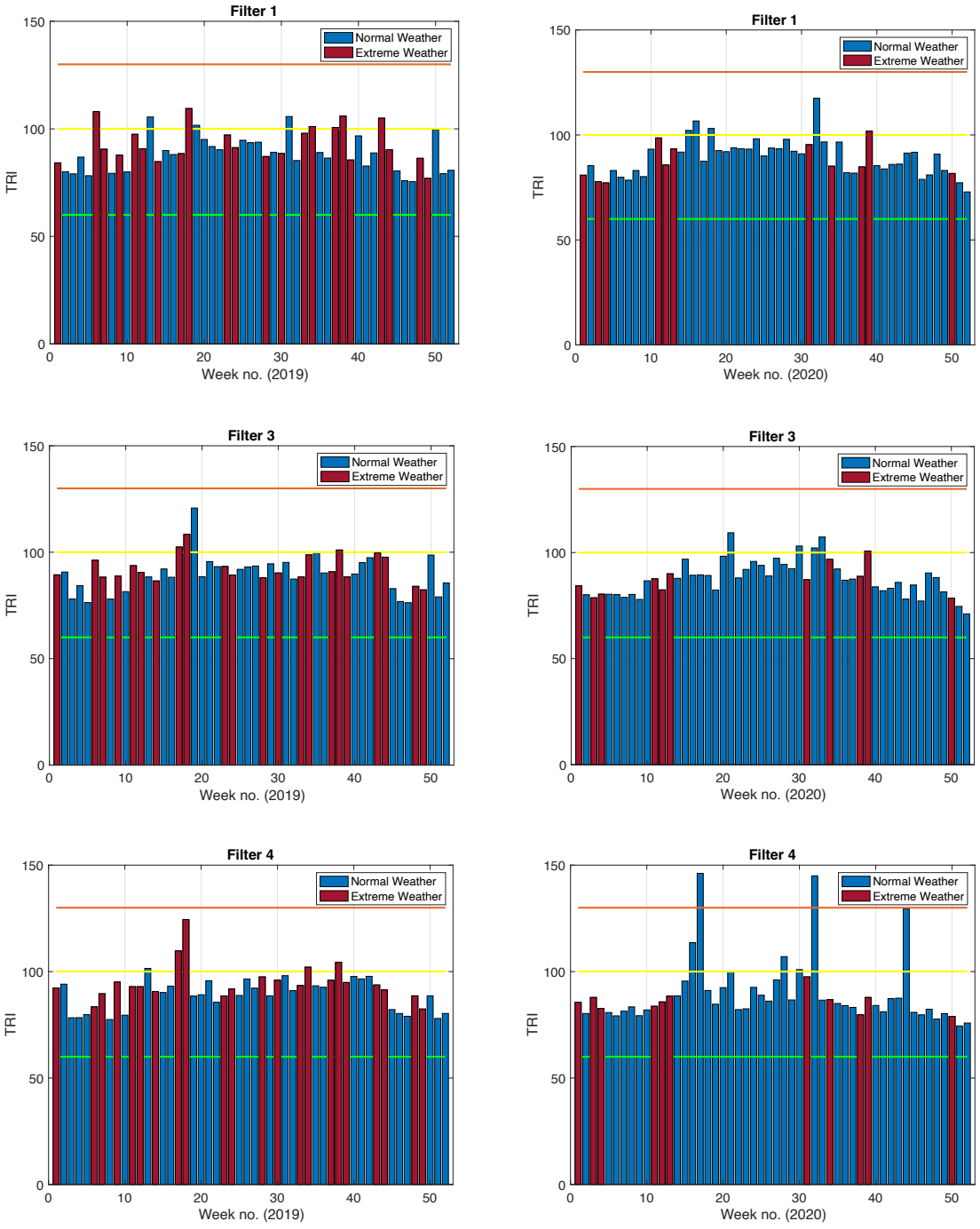


Figure A.6: Weekly TRIs of Filters 1, 3 and 4 during normal weather and weather events characterized by raw water turbidity in 2019 and 2020 (Tgoal = 0.1 NTU)

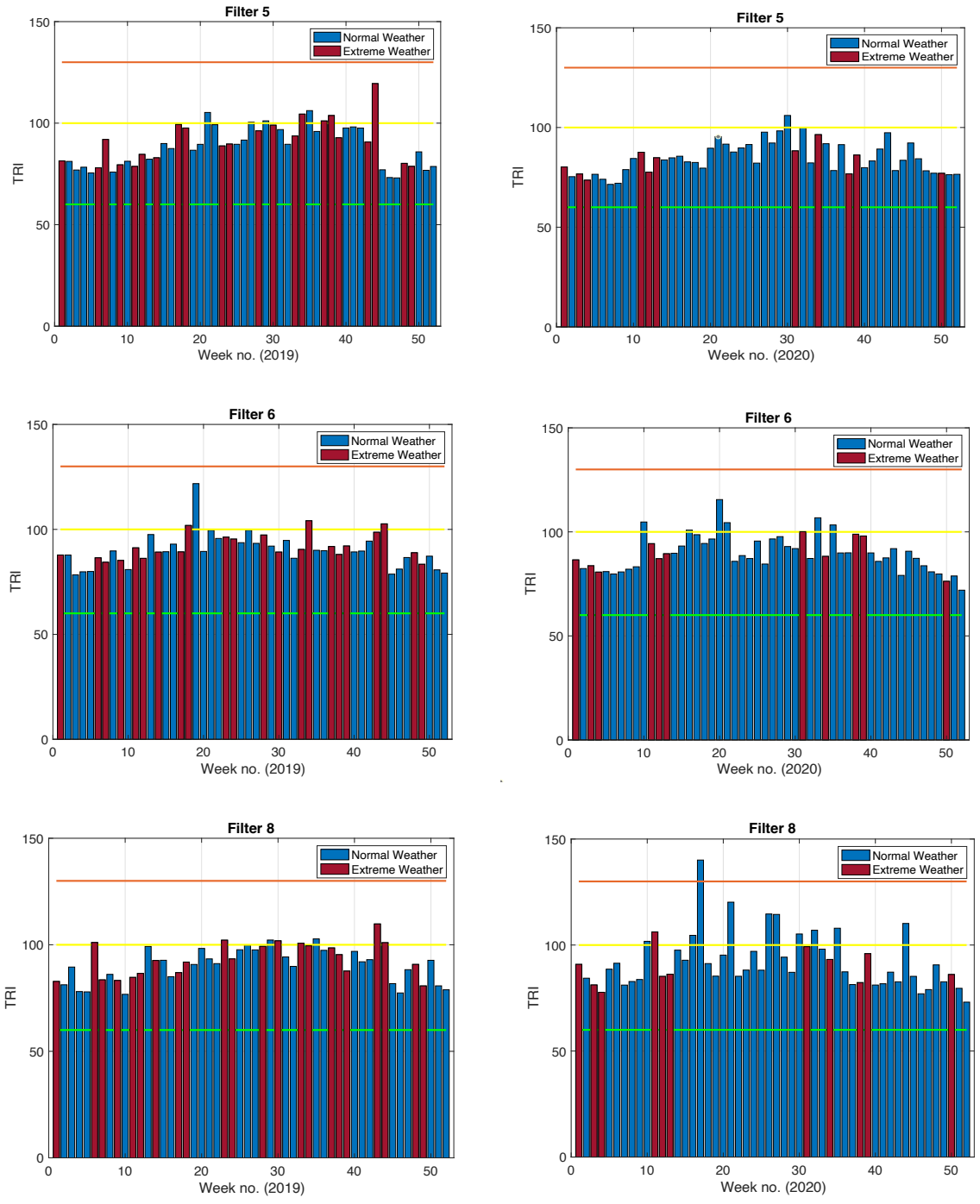


Figure A.7: Weekly TRIs of Filters 5, 6 and 8 during normal weather and weather events characterized by raw water turbidity in 2019 and 2020 (Tgoal = 0.1 NTU)

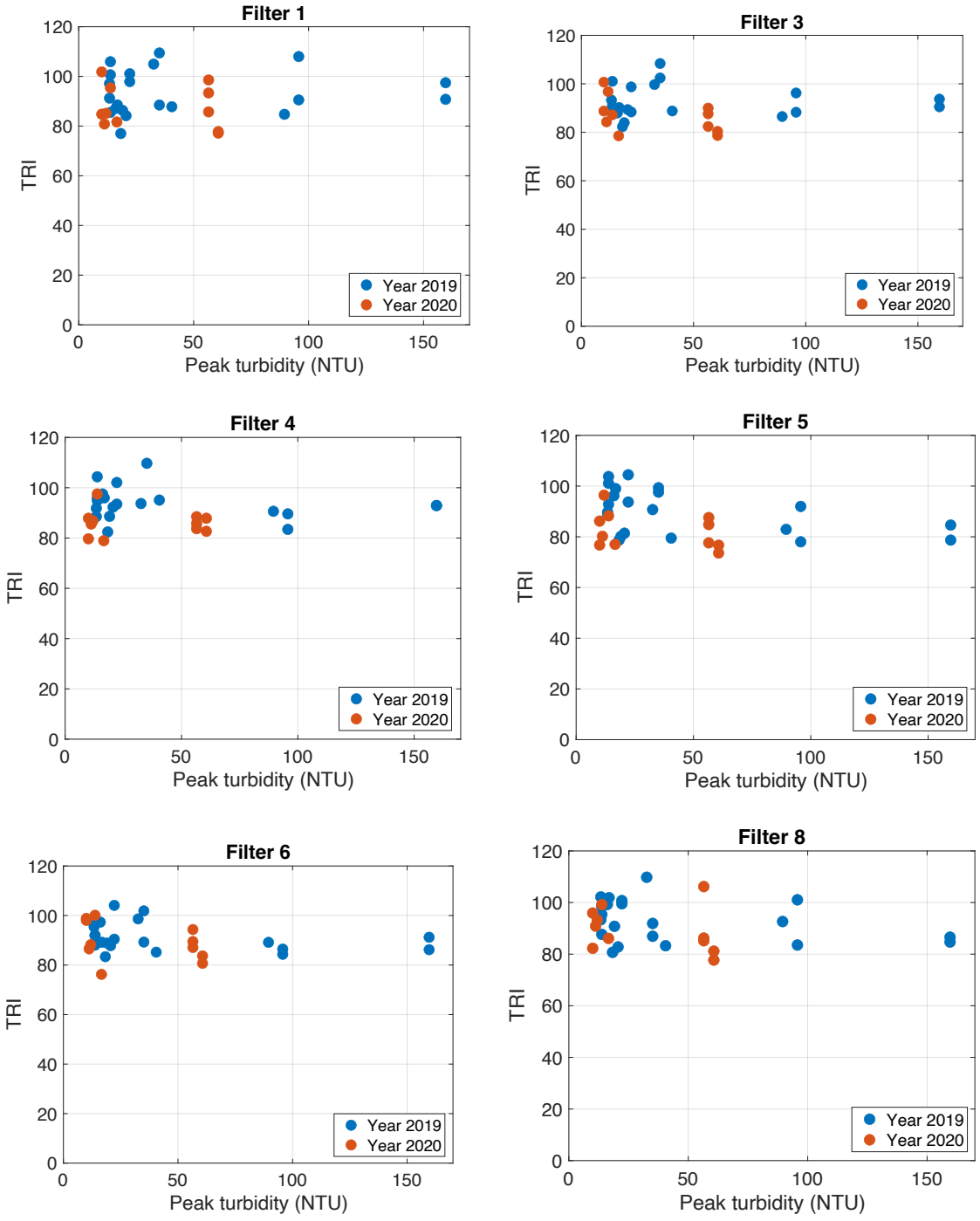


Figure A.8: Weekly TRIs of Filters 1, 3-6 and 8 in relation to the maximum values of raw water turbidities during weather events

Table A.1: Weekly average percentage of turbidity removal by the overall ACTIFLO® (train 1 and 2) and filtration process (Filters 1 to 8)

| Week no. | 2019 | | 2020 | |
|---|---|---|---|---|
| | **Percent turbidity removal by the ACTIFLO® units (%)** | **Percent turbidity removal by the ACTIFLO® units and Filters (%)** | **Percent turbidity removal by the ACTIFLO® units (%)** | **Percent turbidity removal by the ACTIFLO® units and Filters (%)** |
| 1 | 94.4 | 99.5 | 91.2 | 99.2 |
| 2 | 90.0 | 99.2 | 97.5 | 99.8 |
| 3 | 87.6 | 99.0 | 97.2 | 99.9 |
| 4 | 89.0 | 99.2 | 88.9 | 99.4 |
| 5 | 83.3 | 98.8 | 87.0 | 99.2 |
| 6 | 98.0 | 99.9 | 83.1 | 98.9 |
| 7 | 93.0 | 99.6 | 83.2 | 98.9 |
| 8 | 92.0 | 99.4 | 85.0 | 98.8 |
| 9 | 96.4 | 99.8 | 82.7 | 98.9 |
| 10 | 92.0 | 99.4 | 89.8 | 99.3 |
| 11 | 98.7 | 99.9 | 95.9 | 99.8 |
| 12 | 97.0 | 99.7 | 94.2 | 99.6 |
| 13 | 97.5 | 99.7 | 96.0 | 99.6 |
| 14 | 97.7 | 99.8 | 96.3 | 99.6 |
| 15 | 96.3 | 99.6 | 92.8 | 99.2 |
| 16 | 96.4 | 99.6 | 89.6 | 99.1 |
| 17 | 97.4 | 99.7 | 91.6 | 99.1 |
| 18 | 96.7 | 99.6 | 92.6 | 99.3 |
| 19 | 94.1 | 99.3 | 91.1 | 99.3 |
| 20 | 85.4 | 98.1 | 92.7 | 99.4 |
| 21 | 90.7 | 98.9 | 90.1 | 99.1 |
| 22 | 93.7 | 99.3 | 94.3 | 99.3 |
| 23 | 92.3 | 99.1 | 94.7 | 99.3 |

| | | | | |
|---|---|---|---|---|
| 24 | 94.1 | 99.4 | 92.8 | 99.2 |
| 25 | 91.9 | 98.9 | 94.5 | 99.3 |
| 26 | 86.7 | 98.4 | 95.3 | 99.3 |
| 27 | 86.0 | 98.4 | 93.0 | 99.0 |
| 28 | 92.6 | 99.0 | 95.4 | 99.3 |
| 29 | 93.0 | 99.2 | 95.6 | 99.3 |
| 30 | 91.2 | 99.0 | 92.9 | 99.0 |
| 31 | 94.2 | 99.3 | 94.7 | 99.3 |
| 32 | 93.2 | 99.2 | 93.9 | 99.1 |
| 33 | 89.0 | 98.8 | 89.0 | 98.3 |
| 34 | 93.4 | 99.3 | 93.3 | 99.1 |
| 35 | 93.8 | 99.2 | 95.9 | 99.5 |
| 36 | 89.7 | 98.6 | 95.3 | 99.4 |
| 37 | 89.6 | 98.6 | 94.0 | 99.3 |
| 38 | 92.8 | 98.8 | 92.8 | 99.4 |
| 39 | 93.8 | 99.1 | 94.4 | 99.3 |
| 40 | 92.7 | 98.9 | 93.6 | 99.4 |
| 41 | 92.0 | 98.6 | 93.1 | 99.3 |
| 42 | 91.1 | 98.4 | 91.7 | 99.2 |
| 43 | 93.3 | 98.9 | 91.0 | 99.2 |
| 44 | 96.2 | 99.6 | 88.5 | 99.1 |
| 45 | 92.0 | 99.1 | 90.4 | 99.2 |
| 46 | 87.8 | 98.8 | 88.9 | 99.2 |
| 47 | 90.0 | 99.0 | 86.5 | 99.1 |
| 48 | 93.4 | 99.5 | 85.5 | 99.1 |
| 49 | 89.6 | 99.1 | 82.0 | 99.0 |
| 50 | 93.5 | 99.6 | 90.7 | 99.6 |
| 51 | 87.0 | 99.0 | 90.3 | 99.5 |
| 52 | 85.0 | 98.9 | 87.8 | 99.4 |

Table A.2: Overall robustness of Plant A by weeks in 2020 by equal weighting

| Week no. | 2020 | | | | | |
|---|---|---|---|---|---|---|
| | ACTIFLO® Units | | Filters | | Plant | |
| | TRI | Category | TRI | Category | Overall Robustness Category | Overall System Robustness |
| 1 | 100 | 2 | 85 | 2 | 2 | stable |
| 2 | 129 | 3 | 80 | 2 | 3 | slightly disturbed |
| 3 | 101 | 3 | 80 | 2 | 3 | slightly disturbed |
| 4 | 101 | 3 | 78 | 2 | 3 | slightly disturbed |
| 5 | 99 | 2 | 81 | 2 | 2 | stable |
| 6 | 96 | 2 | 80 | 2 | 2 | stable |
| 7 | 93 | 2 | 78 | 2 | 2 | stable |
| 8 | 107 | 3 | 79 | 2 | 3 | slightly disturbed |
| 9 | 103 | 3 | 81 | 2 | 3 | slightly disturbed |
| 10 | 108 | 3 | 92 | 2 | 3 | slightly disturbed |
| 11 | 114 | 3 | 92 | 2 | 3 | slightly disturbed |
| 12 | 118 | 3 | 84 | 2 | 3 | slightly disturbed |
| 13 | 98 | 2 | 89 | 2 | 2 | stable |
| 14 | 95 | 2 | 89 | 2 | 2 | stable |
| 15 | 107 | 3 | 93 | 2 | 3 | slightly disturbed |
| 16 | 97 | 2 | 98 | 2 | 2 | stable |
| 17 | 98 | 2 | 108 | 3 | 3 | slightly disturbed |
| 18 | 94 | 2 | 91 | 2 | 2 | stable |
| 19 | 94 | 2 | 87 | 2 | 2 | stable |
| 20 | 94 | 2 | 97 | 2 | 2 | stable |
| 21 | 99 | 2 | 103 | 3 | 3 | slightly disturbed |
| 22 | 85 | 2 | 89 | 2 | 2 | stable |
| 23 | 90 | 2 | 91 | 2 | 2 | stable |
| 24 | 102 | 3 | 95 | 2 | 3 | slightly disturbed |

| | | | | | | |
|---|---|---|---|---|---|---|
| 25 | 89 | 2 | 91 | 2 | 2 | stable |
| 26 | 86 | 2 | 91 | 2 | 2 | stable |
| 27 | 98 | 2 | 100 | 3 | 3 | slightly disturbed |
| 28 | 89 | 2 | 98 | 2 | 2 | stable |
| 29 | 85 | 2 | 92 | 2 | 2 | stable |
| 30 | 87 | 2 | 101 | 3 | 3 | slightly disturbed |
| 31 | 102 | 3 | 96 | 2 | 3 | slightly disturbed |
| 32 | 101 | 3 | 108 | 3 | 3 | slightly disturbed |
| 33 | 83 | 2 | 96 | 2 | 2 | stable |
| 34 | 80 | 2 | 92 | 2 | 2 | stable |
| 35 | 83 | 2 | 94 | 2 | 2 | stable |
| 36 | 82 | 2 | 85 | 2 | 2 | stable |
| 37 | 90 | 2 | 85 | 2 | 2 | stable |
| 38 | 95 | 2 | 85 | 2 | 2 | stable |
| 39 | 83 | 2 | 93 | 2 | 2 | stable |
| 40 | 92 | 2 | 83 | 2 | 2 | stable |
| 41 | 81 | 2 | 82 | 2 | 2 | stable |
| 42 | 90 | 2 | 86 | 2 | 2 | stable |
| 43 | 105 | 3 | 88 | 2 | 3 | slightly disturbed |
| 44 | 98 | 2 | 98 | 2 | 2 | stable |
| 45 | 88 | 2 | 86 | 2 | 2 | stable |
| 46 | 89 | 2 | 82 | 2 | 2 | stable |
| 47 | 99 | 2 | 83 | 2 | 2 | stable |
| 48 | 96 | 2 | 83 | 2 | 2 | stable |
| 49 | 93 | 2 | 80 | 2 | 2 | stable |
| 50 | 113 | 3 | 80 | 2 | 3 | slightly disturbed |
| 51 | 100 | 3 | 76 | 2 | 3 | slightly disturbed |
| 52 | 98 | 2 | 74 | 2 | 2 | stable |

Table A.3: Overall robustness of Plant A by weeks in 2020 by unequal weighting (considering the ACTIFLO® process is more significant)

| Week no. | 2020 | | | | | |
|---|---|---|---|---|---|---|
| | ACTIFLO® Units | | Filters | | Plant | |
| | TRI | Category | TRI | Category | Overall Robustness Category | Overall System Robustness |
| 1 | 100 | 2 | 85 | 2 | 2 | stable |
| 2 | 129 | 3 | 80 | 2 | 3 | slightly disturbed |
| 3 | 101 | 3 | 80 | 2 | 3 | slightly disturbed |
| 4 | 101 | 3 | 78 | 2 | 3 | slightly disturbed |
| 5 | 99 | 2 | 81 | 2 | 2 | stable |
| 6 | 96 | 2 | 80 | 2 | 2 | stable |
| 7 | 93 | 2 | 78 | 2 | 2 | stable |
| 8 | 107 | 3 | 79 | 2 | 3 | slightly disturbed |
| 9 | 103 | 3 | 81 | 2 | 3 | slightly disturbed |
| 10 | 108 | 3 | 92 | 2 | 3 | slightly disturbed |
| 11 | 114 | 3 | 92 | 2 | 3 | slightly disturbed |
| 12 | 118 | 3 | 84 | 2 | 3 | slightly disturbed |
| 13 | 98 | 2 | 89 | 2 | 2 | stable |
| 14 | 95 | 2 | 89 | 2 | 2 | stable |
| 15 | 107 | 3 | 93 | 2 | 3 | slightly disturbed |
| 16 | 97 | 2 | 98 | 2 | 2 | stable |
| 17 | 98 | 2 | 108 | 3 | 2 | stable |
| 18 | 94 | 2 | 91 | 2 | 2 | stable |
| 19 | 94 | 2 | 87 | 2 | 2 | stable |
| 20 | 94 | 2 | 97 | 2 | 2 | stable |
| 21 | 99 | 2 | 103 | 3 | 2 | stable |
| 22 | 85 | 2 | 89 | 2 | 2 | stable |
| 23 | 90 | 2 | 91 | 2 | 2 | stable |

| | | | | | | |
|---|---|---|---|---|---|---|
| 24 | 102 | 3 | 95 | 2 | 3 | slightly disturbed |
| 25 | 89 | 2 | 91 | 2 | 2 | stable |
| 26 | 86 | 2 | 91 | 2 | 2 | stable |
| 27 | 98 | 2 | 100 | 3 | 2 | stable |
| 28 | 89 | 2 | 98 | 2 | 2 | stable |
| 29 | 85 | 2 | 92 | 2 | 2 | stable |
| 30 | 87 | 2 | 101 | 3 | 2 | stable |
| 31 | 102 | 3 | 96 | 2 | 3 | slightly disturbed |
| 32 | 101 | 3 | 108 | 3 | 3 | slightly disturbed |
| 33 | 83 | 2 | 96 | 2 | 2 | stable |
| 34 | 80 | 2 | 92 | 2 | 2 | stable |
| 35 | 83 | 2 | 94 | 2 | 2 | stable |
| 36 | 82 | 2 | 85 | 2 | 2 | stable |
| 37 | 90 | 2 | 85 | 2 | 2 | stable |
| 38 | 95 | 2 | 85 | 2 | 2 | stable |
| 39 | 83 | 2 | 93 | 2 | 2 | stable |
| 40 | 92 | 2 | 83 | 2 | 2 | stable |
| 41 | 81 | 2 | 82 | 2 | 2 | stable |
| 42 | 90 | 2 | 86 | 2 | 2 | stable |
| 43 | 105 | 3 | 88 | 2 | 3 | slightly disturbed |
| 44 | 98 | 2 | 98 | 2 | 2 | stable |
| 45 | 88 | 2 | 86 | 2 | 2 | stable |
| 46 | 89 | 2 | 82 | 2 | 2 | stable |
| 47 | 99 | 2 | 83 | 2 | 2 | stable |
| 48 | 96 | 2 | 83 | 2 | 2 | stable |
| 49 | 93 | 2 | 80 | 2 | 2 | stable |
| 50 | 113 | 3 | 80 | 2 | 3 | slightly disturbed |
| 51 | 100 | 3 | 76 | 2 | 3 | slightly disturbed |
| 52 | 98 | 2 | 74 | 2 | 2 | stable |

Table A.4: Overall robustness of Plant A by weeks in 2020 by unequal weighting (considering the filtration process is more significant)

| Week no. | 2020 | | | | | |
|---|---|---|---|---|---|---|
| | ACTIFLO® Units | | Filters | | Plant | |
| | TRI | Category | TRI | Category | Overall Robustness Category | Overall System Robustness |
| 1 | 100 | 2 | 85 | 2 | 2 | stable |
| 2 | 129 | 3 | 80 | 2 | 2 | stable |
| 3 | 101 | 3 | 80 | 2 | 2 | stable |
| 4 | 101 | 3 | 78 | 2 | 2 | stable |
| 5 | 99 | 2 | 81 | 2 | 2 | stable |
| 6 | 96 | 2 | 80 | 2 | 2 | stable |
| 7 | 93 | 2 | 78 | 2 | 2 | stable |
| 8 | 107 | 3 | 79 | 2 | 2 | stable |
| 9 | 103 | 3 | 81 | 2 | 2 | stable |
| 10 | 108 | 3 | 92 | 2 | 2 | stable |
| 11 | 114 | 3 | 92 | 2 | 2 | stable |
| 12 | 118 | 3 | 84 | 2 | 2 | stable |
| 13 | 98 | 2 | 89 | 2 | 2 | stable |
| 14 | 95 | 2 | 89 | 2 | 2 | stable |
| 15 | 107 | 3 | 93 | 2 | 2 | stable |
| 16 | 97 | 2 | 98 | 2 | 2 | stable |
| 17 | 98 | 2 | 108 | 3 | 3 | slightly disturbed |
| 18 | 94 | 2 | 91 | 2 | 2 | stable |
| 19 | 94 | 2 | 87 | 2 | 2 | stable |
| 20 | 94 | 2 | 97 | 2 | 2 | stable |
| 21 | 99 | 2 | 103 | 3 | 3 | slightly disturbed |
| 22 | 85 | 2 | 89 | 2 | 2 | stable |
| 23 | 90 | 2 | 91 | 2 | 2 | stable |

| | | | | | | |
|---|---|---|---|---|---|---|
| 24 | 102 | 3 | 95 | 2 | 2 | stable |
| 25 | 89 | 2 | 91 | 2 | 2 | stable |
| 26 | 86 | 2 | 91 | 2 | 2 | stable |
| 27 | 98 | 2 | 100 | 3 | 3 | slightly disturbed |
| 28 | 89 | 2 | 98 | 2 | 2 | stable |
| 29 | 85 | 2 | 92 | 2 | 2 | stable |
| 30 | 87 | 2 | 101 | 3 | 3 | slightly disturbed |
| 31 | 102 | 3 | 96 | 2 | 2 | stable |
| 32 | 101 | 3 | 108 | 3 | 3 | slightly disturbed |
| 33 | 83 | 2 | 96 | 2 | 2 | stable |
| 34 | 80 | 2 | 92 | 2 | 2 | stable |
| 35 | 83 | 2 | 94 | 2 | 2 | stable |
| 36 | 82 | 2 | 85 | 2 | 2 | stable |
| 37 | 90 | 2 | 85 | 2 | 2 | stable |
| 38 | 95 | 2 | 85 | 2 | 2 | stable |
| 39 | 83 | 2 | 93 | 2 | 2 | stable |
| 40 | 92 | 2 | 83 | 2 | 2 | stable |
| 41 | 81 | 2 | 82 | 2 | 2 | stable |
| 42 | 90 | 2 | 86 | 2 | 2 | stable |
| 43 | 105 | 3 | 88 | 2 | 2 | stable |
| 44 | 98 | 2 | 98 | 2 | 2 | stable |
| 45 | 88 | 2 | 86 | 2 | 2 | stable |
| 46 | 89 | 2 | 82 | 2 | 2 | stable |
| 47 | 99 | 2 | 83 | 2 | 2 | stable |
| 48 | 96 | 2 | 83 | 2 | 2 | stable |
| 49 | 93 | 2 | 80 | 2 | 2 | stable |
| 50 | 113 | 3 | 80 | 2 | 2 | stable |
| 51 | 100 | 3 | 76 | 2 | 2 | stable |
| 52 | 98 | 2 | 74 | 2 | 2 | stable |

# Appendix B: Supplementary Information of Plant B

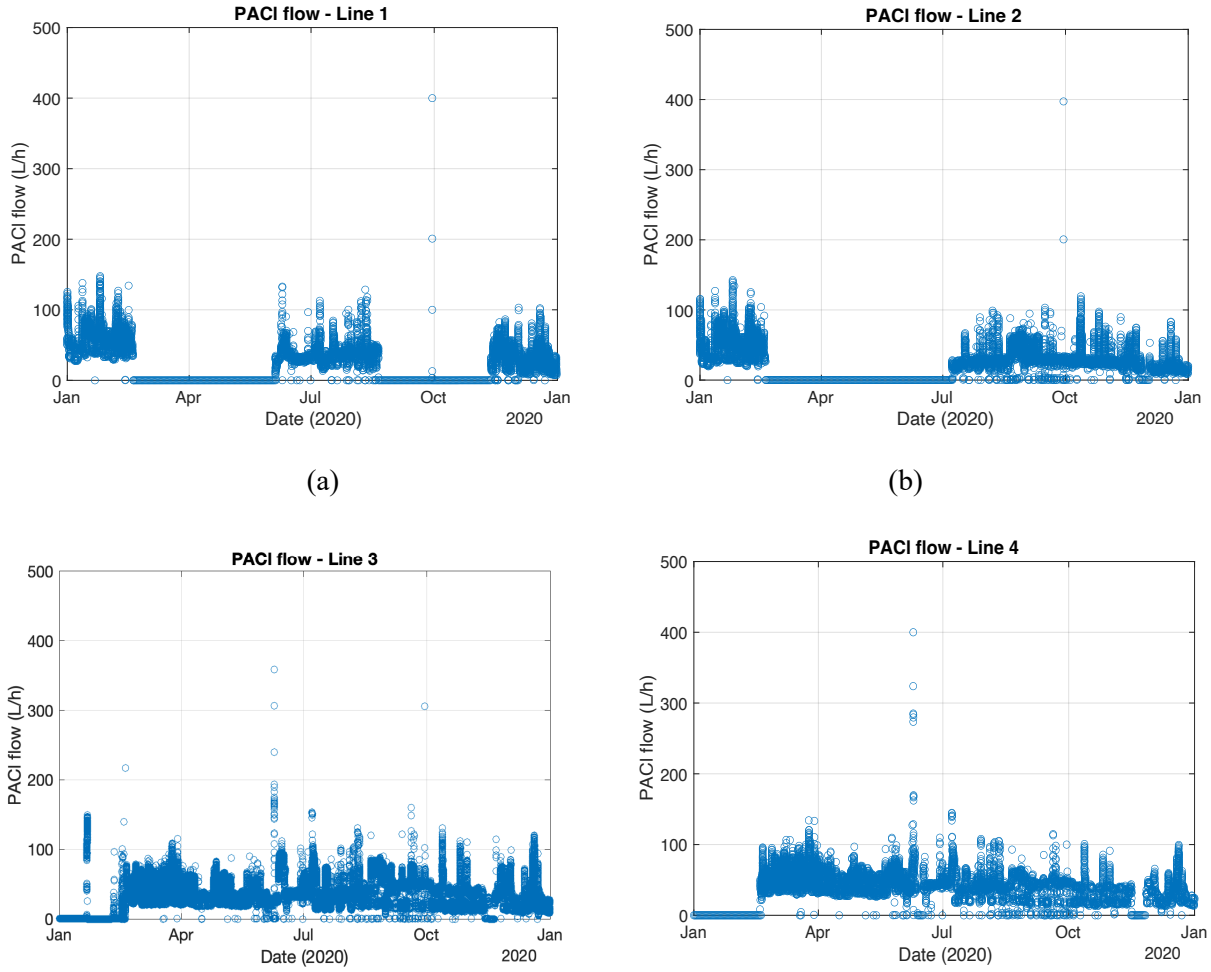


Figure B.1: Timeseries of PACl flow (L/h) – Line 1 to 4 (2020)

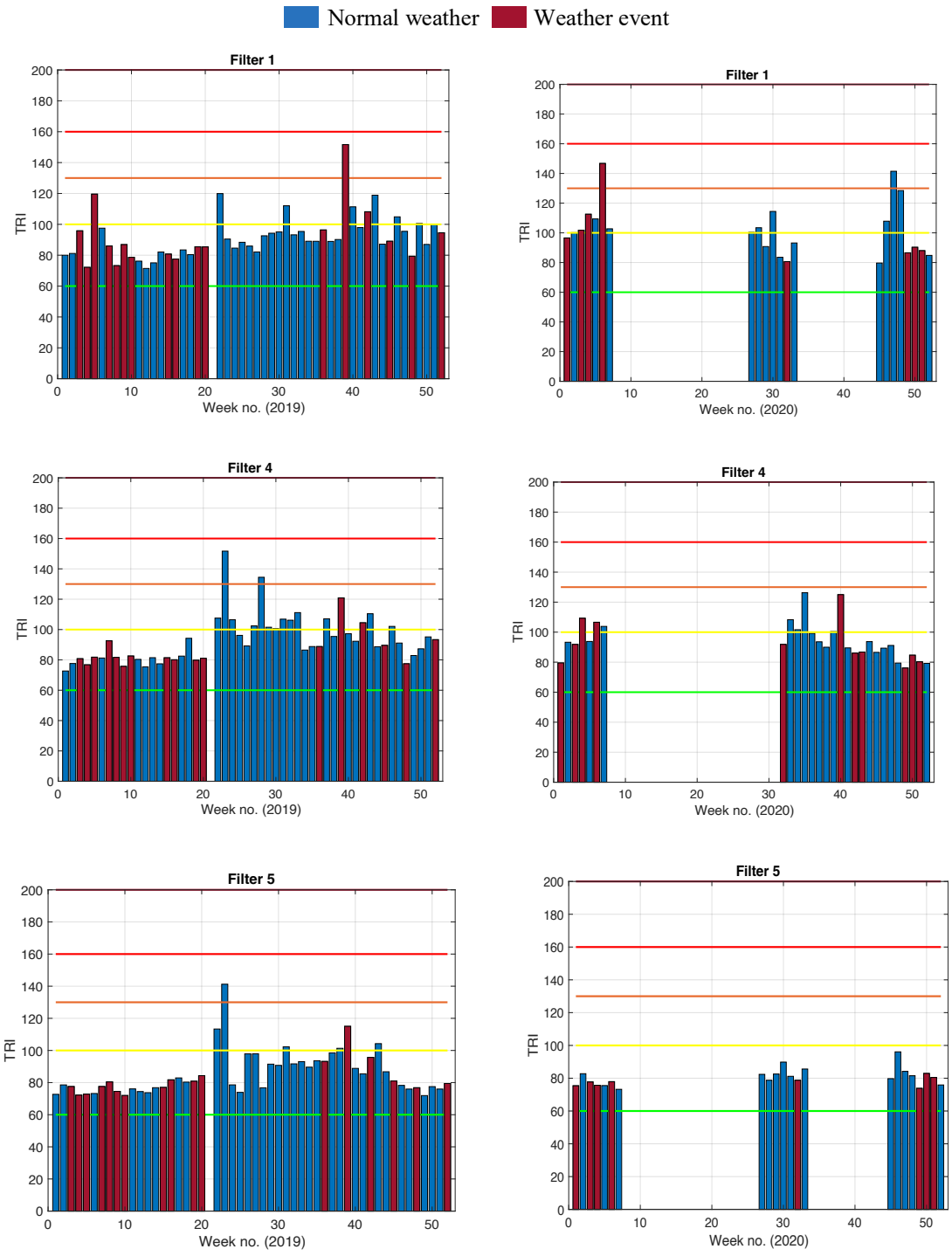


Figure B.2: Weekly TRIs of Filters 1, 4, and 5 during normal weather and weather events characterized by raw water turbidity in 2019 and 2020 (Tgoal = 0.1 NTU)

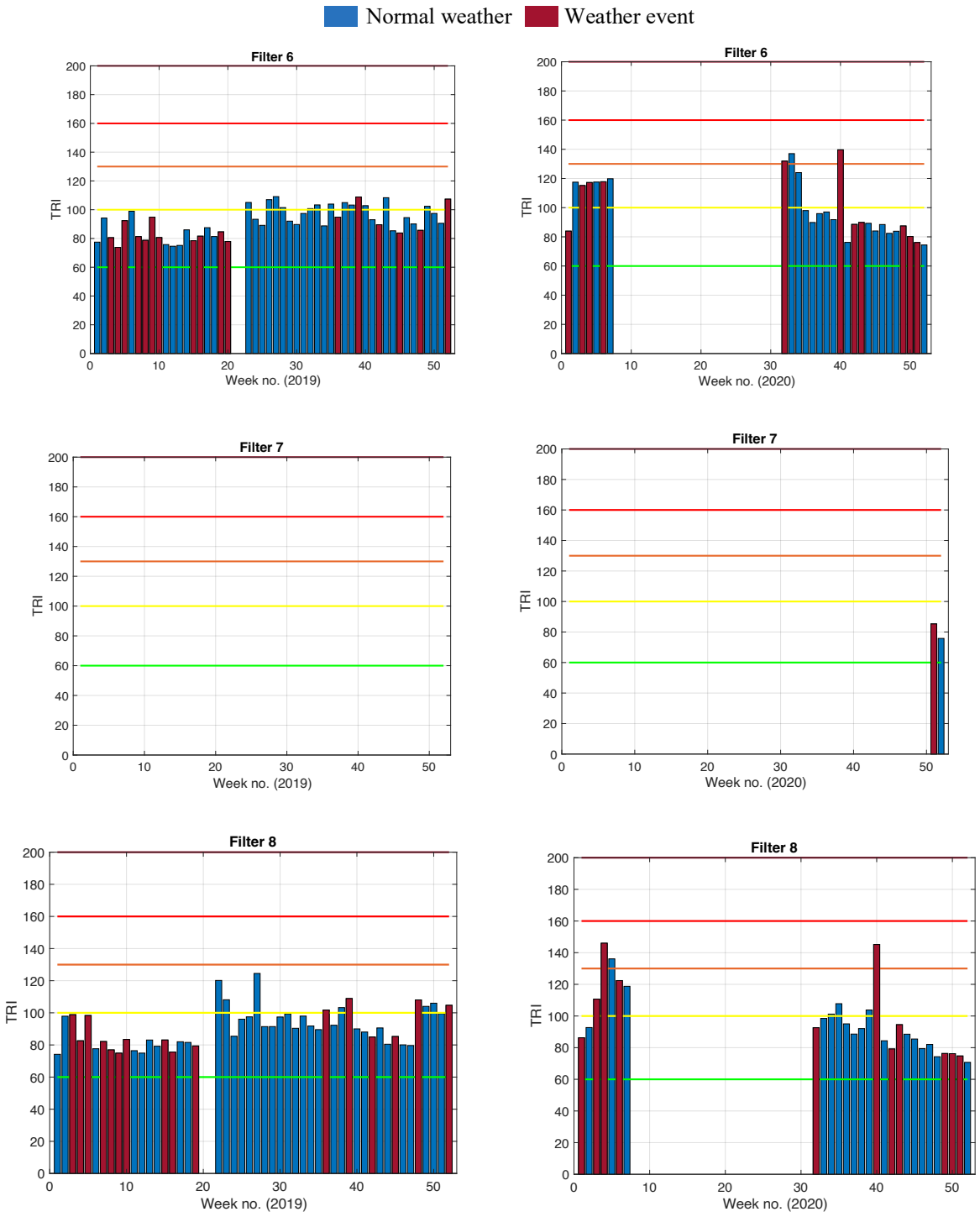


Figure B.3: Weekly TRIs of Filters 6 to 8 during normal weather and weather events characterized by raw water turbidity in 2019 and 2020 (Tgoal = 0.1 NTU)

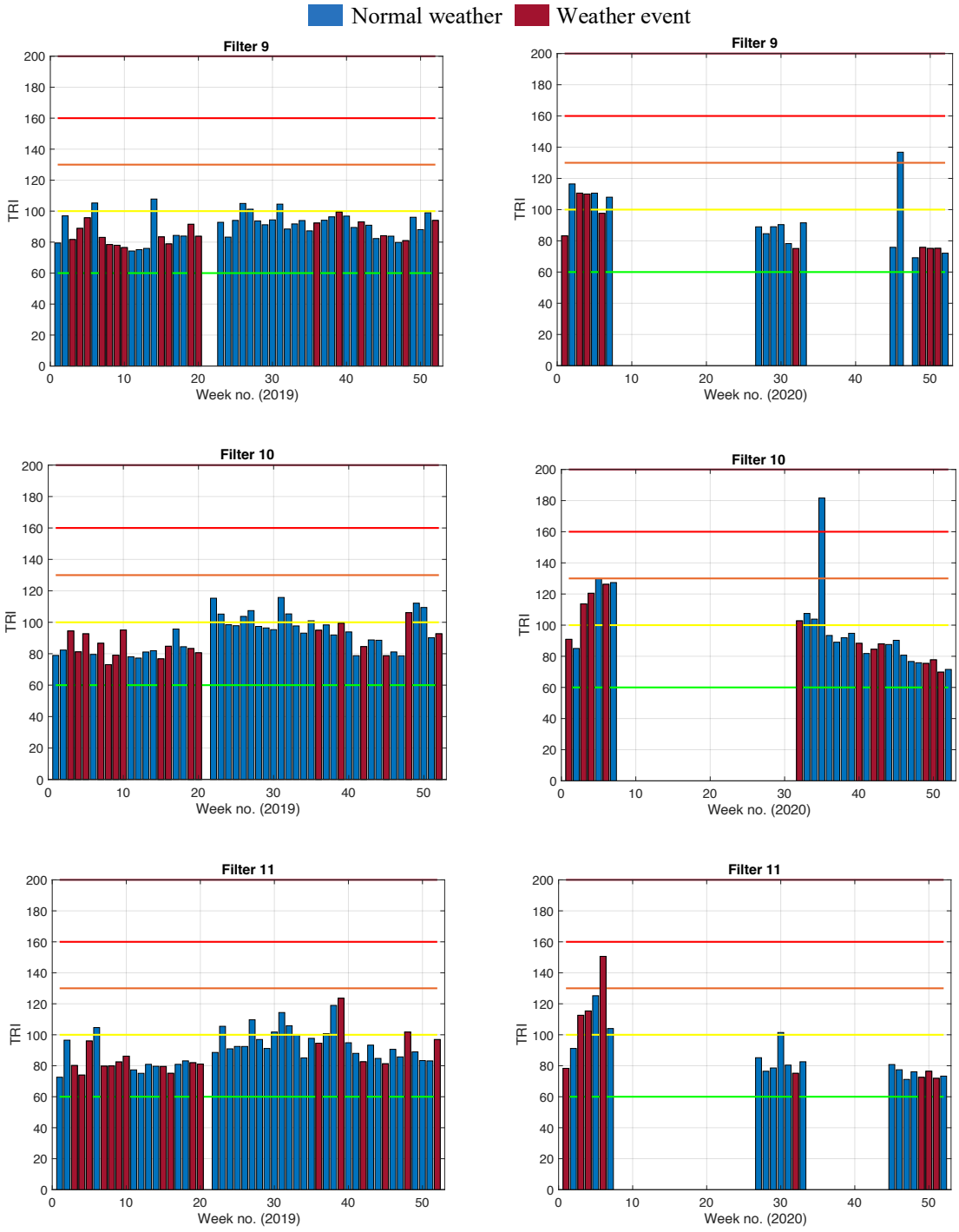


Figure B.4: Weekly TRIs of Filters 9 to 11 during normal weather and weather events characterized by raw water turbidity in 2019 and 2020 (Tgoal = 0.1 NTU)

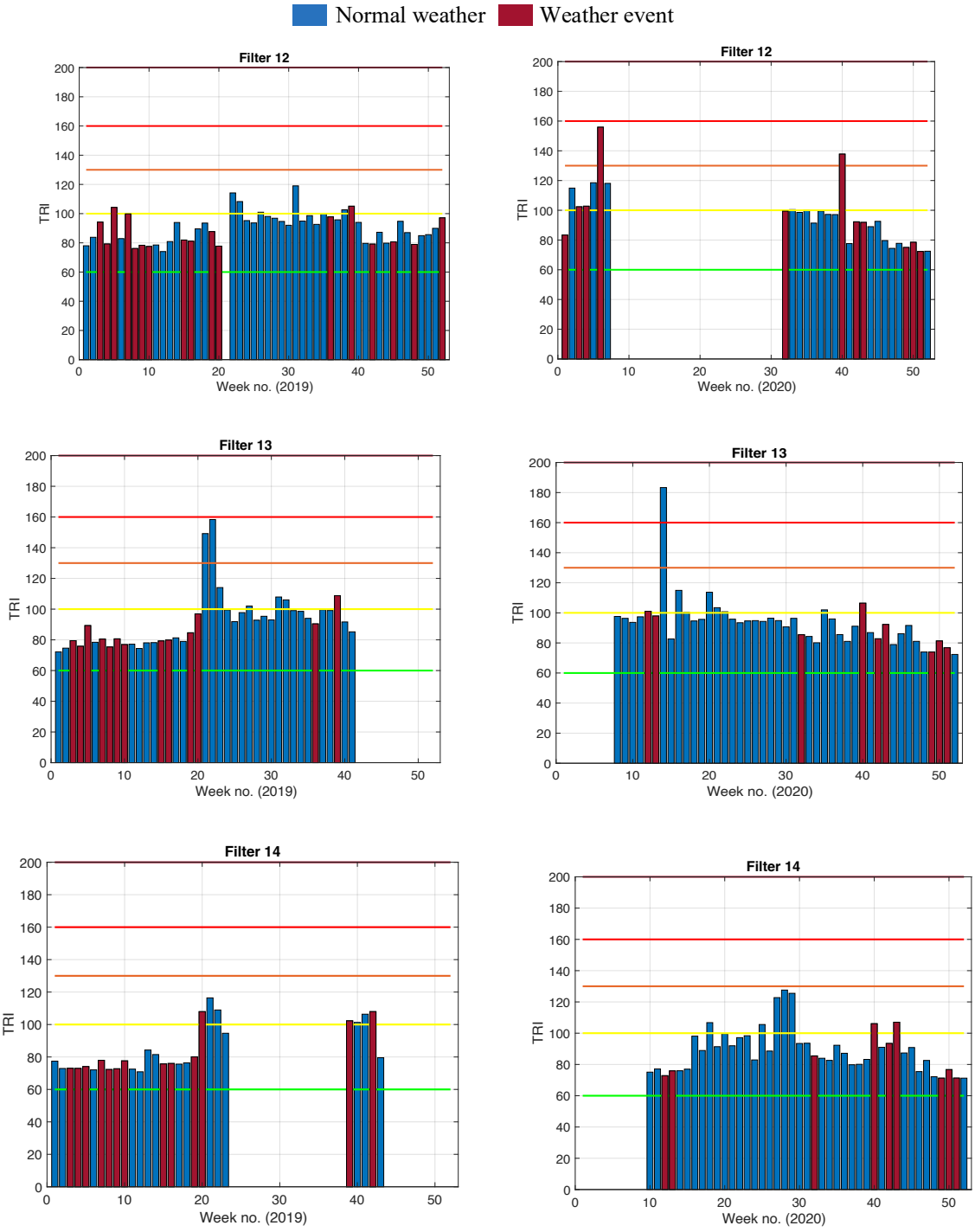


Figure B.5: Weekly TRIs of Filters 12 to 14 during normal weather and weather events characterized by raw water turbidity in 2019 and 2020 (Tgoal = 0.1 NTU)

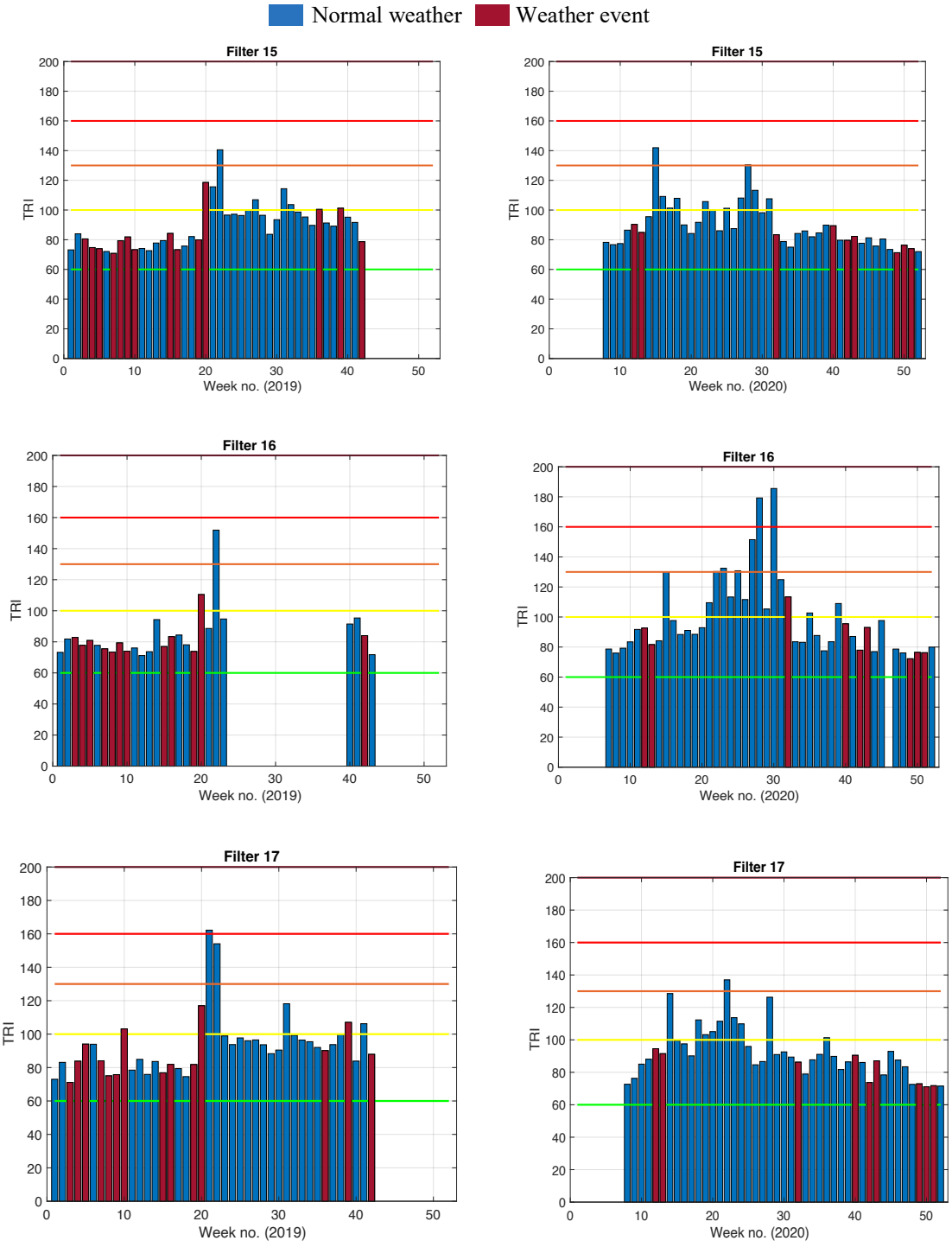


Figure B.6: Weekly TRIs of Filters 15 to 17 during normal weather and weather events characterized by raw water turbidity in 2019 and 2020 (Tgoal = 0.1 NTU)

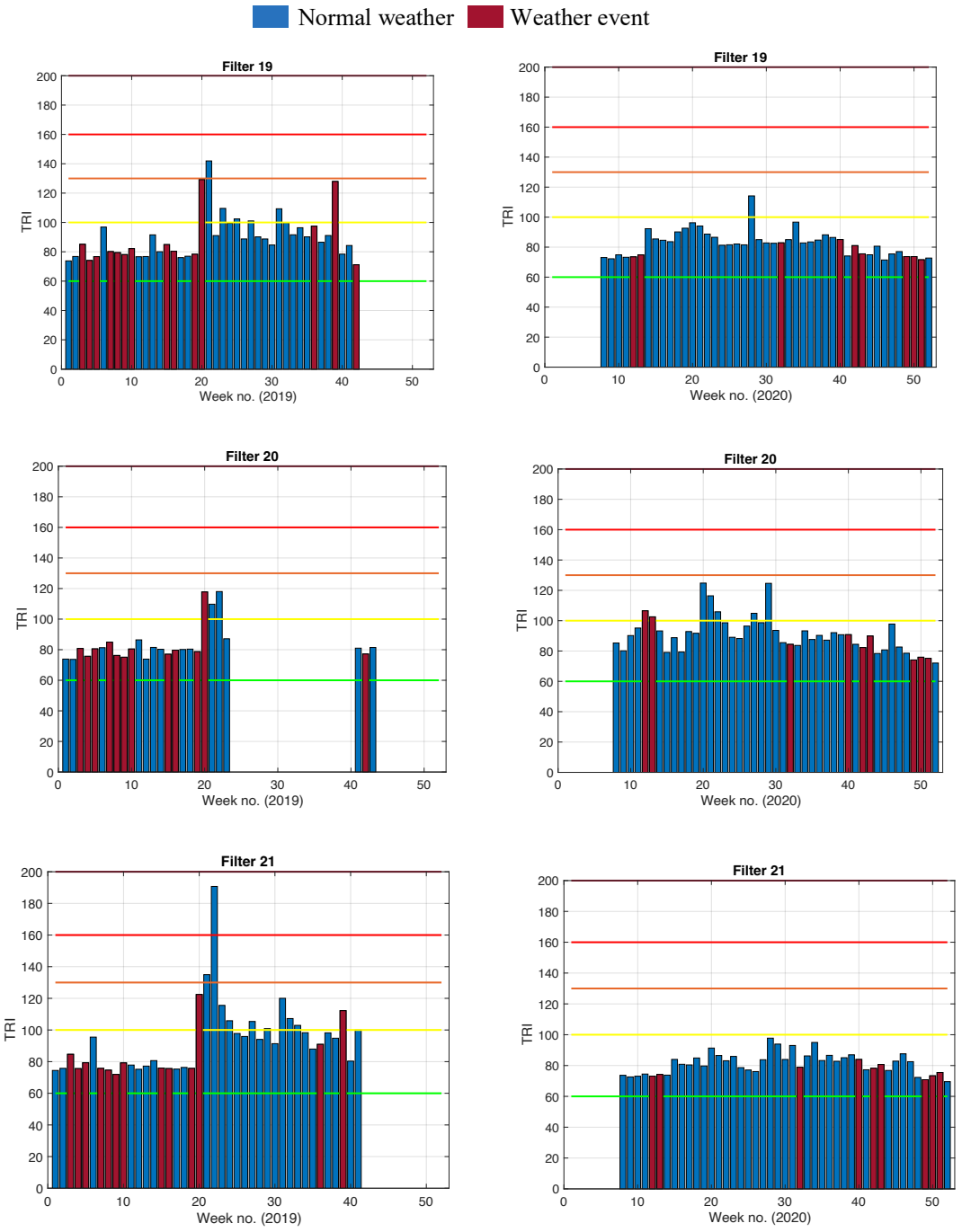


Figure B.7: Weekly TRIs of Filters 19 to 21 during normal weather and weather events characterized by raw water turbidity in 2019 and 2020 (Tgoal = 0.1 NTU)

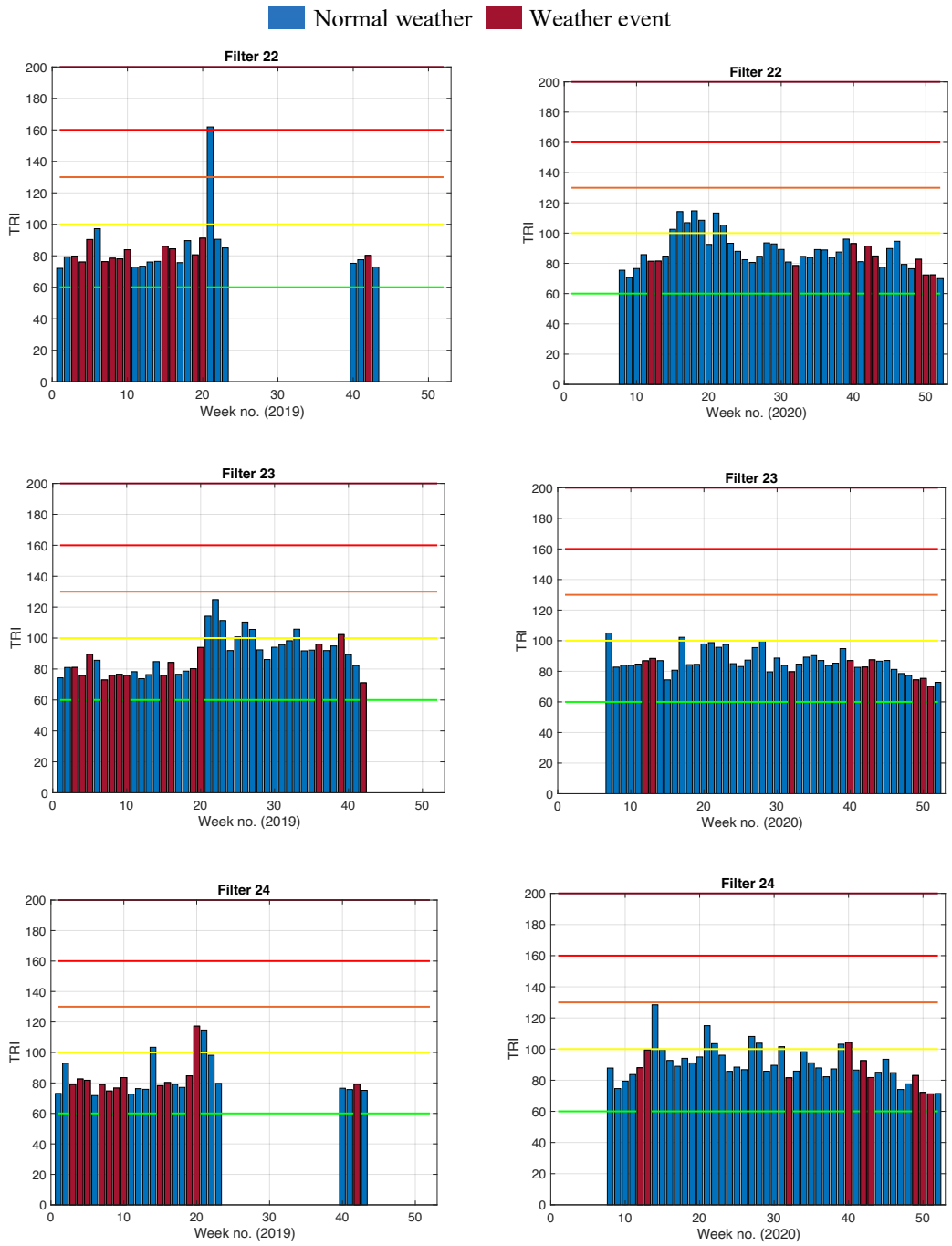


Figure B.8: Weekly TRIs of Filters 22 to 24 during normal weather and weather events characterized by raw water turbidity in 2019 and 2020 (Tgoal = 0.1 NTU)

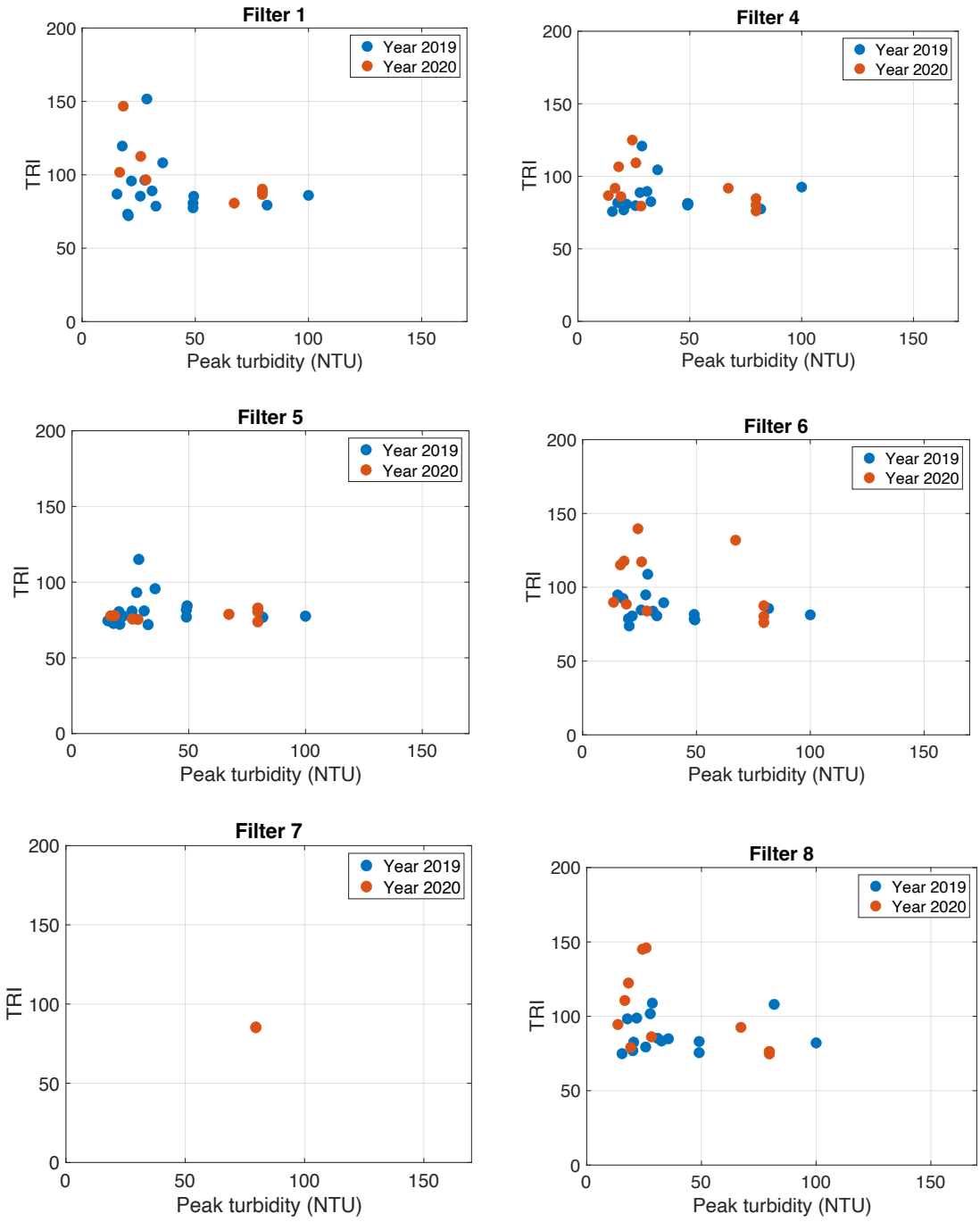


Figure B.9: Weekly TRIs of Filters 1 and 4-8 in relation to the maximum values of raw water turbidities during weather events

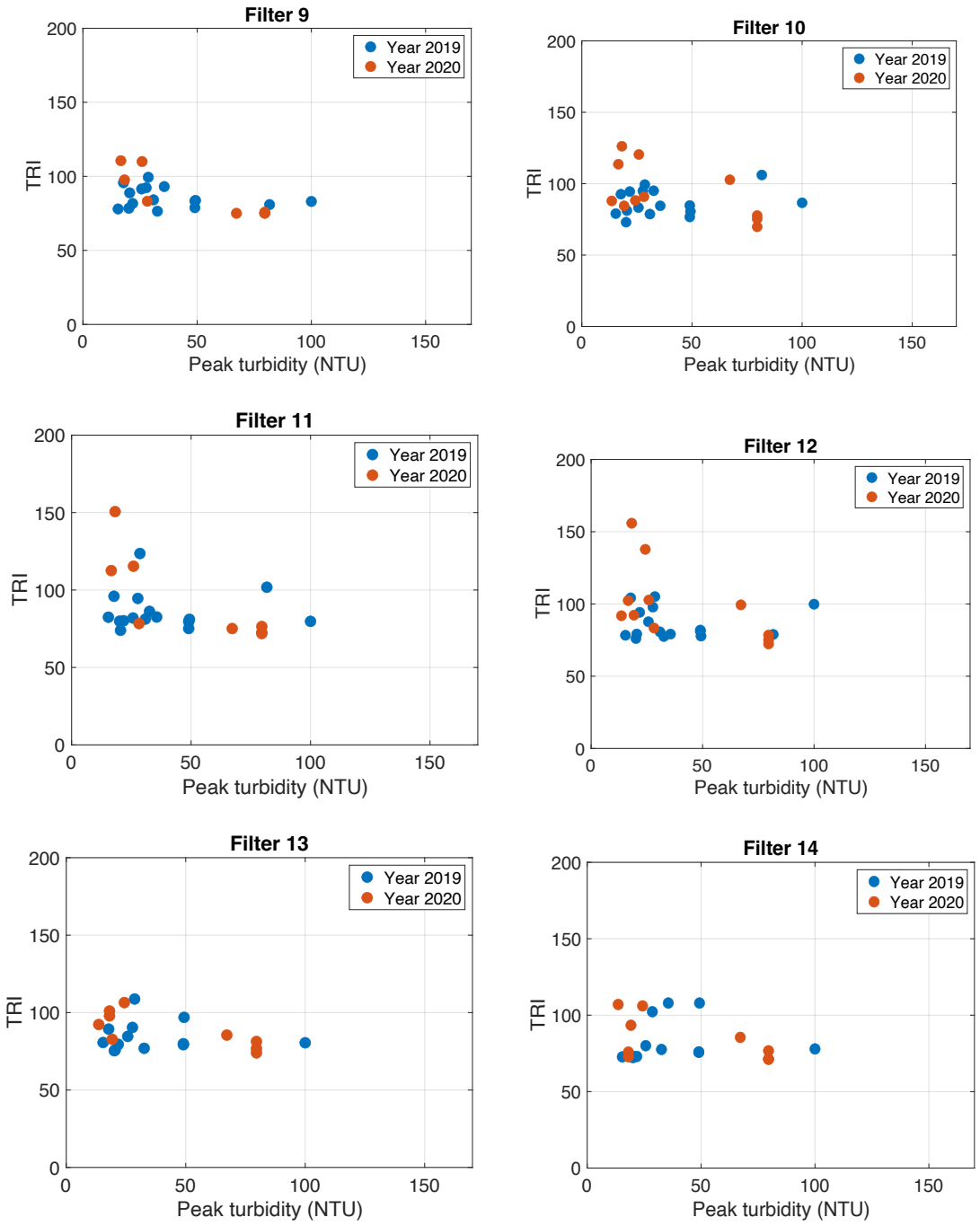


Figure B.10: Weekly TRIs of Filters 9-14 in relation to the maximum values of raw water turbidities during weather events

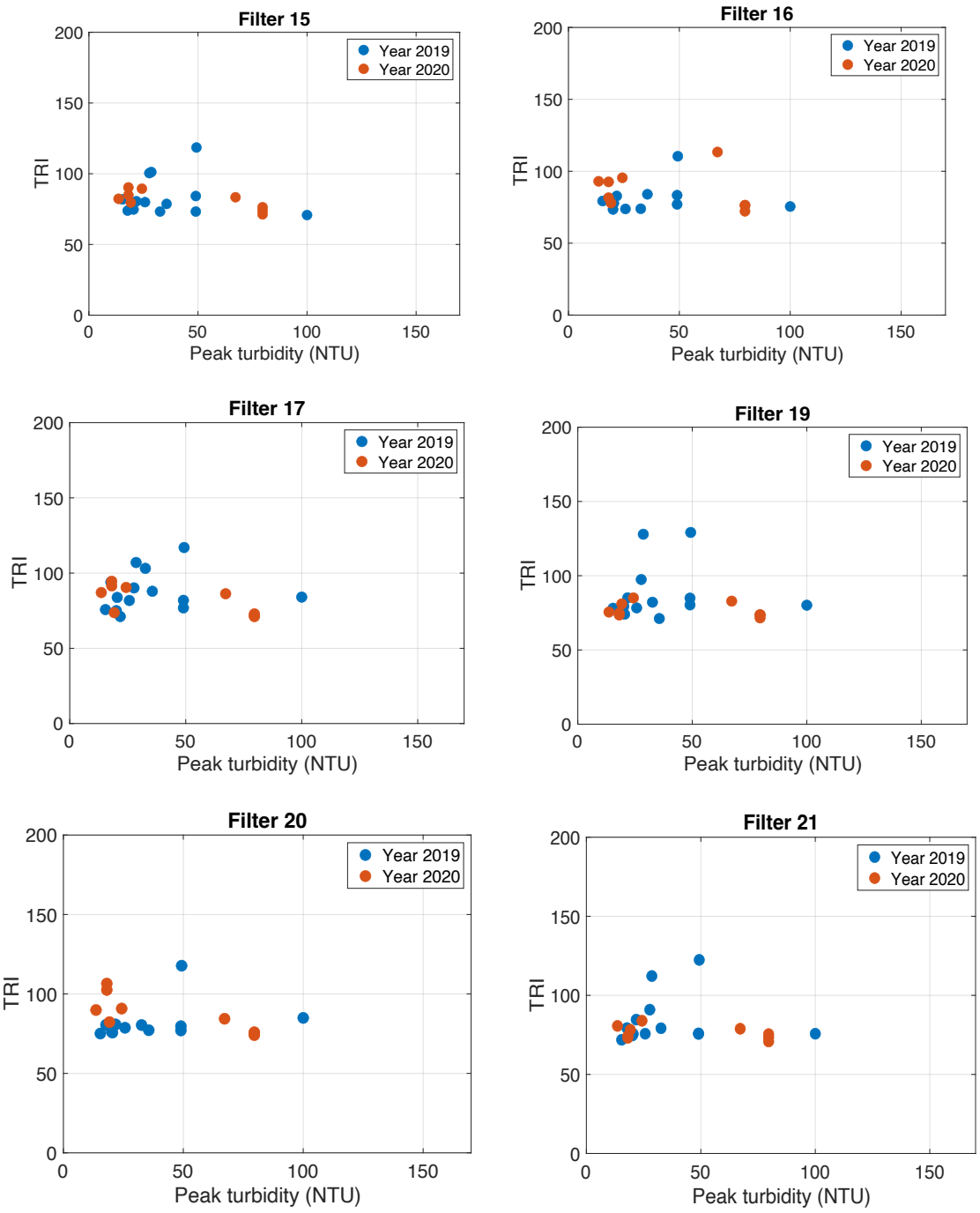


Figure B.11: Weekly TRIs of Filters 15-17 and 19-21 in relation to the maximum values of raw water turbidities during weather events

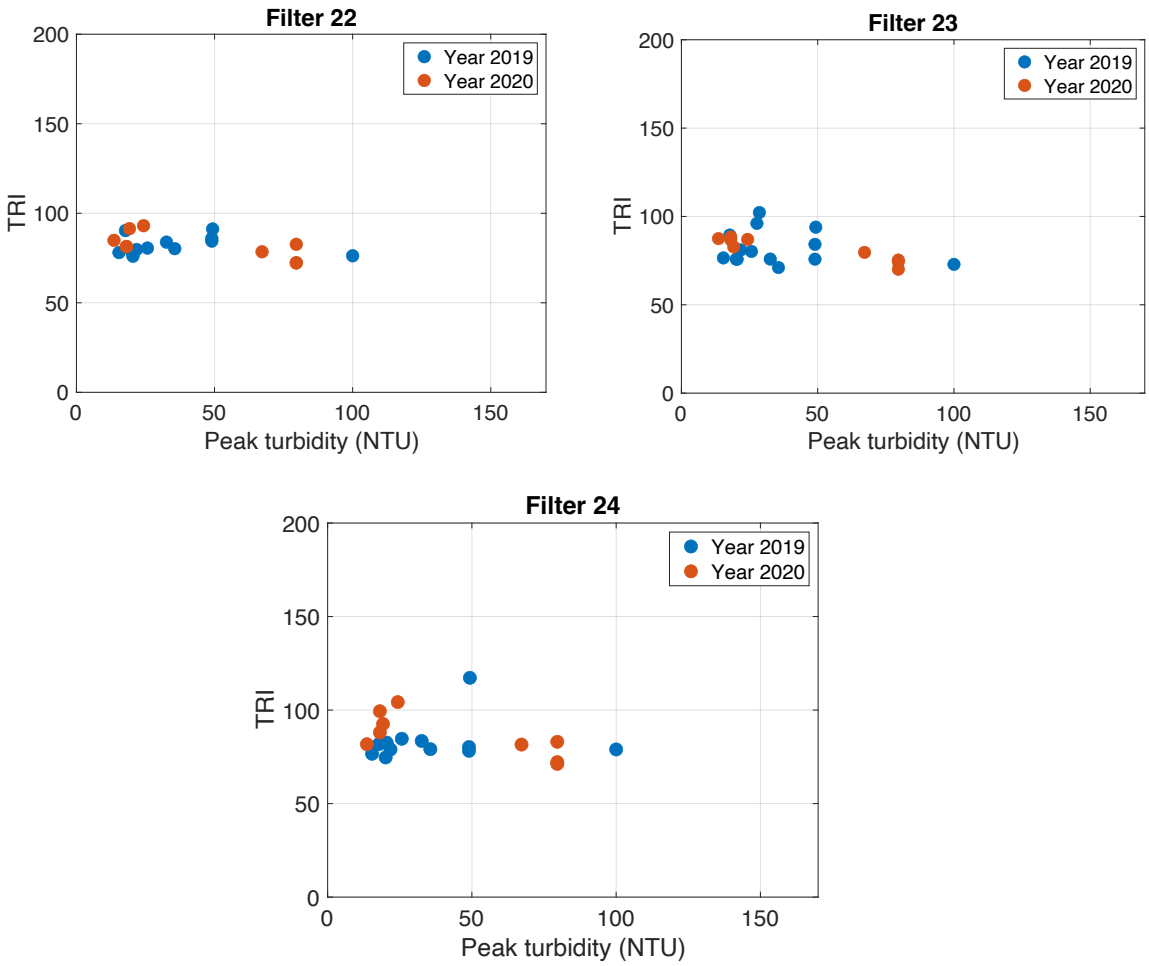


Figure B.12: Weekly TRIs of Filters 22-24 in relation to the maximum values of raw water turbidities during weather events

Table B.1: Weekly average percentage of turbidity removal by the overall CFS (modules 1 and 2) and filtration process (Filters 1 to 24)

| Week no. | 2019 | | 2020 | |
|---|---|---|---|---|
| | **Percent turbidity removal by the CFS units (%)** | **Percent turbidity removal by the CFS units and Filters (%)** | **Percent turbidity removal by the CFS units (%)** | **Percent turbidity removal by the CFS units and Filters (%)** |
| 1 | 27.8 | 78.8 | 95.2 | 99.4 |
| 2 | 59.0 | 68.3 | 98.0 | 99.1 |
| 3 | 70.9 | 83.5 | 98.6 | 99.6 |
| 4 | 61.8 | 86.8 | 97.8 | 99.4 |
| 5 | 72.1 | 66.6 | 98.8 | 98.0 |
| 6 | 72.7 | 81.9 | 98.6 | 99.3 |
| 7 | 94.0 | 81.2 | 99.9 | 98.8 |
| 8 | 89.0 | 67.3 | 99.6 | 97.0 |
| 9 | 80.0 | 59.8 | 99.1 | 97.1 |
| 10 | 88.9 | 61.3 | 99.4 | 97.1 |
| 11 | 81.3 | 57.3 | 98.4 | 97.3 |
| 12 | 79.6 | 84.4 | 98.4 | 99.1 |
| 13 | 74.6 | 82.3 | 98.4 | 98.9 |
| 14 | 81.4 | 59.5 | 98.4 | 97.4 |
| 15 | 92.7 | 48.3 | 99.7 | 96.2 |
| 16 | 83.6 | 5.5 | 99.1 | 91.8 |
| 17 | 78.3 | 63.2 | 98.4 | 97.8 |
| 18 | 92.7 | 62.5 | 99.6 | 97.5 |
| 19 | 95.0 | 57.5 | 99.7 | 95.2 |
| 20 | 80.4 | 62.7 | 99.4 | 96.9 |
| 21 | 54.0 | 65.0 | 97.4 | 97.7 |
| 22 | 61.9 | 37.2 | 97.7 | 94.9 |
| 23 | 63.1 | 62.1 | 96.5 | 96.3 |

| | | | | |
|---|---|---|---|---|
| 24 | 62.1 | 83.9 | 95.4 | 98.3 |
| 25 | 62.8 | 75.7 | 96.0 | 97.1 |
| 26 | 64.0 | 87.4 | 96.2 | 98.4 |
| 27 | 59.9 | 88.6 | 96.1 | 98.4 |
| 28 | 71.8 | 85.9 | 97.3 | 98.2 |
| 29 | 35.7 | 87.0 | 95.7 | 98.0 |
| 30 | 36.6 | 83.6 | 95.2 | 97.7 |
| 31 | 43.8 | 82.9 | 95.0 | 98.4 |
| 32 | 55.4 | 84.5 | 96.4 | 98.4 |
| 33 | 54.6 | 84.9 | 96.0 | 97.9 |
| 34 | 53.2 | 89.5 | 95.4 | 98.4 |
| 35 | 65.2 | 87.7 | 97.1 | 99.1 |
| 36 | 62.7 | 62.8 | 96.8 | 96.9 |
| 37 | 80.0 | 72.6 | 98.4 | 94.9 |
| 38 | 74.9 | 69.6 | 95.9 | 97.1 |
| 39 | 76.4 | 68.8 | 98.1 | 77.9 |
| 40 | 90.2 | 41.9 | 99.1 | 76.8 |
| 41 | 83.9 | 90.0 | 99.0 | 98.1 |
| 42 | 86.2 | 67.1 | 98.8 | 97.3 |
| 43 | 84.0 | 77.0 | 98.9 | 98.5 |
| 44 | 78.1 | 82.9 | 98.2 | 98.5 |
| 45 | 63.6 | 55.4 | 98.5 | 95.5 |
| 46 | 78.7 | 39.3 | 99.0 | 95.5 |
| 47 | 32.5 | 78.7 | 96.3 | 98.7 |
| 48 | 93.2 | 70.6 | 99.8 | 97.8 |
| 49 | 64.5 | 54.9 | 99.1 | 94.8 |
| 50 | -65.8 | 95.5 | 93.6 | 99.7 |
| 51 | -43.9 | 91.4 | 93.5 | 99.8 |
| 52 | 93.2 | 80.4 | 99.8 | 99.3 |

Table B.2: Overall robustness of Plant B by weeks in 2020 by equal weighting

| Week no. | 2020 | | | | | |
|---|---|---|---|---|---|---|
| | CFS Units | | Filters | | Plant | |
| | TRI | Category | TRI | Category | Overall Robustness Category | Overall System Robustness |
| 1 | 136 | 4 | 84 | 2 | 3 | slightly disturbed |
| 2 | 119 | 3 | 99 | 2 | 3 | slightly disturbed |
| 3 | 128 | 3 | 103 | 3 | 3 | slightly disturbed |
| 4 | 116 | 3 | 110 | 3 | 3 | slightly disturbed |
| 5 | 94 | 2 | 112 | 3 | 3 | slightly disturbed |
| 6 | 127 | 3 | 120 | 3 | 3 | slightly disturbed |
| 7 | 96 | 2 | 103 | 3 | 3 | slightly disturbed |
| 8 | 97 | 2 | 80 | 2 | 2 | stable |
| 9 | 105 | 3 | 78 | 2 | 3 | slightly disturbed |
| 10 | 90 | 2 | 81 | 2 | 2 | stable |
| 11 | 102 | 3 | 85 | 2 | 3 | slightly disturbed |
| 12 | 112 | 3 | 86 | 2 | 3 | slightly disturbed |
| 13 | 119 | 3 | 86 | 2 | 3 | slightly disturbed |
| 14 | 100 | 2 | 113 | 3 | 3 | slightly disturbed |
| 15 | 156 | 4 | 102 | 3 | 4 | moderately disturbed |
| 16 | 86 | 2 | 97 | 2 | 2 | stable |
| 17 | 106 | 3 | 92 | 2 | 3 | slightly disturbed |
| 18 | 98 | 2 | 97 | 2 | 2 | stable |
| 19 | 96 | 2 | 93 | 2 | 2 | stable |
| 20 | 121 | 3 | 99 | 2 | 3 | slightly disturbed |
| 21 | 106 | 3 | 104 | 3 | 3 | slightly disturbed |
| 22 | 115 | 3 | 106 | 3 | 3 | slightly disturbed |
| 23 | 119 | 3 | 102 | 3 | 3 | slightly disturbed |
| 24 | 93 | 2 | 91 | 2 | 2 | stable |

| | | | | | | |
|---|---|---|---|---|---|---|
| 25 | 122 | 3 | 95 | 2 | 3 | slightly disturbed |
| 26 | 93 | 2 | 90 | 2 | 2 | stable |
| 27 | 108 | 3 | 100 | 3 | 3 | slightly disturbed |
| 28 | 90 | 2 | 110 | 3 | 3 | slightly disturbed |
| 29 | 97 | 2 | 98 | 2 | 2 | stable |
| 30 | 103 | 3 | 101 | 3 | 3 | slightly disturbed |
| 31 | 109 | 3 | 99 | 2 | 3 | slightly disturbed |
| 32 | 89 | 2 | 90 | 2 | 2 | stable |
| 33 | 95 | 2 | 93 | 2 | 2 | stable |
| 34 | 94 | 2 | 95 | 2 | 2 | stable |
| 35 | 128 | 3 | 101 | 3 | 3 | slightly disturbed |
| 36 | 105 | 3 | 91 | 2 | 3 | slightly disturbed |
| 37 | 92 | 2 | 86 | 2 | 2 | stable |
| 38 | 103 | 3 | 88 | 2 | 3 | slightly disturbed |
| 39 | 93 | 2 | 94 | 2 | 2 | stable |
| 40 | 109 | 3 | 104 | 3 | 3 | slightly disturbed |
| 41 | 131 | 3 | 84 | 2 | 3 | slightly disturbed |
| 42 | 99 | 2 | 84 | 2 | 2 | stable |
| 43 | 147 | 4 | 89 | 2 | 3 | slightly disturbed |
| 44 | 100 | 3 | 83 | 2 | 3 | slightly disturbed |
| 45 | 112 | 3 | 86 | 2 | 3 | slightly disturbed |
| 46 | 103 | 3 | 88 | 2 | 3 | slightly disturbed |
| 47 | 124 | 3 | 83 | 2 | 3 | slightly disturbed |
| 48 | 95 | 2 | 79 | 2 | 2 | stable |
| 49 | 173 | 5 | 76 | 2 | 4 | moderately disturbed |
| 50 | 153 | 4 | 78 | 2 | 3 | slightly disturbed |
| 51 | 113 | 3 | 75 | 2 | 3 | slightly disturbed |
| 52 | 124 | 3 | 74 | 2 | 3 | slightly disturbed |

Table B.3: Overall robustness of Plant B by weeks in 2020 by unequal weighting (considering the CFS process is more significant)

| Week no. | 2020 | | | | | |
|---|---|---|---|---|---|---|
| | CFS Units | | Filters | | Plant | |
| | TRI | Category | TRI | Category | Overall Robustness Category | Overall System Robustness |
| 1 | 136 | 4 | 84 | 2 | 3 | slightly disturbed |
| 2 | 119 | 3 | 99 | 2 | 3 | slightly disturbed |
| 3 | 128 | 3 | 103 | 3 | 3 | slightly disturbed |
| 4 | 116 | 3 | 110 | 3 | 3 | slightly disturbed |
| 5 | 94 | 2 | 112 | 3 | 2 | stable |
| 6 | 127 | 3 | 120 | 3 | 3 | slightly disturbed |
| 7 | 96 | 2 | 103 | 3 | 2 | stable |
| 8 | 97 | 2 | 80 | 2 | 2 | stable |
| 9 | 105 | 3 | 78 | 2 | 3 | slightly disturbed |
| 10 | 90 | 2 | 81 | 2 | 2 | stable |
| 11 | 102 | 3 | 85 | 2 | 3 | slightly disturbed |
| 12 | 112 | 3 | 86 | 2 | 3 | slightly disturbed |
| 13 | 119 | 3 | 86 | 2 | 3 | slightly disturbed |
| 14 | 100 | 2 | 113 | 3 | 2 | stable |
| 15 | 156 | 4 | 102 | 3 | 4 | moderately disturbed |
| 16 | 86 | 2 | 97 | 2 | 2 | stable |
| 17 | 106 | 3 | 92 | 2 | 3 | slightly disturbed |
| 18 | 98 | 2 | 97 | 2 | 2 | stable |
| 19 | 96 | 2 | 93 | 2 | 2 | stable |
| 20 | 121 | 3 | 99 | 2 | 3 | slightly disturbed |
| 21 | 106 | 3 | 104 | 3 | 3 | slightly disturbed |
| 22 | 115 | 3 | 106 | 3 | 3 | slightly disturbed |

| | | | | | | |
|---|---|---|---|---|---|---|
| 23 | 119 | 3 | 102 | 3 | 3 | slightly disturbed |
| 24 | 93 | 2 | 91 | 2 | 2 | stable |
| 25 | 122 | 3 | 95 | 2 | 3 | slightly disturbed |
| 26 | 93 | 2 | 90 | 2 | 2 | stable |
| 27 | 108 | 3 | 100 | 3 | 3 | slightly disturbed |
| 28 | 90 | 2 | 110 | 3 | 2 | stable |
| 29 | 97 | 2 | 98 | 2 | 2 | stable |
| 30 | 103 | 3 | 101 | 3 | 3 | slightly disturbed |
| 31 | 109 | 3 | 99 | 2 | 3 | slightly disturbed |
| 32 | 89 | 2 | 90 | 2 | 2 | stable |
| 33 | 95 | 2 | 93 | 2 | 2 | stable |
| 34 | 94 | 2 | 95 | 2 | 2 | stable |
| 35 | 128 | 3 | 101 | 3 | 3 | slightly disturbed |
| 36 | 105 | 3 | 91 | 2 | 3 | slightly disturbed |
| 37 | 92 | 2 | 86 | 2 | 2 | stable |
| 38 | 103 | 3 | 88 | 2 | 3 | slightly disturbed |
| 39 | 93 | 2 | 94 | 2 | 2 | stable |
| 40 | 109 | 3 | 104 | 3 | 3 | slightly disturbed |
| 41 | 131 | 3 | 84 | 2 | 3 | slightly disturbed |
| 42 | 99 | 2 | 84 | 2 | 2 | stable |
| 43 | 147 | 4 | 89 | 2 | 3 | slightly disturbed |
| 44 | 100 | 3 | 83 | 2 | 3 | slightly disturbed |
| 45 | 112 | 3 | 86 | 2 | 3 | slightly disturbed |
| 46 | 103 | 3 | 88 | 2 | 3 | slightly disturbed |
| 47 | 124 | 3 | 83 | 2 | 3 | slightly disturbed |
| 48 | 95 | 2 | 79 | 2 | 2 | stable |
| 49 | 173 | 5 | 76 | 2 | 4 | moderately disturbed |
| 50 | 153 | 4 | 78 | 2 | 3 | slightly disturbed |
| 51 | 113 | 3 | 75 | 2 | 3 | slightly disturbed |

| | | | | | | |
|---|---|---|---|---|---|---|
| 52 | 124 | 3 | 74 | 2 | 3 | slightly disturbed |

Table B.4: Overall robustness of Plant B by weeks in 2020 by unequal weighting (considering the filtration process is more significant)

| Week no. | 2020 | | | | | |
|---|---|---|---|---|---|---|
| | CFS Units | | Filters | | Plant | |
| | TRI | Category | TRI | Category | Overall Robustness Category | Overall System Robustness |
| 1 | 136 | 4 | 84 | 2 | 3 | slightly disturbed |
| 2 | 119 | 3 | 99 | 2 | 2 | stable |
| 3 | 128 | 3 | 103 | 3 | 3 | slightly disturbed |
| 4 | 116 | 3 | 110 | 3 | 3 | slightly disturbed |
| 5 | 94 | 2 | 112 | 3 | 3 | slightly disturbed |
| 6 | 127 | 3 | 120 | 3 | 3 | slightly disturbed |
| 7 | 96 | 2 | 103 | 3 | 3 | slightly disturbed |
| 8 | 97 | 2 | 80 | 2 | 2 | stable |
| 9 | 105 | 3 | 78 | 2 | 2 | stable |
| 10 | 90 | 2 | 81 | 2 | 2 | stable |
| 11 | 102 | 3 | 85 | 2 | 2 | stable |
| 12 | 112 | 3 | 86 | 2 | 2 | stable |
| 13 | 119 | 3 | 86 | 2 | 2 | stable |
| 14 | 100 | 2 | 113 | 3 | 3 | slightly disturbed |
| 15 | 156 | 4 | 102 | 3 | 3 | slightly disturbed |
| 16 | 86 | 2 | 97 | 2 | 2 | stable |
| 17 | 106 | 3 | 92 | 2 | 2 | stable |
| 18 | 98 | 2 | 97 | 2 | 2 | stable |
| 19 | 96 | 2 | 93 | 2 | 2 | stable |

| | | | | | | |
|---|---|---|---|---|---|---|
| 20 | 121 | 3 | 99 | 2 | 2 | stable |
| 21 | 106 | 3 | 104 | 3 | 3 | slightly disturbed |
| 22 | 115 | 3 | 106 | 3 | 3 | slightly disturbed |
| 23 | 119 | 3 | 102 | 3 | 3 | slightly disturbed |
| 24 | 93 | 2 | 91 | 2 | 2 | stable |
| 25 | 122 | 3 | 95 | 2 | 2 | stable |
| 26 | 93 | 2 | 90 | 2 | 2 | stable |
| 27 | 108 | 3 | 100 | 3 | 3 | slightly disturbed |
| 28 | 90 | 2 | 110 | 3 | 3 | slightly disturbed |
| 29 | 97 | 2 | 98 | 2 | 2 | stable |
| 30 | 103 | 3 | 101 | 3 | 3 | slightly disturbed |
| 31 | 109 | 3 | 99 | 2 | 2 | stable |
| 32 | 89 | 2 | 90 | 2 | 2 | stable |
| 33 | 95 | 2 | 93 | 2 | 2 | stable |
| 34 | 94 | 2 | 95 | 2 | 2 | stable |
| 35 | 128 | 3 | 101 | 3 | 3 | slightly disturbed |
| 36 | 105 | 3 | 91 | 2 | 2 | stable |
| 37 | 92 | 2 | 86 | 2 | 2 | stable |
| 38 | 103 | 3 | 88 | 2 | 2 | stable |
| 39 | 93 | 2 | 94 | 2 | 2 | stable |
| 40 | 109 | 3 | 104 | 3 | 3 | slightly disturbed |
| 41 | 131 | 3 | 84 | 2 | 2 | stable |
| 42 | 99 | 2 | 84 | 2 | 2 | stable |
| 43 | 147 | 4 | 89 | 2 | 3 | slightly disturbed |
| 44 | 100 | 3 | 83 | 2 | 2 | stable |
| 45 | 112 | 3 | 86 | 2 | 2 | stable |
| 46 | 103 | 3 | 88 | 2 | 2 | stable |
| 47 | 124 | 3 | 83 | 2 | 2 | stable |
| 48 | 95 | 2 | 79 | 2 | 2 | stable |

| | | | | | | |
|---|---|---|---|---|---|---|
| 49 | 173 | 5 | 76 | 2 | 3 | slightly disturbed |
| 50 | 153 | 4 | 78 | 2 | 3 | slightly disturbed |
| 51 | 113 | 3 | 75 | 2 | 2 | stable |
| 52 | 124 | 3 | 74 | 2 | 2 | stable |

# Appendix C: Supplementary Information of Chapter 5

Table C.1: DOC and zeta potential of water samples, coagulant and polymer

| Water samples | DOC (mg/L) | Zeta potential (mV) |
|---|---|---|
| Raw water - batch 2 (1) | 8.92 | -13.1 |
| Raw water - batch 2 (2) | 8.80 | -12.8 |
| Raw water - batch 3 (1) | 8.63 | -11.8 |
| Raw water - batch 3 (2) | 7.09 | -11.3 |
| Coagulated water - batch 2 | 12.1 | -13.9 |
| Coagulated water - batch 3 | 8.44 | -13.5 |
| Spiked water (kaolin dosage = 0.025 g/L) | 8.27 | -15.4 |
| Spiked water (kaolin dosage = 0.1 g/L) | 7.79 | -17.9 |
| Spiked water (kaolin dosage = 0.4 g/L) | 8.08 | -18.7 |
| Spiked water (kaolin dosage = 0.5 g/L) | 7.65 | -21.9 |
| FD: spiked water (kaolin dosage = 0.35 g/L) | 8.77 | -18.6 |
| FD: spiked coagulated water (run 1-1) | 9.74 | -15.7 |
| FD: spiked coagulated water (run 2-1) | 8.96 | -14.8 |
| FD: spiked coagulated water (run 3-1) | 9.99 | -16.5 |
| FD: spiked coagulated water (run 4-1) | 9.31 | -16.5 |
| FD: spiked coagulated water (run 5-1) | 10.2 | -16.9 |
| FD: spiked coagulated water (run 6-1) | 10.3 | -17.6 |
| FD: spiked coagulated water (run 7-1) | 9.57 | -17.2 |
| FD: spiked coagulated water (run 8-1) | 10.5 | -16.3 |
| FD: spiked coagulated water (run 9-1) | 10.1 | -17.1 |
| Coagulant (50 mg/L) in ultra-pure water | 0.90 | +26.2 |
| Coagulant (40 mg/L) in ultra-pure water | 0.82 | +18.4 |
| Coagulant (30 mg/L) in ultra-pure water | 0.69 | +18.2 |
| Polymer (0.10 mg/L) in ultra-pure water | 0.10 | |
| Polymer (0.15 mg/L) in ultra-pure water | 0.15 | |
| Polymer (0.20 mg/L) in ultra-pure water | 0.23 | |

FD: factorial design

Table C.2: Residuals values of the model

| **Run** | $\mathbf{Y_{i\ exp}}$ | $\mathbf{Y_{i\ fit}}$ | $\mathbf{e_i = Y_{i\ exp} - Y_{i\ fit}}$ |
|---|---|---|---|
| 1-1 | 93.7 | 95.5 | -1.8 |
| 1-2 | 95.2 | 95.5 | -0.3 |
| 2-1 | 94.6 | 96.2 | -1.6 |
| 2-2 | 95.7 | 96.2 | -0.5 |
| 3-1 | 94.2 | 95.5 | -1.3 |
| 3-2 | 94.7 | 95.5 | -0.8 |
| 4-1 | 90.6 | 92.4 | -1.8 |
| 4-2 | 92.1 | 92.4 | -0.3 |
| 5-1 | 97.6 | 98.2 | -0.7 |
| 5-2 | 96.8 | 98.2 | -1.5 |
| 6-1 | 89.6 | 92.0 | -2.4 |
| 6-2 | 92.3 | 92.0 | 0.3 |
| 7-1 | 68.2 | 63.2 | 5.0 |
| 7-2 | 56.0 | 63.2 | -7.1 |
| 8-1 | 93.1 | 93.4 | -0.3 |
| 8-2 | 91.6 | 93.4 | -1.8 |
| 9-1 | 96.1 | 90.8 | 5.3 |
| 9-2 | 97.1 | 90.8 | 6.3 |
| 9-3 | 96.3 | 90.8 | 5.5 |

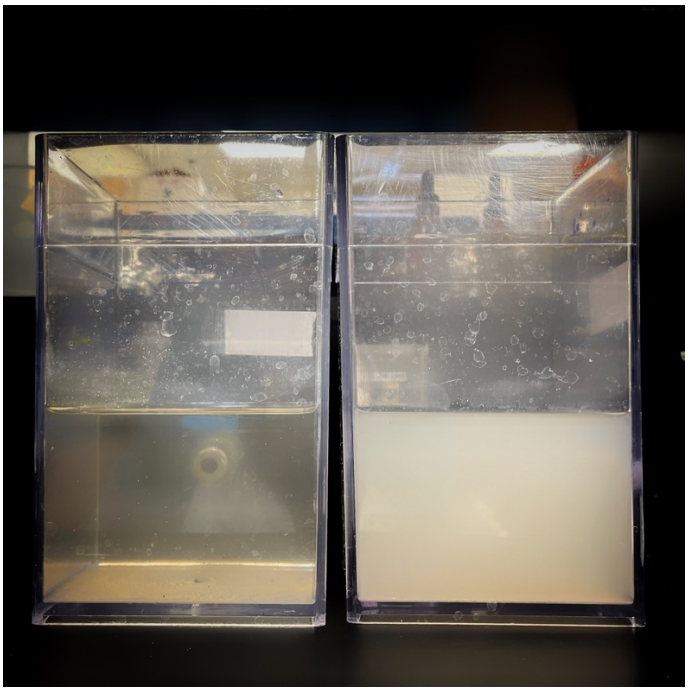

Figure C.1: Raw water (batch 3, turbidity 37.4 NTU) before and after addition of 0.35 g/L of kaolin (spiked water turbidity = 477 NTU)

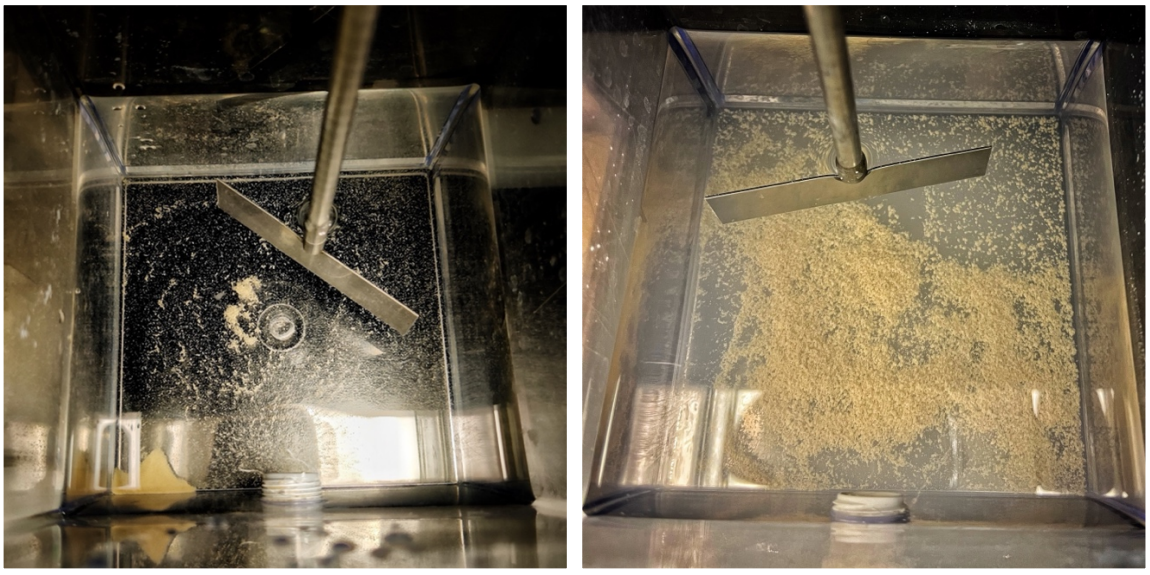

(a) (b)

Figure C.2: Settled floc after jar tests on raw water samples of (a) batch 2 and (b) batch 3

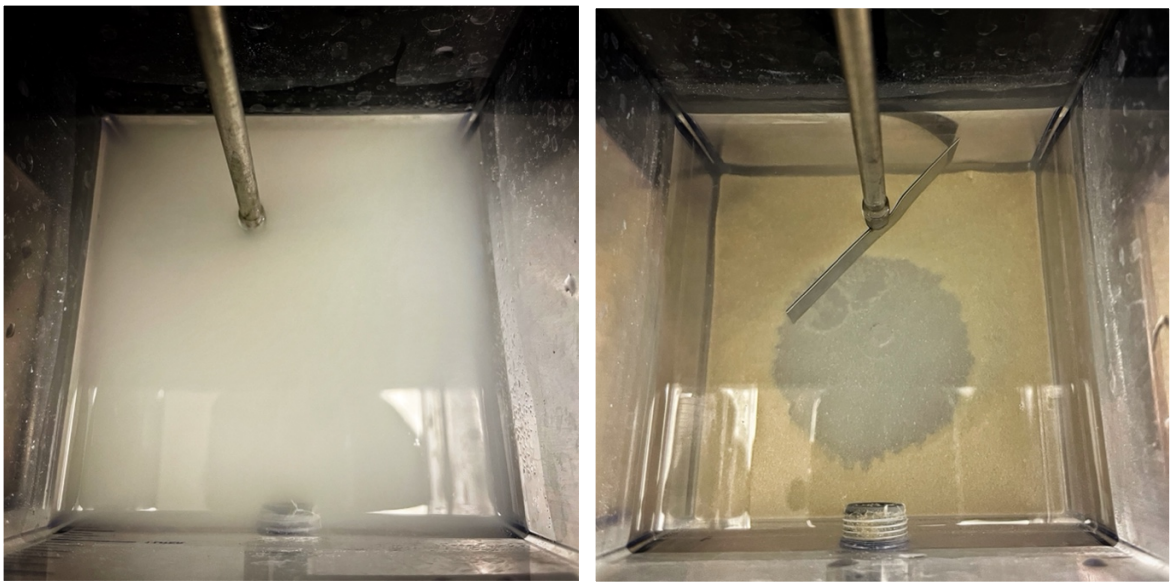

(a) (b)

Figure C.3: Spiked water samples with extremely high turbidity: (a) before and (b) after jar test

# Appendix D: MATLAB Codes

Code D.1: Checks the validity of data for x = 25%, 50%, 75%, 100%, 150% and 200% (invalid data = x% over the hourly median turbidity)

```
function [raw_invalid_yn] = raw_invalid_detect(turb)
n = numel(turb); %n = no of data
for ij = 7:n %validity of the 1st 6 data was checked manually
    if turb(ij,1) > 1.25*median(turb(ij-6:ij+6))
        turb(ij,2) = 1; %1 = invalid, 0 = valid
    else turb(ij,2) = 0;
    end
end
for ij = 7:n
    if turb(ij,1) > 1.5*median(turb(ij-6:ij+6))
        turb(ij,3) = 1;
    else turb(ij,3) = 0;
    end
end
for ij = 7:n
    if turb(ij,1) > 1.75*median(turb(ij-6:ij+6))
        turb(ij,4) = 1;
    else turb(ij,4) = 0;
    end
end
for ij = 7:n
    if turb(ij,1) > 2*median(turb(ij-6:ij+6))
        turb(ij,5) = 1;
    else turb(ij,5) = 0;
    end
end
for ij = 7:n
    if turb(ij,1) > 2.5*median(turb(ij-6:ij+6))
        turb(ij,6) = 1;
    else turb(ij,6) = 0;
    end
end
for ij = 7:n
    if turb(ij,1) > 3*median(turb(ij-6:ij+6))
        turb(ij,7) = 1;
    else turb(ij,7) = 0;
    end
end
raw_invalid_yn = turb; %c1=rawturb c2=25 c3=50 c4=75 c5=100 c6=150 c7=200
```

Code D.2: Removes the invalid data for x = 25%, 50%, 75%, 100%, 150% and 200%

```
function [rawturb_wo_200, rawturb_wo_150, rawturb_wo_100, rawturb_wo_75,
rawturb_wo_50, rawturb_wo_25] = raw_invalid_delete(raw_invalid_yn)
n = height(raw_invalid_yn);
for ij = 1:n
    if raw_invalid_yn(ij,7) == 1 %1 = invalid data
        raw_invalid_yn(ij,1) = NaN;
    end
end
rawturb_wo_200 = raw_invalid_yn(:,1);
for ij = 1:n
    if raw_invalid_yn(ij,6) == 1
        raw_invalid_yn(ij,1) = NaN;
    end
end
rawturb_wo_150 = raw_invalid_yn(:,1);
for ij = 1:n
    if raw_invalid_yn(ij,5) == 1
        raw_invalid_yn(ij,1) = NaN;
    end
end
rawturb_wo_100 = raw_invalid_yn(:,1);
for ij = 1:n
    if raw_invalid_yn(ij,4) == 1
        raw_invalid_yn(ij,1) = NaN;
    end
end
rawturb_wo_75 = raw_invalid_yn(:,1);
for ij = 1:n
    if raw_invalid_yn(ij,3) == 1
        raw_invalid_yn(ij,1) = NaN;
    end
end
rawturb_wo_50 = raw_invalid_yn(:,1);
for ij = 1:n
    if raw_invalid_yn(ij,2) == 1
        raw_invalid_yn(ij,1) = NaN;
    end
end
rawturb_wo_25 = raw_invalid_yn(:,1);
```

Code D.3: Removes corresponding ACTIFLO® effluent turbidity data for flow <35ML/D

```
function [turb_wo_lowflow] = actiflo_low_flow_delete(flow,turb)
n = numel(flow);
for ij = 1:n
    if raw_flow(ij) < 35
```

```
        turb(ij) = NaN;
    end
end
    turb_wo_lowflow = turb([1:end],1);
```

Code D.4: Removes corresponding filter effluent turbidity data for zero flow and filter-to-waste period (Plant A)

```
function [turb_wo] = filter_lowflow_del(turb,flow)
n = numel(flow);
for ij = 1:n
    if flow(ij,1) == 0
        flow(ij,1) = NaN;
    end
end
flow_0 = flow; %all zero flow is replaced by NaN

for ij = 1:n
    if isnan(flow_0(ij,1)) && ~isnan(flow_0(ij+40,1)) %filter is not
running for at least 40 minutes = shutdown or backwash, but not filter-to-
waste
        flow_0(ij:ij+35,1) = NaN; %filter to waste = 1st 35 mins of a
filter cycle
    end
end
flow_0_fw = flow_0; %all zero flow and filter-to-waste flow is replaced by
NaN
for ij = 1:n
    if isnan(flow_0_fw(ij,1))
        turb(ij,1) = NaN;
    end
end
turb_wo = turb;
```

Code D.5: Identifies data over seasonal median turbidity for y = 25%, 50%, 75% and 100% (turbidity event = y% over seasonal median)

```
function [percent_above] = event_detect (event_turb, seas_med)
n = height(event_turb); %n=no. of data
for ij = 1:n
    if event_turb(ij,1) > seas_med*1.25
        event_turb(ij,2) = 1; %1=event
    else event_turb(ij,2) = 0; %0=not event
```

```
    end
end
for ij = 1:n
    if event_turb(ij,1) > seas_med*1.5
        event_turb(ij,3) = 1;
    else event_turb(ij,3) = 0;
    end
end
for ij = 1:n
    if event_turb(ij,1) > seas_med*1.75
        event_turb(ij,4) = 1;
    else event_turb(ij,4) = 0;
    end
end
for ij = 1:n
    if event_turb(ij,1) > seas_med*2
        event_turb(ij,5) = 1;
    else event_turb(ij,5) = 0;
    end
end
%c1=turb c2=25% c3=50% c4=75% c5=100%
percent_above = event_turb;
```

Code D.6: Removes the baseline turbidity for y = 25%, 50%, 75% and 100%

```
function [event25, event50, event75, event100] = event_separation
(event_turb)
n = height(event_turb); % n=no. of data
for ij = 1:n
    if event_turb(ij,2) == 0 %0=not event, 1=event
        event_turb(ij,1) = NaN;
    end
end
event25 = event_turb(1:end,1);
for ij = 1:n
    if event_turb(ij,3) == 0
        event_turb(ij,1) = NaN;
    end
end
event50 = event_turb(1:end,1);
for ij = 1:n
    if event_turb(ij,4) == 0
        event_turb(ij,1) = NaN;
    end
end
event75 = event_turb(1:end,1);
for ij = 1:n
    if event_turb(ij,5) == 0
        event_turb(ij,1) = NaN;
```

```
    end
end
event100 = event_turb(1:end,1);
```

Code D.7: Calculation of TRI

```
function [tri] = tri(turb,tgoal)
m = 1;
w = floor(numel(turb)/52); %1 week = w data points
n = w;
for ii = 1:52 %52 weeks in a year
    x = m;
    y = n;
    t50 = prctile(turb(x:y,1),50);
    t60 = prctile(turb(x:y,1),60);
    t70 = prctile(turb(x:y,1),70);
    t80 = prctile(turb(x:y,1),80);
    t90 = prctile(turb(x:y,1),90);
    w = (t50+t60+t70+t80+t90)*10/tgoal;
    if w <= 50
        a1 = 0.6;
    else
        a1 = 0.4;
    end
    a2 = 1-a1;
    tri90(ii) = ((a1*t90/t50) + (a2*t50/tgoal))*100;
    m = n+1;
    n = n+w;
end
```

Code D.8: Removes corresponding CFS effluent turbidity data for flow <5ML/D and zero PACl flow (Plant B)

```
function [turb_wo_lowflow] = cfs_low_flow_delete(flow,turb,pacl_1,pacl_2)
n = numel(flow);
for ij = 1:n
    if flow(ij) < 5
       turb(ij) = NaN;
    end
end
pacl = pacl_1 + pacl_2;
for ij = 1:n
    if pacl(ij) == 0
        turb(ij) = NaN;
    end
```

```
end
    turb_wo_lowflow = turb([1:end],1);
```

Code D.9: Removes corresponding filter effluent turbidity data for zero flow (Plant B)

```
function [turb_wo_lowflow] = filter_low_flow_delete(flow,turb)
n = numel(flow);
for ij = 1:n
    if flow(ij) == 0
       turb(ij) = NaN;
    end
end
    turb_wo_lowflow = turb([1:end],1);
```